

Universidad de Granada  
Facultad de Ciencias  
Departamento de Microbiología

**DESARROLLO DE ESTRATEGIAS DE  
BIORREMEDIACIÓN DE AGUAS CONTAMINADAS  
CON URANIO BASADAS EN LA INMOVILIZACIÓN DE  
CÉLULAS BACTERIANAS CON ACTIVIDAD  
FOSFATASA**



**UNIVERSIDAD  
DE GRANADA**

Pablo Martínez Rodríguez  
Granada, 2022

Dirigida por el Dr. Mohamed Merroun y Dr. Iván Sánchez Castro

Programa de Doctorado en Biología Fundamental y de Sistemas

Editor: Universidad de Granada. Tesis Doctorales  
Autor: Pablo Martínez Rodríguez  
ISBN: 978-84-1117-708-5  
URI: <https://hdl.handle.net/10481/80347>



Esta Tesis Doctoral ha sido realizada en el Departamento de Microbiología (Facultad de Ciencias) de la Universidad de Granada durante los años 2018-2022 dentro del Grupo de Investigación Mixobacterias (BIO103).

Para la realización de este trabajo el doctorando disfrutó de un contrato de investigador con cargo al Proyecto nº3022 OTRI-UGR, financiado por ORANO Mining (Francia). Parte del tiempo el doctorando también disfrutó del contrato “Personal Contratado del Programa de Joven Personal Investigador Ref. 6019” financiado por el Fondo Social Europeo – Iniciativa de Empleo Juvenil.

Además, el doctorando disfrutó de la beca de movilidad del programa Erasmus Prácticas (Erasmus +) del Vicerrectorado de Estudiantes de la Universidad de Granada para la realización de la estancia en el centro de investigación extranjero *College of Engineering, Swansea University (UK)* bajo la supervisión del Prof. Jesús Ojeda Ledo.





*A mis padres, Belén y Julián,  
para que dejen de preguntarme por la tesis.*



*“Everyone has a plan 'till they get punched in the mouth”*

**Myke Tyson**



Los resultados obtenidos durante la realización de esta Tesis Doctoral han sido publicados o se están preparando para su publicación en revistas científicas de impacto, así como en congresos tanto a nivel nacional como internacional:

- Artículos científicos publicados con los resultados obtenidos durante esta Tesis Doctoral:

- **Martínez-Rodríguez, P.**, Sánchez-Castro, I., Descostes, M., Merroun, M.L., 2020. Draft genome sequence data of *Microbacterium* sp. strain Be9 isolated from uranium-mill tailings porewaters. *Data in Brief*. 31, 10–14. <https://doi.org/10.1016/j.dib.2020.105732>. **IF: 0.2, Q2.**
  - Sánchez-Castro, I., **Martínez-Rodríguez, P.**, Jroundi, F., Lorenzo, P., Descostes, M., L. Merroun, M., 2020. High-efficient microbial immobilization of solved U(VI) by the *Stenotrophomonas* strain Br8. *Water Research*. 183, 116110. <https://doi.org/10.1016/j.watres.2020.116110> **IF: 11.236, Q1.**
  - Sánchez-Castro, I\*, **Martínez-Rodríguez, P\***, Abad, M.M., Descostes, M., Merroun, M.L., 2021. Uranium removal from complex mining waters by alginate beads doped with cells of *Stenotrophomonas* sp. Br8: Novel perspectives for metal bioremediation. *Journal of Environmental Management*. 296, 1–10. <https://doi.org/10.1016/j.jenvman.2021.113411>. **IF: 8.91, Q1.**
- \*These authors contributed equally.
- **Pablo Martínez-Rodríguez**, Iván Sánchez-Castro, Jesús J. Ojeda, María M. Abad, Michael Descostes, Mohamed Larbi Merroun, 2022. Effect of different phosphate sources on uranium biomineralization by the *Microbacterium* sp. Be9 strain: a multidisciplinary approach study. *Frontiers in Microbiology*, *En prensa*. doi: 10.3389/fmicb.2022.1092184. **IF: 6.06, Q1.**

- Resultados obtenidos durante esta Tesis Doctoral presentados en congresos a nivel nacional e internacional:

- **Pablo Martínez-Rodríguez**, Iván Sánchez-Castro, María Pinel-Cabello, Germán Bosch-Estévez, V. Phrommavanh, Michael Descostes, Mohamed Larbi Merroun. Bacterial strain *Microbacterium* sp. Be9: variable behaviour in presence of uranium. Geomicrobiology Network, Research in Progress Meeting, 14 and 15 June, 2018, University of Strathclyde, UK.
- Iván Sánchez-Castro, **Pablo Martínez-Rodríguez**, María Pinel-Cabello, Germán Bosch-Estévez, Vannapha Phrommavanh, Michael Descostes, Mohamed Larbi Merroun. Versatile behaviour of bacterial strain *Microbacterium* sp. Be9 in presence of Uranium and its bioremediation potential. 7th European Bioremediation Conference (EBC-VII) and the 11th International Society for Environmental Biotechnology conference (ISEB 2018). July 4-9, 2018, Crete, Greece.
- **Martínez-Rodríguez, Pablo**; Sánchez-Castro, Iván; Pinel-Cabello, María; Bosh-Estévez, Germán; Descostes, Michael; Merroun, Mohamed. Phosphates speciation influences Be9 bacterial strain uranium bioremediation potential. Final Project annual meeting 2019 of the EU-Project MIND, 7 – 9 May, Vattenfall building, Stockholm, Sweden.
- **Pablo Martínez-Rodríguez**, Iván Sánchez-Castro, María Pinel-Cabello, Germán Bosch-Estévez, Michael Descostes, Mohamed. L. Merroun. Effect of phosphate sources on *Microbacterium* sp. Be9 Uranium removal potential. II Congreso de la Escuela Internacional de Doctorado celebrado los días 27 y 28 de noviembre de 2019, Campus de Móstoles, Madrid.
- **Pablo Martínez Rodríguez**, Iván Sánchez Castro, María M. Abad, Michael Descostes, Mohamed Merroun. Biorremediación de U en aguas mineras mediante microesferas de alginato con células de la cepa *Stenotrophomonas* Br8. XIII Reunión Científica del Grupo de Microbiología del Medio Acuático de las SEM celebrado en Granada los días 22 y 23 de septiembre de 2022.

El doctorando y los directores de la tesis Mohamed Larbi Merroun e Iván Sánchez Castro:  
Garantizamos, al firmar esta tesis doctoral, que el trabajo ha sido realizado por el doctorando bajo la dirección de los directores de la tesis y hasta donde nuestro conocimiento alcanza, en la realización del trabajo, se han respetado los derechos de otros autores a ser citados, cuando se han utilizado sus resultados o publicaciones.

///

The doctoral candidate Pablo Martínez Rodríguez and the thesis supervisors Mohamed Larbi Merroun e Iván Sánchez Castro:

We guarantee, by signing this doctoral thesis, that the work has been done by the doctoral candidate under the direction of the thesis supervisors and, as far as our knowledge reaches, in the performance of the work, the rights of other authors to be cited (when their results or publications have been used) have been respected.

Lugar y fecha / Place and date:

Directores de la Tesis / Thesis supervisors

Doctorando / Doctoral candidate

Firma / Signed

Firma / Signed





# LIST OF ABBREVIATIONS

**ANI:** Average Nucleotide Identity

**BWR:** Boiling Water Reactor

**CANDU:** Canada Deuterium Uranium

**EDAX:** Energy-Dispersive X-Ray

**EDS:** Energy-Dispersive X-Ray Spectroscopy

**EDX:** Energy Dispersive X-Ray

**ESEM:** Environmental Scanning Electron Microscopy

**EXAFS:** Extended X-Ray Absorption Fine Structure

**FDA:** Fluorescein Diacetate

**FT:** Fourier Transforms

**FT-IR:** Fourier Transform Infrared

**FTIR-ATR:** Fourier Transform Infrared Spectroscopy with Attenuated Total Reflectance

**G2P:** Glycerol-2-Phosphate

**G3P:** Glycerol-3-phosphate

**GBDP:** Genome-Blast Distance Phylogeny

**HAADF-STEM:** High-Angle Annular Dark-Field Scanning Transmission Electron Microscopy

**HDPE:** High-Density Polyethylene

**HRTEM:** High-Resolution Transmission Electron Microscopy

**ICP-MS:** Inductively-Coupled Plasma Mass Spectrometry

**IDA:** Inferred from Direct Assay

**ISL:** In Situ Leaching

**ISR:** In Situ Recovery

**LPM:** Low Phosphate Medium

**MIC:** Minimal Inhibitory Concentration

**MM:** Metal/Metalloids

**MOPS:** 3-(N-morpholino) Propanesulphonic Acid

**Ortho-ANI:** Average Nucleotide Identity with Respect to Orthologous Genes

**Pi:** Inorganic Phosphate

**PI:** Propidium Iodide

**Poly-Ps:** Polyphosphates

**PSB:** Phosphate Solubilizing Bacteria

**PWR:** Pressurized Water Reactor

**RAST:** Rapid Annotation System Technology

**RBMK:** Reactor Bolshoy Moshchnosty Kanalny

**SD:** Standard Deviation

**SEM:** Scanning Electron Microscopy

**STEM:** Scanning Transmission Electron Microscopy

**TAS:** Traceable Author Statement

**TEOS:** Tetraethyl Orthosilicate

**TYGS:** Type Strain Genome Server

**XANES:** X-Ray Absorption Near-Edge Structure

**XAS:** X-Ray Absorption Spectroscopy

**XPS:** X-Ray Photoelectron Spectroscopy

**XRD:** X-Ray Diffraction

<b>RESUMEN .....</b>	<b>1</b>
<b>SUMMARY .....</b>	<b>7</b>
<b>INTRODUCCIÓN .....</b>	<b>11</b>
Uranio: Propiedades físico-químicas, fuentes naturales y antropogénicas, y usos industriales. ....	13
Minería de U y la contaminación medioambiental asociada .....	16
Diversidad microbiana de ambientes contaminados con radionucleidos .....	23
Interacciones microbianas con U .....	24
Biorremediación de U: fundamentos y tecnologías usadas a nivel mundial .....	29
Procesos basados en la inmovilización de biomasa sobre soportes sólidos .....	34
<b>OBJETIVOS.....</b>	<b>47</b>
<b>MATERIALS AND METHODS .....</b>	<b>51</b>
Molecular and phenotypic characterization of the strains Br8 and Be9 .....	53
Design and optimization of a method for Br8 bacterial biomass immobilization on inorganic supports. ....	55
Interactions bacteria-U.....	61
Spectroscopic and microscopic characterization of U precipitates .....	65
<b>CAPÍTULO I.....</b>	<b>69</b>
<b>CAPÍTULO II .....</b>	<b>77</b>
<b>CAPÍTULO III.....</b>	<b>93</b>
<b>CAPÍTULO IV .....</b>	<b>131</b>
<b>CAPÍTULO V.....</b>	<b>165</b>
<b>DISCUSIÓN GENERAL .....</b>	<b>203</b>
<b>CONCLUSIONES .....</b>	<b>227</b>
<b>CONCLUSIONS.....</b>	<b>231</b>



## RESUMEN

Actualmente la producción de energía nuclear es una de las actividades más importantes a nivel económico mundial, siendo el uranio, por tanto, un elemento con una importancia en continuo auge. Debido a la expansión de la industria relacionada con estos procesos (p. ej. minas de uranio) se pueden liberar desechos que contienen radionucleidos y metales pesados (el propio uranio entre ellos) al medio ambiente, contaminando las zonas más cercanas, como pueden ser aguas superficiales o subterráneas. Por esta razón es imprescindible el desarrollo de programas de rehabilitación y gestión sostenible de estos residuos con el objetivo de minimizar su impacto medioambiental siendo objeto de estudio, en los últimos años, nuevas estrategias de remediación basadas en el uso de microorganismos y en la capacidad de estos de interactuar con los contaminantes inorgánicos. Ello viene propiciado por ser muy costosas, tanto a nivel económico como ambiental, las estrategias físico-químicas tradicionales para la eliminación del medio ambiente de metales pesados contaminantes, mientras que las tecnologías de inmovilización de metales pesados basadas, con el mismo propósito, en el uso de microorganismos parecen ser una alternativa más sostenible, atractiva, eficiente y menos costosa.

Los mecanismos de interacción microbiana con U y su inmovilización mediante diferentes procesos han sido descritos por numerosos estudios. En este sentido, las principales técnicas propuestas para la biorremediación de uranio son la precipitación por reducción enzimática de U(VI) a U(IV) y la biomineralización de fosfatos de U(VI). En cuanto a la reducción química de U, estas estrategias conllevan la alteración de la especiación química del U(VI), una forma móvil/soluble (más tóxica), a U(IV), una forma insoluble e inmóvil y, consecuentemente, menos tóxica. En condiciones anaerobias, un grupo limitado de bacterias (p. ej. *Geobacter*, *Clostridium*, *Desulfovibrio*, *Shewanella*) son capaces de reducir el U(VI) a U(IV), precipitándolo y formando minerales de uraninita (UO<sub>2</sub>). Sin embargo, estos precipitados presentan poca estabilidad, pudiendo reoxidarse y, por tanto, volviendo a formas móviles ante determinados cambios geoquímicos en las condiciones del sistema. Por el contrario, la biomineralización de uranio, basada en la actividad fosfatasa de algunos microorganismos, facilita la degradación de fosfatos orgánicos liberando fosfatos inorgánicos al medio que pueden precipitar el U móvil presente en el sistema generando

## RESUMEN

fosfatos de uranio. Estas fases minerales de uranio se caracterizan por su gran estabilidad e insolubilidad en un amplio rango de potencial redox y pH, convirtiéndolo en un método muy prometedor para biorremediación.

El desarrollo de estrategias de remediación basadas en el proceso de biomineralización requiere que los microorganismos usados cumplan una serie de requisitos, entre otros: 1) ser altamente tolerantes al metal de interés y otros metales pesados que podrían estar presentes en el medio afectado, 2) presentar una alta versatilidad metabólica que les permita actuar frente a cambios fisicoquímicos, y 3) ser capaces de biomineralizar el metal, inmovilizándolo. Todos estos requisitos deben ser evaluados para el posible desarrollo de estrategias de biorremediación aplicables en ambientes contaminados reales. Adicionalmente, los procesos de inmovilización de biomasa activa pueden ofrecer resultados prometedores aportando ciertas ventajas: un menor espacio necesario en comparación con otras estrategias *ex situ*, una mayor facilidad de manejo del sistema, la posibilidad de reutilizar las matrices, o una recuperación más sencilla, entre otras. Además, estas matrices pueden proporcionar un ambiente adecuado para las bacterias contribuyendo a una mejor preservación de la integridad celular en condiciones limitantes. Por este motivo numerosas técnicas de inmovilización están siendo desarrolladas y mejoradas debido a que las características mencionadas las convierten en las alternativas más eficientes y atractivas para aplicaciones a nivel de campo.

El objetivo de este trabajo de tesis doctoral consistió en estudiar la capacidad de biomineralización de U de las cepas *Microbacterium* sp. Be9 y *Stenotrophomonas* sp. Br8, y desarrollar una estrategia aplicable de biorremediación para eliminar U en aguas mineras contaminadas. Con esta finalidad se empleó una metodología multidisciplinar, combinando técnicas espectroscópicas, microscópicas y microbiológicas.

En primer lugar, ambas cepas fueron caracterizadas fisiológica, bioquímica y filogenéticamente con el objetivo de obtener información de utilidad para la consecución de los objetivos de esta tesis doctoral. En cuanto a la cepa *Microbacterium* sp. Be9, en trabajos anteriores, publicados en el Grupo de Investigación BIO103, se había demostrado su alta tolerancia al U y otros metales pesados, sugiriendo un alto potencial en biorremediación para este radionucleido. En la investigación llevada a cabo, la anotación de su genoma predijo numerosos genes responsables de la resistencia a compuestos tóxicos (*arsD*, *czcD*, *copC*, *copD*), genes que codifican para proteínas de respuesta a estrés

(CoaADR, PrxCat) y transporte de membrana (YbaT, DedA), entre otros. Entre los transportadores de membrana destaca la presencia de sideróforos ABC-type  $\text{Fe}^{3+}$ , los cuales han sido identificados como proteínas responsables de la acumulación intracelular de U. Del mismo modo, la cepa *Stenotrophomonas* sp. Br8 mostró una alta tolerancia al U y otros metales, además de una gran capacidad de biomineralización de fosfatos de U mediada por la actividad fosfatasa. Los análisis filogenéticos y genómicos confirmaron la afiliación de la cepa Br8 al género *Stenotrophomonas*, siendo identificada como la especie *Stenotrophomonas lactitubi*. Mediante la anotación de su genoma se identificaron algunos genes específicos potencialmente relacionados con la biomineralización de U(VI) (p. ej. regiones codificantes relacionadas con la fosfatasa) y, además, se han encontrado numerosas regiones responsables de la resistencia a compuestos tóxicos y respuesta a estrés (*phoU*, *phoB*, *phoR*, *TonB*).

Posteriormente, se evaluó la capacidad de bioprecipitación de U por parte de ambas cepas, con el objetivo de seleccionar aquella con mayor potencial. La cepa *Microbacterium* sp. Be9 demostró una alta capacidad de eliminar el U soluble presente (88%) pero únicamente ante la ausencia de fuentes exógenas de fosfato, de modo que se evaluó el efecto de diferentes fuentes de fosfato (orgánicos e inorgánicos) y su ausencia en el proceso de biomineralización de U. Los resultados mostraron un comportamiento variable bajo las condiciones ensayadas: una alta bioacumulación intracelular de fosfatos de U en ausencia de fosfatos y una solubilización de U cuando este fue, previamente, precipitado abióticamente por fosfatos inorgánicos. En presencia de una fuente de fosfatos orgánicos la capacidad de precipitación disminuyó notablemente. Para confirmar este comportamiento variable de la cepa Be9 se aplicó un enfoque multidisciplinar (determinación de la actividad de fosfatasa, cuantificación de la liberación de fosfatos inorgánicos, viabilidad celular, etc.). Además, se caracterizó su superficie celular mediante análisis XPS (*X-ray photoelectron spectroscopy*) y titulaciones potenciométricas para determinar los grupos funcionales implicados en la bioadsorción de U. Estos estudios determinaron que la superficie celular de Be9 contaba con la presencia de una alta proporción de polisacáridos y una carga neta negativa, lo que puede facilitar la adsorción de iones  $\text{UO}_2^{2+}$ . Estas características favorecerían el proceso de bioacumulación intracelular detectado, consistente en una primera fase pasiva rápida, donde el U se adhiere a la superficie celular y, posteriormente, una fase activa lenta donde fosfatos inorgánicos intracelulares precipitan el metal. Sin embargo, al no detectarse una actividad fosfatasa



## RESUMEN

relevante en la cepa Be9, el proceso responsable de la biomineralización detectada sigue sin estar claro. Mediante micrografías de HAADF-STEM (*High-Angle Annular Dark-Field Scanning Transmission Electron Microscopy*) y análisis por EDX (*Energy Dispersive X-ray*) se observó que los fosfatos de U formados precipitaron intra o extracelularmente, dependiendo del tratamiento.

Por el contrario, la cepa *Stenotrophomonas* sp. Br8 mostró una alta actividad fosfatasa que provocó la liberación de ortofosfatos en presencia de glicerol-2-fosfato (G2P) lo que, a su vez, supuso una alta precipitación del U soluble (90 – 95%). Los iones de U móviles precipitaron como “agujas” (*needle-like fibrils*) en la superficie celular y en el espacio extracelular, según se observó mediante STEM (*Scanning Transmission Electron Microscopy*). Los análisis por espectroscopía EXAFS (*Extended X-ray Absorption Fine Structure*) y XRD (*X-ray Diffraction*) mostraron que la estructura local de los precipitados de U es similar a la del grupo de meta-autunita ( $\text{Ca}(\text{UO}_2)_2(\text{PO}_4)_2 \cdot 6\text{H}_2\text{O}$ ). Esta fase mineral del U ha sido ampliamente estudiada, destacando por su alta estabilidad a lo largo del tiempo. La alta capacidad de biomineralización de U de la cepa Br8 también se llevó a cabo bajo diferentes condiciones fisicoquímicas (p. ej. pH, temperatura, etc.), demostrando una gran habilidad de remediación bajo posibles condiciones ambientales cambiantes.

En definitiva, tras evaluar ambas cepas bacterianas, se seleccionó *Stenotrophomonas* sp. Br8 como la más adecuada para desarrollar la estrategia de eliminación de U mediante la inmovilización de biomasa, gracias a su alta actividad fosfatasa y versatilidad frente a cambios ambientales, capaz de precipitar el metal soluble en forma de fosfatos de U.

Finalmente, se optimizó el protocolo de inmovilización de biomasa de la cepa Br8 en una matriz inorgánica con el objetivo de proporcionar protección a las células, facilitar su manipulación y hacer que el proceso sea más adecuado para su uso a escala industrial. Con esta finalidad se caracterizaron varios métodos de inmovilización de biomasa (microesferas de alginato, matriz TEOS (ortosilicato de tetraetilo) y una matriz híbrida de ambos compuestos) mediante un enfoque multidisciplinar (HAADF-STEM, microscopía ESEM (*Environmental Scanning Electron Microscopy*), FTIR-ATR (*Fourier Transform Infrared Spectroscopy with Attenuated Total Reflectance*), etc.). De esta forma se concluyó que el mejor método de inmovilización era el uso de microesferas de alginato, por ser biocompatibles y altamente porosas para las células de Br8. Esta aproximación fue ensayada con aguas mineras contaminadas con U en presencia de G2P como fuente de

fosfato orgánico para liberar ortofosfatos gracias a la actividad fosfatasa de Br8, logrando altas tasas de precipitación de U (alrededor del 98%) después de incubarse durante 72 h. Además, se optimizaron otros parámetros como la concentración de biomasa y las condiciones de almacenamiento de microesferas inoculadas con Br8 para una correcta aplicación. Los resultados de la cinética de eliminación de U y los análisis por HAADF-STEM/ESEM indicaron que la precipitación de U por parte de las células inmovilizadas es un proceso bifásico que combina una primera sorción pasiva del metal en la superficie de las microesferas o de las propias células, y una segunda biomineralización activa más lenta. En conclusión, este estudio reveló que la eliminación de U presente en aguas mineras complejas empleando microesferas de alginato inoculadas con células de la cepa *Stenotrophomonas* sp. Br8 es una estrategia prometedora, incluso a altas concentraciones de metal.

La eliminación de U en soluciones sintéticas que contienen U ha sido ampliamente estudiada. Sin embargo, la inmovilización de U de aguas residuales mineras permanece relativamente inexplorada hasta el momento. Por ello, la precipitación de U como fosfato de U(VI) en este tipo de aguas es de gran relevancia científica y ambiental para el futuro desarrollo de estrategias apropiadas de biorremediación. Para continuar con la mejora de esta estrategia sería de gran interés centrarse en el escalado del proceso, aumentando los volúmenes ensayados y las tasas de eliminación, logrando recrear estaciones de tratamiento de aguas respetuosas con el medio ambiente.

## RESUMEN

## SUMMARY

Nowadays, production of nuclear energy is one of the most important economic activities worldwide, implying an increasing value of U. However, due to the expansion of related industries (e.g. U mining), radionuclide-containing wastes can be released into the environment (e.g. surface water (e.g. rivers, lakes) and groundwater). For this reason, there is a growing need to develop sustainable strategies, minimizing the environmental impact of this type of wastes. In recent years, new efficient and eco-friendly remediation strategies based on the use of microorganisms and their ability to interact with inorganic contaminants have emerged. Physicochemical remediation strategies for heavy metals are economical and environmentally costly, while microbiological heavy metal immobilization mechanisms seem to be a more sustainable, efficient and less expensive approaches.

Numerous studies have described the mechanisms of U microbial immobilization through different processes, mainly, enzymatic reduction of U(VI) to U(IV) and the U(VI) phosphate biomineralization. Microbial U reduction alters the chemical speciation of U(VI), a mobile/soluble (more toxic) form, to U(IV), an insoluble/immobile and less toxic species. Under anaerobic conditions, a limited group of bacteria (e.g. *Geobacter*, *Clostridium*, *Desulfovibrio*, *Shewanella*) are capable to reduce U(VI) to U(IV), precipitating it as uraninite (UO<sub>2</sub>). But these precipitates have low stability and could be reoxidized into mobile forms under some geochemical changes. However, the U biomineralization is based on microbial phosphatase activity, leading to the degradation of organic phosphates and subsequent release of inorganic phosphates for U biomineralization. The U biomineral phases generated present high stability and insolubility in a wide redox and pH range, becoming a highly promising strategy for bioremediation.

Microbial strains with potential for U bioremediation should fulfil several criteria: 1) high tolerance to U and other heavy metals; 2) high metabolic versatility against physicochemical changes; and 3) high U phosphate biomineralization ability. However, for environmental upscaling of these remediation strategies, in real contaminated environments, biomass immobilization procedures in inorganic matrices are needed. The immobilization of microorganisms in a matrix is a well-studied approach used for efficient

## SUMMARY

removal of organic and inorganic contaminants. The use of matrices provides several advantages: less operation space, ease of handling, reusable matrices, or easiest recovery, among others. In addition, it may provide an appropriate environment for bacteria, preserving the cell integrity under limiting conditions. Biomass immobilization confers favourable characteristics to bioremediation strategies, and therefore, are being developed and improved, becoming more efficient and attractive for real application.

For this reason, the main objective of this doctoral thesis was to study the U biomineralization ability of *Microbacterium* sp. Be9 and *Stenotrophomonas* sp. Br8 strains, isolated from U contaminated waters, and to design a bacteria-based U immobilization strategy for real contaminated water samples. For this purpose, a multidisciplinary methodology was used, combining spectroscopic, microscopic and microbiological techniques.

Firstly, both strains were physiologically, biochemically and phylogenetically characterized in order to obtain useful information for the development of the above-mentioned bioremediation strategy. In previous works published by BIO103 Research Group, *Microbacterium* sp. Be9 strain showed high tolerance to U and other heavy metals, suggesting potential in bioremediation of this radionuclide. In this work, the Be9 genome annotation predicted genes responsible for resistance to toxic metals/metalloids (*arsD*, *czcD*, *copC*, *copD*), in addition to genes codifying for proteins related to stress response (CoaADR, PrxCat) and membrane transport (YbaT, DedA). Interestingly, it is worthy to point out the key role of ABC-type Fe<sup>3+</sup> siderophores, which have been identified as responsible for the uptake of U. Similarly, the *Stenotrophomonas* sp. Br8 strain showed high tolerance to U and other heavy metals and metalloids. Phylogenetic analyses supported the affiliation to the genus *Stenotrophomonas*, specifically as *Stenotrophomonas lactitubi* species. Through genome annotation, some specific genes potentially related to U(VI) biomineralization (e.g., phosphatase-related coding regions), and numerous regions responsible for resistance to toxic compounds and stress response (*phoU*, *phoB*, *phoR*, *TonB*) were identified.

Secondly, the U bioprecipitation ability of the two bacterial strains was evaluated in order to screen for the most suitable one for metal bioremediation. The U removal ability of *Microbacterium* sp. Be9 strain was shown to be affected by the type of exogenous phosphates. While up to 88% of U was removed by the cells in a free phosphate system,

the amendment of organic or inorganic P led to a low U removal ranging between 10% and 23%. Further studies were undertaken to assess the impact of phosphate on U bioprecipitation by both strains. In the case of strain Be9, these results showed that the U interaction is a phosphate-dependent process: a high U bioprecipitation in absence of exogenous phosphates and a U solubilization in an inorganic phosphate-amended system. In presence of an organic phosphate source, the Be9 capacity for U precipitation decreased remarkably. A multidisciplinary approach (phosphatase activity determination, release of inorganic phosphates measurements, cell viability, etc.) was applied to confirm this variable behaviour of Be9 strain as function of phosphate substrate occurring. Firstly, Be9 cell surface was characterized by XPS (X-ray photoelectron spectroscopy) and potentiometric titrations to determine the functional groups involved in U bioadsorption. Be9 cell surface showed a high proportion of polysaccharides and a net negative charge, facilitating the  $\text{UO}_2^{2+}$  ions adsorption, and possibly, being responsible of the bioaccumulation process detected. This mechanism consisted of a first phase (fast and passive), where U adsorbs to the cell surface, and secondly, a slow active phase consisting on the intracellular U phosphate biomineralization. However, no relevant phosphatase activity was detected in Be9 strain, remaining unclear the key process for the detected biomineralization. U phosphates location was observed by HAADF-STEM (High-Angle Annular Dark-Field Scanning Transmission Electron Microscopy) and EDX (Energy Dispersive X-Ray) analysis. Depending on the treatment, the phosphate precipitates were observed intra or extracellularly.

In contrast, *Stenotrophomonas* sp. Br8 strains showed high phosphatase activity that leads to the release of orthophosphates in presence of glycerol-2-phosphate (G2P), resulting in a high U biomineralization ability (removal of 90-95% of soluble U). U phosphates were precipitated as needle-like fibrils on the cell surface and extracellular space, as observed by STEM (Scanning Transmission Electron Microscopy). These results are supported by EXAFS (Extended X-Ray Absorption Fine Structure) spectroscopy and XRD (X-Ray Diffraction) analyses which showed that local structure of U precipitates was similar to meta-autunite ( $\text{Ca}(\text{UO}_2)_2(\text{PO}_4)_2 \cdot 6\text{H}_2\text{O}$ ). This U mineral phase has been extensively studied, being characterized by its high stability over time. High U biomineralization capacity by Br8 strain was also detected under different conditions of pH (pH 5 and 8), temperature (15 and 37 °C), etc., demonstrating a great remediation potential under changing environmental conditions. Therefore, *Stenotrophomonas* sp. Br8 was selected to design a U remediation

## SUMMARY

strategy, mediated by a process of biomass immobilization, due to its high phosphatase activity and metabolic versatility against environmental changes, being capable of precipitating the soluble metal as U phosphates.

Finally, a procedure for biomass immobilization of Br8 strain in an inorganic matrix was optimized to provide protection to the cells, facilitate their handling and make the process more convenient for its future use in the remediation of U at large scale. Several immobilization matrices were characterized (alginate beads, TEOS (Tetraethyl orthosilicate) matrix and a hybrid matrix) through a multidisciplinary approach [HAADF-STEM, ESEM (Environmental Scanning Electron Microscopy), FTIR-ATR (Fourier Transform Infrared Spectroscopy with Attenuated Total Reflectance), etc.]. Alginate beads were selected as the best immobilization material, due to its biocompatibility with Br8 cells and highly porosity. Beads doped with Br8 biomass were tested with real U-contaminated water in the presence of G2P, as organic phosphate substrate, to release orthophosphates as a result of Br8 phosphatase activity. These experiments resulted in high U precipitation rates (around 98%) after 72h of incubation. In addition, experiments for the optimization of biomass concentration in the beads and beads storage conditions were conducted. Results on U elimination kinetics tests and HAADF-STEM/ESEM analyses indicated that the U precipitation by immobilized cells was a biphasic process that combines a first passive sorption of U on the beads surface or Br8 cells, and a second slower active biomineralization phase, as it was observed for Br8 planktonic cells and U.

In conclusion, this study revealed that U removal from complex mining waters using alginate beads doped with *Stenotrophomonas* sp. Br8 cells is a promising U bioremediation strategy, even at high U concentrations. The U removal from synthetic solutions has been extensively studied, however, the U immobilization from real mining wastewater remains relatively unexplored so far. Therefore, the U precipitation as uranyl phosphate in real mining water supposes an outstanding result with a high environmental relevance for the development of future sustainable bioremediation strategies. Further research should focus on the scale-up of this process, increasing the assayed volumes and the metal elimination rates, in order to design eco-friendly water treatment stations.

# INTRODUCCIÓN



## INTRODUCCIÓN

**Uranio: Propiedades físico-químicas, fuentes naturales y antropogénicas, y usos industriales.**

El uranio (U) es el elemento más pesado ( $Z = 92$ ) encontrado en la naturaleza, presente desde el origen de la Tierra al producirse de forma natural durante la formación de las supernovas. Con una densidad de  $19 \text{ g/cm}^3$ , el U fue descubierto por Martin Heinrich Klaproth en 1798, siendo uno de los primeros elementos en atribuírsele propiedades radiactivas gracias a los trabajos de Henry Becquerel en 1896 (Hopkins, 1923). Se trata de un elemento químico metálico, perteneciente a la serie de los actínidos, que puede caracterizarse como metal pesado, dúctil y ligeramente paramagnético (Meinrath et al., 2003; Rivas, 2005). En estado natural el U se encuentra compuesto por tres isótopos:  $^{238}\text{U}$ ,  $^{235}\text{U}$  y  $^{234}\text{U}$ , siendo todos ellos radiactivos (Meinrath et al., 2003) y presentando una vida media de aproximadamente  $4,4 \times 10^9$  y  $7 \times 10^8$  años los dos más abundantes ( $^{238}\text{U}$  y  $^{235}\text{U}$ ) respectivamente (Kathren, 2001). La presencia natural de U en el medio ambiente contribuye a bajos niveles de radiación de fondo en forma de emisiones alfa o beta e incluso, en el caso de algunos isótopos, de radiación gamma de energías variables (Hopkins, 1923). Cada gramo de U natural está constituido por entre un 99,2739 – 99,2752 % de  $^{238}\text{U}$ , 0,7198 – 0,7202 % de  $^{235}\text{U}$  y 0,0050 – 0,0059 % de  $^{234}\text{U}$ . A pesar de este balance, en la naturaleza puede existir un desequilibrio entre  $^{238}\text{U}/^{235}\text{U}$  debido a la descomposición del  $^{238}\text{U}$ , aumentando la disponibilidad de  $^{235}\text{U}$  y su transporte a través de procesos geológicos. Algunas mediciones muestran que la *ratio*  $^{238}\text{U}/^{235}\text{U}$  no es proporcional (Weyer et al., 2008), debido principalmente a la acción química y física del agua. Estos procesos pueden alterar el balance presente de isótopos de uranio en suelos, aire y agua.

El U presenta cuatro estados de oxidación, siendo los más predominantes y estables el estado oxidado (VI) y el estado reducido (IV). El estado de oxidado VI forma principalmente compuestos y especies solubles y, por tanto, más móviles y tóxicas, capaces de incorporarse con mayor facilidad en organismos vivos. Este estado del U es capaz de provocar un mayor daño oxidativo en el ADN, causando efectos genotóxicos a largo plazo como mutagénesis, carcinogénesis y otras patologías (Gudkov et al., 2016). Por otro lado, el estado de reducido IV domina en formas insolubles y menos móviles, siendo especialmente estable como uraninita mineral ( $\text{UO}_2$ ) en condiciones anóxicas.

La abundancia natural de U en la corteza terrestre se estima entre 2 – 4 ppm, y está ampliamente distribuido en rocas, suelos y aguas (Gavrilescu et al., 2009; Stegnar and

## INTRODUCCIÓN

Benedik, 2001). Normalmente se detecta a bajos niveles en una amplia variedad de minerales, siendo mayor su concentración en minerales ácidos que básicos (“NCRP report 77: Exposure from the uranium series with emphasis on radon and its daughters,” 1987). Esta abundancia en suelos se puede ver aumentada a consecuencia de fenómenos naturales, tales como las erupciones volcánicas. Los minerales de U más comunes son la uraninita ( $\text{UO}_2$ ) y la coffinita ( $\text{USiO}_4$ ), mientras que la carnotita  $\text{K}_2(\text{UO}_2)_2(\text{VO}_4)_2 \cdot 3\text{H}_2\text{O}$  o la autunita  $\text{Ca}(\text{UO}_2)_2(\text{PO}_4)_2 \cdot 10\text{-}12\text{H}_2\text{O}$  existen como minerales polimetálicos secundarios. Además, en los últimos años se han identificado formas diferentes a la uraninita como  $\text{U}_2\text{O}(\text{PO}_4)_2$ ,  $\text{CaU}(\text{PO}_4)_2$  y  $\text{U}_2(\text{PO}_4)(\text{P}_3\text{O}_{10})$  (Bargar et al., 2013). Una concentración de U de aproximadamente  $10^{-7}$  g/g se localiza en océanos, plantas y animales debido a la solubilidad del estado oxidado (VI) y a su continua liberación causada por procesos geoquímicos (Frontasyeva et al., 2001). La redistribución de este elemento en el ambiente ocurre de forma natural en estos ciclos biogeoquímicos, comenzando por la meteorización química de las rocas en superficie y continuando su movilización en aguas subterráneas y superficiales. En aguas, la naturaleza del U puede variar en función del potencial redox existente. Aguas anóxicas, cuyo potencial redox es bajo, presentan una mayor cantidad de  $\text{U}^{4+}$  y/o  $\text{UO}_2^+$  debido a su estado de oxidación. Estos estados del U tienen una alta tendencia a precipitar y permanecer inmóviles (Ivanovich and Alexander, 1987). En aguas óxicas el U domina en forma  $\text{UO}_2^{2+}$  creando complejos iónicos y/o neutros solubles, altamente móviles, que juegan un papel importante en el transporte de U durante la meteorización (Ivanovich and Harmon, 1992). La concentración media de U en ríos se estima en  $0,4 \mu\text{g L}^{-1}$ , pero puede variar en función de diferentes factores como el tiempo de contacto con estratos ricos en U, la tasa de evaporación o la disponibilidad de iones complejos (Ivanovich and Harmon, 1992). En mares y océanos la concentración de U aumenta debido a la salinidad, alcanzando una media de  $3,3 \mu\text{g L}^{-1}$ , siendo la afluencia de los ríos el principal aporte de este elemento. La erosión costera y el desprendimiento de partículas procedentes de glaciares también pueden llegar a aportar alrededor de 76.000 toneladas (t) de uranio al año.

Además de estas fuentes naturales, la presencia de U puede verse incrementada debido a diversas actividades antropogénicas. Mientras que los ciclos geoquímicos naturales del U son responsables de gran parte de su redistribución, estos procesos humanos pueden liberar grandes cantidades del metal pesado en localizaciones concretas. Entre estas fuentes antropogénicas destacan las implicadas en el ciclo del combustible nuclear, como la minería

de U y su molienda (o *milling*), la conversión del U y la elaboración de combustible. También la fabricación y uso de fertilizantes de fosfato o la combustión de combustibles fósiles (como el carbón) pueden contribuir al aumento de la presencia de U. Estos procesos generan compuestos con diferentes concentraciones de U, principalmente en forma sólida o líquida, que terminan acumulándose en el medio ambiente si no se controlan. Ya que este tipo de contaminación va ligada a lugares e industria específicos, conlleva una mayor preocupación para su acondicionamiento, tratamiento, almacenamiento y eliminación de forma segura.

El principal uso del U es su aplicación como combustible en centrales nucleares, las cuales está equipadas mayoritariamente con reactores de agua a presión o PWR (*Pressurized Water Reactor*). Otros reactores como los BWR (*Boiling Water Reactor* o reactores de agua en ebullición), RBMK (*Reactor Bolshoy Moshchnosty Kanalny* o reactor de canales de alta potencia) o CANDU (*Canada Deuterium Uranium*) son ampliamente utilizados por diferentes países. En todos ellos, se genera energía mediante la fisión de uranio enriquecido, el cual presenta una mayor proporción de  $^{235}\text{U}$  (entre el 3 - 5%). Este isótopo es fisil al ser atacado por neutrones libres debido a su configuración atómica. Actualmente, la energía nuclear supone el origen del 10% de la electricidad generada a nivel mundial (NEA/IAEA, 2020). El funcionamiento de dichas instalaciones consiste en la generación de calor mediante la fisión del  $^{235}\text{U}$  para aumentar la temperatura del agua y emitir vapor de agua. Para la obtención de este mayor porcentaje de  $^{235}\text{U}$  se requieren procesos de enriquecimiento del dióxido de uranio extraído naturalmente. Como desecho de estas reacciones y de su enriquecimiento se genera uranio empobrecido, el cual presenta una proporción menor a la natural de  $^{235}\text{U}$ . Este es la principal materia prima para la producción de armamento militar, como modelos especiales de munición o blindajes de alta resistencia, gracias a su alta densidad (Bleise et al., 2003). Además, el U en forma metálica presenta aplicaciones en el diagnóstico y la terapia de ciertas enfermedades, al ser usado como blanco en pruebas de rayos X de alta energía. Por otra parte, el largo período de semi-desintegración del  $^{238}\text{U}$  es una característica que permite usar ese isótopo en la estimación y datación de la edad de materiales, restos orgánicos, depósitos de minerales, etc. Asimismo, el U aparece en fertilizantes de fosfatos debido al mineral usado en su fabricación, el cual presenta altas cantidades de este metal pesado (Bleise et al., 2003).

### **Minería de U y la contaminación medioambiental asociada**

La cadena de producción del combustible nuclear está compuesta por una serie de fases, tanto de tratamiento previo del U para su uso como combustible, como de tratamiento a *posteriori* para acondicionar y gestionar los residuos producidos de forma segura. El primer paso para la utilización del U es su extracción desde los recursos naturales disponibles, lo que se realiza a través de la minería de U. Para localizar zonas ricas en minerales de uranio se emplean técnicas geofísicas mediante las que se estiman las cantidades disponibles. El U tiende a concentrarse en rocas ígneas y silíceas, y a niveles de menor concentración en rocas máficas, pero procesos de meteorización y metamorfismo pueden aumentar la concentración de este metal en el medio (Plant et al., 2019). Actualmente los depósitos de U están clasificados en 14 categorías diferentes en función del entorno geológico en el que se encuentran y la importancia económica (NEA/IAEA, 2020). Los minerales uraníferos presentes en estos depósitos naturales dependen del entorno geológico en el que se han formado. El mineral de U más común y de mayor importancia económica es la uraninita  $UO_2$  (Finch and Murakami, 1999), además de la coffinita  $USiO_4$ , la branerita  $U(Ti,Fe)_2O_6$  y varios productos de alteración de estos minerales. El U también se puede encontrar en bajas proporciones en depósitos de minerales de fosfato en sistemas acuáticos, como la autunita  $Ca(UO_2)_2(PO_4)_2 \cdot 10-12 H_2O$  o la zeunerita  $Cu(UO_2)_2(AsO_4)_2 \cdot 12 H_2O$  (Meinrath et al., 2003). Estos sedimentos, al ser usados en la producción de ácido fosfórico en fertilizantes, son los responsables de la presencia del metal en estos productos químicos y en las plantas que los procesan (Bleise et al., 2003). En formaciones naturales de minerales de U pueden encontrarse trazas de otros elementos como Pb, Ca o Th (Finch and Murakami, 1999), pudiendo formar agregados sólidos y causar metamictización en presencia de altas concentraciones de minerales ricos en Ce y Zr (McGloin et al., 2016). Actualmente, los recursos de U conocidos y disponibles a nivel mundial se estima que se agotarían en un tiempo máximo de 85 años, aunque, según la evidencia geológica, se considera que los niveles de minerales de U disponibles para su explotación son mayores de los considerados en estas estimaciones. Este hecho, sumado a los avances en tecnología nuclear que están siendo desarrollados, que permitirían una optimización en la utilización de los recursos, se piensa que las reservas aumentarían su duración hasta unos 2550 años (NEA/IAEA, 2020).

Existen distintos tipos de actividades mineras para extraer U que han ido variando a lo largo de su historia en función de la productividad, costes y disponibilidad:

a. Minería a cielo abierto (*open-pit*):

Se lleva a cabo en aquellas explotaciones mineras que se desarrollan a nivel de la superficie del suelo debido a la proximidad de los depósitos. Mediante el empleo de maquinaria o explosivos se eliminan las capas que recubren el yacimiento de los minerales para dejarlos descubiertos y accesibles. La rentabilidad de este sistema de minería es dependiente del afloramiento de los depósitos, ya que cuanto más cerca de la superficie se encuentren mayor será su extracción y menor su coste. Es uno de los sistemas históricamente más usados y, actualmente, supone a nivel mundial el 16,1% de los métodos de extracción de uranio (NEA/IAEA, 2020). Este tipo de minería se considera rentable gracias al uso de equipos de alta capacidad, pero generalmente produce grandes cantidades de rocas de desecho y minerales de baja ley (aquellos con bajas concentraciones del metal objetivo). El almacenamiento de estos residuos requiere de zonas protegidas y vertederos bien diseñados, siendo usadas las propias minas, en algunas ocasiones, para el almacenamiento de relaves (Falck, 2015).



**Figura 1.** Mina a cielo abierto de uranio en el noroeste de Níger (Foto de ORANO). Fuente: *Mining.com* (<https://www.mining.com/web/arevas-niger-uranium-mines-cut-staff-slash-production-union>).

## INTRODUCCIÓN

### b. Minería subterránea:

Son aquellas explotaciones mineras que se desarrollan por debajo de la superficie a través de galerías o túneles. La realización de este tipo de actividad depende de la localización del yacimiento y su facilidad de extracción. Actualmente alcanza el 31,9% de la distribución mundial de métodos de extracción de uranio, a pesar de ser uno de los sistemas más caros y de mayor riesgo. Este es el caso, principalmente, de las minas subterráneas canadienses, donde se extraen minerales de U altamente concentrados (contienen 50 veces más U por kilogramo que minerales de Australia y 1000 veces más que minerales de África (NEA/IAEA, 2020)).



**Figura 2.** Galería de la mina *Olympic Dam* en Roxby Downs, Australia. Fuente: *Mining News.net* (<https://www.miningnews.net/politics/news/1389002/approvals-for-olympic-dam-expansion-to-be-fast-tracked>).

### c. In Situ Recovery (ISR):

El método ISR para la recuperación de U (también conocido como ISL; *In Situ Leaching*) consiste en la perforación de pozos en los yacimientos de minerales de U y el bombeo de soluciones de lixiviación a través de estos. De este modo, dicha solución disuelve el mineral, recuperándolo mediante pozos de producción y extrayendo el U en solución en una planta de superficie. La solución de lixiviación penetra en los minerales debido tanto a la propia porosidad natural de la roca como a la porosidad generada por la disolución del mineral (lixiviación ácida), o bien por la fragmentación artificial (mediante explosivos o presión hidráulica). La solución de lixiviación usada puede ser tanto alcalina como ácida, dependiendo de las propiedades mineralógicas y geoquímicas del depósito del que se quiera



extraer. Este proceso permite la recuperación de U directamente desde el mineral sin necesidad de métodos tan destructivos como la minería a cielo abierto o subterránea. Actualmente se está estudiando la diversidad microbiana presente en estos acuíferos ya que dichos microorganismos pueden alterar los ciclos biogeoquímicos del U y, por tanto, modificar la movilidad del metal (Jroundi et al., 2020). En las dos últimas décadas este tipo de minería se ha vuelto cada vez más importante, siendo en la actualidad el principal método de extracción de U. A nivel mundial supone un 57,4% de los diferentes métodos de minería (NEA/IAEA, 2020). Actualmente, la minería ISR se está utilizando únicamente para extraer U en depósitos de arenisca (NEA/IAEA, 2020).

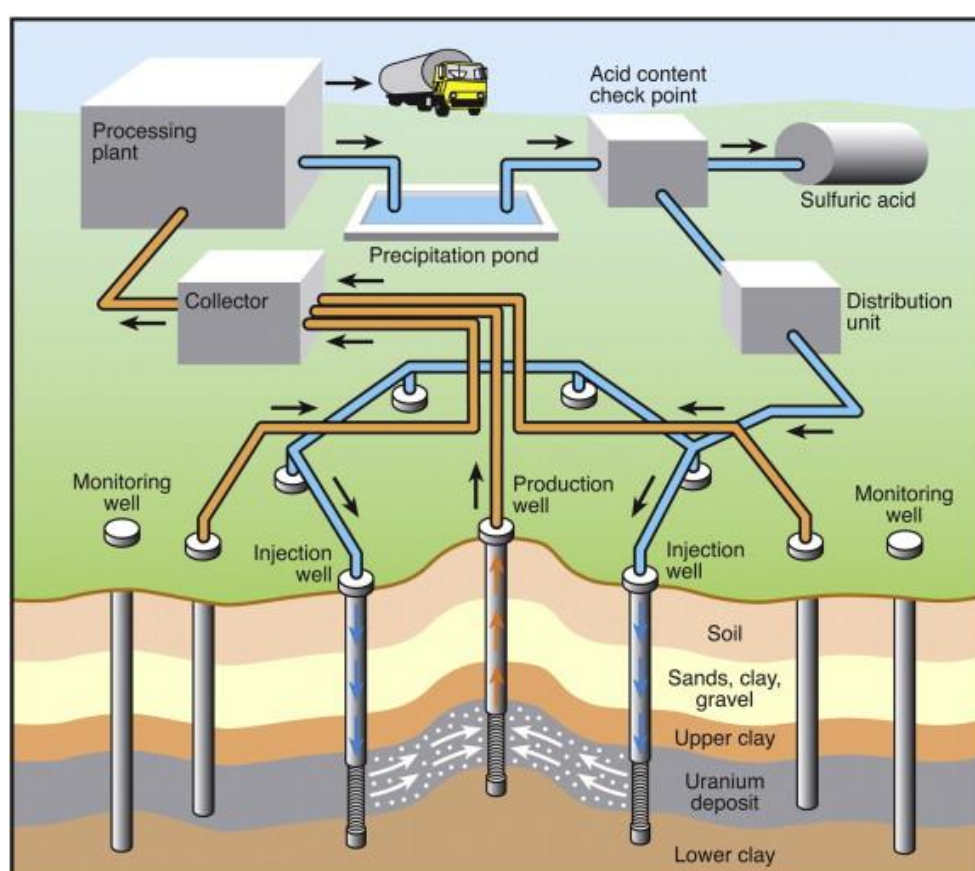


**Figura 3.** Esquema de la recuperación de U mediante ISR (Zammit et al., 2014).

d. Heap Leaching y biolixiviación:

*Heap Leaching* o “Lixiviación en pilas/columnas” consiste en la recolección de U mediante la trituración del mineral que lo contiene y su colocación en sistemas de contención para, posteriormente, rociar soluciones lixivadoras o usar reacciones *in situ* (reacciones de biolixiviación como la oxidación bacteriana para producir ácido sulfúrico). De este modo se moviliza el componente y se transporta por un circuito de concentración. Esta técnica se



## INTRODUCCIÓN

aplica fundamentalmente a minerales de U, Cu y Au, ya que presentan buena permeabilidad y son fácilmente solubles. Este tipo de extracción se encuentra ligada tanto a la minería a cielo abierto como subterránea, al ser complementaria con la recolección de minerales de baja ley. Estos tipos de minería, que además practican operaciones de *Heap leaching*, han sufrido un enriquecimiento natural de microorganismos con el paso del tiempo, debido a la exposición al aire, humedad y lluvia. Este enriquecimiento microbiano supone una mejora en el rendimiento de la lixiviación, y esta mejora, gracias al uso de microorganismos, fue estudiada y comenzó a aplicarse en minas de uranio en los años 50 y 60 (Bryner et al., 1954; Razzel and Trussell, 1962). No obstante, a nivel mundial, la extracción de U mediante esta técnica únicamente supone el 0,2% del total de su extracción (NEA/IAEA, 2020).

### e. Otros métodos:

Además de los métodos convencionales (minería a cielo abierto y subterránea) y de técnicas más novedosas (ISR o *Heap Leaching*), mediante las que el U se extrae como producto primario o como un subproducto de relevancia, existen técnicas no convencionales con las que el U se puede extraer como un subproducto menor. Entre estas destacan el U obtenido al encontrarse asociado a minerales de fosfato (posteriormente usados en la fabricación de fertilizantes de fosfatos (Bleise et al., 2003)), rocas no ferrosas, lutita negra o lignita. Además, en los últimos años se están estudiando nuevas fuentes de U, como es el caso del agua oceánica, en la que se estima que se concentran unos 4 billones de toneladas de U (Dungan et al., 2017).

Debido al aumento de las centrales nucleares y la creciente necesidad del uso de la energía nuclear se estima que la producción de U a lo largo del mundo aumente año tras año. Aproximadamente 10 países son los principales responsables de la producción de U en el mundo, siendo Kazajstán, Australia y Canadá los tres mayores representados, aproximadamente, el 63,5 % de la producción mundial (Zammit et al., 2014). Informes de la Agencia de Energía Nuclear (NEA) y la Agencia Internacional de Energía Atómica (IAEA) estiman los porcentajes de la producción de U mundial de los siguientes países, que suponen el 98% del total, en: Kazajstán (40,6%), Canadá (13,1%), Australia (12,2%), Namibia (10,3%), Uzbekistán (6,4%), Níger (5,4%), Rusia (5,4%), China (3,0%), Ucrania (1,5%) e India (0,7%) (NEA/IAEA, 2020). En la Unión Europea, la producción primaria

de U en 2016 se realizó, exclusivamente, por parte de la República Checa, mientras que países como Francia, Alemania y Hungría produjeron cantidades menores únicamente a partir de actividades de remediación de minas. La producción total de la UE se ha ido reduciendo a lo largo de los años, desde las 272 t de U en 2014, 190 t de U en 2016 hasta 39 t de U en 2018 (NEA/IAEA, 2020). Esta disminución se ha debido al descenso de la producción en República Checa, en su principal instalación Dolní Rozínka, como consecuencia del agotamiento de los recursos y al cierre definitivo en 2017 de la mina subterránea de Rozná (NEA/IAEA, 2020).

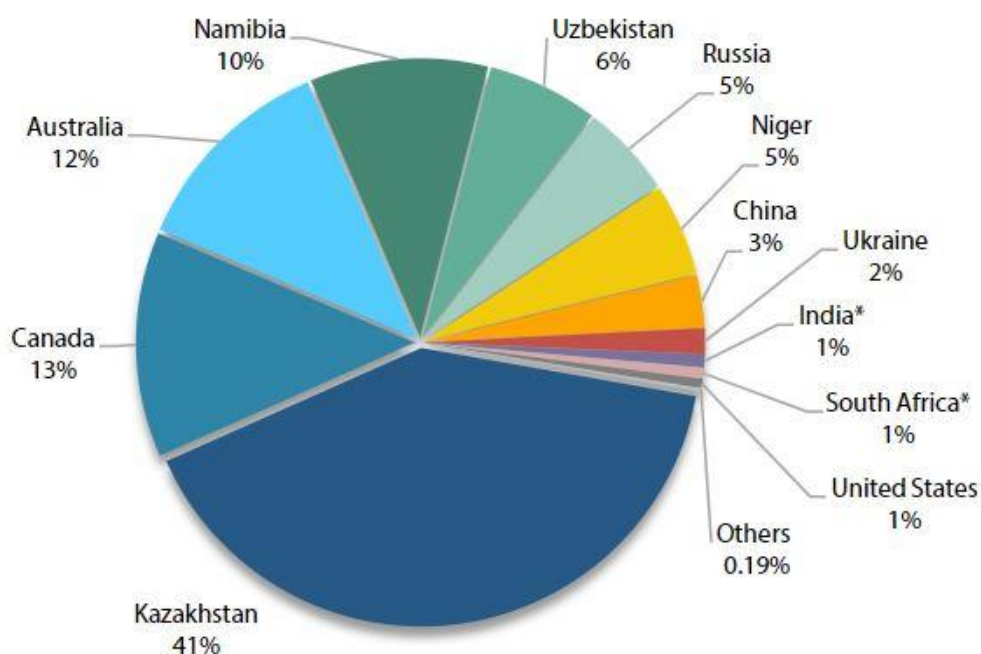


**Figura 4.** Producción mundial de U durante 2018 en los principales países productores (NEA/IAEA, 2020).

Existen diversas actividades, tanto antropogénicas como naturales, que provocan un aumento de los niveles de U en el medio ambiente, pudiendo llegar a producir problemas de contaminación. Procesos de lixiviación natural o meteorización de rocas y suelos de acuíferos movilizan el U de los minerales presentes. Pero las mayores concentraciones se alcanzan debido a la actividad humana. Antiguas localizaciones de pruebas nucleares (Child and Hotchkis, 2013) o vertidos de desechos de forma descontrolada son algunas de las causas de esta actividad humana. Debido a ello, tanto suelos como acuíferos contaminados con U se han convertido en la principal preocupación por la amenaza ecológica que suponen. Esta presencia de U provoca alteraciones en el ambiente, evitando

## INTRODUCCIÓN

que sea apto para los microorganismos, flora y fauna naturales. Además, la solubilidad del U y su presencia en formas móviles conlleva su incorporación en los organismos, provocando diversos efectos tóxicos y desequilibrios ecológicos al afectar las cadenas tróficas.

La minería de U y su molienda (o *milling*) se encuentra entre las actividades industriales que más atención han atraído a nivel mundial debido a su impacto en el medio ambiente. Sus procesos movilizan grandes cantidades del radionucleido, además de otros elementos tóxicos, siendo liberados a la hidrosfera y suelos. Muchas instalaciones antiguas de producción, a menudo abandonadas, necesitan de medidas de corrección para minimizar sus efectos ambientales dañinos. Para aquellas que aún se encuentran en funcionamiento se están realizando mejoras en sus métodos de producción y en la planificación de su desmantelamiento al terminar su “vida útil”. Dependiendo del tipo de minería que se realice, el impacto ambiental que produce varía (Benes, 1999). La minería a cielo abierto se caracteriza por un mayor impacto debido a una gran alteración del terreno, destruyendo la flora presente y cambiando de posición grandes cantidades de tierra y minerales, y permitiendo el acceso de aire y agua a las superficies ahora descubiertas. El proceso de desmantelamiento de estas minas suele consistir en rellenar los terrenos alterados con los relaves o rocas de desecho producidas en la propia extracción, o inundando toda la zona tratada (Benes, 1999). En la minería subterránea se extraen grandes cantidades de rocas y minerales de desecho, que se almacenan o son utilizados con otra finalidad. A menudo son usadas para rellenar galerías o pozos, evitando así el colapso de estos. Durante su almacenamiento en el exterior, altas cantidades de radionucleidos y elementos tóxicos pueden ser lixiviados de forma natural mediante la lluvia o el viento, al arrastrar las partículas más pequeñas. El caso del ISR se considera la técnica de extracción que menos impacto ambiental genera. Al no extraer directamente ni transportar el mineral de U evita la contaminación de las aguas y suelos cercanos. Las zonas más cercanas a los pozos de bombeo/extracción pueden contaminarse debido al derrame accidental del lixiviado. Algunos estudios han señalado que suelos de zonas próximas a los pozos de extracción pueden alcanzar altas concentraciones de U y Ra (Benes, 1999; Gallegos et al., 2015).

**Diversidad microbiana de ambientes contaminados con radionucleidos.**

La presencia de bajas concentraciones de metales esenciales es indispensable para la vida y actividad de los organismos. Sin embargo, la acumulación de metales pesados en altos niveles es perjudicial tanto para el medio ambiente como para la salud humana. Se ha observado que los microorganismos que habitan en zonas naturales de alta concentración de U (además de otros radionucleidos) se encuentran bien adaptados a las condiciones de estrés y juegan un papel importante en el ciclo biogeoquímico de dichos elementos (Choudhary and Sar, 2015). Pueden tomar parte, entre otras funciones, en los procesos de humificación, degradación de contaminantes o en el mantenimiento de la estructura del suelo. Estos microorganismos pueden usarse como indicadores del estrés ambiental presente (Bano et al., 2018). En concreto, la investigación sobre las comunidades bacterianas y su diversidad en ambientes contaminados con U no solo ayudará a comprender las características bacterianas en presencia de este metal pesado, sino que también planteará nuevas posibilidades de biorremediación de estas zonas contaminadas con U. En los últimos años las técnicas de secuenciación de última generación se han utilizado en la investigación sobre microbiomas y diversidad microbiana (Hao et al., 2021; Jroundi et al., 2020, 2022; Povedano-Priego et al., 2019; Qi et al., 2022), al poder obtener una enorme cantidad de secuencias en poco tiempo. Tanto suelos como aguas son los principales focos de estudio de la diversidad bacteriana ya que son los ecosistemas donde las formas móviles del radionucleido afectan en mayor medida.

En suelos, conocer la diversidad microbiana puede servir de diagnóstico de la calidad de los mismos. Al llevar a cabo un monitoreo de los suelos a lo largo del tiempo, y estudiando los indicadores microbianos, se puede comparar el estado previo y posterior a la contaminación (Tang et al., 2019). En general, los suelos con mayor abundancia o actividad bacteriana presentan mejores funciones y, por tanto, mejor calidad. A lo largo de los últimos años se ha comprobado que la actividad y diversidad bacteriana se ve afectada en zonas contaminadas con U (Islam and Sar, 2011; Yan and Luo, 2015), llegando en algunos casos concretos a reducir la biodiversidad hasta un 66% (Kenarova et al., 2010). En antiguas minas de U se ha observado que la diversidad bacteriana es específica de esas zonas (Kenarova et al., 2014). Algunos estudios indican que la presencia de bacterias reductoras y oxidantes de hierro son abundantes en muestras de suelos con altos niveles de U (Mondani et al., 2011). Otras investigaciones también han destacado la presencia del género *Proteobacteria* como el dominante en relaves de minas de U (Yan and Luo, 2015).

## INTRODUCCIÓN

En aguas, las comunidades microbianas presentan amplias diferencias en función de numerosos factores. En este medio, el U y sus formas más solubles dependen en gran medida del pH, las concentraciones de solutos, el estado redox del medio y la conductividad, entre otras propiedades (Ivanovich and Harmon, 1992). También difieren debido a la procedencia del agua (salada o dulce) o a la propia localización (como pueden ser lagos (Edberg et al., 2012) o aguas subterráneas (Cho et al., 2012)). Al igual que en otros ambientes, la diversidad microbiana decrece en relación a los niveles de contaminación de U; cuanto mayor son las concentraciones de este metal, menores son los índices de diversidad microbiana (Cho et al., 2012; Dhal and Sar, 2014; He et al., 2018). Algunos estudios han señalado que la radiación en un medio oligotrófico conduce a una presión selectiva que adapta a ciertas bacterias, alterando significativamente la riqueza, diversidad y abundancia en ese entorno (Tišáková et al., 2013). Esta diversidad reducida sugiere que aquellas bacterias que sobreviven en aguas altamente contaminadas pueden usar dichos contaminantes en sus procesos celulares o expresar mecanismos de defensa contra ellos (Cho et al., 2012). Algunos análisis de la comunidad bacteriana presente en acuíferos contaminados con U han mostrado el predominio de los géneros *Desulfococcus*, *Desulfobacterium* y *Desulfovibrio* (Zhang et al., 2017). Otros estudios, llevados a cabo en sedimentos con altas concentraciones de U señalan a los géneros *Geobacter*, *Geothrix*, *Dyella*, *Bacteroidetes* y *Chloroflexi* como los más dominantes (Sutcliffe et al., 2017). Otros géneros, como *Arthrobacter* y *Microbacterium* también han sido identificados en áreas contaminadas con metales pesados, siendo conocidos por eliminar grandes cantidades de U en ambientes cuya concentración es alta (Islam and Sar, 2016). Ciertos miembros del subfilo *Acidobacteria* son encontrados frecuentemente en suelos contaminados con radionucleidos, ya que toleran condiciones extremas como pH ácidos o limitación de nutrientes (Kielak et al., 2016; Mumtaz et al., 2018).

### **Interacciones microbianas con U**

Dado que numerosos microorganismos son capaces de sobrevivir en condiciones de altas concentraciones de U, el estudio y comprensión de los mecanismos e interacciones que se producen serán útiles para desarrollar una remediación adecuada y un plan de gestión a largo plazo para los sitios contaminados con U. Estas bacterias han sido aisladas en numerosos trabajos, demostrando una alta tolerancia al U (Banala et al., 2021b; Gallois et

al., 2018; Gerber et al., 2018; Khare et al., 2022; Sánchez-Castro et al., 2017; Sowmya et al., 2020). Los principales mecanismos que expresan frente al U son la biosorción, biomineralización, bio-reducción y la bioacumulación intracelular.

- a. **Biosorción:** este proceso consiste en interacciones fisicoquímicas entre los iones metálicos y las superficies celulares uniéndose, mediante los ligandos presentes en dichas superficies, los iones disueltos en las soluciones acuosas (Prakash et al., 2013; Volesky and Holan, 1995; Xu et al., 2020). Este es un proceso pasivo debido, fundamentalmente, a las diferencias de cargas entre la superficie bacteriana (negativa) y la de los metales (positiva), pudiendo producirse tanto en microorganismos vivos como muertos (Ayangbenro and Babalola, 2017). Al no requerir de rutas metabólicas estas uniones son rápidas y no dependientes de crecimiento, y presentan una alta eficiencia y selectividad para iones metálicos en un amplio rango de temperatura y pH (Kolhe et al., 2018). Esta interacción se puede producir directamente entre los grupos funcionales propios de las paredes bacterianas (grupos fosfato, carboxilo...) o indirectamente a través de componentes específicos (proteínas de la capa S, polímeros extracelulares, cápsulas bacterianas, etc...).

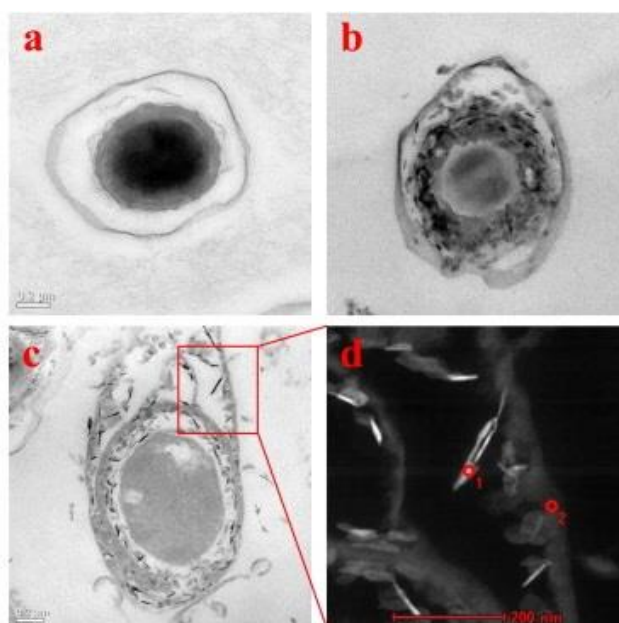


**Figura 5.** Imágenes TEM de la cepa *Bacillus* sp. dwc-2 sin tratar (a) y cargadas con U, provocando su biosorción (b–d) (Li et al., 2014).

## INTRODUCCIÓN

- b. Bioacumulación intracelular: este mecanismo consiste en la internalización de metales en el citoplasma de forma activa, es decir, dependiente de metabolismo. El proceso suele producirse en dos fases: en primer lugar, una unión rápida de los iones metálicos seguida de la acumulación, relativamente lenta, en el interior de la célula debido al transporte activo (Aksu and Dönmez, 2000; Gerber et al., 2016), el cual requiere de un mayor consumo energético. Con determinados metales esta captación puede producirse de forma accidental debido a la similitud entre el ion y los elementos esenciales necesarios para la bacteria. En el caso del U no se le conoce ninguna función biológica en el metabolismo de las células, por lo que se sugiere que su captación sea debida a la alteración de la permeabilidad de la membrana (Suzuki and Banfield, 1999) o a transportadores específicos del Fe (Gallois et al., 2018). Estudios transcriptómicos en presencia de U demuestran que ciertos genes relacionados con la resistencia al cobre y a la plata están involucrados en la bioacumulación de U por *Cupriavidus metallidurans* (Rogiers et al., 2022).

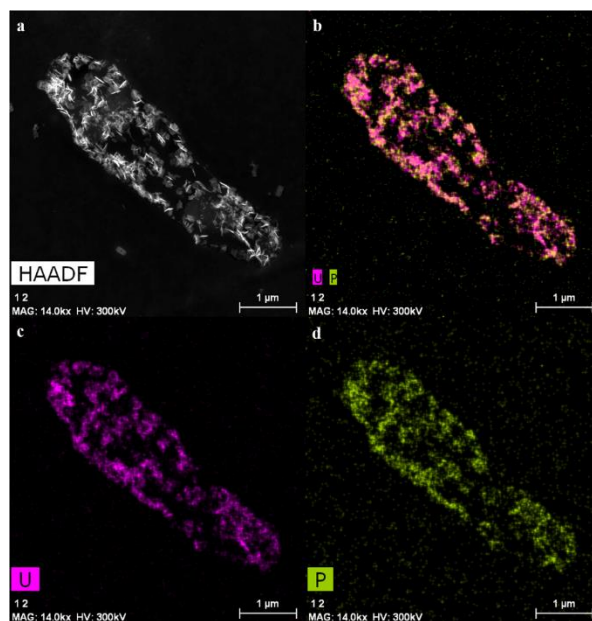


**Figura 6.** Imágenes HAADF-STEM de la bioacumulación de U en forma de fosfatos por parte de la cepa *Rhodosporidium toruloides* KS5 (Gerber et al., 2018).

- c. Bioreducción: mediante la actividad bacteriana se produce la inmovilización de los metales solubles en formas inmóviles debido a la alteración de sus estados de oxidación. Numerosas bacterias son capaces de usar directamente el U(VI) como aceptor final de electrones, reduciéndolo a U(IV) (Newsome et al., 2014), aunque

esta transformación también puede ocurrir de forma indirecta debido a la reducción metabólica del Fe(III) (Liger et al., 1999). La bioreducción ocurre principalmente con bacterias anaerobias de diversas especies a través de diferentes mecanismos que aún no han sido completamente descritos. Sobre todo, queda por aclarar la implicación que tienen elementos como los nanotubos o los citocromos (Newsome et al., 2014). En este sentido, bacterias del género *Thermus*, *Bacillus*, *Clostridium*, *Desulfovibrio* o *Geobacter* (Cason et al., 2012; Gao and Francis, 2008; Li et al., 2018) han sido estudiadas como reductoras de iones metálicos de U.

- d. Biomíneralización: este proceso consiste en la precipitación de los metales en forma de carbonatos, fosfatos e hidróxidos mediante ligandos generados por los microorganismos. Los complejos formados son insolubles, alterando la movilidad de los iones metálicos y reduciendo su toxicidad, pero sin cambiar el estado de oxidación del metal. La liberación de estos ligandos está mediada por la actividad enzimática bacteriana, entre la que destaca el papel de las fosfatasa. Estas se expresan de forma natural en las bacterias e hidrolizan compuestos de fosfatos orgánicos, liberando fosfato inorgánico (Pi). Numerosas bacterias aisladas de ambientes contaminados, o con altos niveles de U, expresan actividad fosfatasa, precipitando el metal como fosfatos de U (Huang et al., 2017; Merroun et al., 2011; Sánchez-Castro et al., 2020; Shukla et al., 2019). Esta precipitación suele producirse en forma de diferentes minerales compuestos por fosfatos de U, como la autunita, chernikovita o la uranfita. La inmovilización del U en minerales de fosfato es uno de los mecanismos más estudiados debido a su alta estabilidad al no ser susceptibles a cambios producidos por las condiciones redox del ambiente. También se ha demostrado la precipitación de U como minerales de carbonato en forma de calcita (Brook et al., 2001; Doudou et al., 2012).



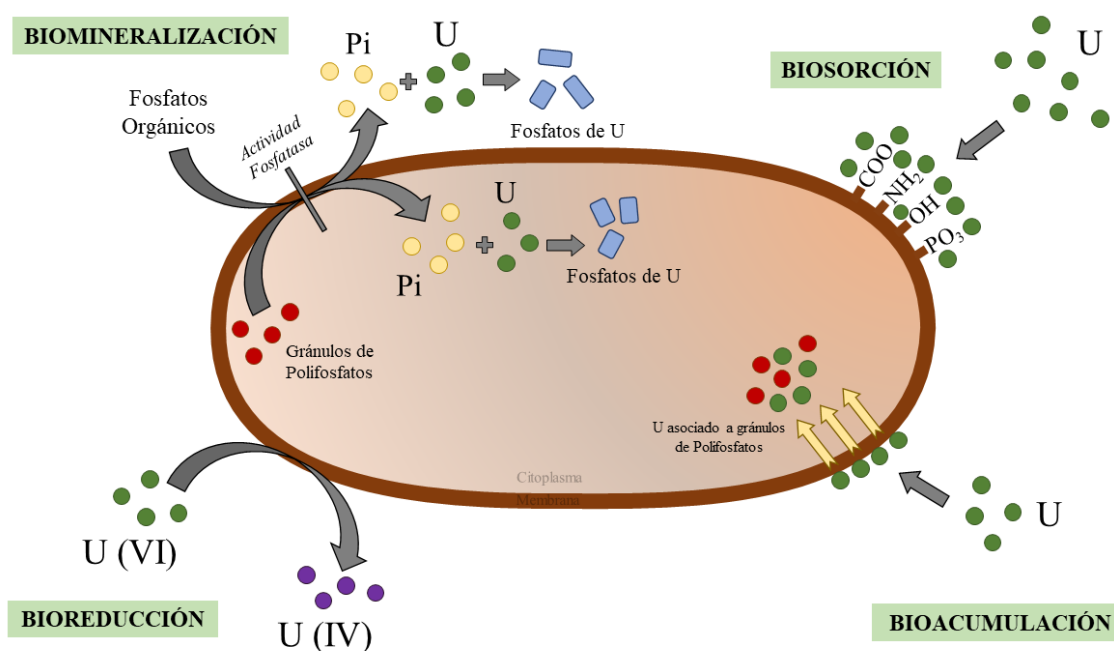


**Figura 7.** Esquema de las interacciones microbianas con el U

Estas interacciones entre los microorganismos y el U son los principales mecanismos en los que se basan las nuevas tecnologías de biorremediación, principalmente en la bioreducción y la biomineralización. La bioreducción de U(VI) ha demostrado ser una eliminación sostenida en ensayos de aguas subterráneas, pero, sin embargo, la estabilidad y perdurabilidad del U reducido sigue siendo cuestionable. Debido a numerosos factores ambientales (como el pH, hidrólisis, potencial redox o la formación de complejos) se puede provocar la reoxidación del U, devolviéndolo a un estado móvil (You et al., 2021). En comparación con la bioreducción, se ha ensayado la biomineralización en diversos entornos y en diferentes condiciones (distintos valores de pH, condiciones aeróbicas y anaeróbicas o una alta presencia de ácidos), lo que le permite ser una estrategia más versátil (Zhang et al., 2020). Aun así, ciertos inconvenientes, como el coste de las fuentes de fosfatos, han limitado la aplicación de esta técnica a escala de laboratorio. Para realizar ensayos a mayor escala es necesario elegir la técnica de tratamiento del U correcta, considerando tanto los factores ambientales como los económicos, a fin de lograr la mejor estrategia posible de inmovilización y eliminación (Wufuer et al., 2017).

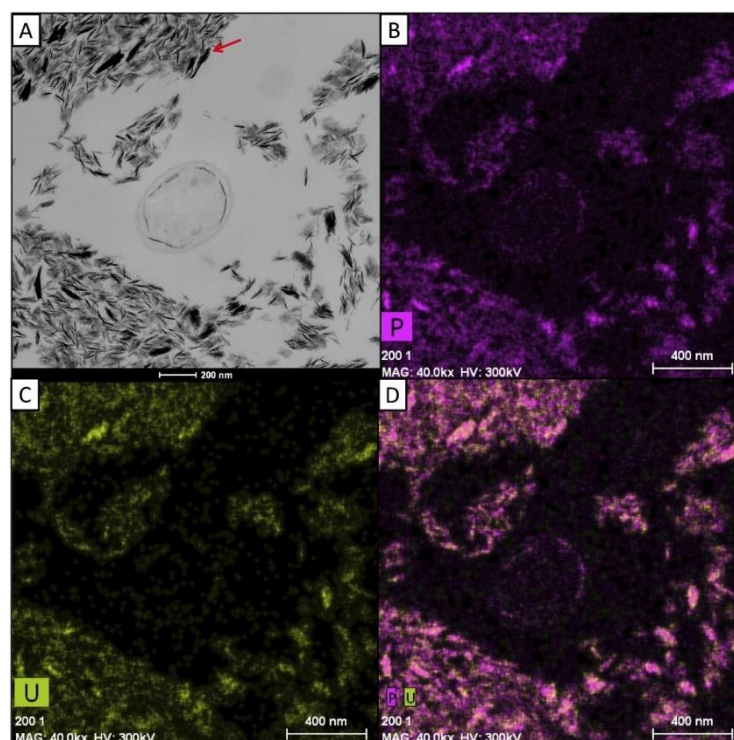


**Figura 8.** Bioprecipitación de U en el medio extracelular por células de *Stenotrophomonas bentonitica* BII-R7 tras su exposición al metal (Pinel-Cabello et al., 2021).

### **Biorremediación de U: fundamentos y tecnologías usadas a nivel mundial.**

La actividad humana aumenta constantemente debido al crecimiento de la población y de la industria asociada. Este tipo de industrialización, en especial la relacionada con el ciclo de la energía nuclear, puede conllevar a la contaminación de ciertos ambientes con altas concentraciones de U, ya sea accidentalmente o debido a la minería y su tratamiento. Elevados niveles de U pueden suponer un problema ambiental y para la salud humana debido a la presencia de compuestos de U solubles y móviles. A lo largo del tiempo se han utilizado diversas estrategias para abordar este problema, pero en los últimos años ha destacado el desarrollo de tecnologías basadas en el uso de microorganismos, lo que se conoce como la biorremediación. De hecho, la biorremediación se define como cualquier proceso que involucra al uso de organismos vivos (p. ej. microorganismos) o sus enzimas para reducir o eliminar contaminantes o toxinas presentes en suelos o aguas. En el caso del U, las interacciones biogeoquímicas desempeñan un papel muy importante en el balance de la especiación del metal y su movilidad, y, por tanto, de su toxicidad (Gudkov et al., 2016). El principal riesgo para los seres vivos es la inclusión de compuestos de U en el organismo, y este riesgo aumenta cuando estos compuestos son solubles. Por tanto, el uso

## INTRODUCCIÓN

de microorganismos y sus procesos metabólicos naturales como técnica de remediación de U es una estrategia prometedora que está siendo estudiada y desarrollada.

La biorremediación de U está basada en aquellos procesos metabólicos presentes en las bacterias capaces de reducir o inmovilizar el ion metálico, como la alteración de las condiciones redox o de pH, o la producción de ligandos o formas minerales. Todos ellos se producen debido a los mecanismos de interacción con U enumerados más arriba. Las técnicas de biorremediación, además de ser unas herramientas efectivas para contrarrestar los efectos nocivos del U, han surgido como alternativas más económicas que otros procesos fisicoquímicos (Lopez-Fernandez et al., 2020). Estos métodos tradicionales, basados en técnicas fisicoquímicas, como la precipitación, evaporación, extracción o lixiviación química, entre otros, son más costosos económica y ambientalmente. Hoy en día existe un mayor interés en la biorremediación bacteriana ya que aspira a reducir la contaminación mediante métodos más sostenibles y rentables (Kumar et al., 2016; Raghunandan et al., 2018).

Existen dos tipos generales de clasificación de biorremediación en función de su localización:

- *In situ*: Son aquellas técnicas que se realizan en el mismo lugar donde se detecta la contaminación. Con esta finalidad en ocasiones se estimula la propia biodegradación natural en suelos o aguas subterráneas únicamente aplicando oxígeno y nutrientes mediante sistemas de circulación. Estos sistemas de descontaminación son los más baratos y utilizan microorganismos no nocivos al usar la biomasa autóctona.
- *Ex situ*: Al contrario que en los procesos *in situ*, la contaminación es retirada de su lugar de origen y es tratada de forma externa. Estos procesos requieren de la excavación de los suelos o el bombeo de las aguas para aplicar el mecanismo de remediación, de modo que presentan mayores desventajas frente a otros métodos. Destacan el *landfarming* o las biopilas, ambos consistentes en la excavación de tierras contaminadas y su depósito como finas capas sobre diferentes tipos de aislantes, favoreciendo la actividad bacteriana.

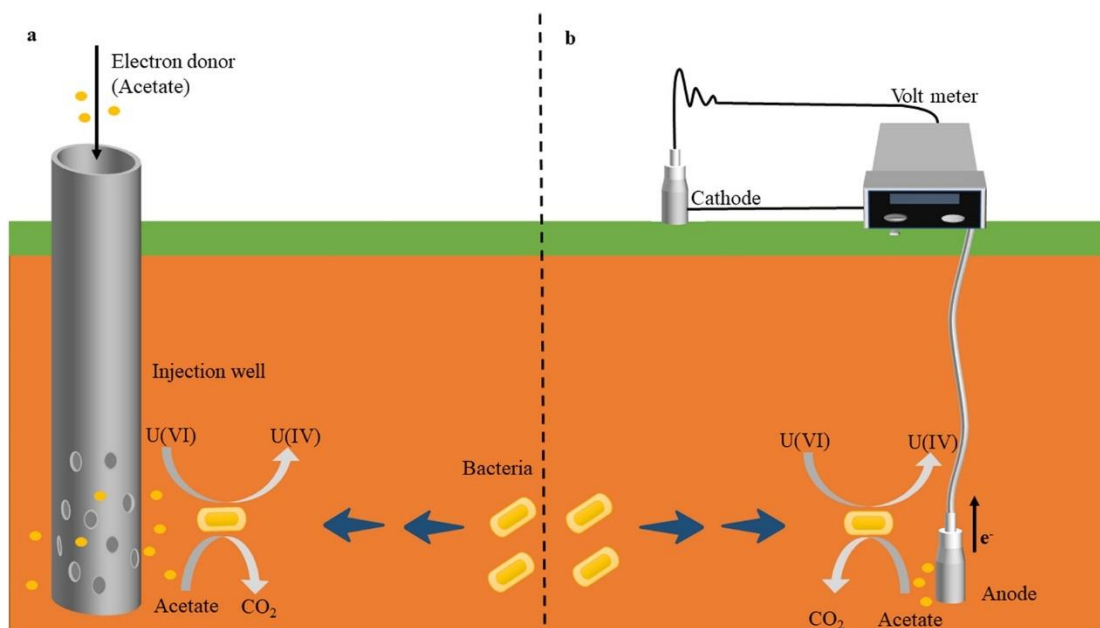


**Figura 9.** Esquema general de la biorremediación *in situ* de U mediante la introducción de compuestos orgánicos (p. ej. acetato) (You et al., 2021).

Dentro de estos casos existe otro tipo de clasificación según el modelo de comunidad microbiana usada:

- Atenuación natural (o bioatenuación): consistente en el efecto de procesos naturales (como la biodegradación, sorción, estabilización (bio)química... etc.) producidos por la propia comunidad microbiana existente en el lugar afectado por la contaminación. Esta biodegradación por parte de las comunidades microbianas autóctonas es considerada con frecuencia como la primera barrera y el mecanismo principal para la atenuación de los contaminantes. Sin embargo, suele ser un proceso de eliminación muy lento.
- Bioestimulación: mediante la adición de nutrientes específicos o la modificación de características fisicoquímicas del medio en la zona afectada (pH, oxígeno, temperatura... etc.) se provoca un aumento de la actividad de la comunidad microbiana autóctona. De esta forma se potencian los mecanismos existentes por parte de los organismos frente a los contaminantes, acelerando su eliminación.
- Bioaumentación: consiste en la adición de microorganismos o consorcios especializados en la degradación del contaminante. Estas cepas pueden ser tanto

## INTRODUCCIÓN

autóctonas como alóctonas o modificadas genéticamente, y permiten aumentar la capacidad de eliminación ya que poseen las características catalíticas deseadas.

Estos tres tipos han sido ampliamente estudiados en los últimos años frente a diferentes contaminantes (sobre todo hidrocarburos y residuos de refinerías) concluyendo, en la mayoría de los casos, que la combinación de dos o tres de las estrategias proporciona mejores resultados de eliminación (Agnello et al., 2016; Guarino et al., 2017; Roy et al., 2018; Varjani and Upasani, 2019). A nivel de aplicación industrial frente a contaminación de U los mecanismos de bioreducción y biomineralización son los más usados, gracias a su mayor efectividad en comparación con otros. La estabilidad a largo plazo de los compuestos formados es crucial para el éxito de la biorremediación *in situ*, ya que cuanto más insoluble es la forma del U es menos probable que se vuelva a movilizar. La bioreducción de U en ensayos de campo *in situ* se han demostrado con éxito a escala piloto (Maleke et al., 2015), aunque mantener bajos los niveles de concentración en aguas subterráneas durante largos periodos de tiempo requiere de un suministro continuo de donante de electrones. El buen funcionamiento dependerá de diferentes factores como el uso de un donador de electrones adecuado, la posible interferencia con otros procesos (como la reducción de nitratos, Fe(III), sulfatos) o la propia composición de la comunidad microbiana. Aunque el papel principal en la bioreducción de U se atribuye normalmente a los microorganismos más predominantes en el medio, un componente de menor abundancia puede ser lo suficientemente importante en dicho proceso para alterarlo (Williams et al., 2013). Algunos estudios han demostrado que, aunque se consideren radiotolerantes a las bacterias presentes, concentraciones de U demasiado altas pueden tener un efecto de inhibición debido a la quimitoxicidad, llegando a reducir su tasa de rendimiento y crecimiento un 50% (Nyman et al., 2007).

La biomineralización de U puede producirse debido a la actuación de diferentes ligandos en función de la actividad enzimática, como carbonatos o silicatos, pero la más estudiada es la bioprecipitación mediante fosfatos. Esta técnica es especialmente prometedora para la biorremediación *in situ* de zonas donde la bioreducción es inviable debido a altas concentraciones de nitratos o por riesgo de reoxidación de las formas de U (Newsome et al., 2014). La biomineralización de U mediante la actividad fosfatasa se ha estudiado, entre otras, con cepas bacterianas de los géneros *Bacillus*, *Serratia*, *Pseudomonas*, o *Caulobacter* (Chandwadkar et al., 2018; Choudhary and Sar, 2011; Morrison et al., 2021; Pinel-Cabello et al., 2021; Tu et al., 2019) y del género *Saccharomyces* de levadura (Shen et al., 2018).

Los precipitados formados difieren en cada estudio en función de la actividad enzimática del microorganismo y de las condiciones fisicoquímicas. Los minerales de fosfatos de U más comúnmente formados en estos casos son la autunita / meta-autunita  $\text{Ca}(\text{UO}_2)_2(\text{PO}_4)_2 \cdot 6\text{H}_2\text{O}$ , la uranfita  $(\text{NH}_4)(\text{UO}_2)\text{PO}_4 \cdot 3\text{H}_2\text{O}$  y la chernikovita  $(\text{UO}_2\text{HPO}_4 \cdot 4\text{H}_2\text{O})$  (Morrison et al., 2021; Shen et al., 2018; Sklodowska et al., 2018). Es un hecho bien conocido que la actividad fosfatasa está presente en la mayoría de las bacterias ya que los fosfatos inorgánicos son un nutriente esencial de P para los microorganismos. Las principales enzimas fosfatasas expresadas por las bacterias son la fosfatasa ácida periplásmica (PhoN) y la fosfatasa extracelular alcalina (PhoK). En casos de exceso de P, algunas bacterias acumulan el fosfato inorgánico almacenándolo como gránulos de polifosfatos de forma intracelular para garantizar su uso en situaciones de escasez (Hirota et al., 2010).

Aún quedan limitaciones en la implantación de este tipo de remediación, como la viabilidad económica de la fuente necesaria de fosfatos orgánicos (Banala et al., 2021a; Lloyd and Macaskie, 2000), pero en los últimos años se han desarrollado algunos estudios para su optimización y en la búsqueda de alternativas, como el ácido fítico procedente de desechos vegetales (Paterson-Beedle et al., 2010). No obstante, a pesar de estas limitaciones, actualmente la biomineralización de U se considera más prometedora que la bioreducción ya que los productos resultantes presentan mayor estabilidad en condiciones ambientales variables (Wufuer et al., 2017).

En los últimos años se está desarrollando la aplicación de la ingeniería genética con el objetivo de mejorar la productividad y el coste, debido a que son los principales inconvenientes que presenta el uso de microorganismos como sistema de biorremediación. Efectivamente, el uso de bacterias ha demostrado una alta capacidad de eliminación de contaminantes, pero, como señalan algunos autores, sería necesaria la aplicación de herramientas de mejora genética para aumentar su uso a gran escala y a largo plazo (Tylecote, 2019). Para la eliminación de U se han llevado a cabo algunos trabajos con la finalidad de conseguir la sobreexpresión de la actividad fosfatasa de *Deinococcus radiodurans* (Kulkarni et al., 2013) o *Escherichia coli* (Basnakova et al., 1998).

### **Procesos basados en la inmovilización de biomasa sobre soportes sólidos.**

Algunos tratamientos y técnicas empleados en biorremediación de metales pesados han resultado ser efectivos, aunque presentan baja eficiencia en cuanto a productividad y costo. Es por ello que se están optimizando estas estrategias mediante diferentes procesos. Una de estas nuevas estrategias es la inmovilización de microorganismos (o biomasa) en diferentes soportes y por diferentes técnicas. La inmovilización de biomasa, es decir, la retención de microorganismos ya sean vivos o muertos en materiales de soporte o en el interior de una matriz, ha demostrado ser un importante mecanismo para la aplicación exitosa de dichas estrategias de remediación (Gopi Kiran et al., 2018; Soltmann et al., 2010). Para su inmovilización en matrices se han utilizado una gran variedad tanto de organismos (como bacterias (cultivos puros y mixtos), algas, hongos, levaduras), como de sus propias enzimas, debido a que estas técnicas son altamente compatibles con diversos sistemas biológicos (Girijan and Kumar, 2019).

En comparación con el uso de microorganismos no inmovilizados, la incorporación de un soporte presenta una serie de ventajas. El empleo de células planctónicas “libres” (no inmovilizadas) en técnicas de biorremediación conlleva algunos problemas como son el lavado de los microorganismos, su susceptibilidad a factores externos o una menor concentración de biomasa en contacto (Mehrotra et al., 2021). En cambio, la inmovilización tiene ventajas para la biorremediación como son la reducción del espacio necesario para el tratamiento, una mayor facilidad de manejo en su aplicación o una mayor capacidad de supervivencia de los microorganismos empleados, lo que conlleva, además, la posibilidad de su reutilización, reduciendo los costes de forma importante (Mallik, 2002). Además, logra una mayor estabilidad mecánica en el sistema, y en algunos casos, se ha propuesto como mejora en la capacidad de retención y en la actividad de la propia biomasa (Covarrubias et al., 2012). La gran diversidad de microorganismos que pueden ser empleados, así como la facilidad de manejo a gran escala de los biomateriales generados, son ventajas que impulsan esta tecnología. Además de no producir riesgos para la salud ni para el medioambiente, su uso se está llevando a cabo tanto en medios sólidos como acuosos. Por otro lado, aparte del campo de la biorremediación, la inmovilización de células está siendo utilizado en numerosas aplicaciones como la farmacéutica, procesos de la industria alimentaria o biosensores (Mehrotra et al., 2021).

En función de la aplicación que vayan a desarrollar los microorganismos se debe seleccionar adecuadamente la técnica de inmovilización. Existen diferentes procesos de inmovilización según la forma de anclaje de la biomasa:

- Procesos de adsorción: esta técnica consiste en la inmovilización de la biomasa en un soporte base a través de interacciones físicas, tanto enlaces de Van der Waals como uniones hidrofóbicas, o interacciones químicas como enlaces iónicos o covalentes (Kisukuri and Andrade, 2015). Esta metodología se ha usado desde hace más de 100 años (Nelson and Griffin, 1916) debido a su bajo coste y su simplicidad. Sin embargo, presenta ciertas desventajas frente a otras técnicas de inmovilización ya que, a causa de la debilidad de dichos enlaces, conlleva una eficiencia menor y pérdida de biomasa.
- Encapsulación: mediante este método la biomasa microbiana queda incluida en el interior de una matriz polimérica (p. ej. agarosa, alginato, chitosan o poliacrilamida, entre otras). Para este tipo de inmovilización es necesario que los poros de estos materiales sean lo suficientemente pequeños para que no haya una pérdida de la biomasa, y, al mismo tiempo, lo suficientemente grandes para permitir el flujo de los sustratos que se quieran tratar. Aunque esta técnica presenta algunas limitaciones, como las bajas tasas de difusión mostradas por ciertos materiales, sus ventajas la convierten en una alternativa prometedora para múltiples aplicaciones.
- Unión en superficie: método similar a los procesos de adsorción, pero con una mayor capacidad de unión a los microorganismos. Este sistema requiere tanto de un agente aglutinante como de la obtención de una superficie hidrofílica capaz de atraer a las células o enzimas (Lee and Tsai, 2009). Es usado principalmente en la inmovilización de enzimas debido a que los agentes aglutinantes suelen ser tóxicos para las células, reduciendo la viabilidad microbiana.
- Inmovilización en matrices porosas: en este tipo de encapsulación los microorganismos quedan retenidos en una matriz heterogénea manteniendo la capacidad de moverse dentro de ella. Esto evita que la biomasa se filtre hacia el exterior, pero puede limitar el intercambio de nutrientes y sustancias. Es un sistema



## INTRODUCCIÓN

rápido, económico, no tóxico y versátil para adaptarse a la morfología del organismo usado (Wojcieszńska et al., 2013).

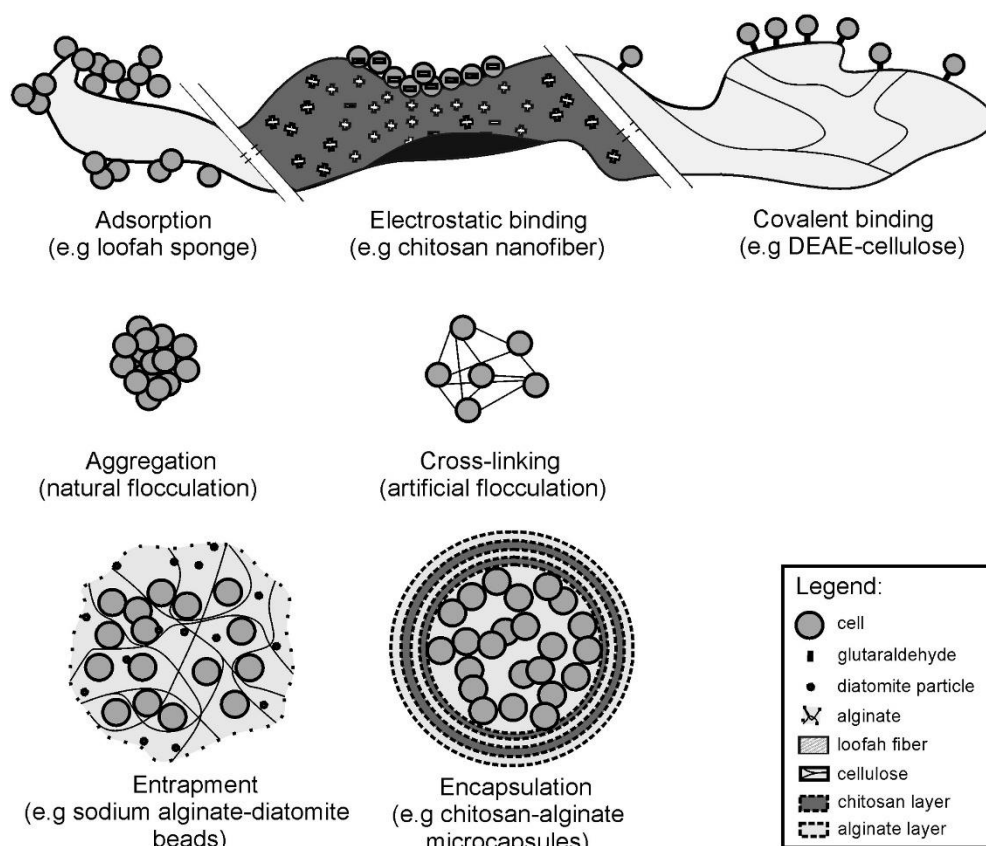


**Figura 10.** Procesos de inmovilización de biomasa para técnicas de biorremediación (Dziona et al., 2016).

La aplicación de los procesos de inmovilización de biomasa en biorremediación ha tenido un notable auge en los últimos años. En el caso de la inmovilización de bacterias (tanto en cultivos puros como en consorcios) se realiza de forma más sencilla y es más eficiente que en el caso de otros microorganismos debido a su morfología y fisiología. En algunos trabajos se ha incluido la cepa *Bacillus sphaericus* en geles de sílice en ensayos de eliminación de U, consiguiendo una alta tasa de remediación, y observando que el metal precipitaba al unirse tanto a los componentes bacterianos como a la propia red de sílice (Soltmann et al., 2003). La cepa *Pseudomonas putida* ha sido inmovilizada tanto en polímeros de arcilla (Zvulunov et al., 2019) como en compuestos de espuma polimérica (Robledo-Ortíz et al., 2011). En otros estudios se han usado esferas de PVA junto con alginato y óxido de grafeno para eliminación de U mediante biomasa de *Saccharomyces cerevisiae* (Chen and Wang, 2016). Angelim et al., (2013) usaron un consorcio bacteriano compuesto por 17 cepas

inmovilizadas en cápsulas de quitosán. Otros autores han logrado reducir la demanda química de oxígeno y nitrógeno procedente de aguas residuales mediante “lodos activados” inmovilizados en cápsulas de alginato-Ca (Martinez et al., 2009). Por otro lado, varios tipos de materiales como alginato, poliacrilamida o poliuretano han sido ensayados como matrices de inmovilización con la cepa *Pseudomonas aeruginosa* para eliminar U procedente de aguas residuales (Hu and Reeves, 1997). En el caso de hongos también se han realizado avances en la eliminación de U con biomasa inmovilizada. Mediante cápsulas de alginato-Ca, Akhtar et al., (2009) lograron una mejora en la biosorción de U por parte del hongo *Trichoderma harzianum*. Por otra parte, recientemente se ha inmovilizado la cepa *Yarrowia lipolytica* mediante cápsulas de alginato-Ca y poliacrilamida con el objetivo de aumentar la captación de U tanto en sistema de lotes como en flujo continuo (Kolhe et al., 2020).

Hoy en día los procesos de inmovilización bacteriana aplicados a la biorremediación de metales pesados se consideran como una alternativa prometedora frente a métodos más convencionales. El uso de la encapsulación de bacterias ha demostrado un rendimiento muy prometedor en la eliminación de contaminantes. Sin embargo, la gran mayoría de trabajos se han desarrollado a escala de laboratorio ya que aún existen ciertos desafíos asociados a este tipo de tecnología, como la estabilidad de las matrices, la presencia de diferentes contaminantes, la inhibición microbiana... etc. Por tanto, la investigación y mejora de estas técnicas es necesaria para poder progresar en la mejora de la estabilidad de las matrices y el aumento de las tasas de difusión de los contaminantes, y poder aplicar los avances realizados de forma preliminar desde escala de laboratorio a ensayos *in situ* y, eventualmente, a una aplicación a escala industrial.

## Bibliografía

- Agnello, A.C., Bagard, M., van Hullebusch, E.D., Esposito, G., Huguenot, D., 2016. Comparative bioremediation of heavy metals and petroleum hydrocarbons co-contaminated soil by natural attenuation, phytoremediation, bioaugmentation and bioaugmentation-assisted phytoremediation. *Sci. Total Environ.* 563–564, 693–703. <https://doi.org/10.1016/j.scitotenv.2015.10.061>
- Akhtar, K., Khalid, A.M., Akhtar, M.W., Ghauri, M.A., 2009. Removal and recovery of uranium from aqueous solutions by Ca-alginate immobilized *Trichoderma harzianum*. *Bioresour. Technol.* 100, 4551–4558. <https://doi.org/10.1016/j.biortech.2009.03.073>
- Aksu, Z., Dönmez, G., 2000. The use of molasses in copper(II) containing wastewaters: Effects on growth and copper(II) bioaccumulation properties of *Kluyveromyces marxianus*. *Process*

## INTRODUCCIÓN

- Biochem. 36, 451–458.  
[https://doi.org/10.1016/S0032-9592\(00\)00234-X](https://doi.org/10.1016/S0032-9592(00)00234-X)
- Angelim, A.L., Costa, S.P., Farias, B.C.S., Aquino, L.F., Melo, V.M.M., 2013. An innovative bioremediation strategy using a bacterial consortium entrapped in chitosan beads. *J. Environ. Manage.* 127, 10–17.  
<https://doi.org/10.1016/j.jenvman.2013.04.014>
- Ayangbenro, A.S., Babalola, O.O., 2017. A new strategy for heavy metal polluted environments: A review of microbial biosorbents. *Int. J. Environ. Res. Public Health* 14.  
<https://doi.org/10.3390/ijerph14010094>
- Banala, U.K., Das, N.P.I., Toleti, S.R., 2021a. Microbial interactions with uranium: Towards an effective bioremediation approach. *Environ. Technol. Innov.* 21, 101254.  
<https://doi.org/10.1016/j.eti.2020.101254>
- Banala, U.K., Indradyumna Das, N.P., Toleti, S.R., 2021b. Uranium sequestration abilities of *Bacillus* bacterium isolated from an alkaline mining region. *J. Hazard. Mater.* 411, 125053.  
<https://doi.org/10.1016/j.jhazmat.2021.125053>
- Bano, A., Hussain, J., Akbar, A., Mehmood, K., Anwar, M., Hasni, M.S., Ullah, S., Sajid, S., Ali, I., 2018. Biosorption of heavy metals by obligate halophilic fungi. *Chemosphere* 199, 218–222.  
<https://doi.org/10.1016/j.chemosphere.2018.02.043>
- Bargar, J.R., Williams, K.H., Campbell, K.M., Long, P.E., Stubbs, J.E., Suvorova, E.I., Lezama-Pacheco, J.S., Alessi, D.S., Stylo, M., Webb, S.M., Davis, J.A., Giammar, D.E., Blue, L.Y., Bernier-Latmani, R., 2013. Uranium redox transition pathways in acetate-amended sediments. *Proc. Natl. Acad. Sci. U. S. A.* 110, 4506–4511.  
<https://doi.org/10.1073/pnas.1219198110>
- Basnakova, G., Stephens, E.R., Thaller, M.C., Rossolini, G.M., Macaskie, L.E., 1998. The use of *Escherichia coli* bearing a *phoN* gene for the removal of uranium and nickel from aqueous flows. *Appl. Microbiol. Biotechnol.* 50, 266–272.  
<https://doi.org/10.1007/s002530051288>
- Benes, P., 1999. The Environmental Impacts of Uranium Mining and Milling and the Methods of Their Reduction, Chemical Separation Technologies and Related Methods of Nuclear Waste Management.
- Bleise, A., Danesi, P.R., Burkart, W., 2003. Properties, use and health effects of depleted uranium (DU): a general overview. *J. Environ. Radioact.* 64, 93–112.
- Brook, S., Division, C., Alamos, L., Molecular, E., Northwest, P., 2001. Coprecipitation of Uranium(VI) with Calcite: XAFS, micro-XAS, and luminescence characterization. *Geochim. Cosmochim. Acta* 65, 1–13.
- Bryner, L.C., Beck, J. V., Davis, D.B., Wilson, D.G., 1954. Microorganisms in Leaching Sulfide Minerals. *Ind. Eng. Chem.* 46, 2587–2592.
- Cason, E.D., Piater, L.A., Heerden, E. van, 2012. Reduction of U(VI) by the deep subsurface bacterium, *Thermus scotoductus* SA-01, and the involvement of the ABC transporter protein. *Chemosphere* 86, 572–577.  
<https://doi.org/10.1016/j.chemosphere.2011.10.006>
- Chandwadkar, P., Misra, H.S., Acharya, C., 2018. Uranium biomineralization induced by a metal tolerant: *Serratia* strain under acid, alkaline and irradiated conditions. *Metallomics* 10, 1078–1088.  
<https://doi.org/10.1039/c8mt00061a>
- Chen, C., Wang, J., 2016. Uranium removal by novel graphene oxide-immobilized *Saccharomyces cerevisiae* gel beads. *J. Environ. Radioact.* 162–163, 134–145.  
<https://doi.org/10.1016/j.jenvrad.2016.05.012>
- Child, D.P., Hotchkis, M.A.C., 2013. Plutonium and uranium contamination in soils from former nuclear weapon test sites in Australia. *Nucl. Instruments Methods Phys. Res. Sect. B Beam Interact. with Mater. Atoms* 294, 642–646.  
<https://doi.org/10.1016/j.nimb.2012.05.018>
- Cho, K., Zholi, A., Frabutt, D., Flood, M., Floyd, D., Tiquia, S.M., 2012. Linking bacterial diversity and geochemistry of uranium-contaminated groundwater. *Environ. Technol. (United Kingdom)* 33, 1629–1640.  
<https://doi.org/10.1080/09593330.2011.641036>
- Choudhary, S., Sar, P., 2015. Interaction of uranium (VI) with bacteria: potential applications in bioremediation of U

- contaminated oxic environments. *Rev. Environ. Sci. Biotechnol.* 14, 347–355. <https://doi.org/10.1007/s11157-015-9366-6>
- Choudhary, S., Sar, P., 2011. Uranium biomineralization by a metal resistant *Pseudomonas aeruginosa* strain isolated from contaminated mine waste. *J. Hazard. Mater.* 186, 336–343. <https://doi.org/10.1016/j.jhazmat.2010.11.004>
- Covarrubias, S.A., De-Bashan, L.E., Moreno, M., Bashan, Y., 2012. Alginate beads provide a beneficial physical barrier against native microorganisms in wastewater treated with immobilized bacteria and microalgae. *Appl. Microbiol. Biotechnol.* 93, 2669–2680. <https://doi.org/10.1007/s00253-011-3585-8>
- Dhal, P.K., Sar, P., 2014. Microbial communities in uranium mine tailings and mine water sediment from Jaduguda U mine, India: A culture independent analysis. *J. Environ. Sci. Heal. - Part A Toxic/Hazardous Subst. Environ. Eng.* 49, 694–709. <https://doi.org/10.1080/10934529.2014.865458>
- Doudou, S., Vaughan, D.J., Livens, F.R., Burton, N.A., 2012. Atomistic simulations of calcium uranyl(VI) carbonate adsorption on calcite and stepped-calcite surfaces. *Environ. Sci. Technol.* 46, 7587–7594. <https://doi.org/10.1021/es300034k>
- Dungan, K., Butler, G., Livens, F.R., Warren, L.M., 2017. Uranium from seawater – Infinite resource or improbable aspiration? *Prog. Nucl. Energy* 99, 81–85. <https://doi.org/10.1016/j.pnucene.2017.04.016>
- Dzionic, A., Wojcieszynska, D., Guzik, U., 2016. Natural carriers in bioremediation: A review. *Electron. J. Biotechnol.* 23, 28–36. <https://doi.org/10.1016/j.ejbt.2016.07.003>
- Edberg, F., Andersson, A.F., Holmström, S.J.M., 2012. Bacterial Community Composition in the Water Column of a Lake Formed by a Former Uranium Open Pit Mine. *Microb. Ecol.* 64, 870–880. <https://doi.org/10.1007/s00248-012-0069-z>
- Falck, W.E., 2015. Radioactive and other environmental contamination from uranium mining and milling, *Environmental Remediation and Restoration of Contaminated Nuclear and Norm Sites.* Elsevier Ltd. <https://doi.org/10.1016/B978-1-78242-231-0.00001-6>
- Finch, R., Murakami, T., 1999. Systematics and paragenesis of uranium minerals. *Uranium Mineral. Geochemistry, Environ.* 38, 91–179.
- Frontasyeva, M. V., Pereygin, V.P., Vater, P., 2001. *Radionuclides and Heavy Metals in Environment,* Springer. <https://doi.org/10.1017/CBO9781107415324.004>
- Gallegos, T.J., Campbell, K.M., Zielinski, R.A., Reimus, P.W., Clay, J.T., Janot, N., Bargar, J.R., Benzel, W.M., 2015. Persistent U(IV) and U(VI) following in-situ recovery (ISR) mining of a sandstone uranium deposit, Wyoming, USA. *Appl. Geochemistry* 63, 222–234. <https://doi.org/10.1016/j.apgeochem.2015.08.017>
- Gallois, N., Alpha-Bazin, B., Ortet, P., Barakat, M., Piette, L., Long, J., Berthomieu, C., Armengaud, J., Chapon, V., 2018. Proteogenomic insights into uranium tolerance of a Chernobyl's Microbacterium bacterial isolate. *J. Proteomics* 177, 148–157. <https://doi.org/10.1016/j.jprot.2017.11.021>
- Gao, W., Francis, A.J., 2008. Reduction of uranium(VI) to uranium(IV) by clostridia. *Appl. Environ. Microbiol.* 74, 4580–4584. <https://doi.org/10.1128/AEM.00239-08>
- Gavrilescu, M., Pavel, L.V., Cretescu, I., 2009. Characterization and remediation of soils contaminated with uranium. *J. Hazard. Mater.* 163, 475–510. <https://doi.org/10.1016/j.jhazmat.2008.07.103>
- Gerber, U., Hübner, R., Rossberg, A., Krawczyk-Bärsch, E., Merroun, M.L., 2018. Metabolism-dependent bioaccumulation of uranium by *Rhodospiridium toruloides* isolated from the flooding water of a former uranium mine. *PLoS One* 13, 1–20. <https://doi.org/10.1371/journal.pone.0201903>
- Gerber, U., Zirnstein, I., Krawczyk-bärsch, E., Lünsdorf, H., Arnold, T., Merroun, M.L., 2016. Combined use of flow cytometry and microscopy to study the interactions between the gram-negative betaproteobacterium *Acidovorax facilis* and uranium(VI). *J. Hazard. Mater.* 317, 127–134. <https://doi.org/10.1016/j.jhazmat.2016.05.062>

## INTRODUCCIÓN

- Girijan, S., Kumar, M., 2019. Immobilized biomass systems: an approach for trace organics removal from wastewater and environmental remediation. *Curr. Opin. Environ. Sci. Heal.* 12, 18–29. <https://doi.org/10.1016/j.coesh.2019.08.005>
- Gopi Kiran, M., Pakshirajan, K., Das, G., 2018. Heavy metal removal from aqueous solution using sodium alginate immobilized sulfate reducing bacteria: Mechanism and process optimization. *J. Environ. Manage.* 218, 486–496. <https://doi.org/10.1016/j.jenvman.2018.03.020>
- Guarino, C., Spada, V., Sciarrillo, R., 2017. Assessment of three approaches of bioremediation (Natural Attenuation, Landfarming and Bioaugmentation – Assisted Landfarming) for a petroleum hydrocarbons contaminated soil. *Chemosphere* 170, 10–16. <https://doi.org/10.1016/j.chemosphere.2016.11.165>
- Gudkov, S. V., Chernikov, A. V., Bruskov, V.I., 2016. Chemical and radiological toxicity of uranium compounds. *Russ. J. Gen. Chem.* 86, 1531–1538. <https://doi.org/10.1134/S1070363216060517>
- Hao, X., Zhu, J., Rensing, C., Liu, Y., Gao, S., Chen, W., Huang, Q., Liu, Y.R., 2021. Recent advances in exploring the heavy metal(loid) resistant microbiome. *Comput. Struct. Biotechnol. J.* 19, 94–109. <https://doi.org/10.1016/j.csbj.2020.12.006>
- He, Z., Zhang, P., Wu, L., Rocha, A.M., Tu, Q., Shi, Z., Wu, B., Qin, Y., Wang, J., Yan, Q., Curtis, D., Ning, D., Joy D. Van Nostrand, L.W., Yang, Y., Elias, D.A., Watson, D.B., Michael W. W. Adams, M.W.F., Alm, E.J., Hazen, T.C., Adams, P.D., Arkin, A.P., Zhou, J., 2018. Microbial Functional Gene Diversity Predicts Groundwater Contamination and Ecosystem Functioning. *Am. Soc. Microbiol. Journals* 9, 1–15.
- Hirota, R., Kuroda, A., Kato, J., Ohtake, H., 2010. Bacterial phosphate metabolism and its application to phosphorus recovery and industrial bioprocesses. *J. Biosci. Bioeng.* 109, 423–432. <https://doi.org/10.1016/j.jbiosc.2009.10.018>
- Hopkins, B.S., 1923. The geochemistry of the rarer elements. D.C. Heath Company, Boston/New York/Chicago/London 203, 350. <https://doi.org/10.1038/203350c0>
- Hu, M.Z.C., Reeves, M., 1997. Biosorption of uranium by *Pseudomonas aeruginosa* strain CSU immobilized in a novel matrix. *Biotechnol. Prog.* 13, 60–70. <https://doi.org/10.1021/bp9600849>
- Huang, W., Nie, X., Dong, F., Ding, C., Huang, R., Qin, Y., Liu, M., Sun, S., 2017. Kinetics and pH-dependent uranium bioprecipitation by *Shewanella putrefaciens* under aerobic conditions. *J. Radioanal. Nucl. Chem.* 312, 531–541. <https://doi.org/10.1007/s10967-017-5261-7>
- Islam, E., Sar, P., 2016. Diversity, metal resistance and uranium sequestration abilities of bacteria from uranium ore deposit in deep earth stratum. *Ecotoxicol. Environ. Saf.* 127, 12–21. <https://doi.org/10.1016/j.ecoenv.2016.01.001>
- Islam, E., Sar, P., 2011. Culture-dependent and -independent molecular analysis of the bacterial community within uranium ore. *J. Basic Microbiol.* 51, 372–384. <https://doi.org/10.1002/jobm.201000327>
- Ivanovich, M., Alexander, J., 1987. Application of uranium-series disequilibrium to studies of groundwater mixing in the Harwell region, U.K. 66, 279–291.
- Ivanovich, M., Harmon, R.S. (Russell S., 1992. Uranium-series disequilibrium : applications to earth, marine, and environmental sciences. Clarendon Press.
- Fadwa Jroundi, Cristina Povedano-Priego, María Pinel-Cabello, Michael Descostes, Pierre Grizard, Bayarma Purevsan, Mohamed L. Merroun. 2022. Evidence of microbial activity in a uranium roll-front deposit: Unlocking their potential role as bioenhancers of the ore genesis, *Science of The Total Environment* -160636. <https://doi.org/10.1016/j.scitotenv.2022.160636>.
- Jroundi, F., Descostes, M., Povedano-Priego, C., Sánchez-Castro, I., Suvannagan, V., Grizard, P., Merroun, M.L., 2020. Profiling native aquifer bacteria in a uranium roll-front deposit and their role in biogeochemical cycle dynamics: Insights regarding in situ recovery mining. *Sci. Total Environ.* 721. <https://doi.org/10.1016/j.scitotenv.2020.137758>

- Kathren, R.L., 2001. The Health Hazards of Depleted Uranium Munitions Part I. *J. Radiol. Prot.* 21, 331–332.  
<https://doi.org/10.1088/0952-4746/21/3/701>
- Kenarova, A., Radeva, G., Danova, I., Boteva, S., Dimitrova, I., 2010. Soil bacterial abundance and diversity of uranium impacted area in north western pirin mountain. *Biotechnol. Biotechnol. Equip.* 24, 469–473.  
<https://doi.org/10.1080/13102818.2010.10817885>
- Kenarova, A., Radeva, G., Traykov, I., Boteva, S., 2014. Community level physiological profiles of bacterial communities inhabiting uranium mining impacted sites. *Ecotoxicol. Environ. Saf.* 100, 226–232.  
<https://doi.org/10.1016/j.ecoenv.2013.11.012>
- Khare, D., Chandwadkar, P., Acharya, C., 2022. Gliding motility of a uranium-tolerant Bacteroidetes bacterium *Chryseobacterium* sp. strain PMSZPI: insights into the architecture of spreading colonies. *Environ. Microbiol. Rep.* 14, 453–463.  
<https://doi.org/https://doi.org/10.1111/1758-2229.13034>
- Kielak, A.M., Barreto, C.C., Kowalchuk, G.A., van Veen, J.A., Kuramae, E.E., 2016. The ecology of Acidobacteria: Moving beyond genes and genomes. *Front. Microbiol.* 7, 1–16.  
<https://doi.org/10.3389/fmicb.2016.00744>
- Kisukuri, C.M., Andrade, L.H., 2015. Production of chiral compounds using immobilized cells as a source of biocatalysts. *Org. Biomol. Chem.* 13, 10086–10107.  
<https://doi.org/10.1039/c5ob01677k>
- Kolhe, N., Zinjarde, S., Acharya, C., 2020. Removal of uranium by immobilized biomass of a tropical marine yeast *Yarrowia lipolytica*. *J. Environ. Radioact.* 223–224, 106419.  
<https://doi.org/10.1016/j.jenvrad.2020.106419>
- Kolhe, N., Zinjarde, S., Acharya, C., 2018. Responses exhibited by various microbial groups relevant to uranium exposure. *Biotechnol. Adv.* 36, 1828–1846.  
<https://doi.org/10.1016/j.biotechadv.2018.07.002>
- Kulkarni, S., Ballal, A., Apte, S.K., 2013. Bioprecipitation of uranium from alkaline waste solutions using recombinant *Deinococcus radiodurans*. *J. Hazard. Mater.* 262, 853–861.  
<https://doi.org/10.1016/j.jhazmat.2013.09.057>
- Kumar, A., Chanderman, A., Makolomakwa, M., Perumal, K., Singh, S., 2016. Microbial production of phytases for combating environmental phosphate pollution and other diverse applications. *Crit. Rev. Environ. Sci. Technol.* 46, 556–591.  
<https://doi.org/10.1080/10643389.2015.1131562>
- Lee, C.A., Tsai, Y.C., 2009. Preparation of multiwalled carbon nanotube-chitosan-alcohol dehydrogenase nanobiocomposite for amperometric detection of ethanol. *Sensors Actuators, B Chem.* 138, 518–523.  
<https://doi.org/10.1016/j.snb.2009.01.001>
- Li, B., Wu, W., Watson, D.B., Cardenas, E., Chao, Y., Phillips, D.H., Mehlhorn, T., 2018. Bacterial Community Shift and Coexisting/Coexcluding Patterns Revealed by Network Analysis in a Uranium-Contaminated Site after Bioreduction Followed by Reoxidation. *Appl. Environ. Microbiol.* 84.  
<https://doi.org/https://doi.org/10.1128/AEM.02885-17>
- Li, X., Ding, C., Liao, J., Lan, T., Li, F., Zhang, D., Yang, J., Yang, Y., Luo, S., Tang, J., Liu, N., 2014. Biosorption of uranium on *Bacillus* sp. dwc-2: Preliminary investigation on mechanism. *J. Environ. Radioact.* 135, 6–12.  
<https://doi.org/10.1016/j.jenvrad.2014.03.017>
- Liger, E., Charlet, L., Van Cappellen, P., 1999. Surface catalysis of uranium(VI) reduction by iron(II). *Geochim. Cosmochim. Acta* 63, 2939–2955.  
[https://doi.org/10.1016/S0016-7037\(99\)00265-3](https://doi.org/10.1016/S0016-7037(99)00265-3)
- Lloyd, J.R., Macaskie, L.E., 2000. Bioremediation of Radionuclide-Containing Wastewaters, in: *Environmental Microbe-Metal Interactions*. pp. 277–327.  
<https://doi.org/10.1128/9781555818098.ch13>
- Lopez-Fernandez, M., Jroundi, F., Ruiz-Fresneda, M.A., Merroun, M.L., 2020. Microbial interaction with and tolerance of radionuclides: underlying mechanisms and biotechnological applications. *Microb. Biotechnol.* 00.

## INTRODUCCIÓN

- <https://doi.org/10.1111/1751-7915.13718>
- Maleke, M., Williams, P., Castillo, J., Botes, E., Ojo, A., DeFlaun, M., van Heerden, E., 2015. Optimization of a bioremediation system of soluble uranium based on the biostimulation of an indigenous bacterial community. *Environ. Sci. Pollut. Res.* 22, 8442–8450.  
<https://doi.org/10.1007/s11356-014-3980-7>
- Mallik, N., 2002. Biotechnological potential of immobilised algae for wastewater N, P and metal removal: a review. *BioMetals* 15, 377–390.
- Martinez, A., Sergio, D., Yaneth Bustos, T., 2009. Biodegradation of wastewater pollutants by activated sludge encapsulated inside calcium-alginate beads in a tubular packed bed reactor. *Biodegradation* 20, 709–715. <https://doi.org/10.1007/s10532-009-9258-y>
- McGloin, M. V., Tomkins, A.G., Webb, G.P., Spiers, K., MacRae, C.M., Paterson, D., Ryan, C.G., 2016. Release of uranium from highly radiogenic zircon through metamictization: The source of orogenic uranium ores. *Geology* 44, 15–18.  
<https://doi.org/10.1130/G37238.1>
- Mehrotra, T., Dev, S., Banerjee, A., Chatterjee, A., Singh, R., Aggarwal, S., 2021. Use of immobilized bacteria for environmental bioremediation: A review. *J. Environ. Chem. Eng.* 9, 105920.  
<https://doi.org/10.1016/j.jece.2021.105920>
- Meinrath, A., Schneider, P., Meinrath, G., 2003. Uranium ores and depleted uranium in the environment, with a reference to uranium in the biosphere from the Erzgebirge/Sachsen, Germany. *J. Environ. Radioact.* 64, 175–193.  
[https://doi.org/10.1016/S0265-931X\(02\)00048-6](https://doi.org/10.1016/S0265-931X(02)00048-6)
- Merroun, M.L., Nedelkova, M., Ojeda, J.J., Reitz, T., Fernández, M.L., Arias, J.M., Romero-González, M., Selenska-Pobell, S., 2011. Bio-precipitation of uranium by two bacterial isolates recovered from extreme environments as estimated by potentiometric titration, TEM and X-ray absorption spectroscopic analyses. *J. Hazard. Mater.* 197, 1–10.  
<https://doi.org/10.1016/j.jhazmat.2011.09.049>
- Mondani, L., Benzerara, K., Carrière, M., Christen, R., Mamindy-Pajany, Y., Février, L., Marmier, N., Achouak, W., Nardoux, P., Berthomieu, C., Chapon, V., 2011. Influence of uranium on bacterial communities: A comparison of natural uranium-rich soils with controls. *PLoS One* 6.  
<https://doi.org/10.1371/journal.pone.0025771>
- Morrison, K.D., Zavarin, M., Kersting, A.B., Begg, J.D., Mason, H.E., Balboni, E., Jiao, Y., 2021. Influence of Uranium Concentration and pH on U-Phosphate Biomineralization by *Caulobacter* OR37. *Environ. Sci. Technol.* 55, 1626–1636.  
<https://doi.org/10.1021/acs.est.0c05437>
- Mumtaz, S., Stretten, C., Parry, D.L., McGuinness, K.A., Lu, P., Gibb, K.S., 2018. Soil uranium concentration at Ranger Uranium Mine Land Application Areas drives changes in the bacterial community. *J. Environ. Radioact.* 189, 14–23.  
<https://doi.org/10.1016/j.jenvrad.2018.03.003>
- NCRP report 77: Exposure from the uranium series with emphasis on radon and its daughters, 1987. . *Natl. Counc. Radiat. Prot. Meas.* 1987.
- NEA/IAEA, 2020. Uranium Resources, Production and Demand: A Joint Report by the Nuclear Energy Agency and the International Atomic Energy Agency.
- Nelson, J.M., Griffin, E.G., 1916. Adsorption of invertase. *J. Am. Chem. Soc.* 38, 1109–1115. <https://doi.org/10.1021/ja02262a018>
- Newsome, L., Morris, K., Lloyd, J.R., 2014. The biogeochemistry and bioremediation of uranium and other priority radionuclides. *Chem. Geol.* 363, 164–184.  
<https://doi.org/10.1016/j.chemgeo.2013.10.034>
- Nyman, J.L., Wu, H.I., Gentile, M.E., Kitanidis, P.K., Criddle, C.S., 2007. Inhibition of a U(VI)- and sulfate-reducing consortia by U(VI). *Environ. Sci. Technol.* 41, 6528–6533. <https://doi.org/10.1021/es062985b>
- Paterson-Beedle, M., Readman, J.E., Hriljac, J.A., MacAskie, L.E., 2010. Biorecovery of uranium from aqueous solutions at the expense of phytic acid. *Hydrometallurgy* 104, 524–528.  
<https://doi.org/10.1016/j.hydromet.2010.01.019>
- Pinel-Cabello, M., Jroundi, F., López-Fernández, M., Geffers, R., Jarek, M., Jauregui, R.,

- Link, A., Vílchez-Vargas, R., Merroun, M.L., 2021. Multisystem combined uranium resistance mechanisms and bioremediation potential of *Stenotrophomonas bentonitica* BII-R7: Transcriptomics and microscopic study. *J. Hazard. Mater.* 403. <https://doi.org/10.1016/j.jhazmat.2020.123858>
- Plant, J.A., Simpson, P.R., Smith, B., Windley, B.F., 2019. Uranium ore deposits-products of the radioactive earth. *Uranium Mineral. Geochemistry, Environ.* 255–319.
- Povedano-Priego, C., Jroundi, F., Lopez-Fernandez, M., Sánchez-Castro, I., Martín-Sánchez, I., Huertas, F.J., Merroun, M.L., 2019. Shifts in bentonite bacterial community and mineralogy in response to uranium and glycerol-2-phosphate exposure. *Sci. Total Environ.* 692, 219–232. <https://doi.org/10.1016/j.scitotenv.2019.07.228>
- Prakash, D., Gabani, P., Chandel, A.K., Ronen, Z., Singh, O. V., 2013. Bioremediation: A genuine technology to remediate radionuclides from the environment. *Microb. Biotechnol.* 6, 349–360. <https://doi.org/10.1111/1751-7915.12059>
- Qi, Q., Hu, C., Lin, J., Wang, X., Tang, C., Dai, Z., Xu, J., 2022. Contamination with multiple heavy metals decreases microbial diversity and favors generalists as the keystones in microbial occurrence networks. *Environ. Pollut.* 306, 119406. <https://doi.org/10.1016/j.envpol.2022.119406>
- Raghunandan, K., Kumar, A., Kumar, S., Permaul, K., Singh, S., 2018. Production of gellan gum, an exopolysaccharide, from biodiesel-derived waste glycerol by *Sphingomonas* spp. *3 Biotech* 8, 1–13. <https://doi.org/10.1007/s13205-018-1096-3>
- Razzel, W.E., Trussell, P.C., 1962. Isolation and properties of an iron-oxidizing *Thiobacillus*. *Am. Soc. Microbiol. Journals* 595–603.
- Rivas, M., 2005. Interactions between soil uranium contamination and fertilization with N, P and S on the uranium content and uptake of corn, sunflower and beans, and soil microbiological parameters, *Landbauforschung Völkenrode*.
- Robledo-Ortíz, J.R., Ramírez-Arreola, D.E., Pérez-Fonseca, A.A., Gómez, C., González-Reynoso, O., Ramos-Quirarte, J., González-Núñez, R., 2011. Benzene, toluene, and o-xylene degradation by free and immobilized *P. putida* F1 of postconsumer agave-fiber/polymer foamed composites. *Int. Biodeterior. Biodegrad.* 65, 539–546. <https://doi.org/10.1016/j.ibiod.2010.12.011>
- Rogiers, T., Merroun, M.L., Williamson, A., Leys, N., Houdt, R. Van, Boon, N., Mijndonckx, K., 2022. *Cupriavidus metallidurans* NA4 actively forms polyhydroxybutyrate-associated uranium-phosphate precipitates. *J. Hazard. Mater.* 421, 126737. <https://doi.org/10.1016/j.jhazmat.2021.126737>
- Roy, A., Dutta, A., Pal, S., Gupta, A., Sarkar, J., Chatterjee, A., Saha, A., Sarkar, P., Sar, P., Kazy, S.K., 2018. Biostimulation and bioaugmentation of native microbial community accelerated bioremediation of oil refinery sludge. *Bioresour. Technol.* 253, 22–32. <https://doi.org/10.1016/j.biortech.2018.01.004>
- Sánchez-Castro, I., Amador-García, A., Moreno-Romero, C., López-Fernández, M., Phrommavanh, V., Nos, J., Descostes, M., Merroun, M.L., 2017. Screening of bacterial strains isolated from uranium mill tailings porewaters for bioremediation purposes. *J. Environ. Radioact.* 166, 130–141. <https://doi.org/10.1016/j.jenvrad.2016.03.016>
- Sánchez-Castro, I., Martínez-Rodríguez, P., Jroundi, F., Lorenzo, P., Descostes, M., L. Merroun, M., 2020. High-efficient microbial immobilization of solved U(VI) by the *Stenotrophomonas* strain Br8. *Water Res.* 183. <https://doi.org/10.1016/j.watres.2020.116110>
- Shen, Y., Zheng, X., Wang, X., Wang, T., 2018. The biomineralization process of uranium(VI) by *Saccharomyces cerevisiae* — transformation from amorphous U(VI) to crystalline chernikovite. *Appl. Microbiol. Biotechnol.* 102, 4217–4229. <https://doi.org/10.1007/s00253-018-8918-4>
- Shukla, S.K., Hariharan, S., Rao, T.S., 2019. Uranium bioremediation by acid phosphatase activity of *Staphylococcus aureus* biofilms: Can a foe turn a friend? *J. Hazard. Mater.* 384, 121316.



## INTRODUCCIÓN

- <https://doi.org/10.1016/j.jhazmat.2019.121316>
- Skłodowska, A., Mielnicki, S., Drewniak, L., 2018. Raoultella sp. SM1, a novel iron-reducing and uranium-precipitating strain. *Chemosphere* 195, 722–726. <https://doi.org/10.1016/j.chemosphere.2017.12.123>
- Soltmann, U., Matys, S., Kieszig, G., Pompe, W., Bottcher, H., 2010. Algae-Silica Hybrid Materials for Biosorption of Heavy Metals. *J. Water Resour. Prot.* 02, 115–122. <https://doi.org/10.4236/jwarp.2010.22013>
- Soltmann, U., Raff, J., Selenska-Pobell, S., Matys, S., Pompe, W., Böttcher, H., 2003. Biosorption of heavy metals by sol-gel immobilized bacillus sphaericus cells, spores and S-layers. *J. Sol-Gel Sci. Technol.* 26, 1209–1212. <https://doi.org/10.1023/A:1020768420872>
- Sowmya, S., Rekha, P.D., Yashodhara, I., Karunakara, N., Arun, A.B., 2020. Uranium tolerant phosphate solubilizing bacteria isolated from Gogi, a proposed uranium mining site in South India. *Appl. Geochemistry* 114, 104523. <https://doi.org/10.1016/j.apgeochem.2020.104523>
- Stegnar, P., Benedik, L., 2001. Depleted uranium in the environment - An issue of concern? *Arch. Oncol.* 9, 251–255.
- Sutcliffe, B., Chariton, A.A., Harford, A.J., Hose, G.C., Stephenson, S., Greenfield, P., Midgley, D.J., Paulsen, I.T., 2017. Insights from the Genomes of Microbes Thriving in Uranium-Enriched Sediments. *Microb. Ecol.* 75, 970–984. <https://doi.org/10.1007/s00248-017-1102-z>
- Suzuki, Y., Banfield, J.F., 1999. 8. Geomicrobiology of Uranium. De Gruyter, Berlin, Boston, pp. 393–432. <https://doi.org/https://doi.org/10.1515/9781501509193-013>
- Tang, J., Zhang, J., Ren, L., Zhou, Y., Gao, J., Luo, L., Yang, Y., Peng, Q., Huang, H., Chen, A., 2019. Diagnosis of soil contamination using microbiological indices: A review on heavy metal pollution. *J. Environ. Manage.* 242, 121–130. <https://doi.org/10.1016/j.jenvman.2019.04.061>
- Tišáková, L., Pipiška, M., Godány, A., Horník, M., Vidová, B., Augustín, J., 2013. Bioaccumulation of <sup>137</sup>Cs and <sup>60</sup>Co by bacteria isolated from spent nuclear fuel pools. *J. Radioanal. Nucl. Chem.* 295, 737–748. <https://doi.org/10.1007/s10967-012-1932-6>
- Tu, H., Yuan, G., Zhao, C., Liu, J., Li, F., Yang, J., Liao, J., Yang, Y., Liu, N., 2019. U-phosphate biomineralization induced by *Bacillus* sp. dw-2 in the presence of organic acids. *Nucl. Eng. Technol.* 51, 1322–1332. <https://doi.org/10.1016/j.net.2019.03.002>
- Tylecote, A., 2019. Biotechnology as a new techno-economic paradigm that will help drive the world economy and mitigate climate change. *Res. Policy* 48, 858–868. <https://doi.org/10.1016/j.respol.2018.10.001>
- Varjani, S., Upasani, V.N., 2019. Influence of abiotic factors, natural attenuation, bioaugmentation and nutrient supplementation on bioremediation of petroleum crude contaminated agricultural soil. *J. Environ. Manage.* 245, 358–366. <https://doi.org/10.1016/j.jenvman.2019.05.070>
- Volesky, B., Holan, Z., 1995. Biosorption of heavy metals. *Biotechnol. Prog.* 11, 235–250.
- Weyer, S., Anbar, A.D., Gerdes, A., Gordon, G.W., Algeo, T.J., Boyle, E.A., 2008. Natural fractionation of <sup>238</sup>U/<sup>235</sup>U. *Geochim. Cosmochim. Acta* 72, 345–359. <https://doi.org/10.1016/j.gca.2007.11.012>
- Williams, K.H., Bargar, J.R., Lloyd, J.R., Lovley, D.R., 2013. Bioremediation of uranium-contaminated groundwater: A systems approach to subsurface biogeochemistry. *Curr. Opin. Biotechnol.* 24, 489–497. <https://doi.org/10.1016/j.copbio.2012.10.008>
- Wojcieszńska, D., Hupert-Kocurek, K., Guzik, U., 2013. Factors affecting activity of catechol 2,3-dioxygenase from 2-chlorophenol-degrading *Stenotrophomonas maltophilia* strain KB2. *Biocatal. Biotransformation* 31, 141–147. <https://doi.org/10.3109/10242422.2013.796456>
- Wufuer, R., Wei, Y., Lin, Q., Wang, H., Song, W., Liu, W., Zhang, D., Pan, X., Gadd, G.M., 2017. Uranium Bioreduction and Biomineralization, in: *Advances in Applied Microbiology*.

- <https://doi.org/10.1016/bs.aambs.2017.01.003>
- Yan, X., Luo, X., 2015. Radionuclides distribution, properties, and microbial diversity of soils in uranium mill tailings from southeastern China. *J. Environ. Radioact.* 139, 85–90.  
<https://doi.org/10.1016/j.jenvrad.2014.09.019>
- You, W., Peng, W., Tian, Z., Zheng, M., 2021. Uranium bioremediation with U(VI)-reducing bacteria. *Sci. Total Environ.* 798, 149107.  
<https://doi.org/10.1016/j.scitotenv.2021.149107>
- Zammit, C.M., Brugger, J., Southam, G., Reith, F., 2014. In situ recovery of uranium - The microbial influence. *Hydrometallurgy* 150, 236–244.  
<https://doi.org/10.1016/j.hydromet.2014.06.003>
- Zhang, D., Chen, X., Larson, S.L., Ballard, J.H., Knotek-Smith, H.M., Ding, D., Hu, N., Han, F.X., 2020. Uranium Biomineralization with Phosphate - Biogeochemical Process and Its Application. *ACS Earth Sp. Chem.* 4, 2205–2214.
- <https://doi.org/10.1021/acsearthspacechem.0c00252>
- Xu, Shaozu, Yonghui Xing, Song Liu, Xiuli Hao, Wenli Chen, Qiaoyun Huang. 2020, Characterization of Cd<sup>2+</sup> biosorption by *Pseudomonas* sp. strain 375, a novel biosorbent isolated from soil polluted with heavy metals in Southern China, *Chemosphere*, Volume 240 - 124893, <https://doi.org/10.1016/j.chemosphere.2019.124893>.
- Zhang, P., He, Z., Van Nostrand, J.D., Qin, Y., Deng, Y., Wu, L., Tu, Q., Wang, J., Schadt, C.W., Fields, M.W., Hazen, T.C., Arkin, A.P., Stahl, D.A., Zhou, J., 2017. Dynamic Succession of Groundwater Sulfate-Reducing Communities during Prolonged Reduction of Uranium in a Contaminated Aquifer. *Environ. Sci. Technol.* 51, 3609–3620.  
<https://doi.org/10.1021/acs.est.6b02980>
- Zvulunov, Y., Ben-Barak-Zelas, Z., Fishman, A., Radian, A., 2019. A self-regenerating clay-polymer-bacteria composite for formaldehyde removal from water. *Chem. Eng. J.* 374, 1275–1285.  
<https://doi.org/10.1016/j.cej.2019.06.017>

## OBJETIVOS

## **OBJETIVOS**

## OBJETIVOS

La generación de energía nuclear incluye una serie de actividades, como la minería, que provocan la liberación de residuos que contienen uranio cuya presencia puede contaminar amplias áreas, principalmente del medio acuático, como aguas superficiales o subterráneas. Por esta razón, es necesario el desarrollo de programas de gestión sostenible de estos residuos y métodos de reducción de los niveles de contaminación producida, con el objetivo de minimizar el impacto ambiental. Recientemente han surgido nuevas estrategias de remediación basadas en el uso de microorganismos capaces de interactuar con metales pesados. Por ello, el objetivo general de esta tesis doctoral ha sido el estudio de los mecanismos de interacción del U con dos cepas bacterianas que presentan alta tolerancia a este metal pesado, y el desarrollo de una estrategia de biorremediación de aguas contaminadas basada en la inmovilización de biomasa. Para lograr este objetivo general se establecieron los siguientes objetivos específicos:

1. Caracterizar molecular, fisiológica y bioquímicamente las cepas bacterianas *Microbacterium* sp. Be9 y *Stenotrophomonas* sp. Br8, seleccionadas como posibles candidatas para la biorremediación de U.
2. Elucidar, mediante una metodología multidisciplinar, los diferentes mecanismos de precipitación que tienen lugar durante la interacción de *Microbacterium* sp. Be9 y *Stenotrophomonas* sp. Br8 con U, además de evaluar el efecto de diferentes parámetros (fuente de fosfatos, pH, temperatura) sobre dichos mecanismos.
3. Estudiar la capacidad de eliminación de U soluble en soluciones sintéticas mediante los mecanismos previamente descritos por parte de *Microbacterium* sp. Be9 y *Stenotrophomonas* sp. Br8, mediante la aplicación de los mecanismos elucidados en el desarrollo del objetivo específico 2, con la finalidad de seleccionar la cepa más eficiente.
4. Optimizar una metodología para la inmovilización de biomasa de la cepa bacteriana seleccionada en el objetivo anterior para su uso en la eliminación de U de aguas procedentes de la minería de U.

## OBJETIVOS

# **MATERIALS AND METHODS**



## MATERIALS AND METHODS

### **Molecular and phenotypic characterization of the strains Br8 and Be9**

Around 33 bacterial strains were previously isolated from uranium tailing porewaters and characterized at different levels in order to predict their role in the biogeochemical cycle of U (Sánchez-Castro et al., 2017). Multidisciplinary studies were conducted to screen those strains with potential for U bioremediation purposes. The strains named as Br8 and Be9, affiliated to the genera *Stenotrophomonas* and *Microbacterium* respectively, were selected for further investigation due to their biochemical characteristics and U interaction mechanisms.

#### ***Phenotypic analysis***

Br8 and Be9 strains were isolated in R2A oligotrophic medium and incubated at 28°C for 3 days. Gram staining, cell motility and the presence of flagella were determined in both strains according to the method described by Clark (1976). For enzymatic characterization some enzyme activities were determined for Be9 and Br8 bacterial isolates by using API ZYM (4h, 28°C) and API 20NE (48h, 28°C) galleries (bioMérieux, France), according to the manufacturer's instructions. Moreover, the oxidase activity (not included in the API galleries) was recorded by contacting the bacterial biomass with a 1% aqueous tetramethyl-p-phenylenediamine dihydrochloride solution. When the bacterial biomass turned to blue colour, the strains were considered as oxidase-positive.

To evaluate the tolerance of both selected bacterial strains to the different metal/metalloids (MM) as U, Cr, Pb, La, Cd, Ni, Zn, Mo, V, Eu and Cu, a standard method for the determination of the minimum inhibitory concentration (MIC) was performed by using low phosphate medium (LPM) agar (pH 7.2; Rossbach et al., 2000). This standard method is used to determine the tolerance levels of the bacterial strains in presence of MM, and in turn to screen for those with potential in bioremediation. 0.1 M stock solutions of  $\text{UO}_2(\text{NO}_3)_2 \cdot 6\text{H}_2\text{O}$ ,  $\text{Cr}(\text{NO}_3)_3 \cdot 9\text{H}_2\text{O}$ ,  $\text{Pb}(\text{NO}_3)_2$ ,  $\text{LaN}_3\text{O}_9 \cdot 6\text{H}_2\text{O}$ ,  $\text{Cd}(\text{NO}_3)_2 \cdot 4\text{H}_2\text{O}$ ,  $\text{Ni}(\text{NO}_3)_2 \cdot 6\text{H}_2\text{O}$ ,  $\text{ZnSO}_4 \cdot 7\text{H}_2\text{O}$ ,  $\text{Na}_2\text{MoO}_4 \cdot 2\text{H}_2\text{O}$ ,  $\text{VOSO}_4$ ,  $\text{Eu}_2\text{O}_3$ , and  $\text{Cu}(\text{NO}_3)_2 \cdot 3\text{H}_2\text{O}$  were prepared by dissolving appropriate quantities of the MM salts in 0.1 M  $\text{NaClO}_4$ . In the case of Ag and Se, 1 M stock solutions of  $\text{AgNO}_3$  and  $\text{Na}_2\text{SeO}_3$  were prepared by dissolving the appropriate quantity in distilled water. The MM solutions were sterilized by filtration through 0.22-mm nitrocellulose membrane filter (Millipore, Bedford, MA, USA).

## MATERIALS AND METHODS

Cells were grown to mid-exponential phase in LB medium, washed twice with 0.9% NaCl, and 10 mL aliquots of the cell suspensions were spotted onto LPM-agar. The solid medium contained increasing MM concentrations in twofold increments as follows: for U and Eu, increasing concentrations from 0.5 to 4 mM; for Cr, Pb, and La, from 2 to 16 mM; for Cd and Ag, from 0.25 to 2 mM; for Ni, Zn, Mo, V and Cu, from 1 to 8 mM; and for Se from 2 to 100 mM (instead of 128 mM to avoid abiotic precipitation of the metal). After spreading the inoculum, the plates were incubated at 28°C for 1 week. The MIC was defined as the lowest concentration of each of the MM at which complete inhibition of colony formation was observed (Rossbach et al., 2000).

### *Molecular analysis*

Biomass of Br8 and Be9 strains was grown in LB solid medium for 24h at 28 °C for DNA isolation, and both genomic DNA extractions were performed as described by Martín-Platero et al. (2007). For detailed phylogenetic placement of Br8 and Be9 strains, nearly the complete small ribosomal subunits 16S rRNA gene was amplified, with primers 8F (50-AGAGTTTGATYMTGGCTCAG-30) and 1492R (50-TACGGY-TACCTTGTTACGACTT-30). PCR amplifications were conducted in 20 mL reactions using approximately 30 ng template. All PCRs were performed in a Mastercycler Nexus PCR cycler (Eppendorf, Hamburg, Germany). Templates replaced with sterile water were always used as negative controls. PCR products were separated electrophoretically on 1% agarose gels, stained with Redsafe DNA dye and visualized by UV illumination. Sequences were compared with those available in the GenBank and EzTaxon-e Type Strains (Chun et al., 2007) databases by BLAST (Basic Local Alignment Search Tool; Altschul et al., 1990). Alignments of the two sequences of each isolate and similarity levels were obtained by using MAFFT (<http://www.ebi.ac.uk/Tools/msa/mafft/>).

In genomic sequencing one µL of gDNA of each sample was used to test the integrity and purity by 1.5% agarose gel electrophoresis. Afterwards, the samples were quantified using the Qubit 3.0 Fluorometer (Life Technology) and used for library construction using the TruSeq DNA Whole genome library preparation kit (Illumina, USA). The generated DNA fragments (DNA libraries) were sequenced using the Illumina Novaseq platform, using 150bp paired-end sequencing reads. Low-quality reads were trimmed by CLC Genomics

Workbench 12.0 to generate 14,144,710 and 16,919,206 reads in Be9 and Br8 strains respectively.

Afterwards, genomes of Br8 and Be9 were assembled and annotated. Quality-filtered reads were *de novo* assembled using an algorithm based on de Bruijn graphs performed by CLC Genomics Workbench 12.0 and resultant genome assemblies were evaluated with QUAST 5.0.2 (Gurevich et al., 2013). The final 4,578,245 and 4,046,806 bp-long genome assemblies (Br8 and Be9 respectively) were functionally annotated through Rapid Annotation System Technology (RAST) server using the default RASTtk parameter (Brettin et al., 2015). Additionally, assembled sequences were uploaded to RNAmmer v1.2 (Lagesen et al., 2007) and tRNAscan-SE v. 2.0 (Lowe and Chan, 2006) to predict the rRNA and tRNA genes respectively.

### **Design and optimization of a method for Br8 bacterial biomass immobilization on inorganic supports.**

In order to obtain an optimized matrix for efficient immobilization of bacterial cells with activity for uranium removal, different alginate/silica materials and hybrid systems were prepared and characterized.

#### ***Design and preparation***

##### *TEOS-based matrix*

Tetraethyl orthosilicate (TEOS) is the main component of the matrix for cell immobilization, being the most prevalent alkoxide of silicon. Procedure included two steps: First, the pure inorganic matrix (silica nanosol) fabrication and then the addition of immobilized cells to the inorganic matrix (silica bio-gel). A modified protocol fitting with our needs has been generated after optimization tests performed during this work. This step consists on the hydrolysis of the precursor (TEOS) and the formation of silica nanosol particles.

Initially, the aqueous silica nanosols were prepared by stirring 5 mL (14% v/v) of TEOS, 20 mL of ethanol, and 10 mL of 0.01 N HCl catalyst for 20 hours at room temperature for achieving TEOS hydrolysis. To prevent microbial contaminations nanosol components,

## MATERIALS AND METHODS

except ethanol, were sterilized either by autoclaving (HCl solution) or 0.22  $\mu\text{m}$  filtering. In order to make this material suitable for hosting bacteria, the ethanol should be removed. This elimination was carried out through evaporation by stirring the solution under slight warming for several hours, resulting in an ethanol evaporation rate about 0.9 mL/h. Then, resulting silica nanosol (TEOS hydrolyzed) was mixed with 27.5 ml water and concentrated to a final volume of 35 ml (in order to remove ethanol) by slightly warming up and stirring. To produce these biocompatible gelled matrices its pH should be increased to a value about 6-7.5, due to initial pH was around 2 to 3. The increase of pH to 6.8 was achieved with the addition of 40 $\mu\text{L}$  of NaOH (5N) in 35 mL of nanosol produced. In this way, no need of pH adjustment by using pH-meter is needed and therefore, sterile conditions can be maintained. Once pH is neutralized the gelation occurred after 1 - 20 minutes depending on TEOS concentration. For bacteria immobilization in this support, fresh Br8 cell cultures were prepared and recovered as explained below. A determined volume of this concentrated bacteria solution was added just after neutralization in order to make a homogeneous mix before gelation in a sterile Petri dish. Silica bio-gel was poured into dishes to get a layer thickness of approximately 7 mm. The solid bio-gel produced was stored at 4°C for 3 days.

### *Na-alginate beads*

In this case, sodium alginate (Na-alginate) was the main component of the matrix, a natural polysaccharide extracted from brown seaweed. One of its principal characteristics is the solidification in presence of calcium ( $\text{CaCl}_2$ ) without the need of heat. Formed gel is heat stable up to 150°C as well as highly stable to freeze/thaw cycles. Additionally, it shows high porosity allowing high diffusion rates for substrates, and high biocompatibility, making this material a “bacteria-friendly” environment. Sodium-alginate concentration in the beads is a key factor affecting their behaviour at mechanical stability and activity level. However, this material has some limitations like its low stability, since substances such as phosphate or citrate, which have a high affinity for  $\text{Ca}^{2+}$ , may sequester the cross-linking calcium ions and destabilize the gel. Since  $\text{Ca}^{2+}$  can be exchanged with other cations, the gel might also be destabilized by high concentrations of non-gel-inducing ions, such as  $\text{Na}^+$  and  $\text{Mg}^{2+}$ .

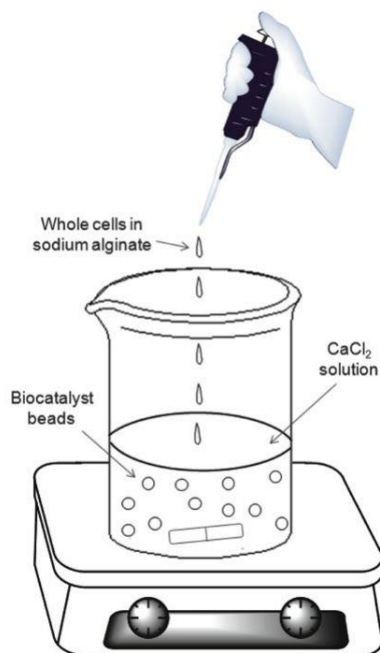


**Figure 1.** Schematic drawing of the alginate immobilization procedure (Rivero, 2013)

Protocol obtained from a previous publication (Smidsrød and Skjakbraek, 1990) was originally used in order to produce Na-alginate beads with the capacity of hosting bacterial cells which may remain under viable conditions for long time. A modified protocol fitting with our needs was generated after optimization tests performed during this work. Between 2% and 4% (w/v) aqueous stock solutions of Na-alginate were prepared in distilled water and sterilized by autoclaving. Washed *Stenotrophomonas* sp. Br8 living cells resuspended in saline solution (0.9%) were mixed with any of these solutions in the right proportion to obtain bacteria-doped 1.5%, 2%, 3% and 4% Na-alginate beads. Abiotic beads with the same Na-alginate concentrations were prepared for comparative purposes. Mixed solutions were dropped through a syringe (inner diameter of 0.3 – 0.6 mm) into a solution containing 2.5% (0.3 M) CaCl<sub>2</sub> (Fig. 1). Beads were left in solution for 1 – 2 hours at room temperature for hardening and washed with 0.9% saline solution. Finally, Na-alginate beads were transferred to new saline solution until further use.

### *Hybrid material*

Amino-functionalized silica nanosols formed with hydrolyzed TEOS and a diamino-functional silane (N-(2-aminoethyl)-3-aminopropyltrimethoxysilane) were used as the

## MATERIALS AND METHODS

matrix where alginate beads were embedded. Different versions of this hybrid material were generated by embedding Br8-doped alginate beads in an amino-functionalized silica gel which had been also doped or not with Br8 cells. Preparation protocol consisted in a first step where a silica sol was prepared similarly as described above by using TEOS, ethanol, 0.01 N HCl as catalyst and de-ionized water. Mix solution was incubated overnight and just when pH was increased and Br8 incorporated to the nanosol (in the case of double-doped version), 2% alginate beads including bacteria were amended. Then, the mix was homogenized and poured in a Petri dish where it gelled after incubation for some minutes at room temperature.

### *Characterization of immobilization matrices*

#### *Physico-chemical characterization and determination of the functional groups implicated in the interaction cells/matrix*

All different proposed matrices were dried until achieving a dust sample through a soft pounding. Average particle size was measured in the different nanosols and bio-gels generated. This determination was performed by using a *Nanosizer* equipment (Zetasizer 1000HS) available at Applied Physics Department of the University of Granada. Moreover, by using Fourier Transform Infrared (FT-IR) method through the equipment JASCO 6200 (4000-400  $\text{cm}^{-1}$ ; resolution 0,25  $\text{cm}^{-1}$ ) available in the Technical Services (Centro de Instrumentación Científica, CIC) of the University of Granada, main functional groups implicated in the interaction cells/matrix were identified as well as background spectra of materials used as immobilizing materials. Infrared spectroscopy uses the absorption of IR radiation by the molecular bonds to identify the bond types that can absorb energy by oscillating, vibrating, and rotating (Fig. 2). FT-IR technique is commonly used for the study of microbiological samples due to absorption bands are observed in the region between approximately 800 and 4000  $\text{cm}^{-1}$  and can often be assigned to particular functional groups (Lasch and Naumann, 2015). Software Spectra Manager v.2 was employed for analysing the obtained spectra.

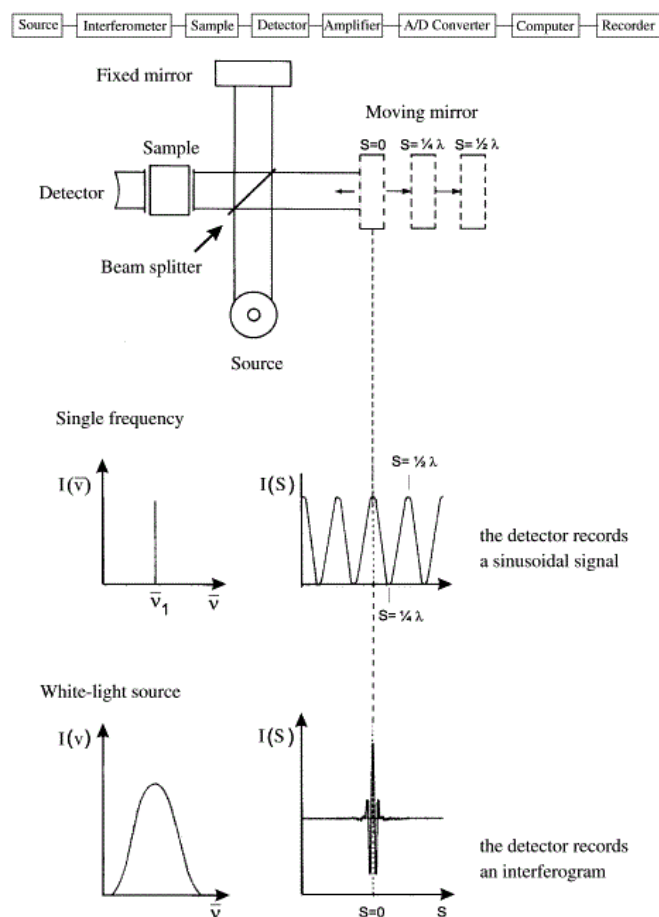


**Figure 2.** Schematic representation of the basic components of an FT-IR spectrometer (Beekes et al., 2007).

### *Cell distribution and effect of the immobilization process in the matrix*

Scanning Electron Microscopy (SEM) and Scanning Transmission Electron Microscopy (STEM) images were used for evaluation of cell distribution within the Br8-doped biomaterials. Microstructural features of different abiotic and biotic immobilization matrices were determined by scanning electron microscopy (Zeiss VPSEM, LEO 1430-VP and Zeiss FESEM, AURIGA) equipped with Energy-dispersive X-ray spectroscopy (EDS) microanalysis. Samples were carbon coated prior to SEM observations. This feature indicates how homogeneous or heterogeneous were organized the cells, what could be related with the efficiency of the matrix at activity level. Also, the general structure of the different matrices analysed was precisely described. Moreover, the comparison of these characteristics in bacteria-doped immobilization supports and abiotic ones, allowed the observation of potential effects of the biotic agent in the inorganic support.



## MATERIALS AND METHODS

### *Mechanical and chemical stability of the materials*

Stability assays were performed to confirm microscopy observations and therefore to assign their real stability in presence of variable conditions. At mechanical stability level, biotic and abiotic beads with different Na-alginate concentration were incubated during 4 and 8 weeks in saline solution under agitation conditions (120 – 130 rpm). At chemical stability, several tests were performed by contacting the different bead variants with a Na-citrate solution (50 mM) and incubated under agitation. As stated above, citrate may act as a calcium chelator due to its high affinity for calcium ions, destabilizing the structure of Na-alginate beads which are crosslinked with  $\text{Ca}^{2+}$ . In this way, citrate shows an analogue behaviour as other compounds like phosphates, lactate or EDTA.

### *Bacterial viability and purity within the matrix*

In order to evaluate the biocompatibility and bacterial viability, different variants of the matrices were tested by using LB culture medium. The biocompatibility determines the viability of the cells once they are immobilized in the matrix, and therefore, their associated bio-activity. Br8 doped matrices were incubated in saline solution at room temperature for certain periods of time (1 day, 20 days, 60 days and 120 days). After the incubation, these samples were crushed under sterile conditions on a LB plate and incubated for 48h at 28°C. Purity of the system was determined by checking that only the bacterial strain Br8 was present in it.

### *Evaluation of storage procedures*

For an optimal long-term preservation of Br8 bioactivity within the immobilization matrices proposed, two different approaches were assayed: drying and freeze-drying. In this way, activities such as conservation, manipulation or transportation of these biomaterials become more convenient. TEOS-based silica bio-gels and Na-alginate beads were lyophilized and maintained for 1 and 2 weeks. After that time, they were rehydrated during two hours in sterile water and tested for Br8 viability in LB culture medium. Fresh silica bio-gels were also air-dried at room temperature under sterile conditions and resultant weight reductions were continuously monitored.

## **Interactions bacteria-U**

### ***Bacterial strains and growth conditions***

*Stenotrophomonas* sp. Br8 and *Microbacterium* sp. Be9 cells were grown aerobically in LB medium (tryptone 10 g/l, yeast extract 5 g/l and NaCl 10 g/l, pH  $7.0 \pm 0.2$ ) at 28 – 30°C and 165 rpm on a rotary shaker. After 24h biomass was centrifuged at 8,000 g for 5 min and washed twice with 0.9% NaCl solution to eliminate growth interferences. Bacterial growth was followed by measuring optical densities at 600 nm. For optimized protocol of Na-alginate beads preparation, Br8 biomass were re-dissolved in a small volume (1 – 2 mL) of isotonic saline solution.

### ***Uranium sources***

#### ***Synthetic U stock solution***

Uranyl nitrate hexahydrate ( $\text{UO}_2(\text{NO}_3)_2 \cdot 6\text{H}_2\text{O}$ ) (Sigma-Aldrich) was prepared as a 0.1M stock solution by dissolving appropriate quantities in 0.1 M sodium perchlorate ( $\text{NaClO}_4$ ).

#### ***U-rich natural waters***

Five samples of natural field-waters containing different U concentrations and chemical composition were obtained (Fig. 3). For the realisation of various experiments, two different pre-treatments were considered in each sample: (1) Natural-water, samples were assayed without any preliminary treatment, conserving intact their microbial activity; (2) Sterile-water, pre-treatment consisted in the filter-sterilization of the samples in order to remove microbes present without modifying their physicochemical properties. By using natural and sterile sub-samples, the role of the bacterial strains independently of other microbes occurring spontaneously in the studied water-samples was expected to be ascertained.



**Figure 3.** Uranium-containing mining water samples used for the different assays.

### *General experimental setup*

Every assay performed consisted in a number of acid-washed glass Erlenmeyer flasks representing different treatments which included abiotic (without bacteria) and no-uranium control treatments.

Flasks included a different U source depending on the assay: in unnatural U solutions, MOPS-buffered medium was supplemented with different concentrations (0.01 to 1 mM) of U(VI) and/or 5 mM glycerol-2-phosphate (G2P) as the sole organic phosphates source. When U-rich natural waters (natural and sterile) were assayed, 5 mM G2P was also added. Free-G2P and free-bacteria treatments were included as controls.

Biotic treatments were inoculated with mid-exponential phase washed biomass grown in LB medium or Br8 doped Na-alginate beads. Optical density (O.D.) was in all cases established between 0.6 – 0.8 by measuring at 600 nm with Thermo Scientific™ GENESYS 10S UV-Vis spectrophotometer. For the assay with dead cells, the recovered biomass was exposed to 80°C incubation for 1h and applied to the experimental flasks as performed in all other experiments. Incubations were always conducted under control temperature conditions (28 – 30°C) and continuous shaking (145 - 165 rpm) to maintain aerobic conditions. Time of incubation was 48h in all cases, except the kinetics experiment, whose sampling times varied in each assay. Once incubations were completed, all replicate liquid samples were centrifuged at 10,000 g for 10 min at 4°C, and supernatants and solid pellets analysed separately by using different techniques described afterwards. Solid phase

precipitates recovered were washed twice with 0.9% NaCl to remove the interfering elements of the incubating solution.

Aseptic techniques were followed during assembly and sub-sampling of all treatments. All treatments were conducted in triplicate and all subsequent analyses utilized all replicates data from each respective treatment for statistics.

### *Quantification of U removal*

In recovered supernatants (from experiments described above), U concentration was analysed spectrophotometrically using the Arsenazo III method (Jauberty et al., 2013). Reagent was prepared by dissolving 70 mg of 2,7-bis(2-arsenophenylazo)-1,8-dihydroxynaphthalene-3,6-disulfonic acid (Arsenazo-III) into 1 L of 3 M HClO<sub>4</sub>. Each time the reagent was prepared, a calibration curve was realised using different U concentration samples (1, 2.5, 5, 10, 20, 40, 60, 80 and 100 ppm), fitting by polynomial approximation. To realise the measures, 250 µl from each subsample were mixed with 1 mL of reagent. Absorbance was measured at 651 nm with Thermo Scientific™ GENESYS 10S UV-Vis spectrophotometer. Also, the final concentration of U(VI) remaining in solution was determined by inductively-coupled plasma mass spectrometry (ICP-MS) with a NexION 300d (PerkinElmer) system after HNO<sub>3</sub> acidification using multi-element standard solutions for calibration. The concentration of U removed in treatments was calculated as the difference between the initial and final U concentrations.

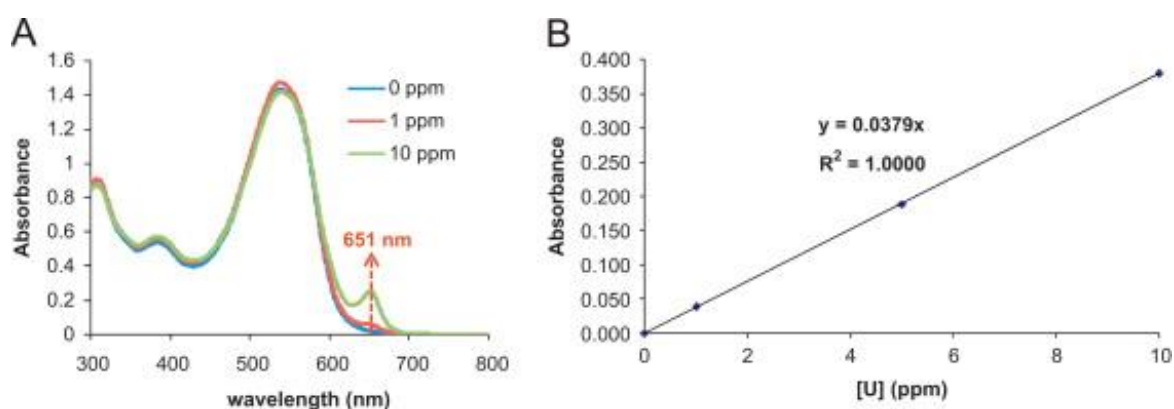


**Figure 4.** (A) UV spectra of assay mixture in presence of different uranium concentrations (0, 1 and 10 ppm). (B) Correlation curve between uranium concentration (ppm) and absorbance at 651 nm (Jauberty et al., 2013).

### ***Calculation of inorganic phosphates release***

After every incubation, inorganic phosphate (Pi) concentration in recovered supernatants was quantified by ammonium-molybdate and ascorbic acid method (Murphy and Riley, 1962). This colorimetric procedure is based in the reaction of the orthophosphate ions with ammonium-molybdate in acidic solution forming phosphomolybdic acid. After reduction with ascorbic acid, the resultant compound shows an intensely blue complex measurable at 850 nm after exactly 30 minutes. A standard curve was determined in order to obtain a linear fit value for correct calculations. Antimony potassium tartrate is added to increase the rate of reduction.

### ***Determination of phosphatase enzymatic activity***

Phosphatase activity calculation was carried out using Methylumbelliferyl (MUB)-linked phosphate as optimized and described German et al., 2011. Cell samples from different assays were dissolved in sodium perchlorate buffer (pH 5) and MUB standards (0.16  $\mu$ M, 0.625  $\mu$ M, 1.25  $\mu$ M and 2.50  $\mu$ M) in order to calculate the emission and quench coefficients using an automatic fluorometer NanoQuant Infinite 200 PRO Tecan. Enzyme activity calculations were performed following German et al. (2011).

### ***Cell viability and activity***

The cell viability and the metabolic activity of *Stenotrophomonas* Br8 and *Microbacterium* Be9 strains in the presence of U(VI) were determined by using flow cytometry technique. Flow cytometry is a multiparametric analysis technique where cells flow one by one through an area illuminated by a laser beam. Information about the cells is obtained using different fluorescent labels (Lakowicz, 2006), being the emission fluorescence from the cells quantitatively proportional to excitation intensity of the fluorochrome employed. Cultures were prepared as stated above with an initial concentration of U (0.01 – 1 mM). After 24 h and 48 h incubation cells were collected by centrifugation at 11.000 g and 4°C for 10 min. The resultant pellets were washed three times and dissolved in phosphate buffered saline (PBS) solution at pH 7. For the cell viability test, fluorescein diacetate (FDA) and propidium iodide (PI) were added to each sample to a final concentration of 20  $\mu$ L/mL and 2  $\mu$ L/mL, respectively. The fluorescent dye FDA can diffuse across intact cell

membranes (living cells) being enzymatically hydrolysed to green fluorescent products and, in contrast, PI is an intercalating DNA-binding dye exclusive of dead cells with injured cell membranes, which stains them in red. In the case of metabolic activity, 3,3'-dihexyloxycarbocyanine iodide (DiOC<sub>6</sub>) was used at a final concentration of 20 µL/mL. DiOC<sub>6</sub> is a positively charged lipophilic dye which binds to the membrane of actively growing cells. Finally, all samples were analysed by Forward Scatter using a FACSCanto IITM cytometer (Becton Dickinson, San Jose, CA, USA) available from *Centro de Instrumentación Científica at Universidad de Granada* (Granada, Spain).

### **Spectroscopic and microscopic characterization of U precipitates**

Once solid pellets were recovered separately and washed twice with 0.9% NaCl, U precipitates present were analysed by spectroscopic and microscopic techniques.

#### ***Cellular localization of U (HAADF/STEM, HRTEM/EDAX)***

High Angle Annular Dark Field (HAADF) Scanning Transmission Electron Microscopy (STEM) and High-Resolution Transmission Electron Microscopy / Energy-Dispersive X-Ray analyser (HRTEM/EDAX) microscopic techniques were employed for localizing the U precipitates at cellular level and to determine their chemical composition. Uranium-treated cells in suspension were harvested by centrifugation at 15000 x g for 15 min at 4°C, washed twice with sodium cacodylate buffer (pH 7.2), fixed with glutaraldehyde in cacodylate buffer (4%) and stained with osmium tetroxide (1%, 1 h) in the same buffer before being dehydrated through graded alcohol followed by propylene oxide treatment and finally was embedded in epoxy resin. Ultrathin sections (0.1 µm) of the samples, obtained using an ultra-microtome, were loaded in carbon coated copper grid and analysed by high-angle annular dark field scanning transmission electron microscope (HAADF-STEM), conducted using a FEI TITAN G2 80-300. The TEM specimen's holders were clean by plasma prior to STEM analysis to minimize contamination. The high-resolution STEM is equipped with HAADF detector and EDAX energy dispersive X-ray, which provides elemental information via the analysis of X-ray emissions caused by a high-energy electron beam.



**Figure 5.** High-Angle Annular Dark Field Scanning Transmission Electron Microscope FEI TITAN G2 80-300 available at *Centro de Instrumentación Científica (Universidad de Granada)*.

### *Characterization of U precipitates by X-Ray Absorption Spectroscopy (XAS)*

X-ray absorption spectra analysis consists in an atomic or molecular characterization of any material by X-ray photon energies. These energies produce sharp increases in detected absorption which are characteristic of the absorbing element (Yano and Yachandra, 2009). X-ray absorption near-edge structure (XANES) spectra provide detailed information about the oxidation state and coordination environment of the metal atoms, while extended X-ray absorption fine structure (EXAFS) studies the fine structure in the absorption at energies greater than the threshold for electron release. These two methods provide complementary structural information about electronic structure / symmetry and numbers, types and distances to atoms from the absorbing element respectively (Yano and Yachandra, 2009).

With the purpose of characterizing the uranium solid phases precipitated during assays performance, Extended X-Ray Absorption Fine Structure (EXAFS) spectroscopy was applied. This technique is a medium energy third-generation synchrotron optimized for the production of vacuum-ultraviolet (VUV) and soft X-ray light from undulators and operated with electrons at energy of 2.75 GeV. In particular, the MARS beamline was built on the bending magnet port D03-1 of the SOLEIL storage ring. The 1.71 T bending magnet field provides a continuous spectrum of photons with a critical energy of 8.6 keV. After

incubation, cells were harvested and washed with 0.1 M NaClO<sub>4</sub>. The pellets were dried in an oven at 30°C for 24 h and subsequently powdered. Data were collected in fluorescence mode using a 13-element Ge detector (EG & G ORTEC, USA) and processed by using the ATHENA code (Ravel and Newville, 2005). FEFF is an automated program for ab initio multiple scattering calculations of EXAFS, X-ray Absorption Near-Edge Structure (XANES) and various other spectra for clusters of atoms. EXAFS analyses were performed in the SOLEIL synchrotron (Paris, France).

### *Characterization of U precipitates by X-Ray Diffraction (XRD)*

X-ray diffraction is a non-destructive and analytical technique used for the identification and characterization of crystalline materials, recognition of crystalline phases (polymorphism), and orientation of polymers (Visakh et al., 2016). The local structure of biogenic U precipitates produced in the different assays was determined by XRD analyses. U treated samples were dried in an oven at 70°C for 6 h, scraped and crushed into a fine powder that was analysed using a X'Pert PRO (PANalytical B-V.) equipped with Cu-K $\alpha$  radiation; Ni filter; 45 kV voltage; 40 mA intensity; exploration range of 3° - 60° 2 $\theta$ ; and goniometer speed of 0.05° 2 $\theta$  s<sup>-1</sup>. Patterns obtained were analysed with X Powder software.

### References

- Altschul, S.F., Gish, W., Miller, W., Myers, E.W., Lipman, D.J., 1990. Basic local alignment search tool. *J. Mol. Biol.* 215, 403–410. [https://doi.org/10.1016/S0022-2836\(05\)80360-2](https://doi.org/10.1016/S0022-2836(05)80360-2)
- Beekes, M., Lasch, P., Naumann, D., 2007. Analytical applications of Fourier transform-infrared (FT-IR) spectroscopy in microbiology and prion research. *Vet. Microbiol.* 123, 305–319. <https://doi.org/10.1016/j.vetmic.2007.04.010>
- Brettin, T., Davis, J.J., Disz, T., Edwards, R.A., Gerdes, S., Olsen, G.J., Olson, R., Overbeek, R., Parrello, B., Pusch, G.D., Shukla, M., Thomason, J.A., Stevens, R., Vonstein, V., Wattam, A.R., Xia, F., 2015. RASTtk: A modular and extensible implementation of the RAST algorithm for building custom annotation pipelines and annotating batches of genomes. *Sci. Rep.* 5. <https://doi.org/10.1038/srep08365>
- Chun, J., Lee, J.H., Jung, Y., Kim, M., Kim, S., Kim, B.K., Lim, Y.W., 2007. EzTaxon: A web-based tool for the identification of prokaryotes based on 16S ribosomal RNA gene sequences. *Int. J. Syst. Evol. Microbiol.* 57, 2259–2261. <https://doi.org/10.1099/ijs.0.64915-0>
- Clark, W.A., 1976. A Simplified Leifson Flagella Stain. *J. Clin. Microbiol.* 3, 632–634.
- German, D.P., Weintraub, M.N., Grandy, A.S., Lauber, C.L., Rinkes, Z.L., Allison, S.D., 2011. Optimization of hydrolytic and oxidative enzyme methods for ecosystem studies. *Soil Biol. Biochem.* 43, 1387–1397. <https://doi.org/10.1016/j.soilbio.2011.03.017>
- Gurevich, A., Saveliev, V., Vyahhi, N., Tesler,



## MATERIALS AND METHODS

- G., 2013. QUASt: Quality assessment tool for genome assemblies. *Bioinformatics* 29, 1072–1075.  
<https://doi.org/10.1093/bioinformatics/btt086>
- Jauberty, L., Drogat, N., Decossas, J.L., Delpech, V., Gloaguen, V., Sol, V., 2013. Optimization of the arsenazo-III method for the determination of uranium in water and plant samples. *Talanta* 115, 751–754.  
<https://doi.org/10.1016/j.talanta.2013.06.046>
- Lagesen, K., Hallin, P., Rødland, E.A., Stærfeldt, H.H., Rognes, T., Ussery, D.W., 2007. RNAmmer: Consistent and rapid annotation of ribosomal RNA genes. *Nucleic Acids Res.* 35, 3100–3108.  
<https://doi.org/10.1093/nar/gkm160>
- Lakowicz, J.R., 2006. Principles of fluorescence spectroscopy, 3rd Edition, Joseph R. Lakowicz, editor, Principles of fluorescence spectroscopy, Springer, New York, USA, 3rd edn, 2006.  
<https://doi.org/10.1007/978-0-387-46312-4>
- Lasch, P., Naumann, D., 2015. Infrared Spectroscopy in Microbiology. *Encycl. Anal. Chem., Major Reference Works.*  
<https://doi.org/https://doi.org/10.1002/9780470027318.a0117.pub2>
- Lowe, T.M., Chan, P.P., 2006. tRNAscan-SE: Searching for tRNA Genes in Genomic Sequences 1962, 1–21.
- Martín-Platero, A.M., Valdivia, E., Maqueda, M., Martínez-Bueno, M., 2007. Fast, convenient, and economical method for isolating genomic DNA from lactic acid bacteria using a modification of the protein “salting-out” procedure. *Anal. Biochem.* 366, 102–104.  
<https://doi.org/10.1016/j.ab.2007.03.010>
- Murphy, J., Riley, J.P., 1962. Determination Single Solution Method For The In Natural Waters. *Anal. Chim. Act* 27, 31–36.
- Ravel, B., Newville, M., 2005. ATHENA, ARTEMIS, HEPHAESTUS: data analysis for X-ray absorption spectroscopy using IFEFFIT. *J. Synchrotron Radiat.* 12, 537–541.  
<https://doi.org/10.1107/S0909049505012719>
- Rivero, J.A.T. and C.W., 2013. Whole Cell Entrapment Techniques. In: Guisan J. (eds) *Immobilization of Enzymes and Cells.* *Immobil. Enzym. Cells* 1051, 365–374.  
<https://doi.org/10.1007/978-1-62703-550-7>
- Rossbach, S., Wilson, T.L., Kukuk, M.L., Carty, H.A., 2000. Elevated zinc induces siderophore biosynthesis genes and a zntA-like gene in *Pseudomonas fluorescens*. *FEMS Microbiol. Lett.* 191, 61–70.  
[https://doi.org/10.1016/S0378-1097\(00\)00371-2](https://doi.org/10.1016/S0378-1097(00)00371-2)
- Sánchez-Castro, I., Amador-García, A., Moreno-Romero, C., López-Fernández, M., Phrommavanh, V., Nos, J., Descostes, M., Merroun, M.L., 2017. Screening of bacterial strains isolated from uranium mill tailings porewaters for bioremediation purposes. *J. Environ. Radioact.* 166, 130–141.  
<https://doi.org/10.1016/j.jenvrad.2016.03.016>
- Smidsrød, O., Skjakbraek, G., 1990. Alginate as immobilization matrix for cells. *Rev. Philos. Psychol.* 8, 71–78.  
[https://doi.org/10.1016/0167-7799\(90\)90139-O](https://doi.org/10.1016/0167-7799(90)90139-O)
- Visakh, P.M., Markovic, G., Pasquini, D., 2016. *Recent Developments in Polymer Macro, Micro and Nano Blends: Preparation and Characterisation.* Woodhead Publishing.
- Yano, J., Yachandra, V.K., 2009. X-ray absorption spectroscopy. *Photosynth. Res.* 102, 241–254.  
<https://doi.org/10.1007/s11120-009-9473-8>

## CAPÍTULO I:

### **Draft genome sequence data of *Microbacterium* sp. strain Be9 isolated from uranium-mill tailings porewaters**

Pablo Martínez-Rodríguez<sup>1</sup>, Iván Sánchez-Castro<sup>1</sup>, Michael Descostes<sup>2,3</sup>, Mohamed L. Merroun<sup>1</sup>

<sup>1</sup> Department of Microbiology, University of Granada, Campus Fuentenueva s/n, 18071 Granada, Spain.

<sup>2</sup> ORANO Mining, Environmental R&D Department, 125 Avenue de Paris, 92330, Châtillon, France.

<sup>3</sup> PSL University/Mines ParisTech, Centre de Géosciences, 35 rue Saint-Honoré, 77305, Fontainebleau, France.

Este capítulo ha sido publicado en la revista Data in Brief:

Martínez-Rodríguez, P., Sánchez-Castro, I., Descostes, M., Merroun, M.L., 2020. Draft genome sequence data of *Microbacterium* sp. strain Be9 isolated from uranium-mill tailings porewaters. Data Br. 31, 10–14. <https://doi.org/10.1016/j.dib.2020.105732>



**Abstract**

*M*icrobacterium are Gram-positive, nonspore-forming, rod-shaped bacteria inhabiting a wide range of environments including soil, water, dairy products, other living organisms, etc. *Microbacterium* sp. strain Be9, isolated from mill tailings porewaters in France, shows a remarkable behavior in presence of uranium under distinct conditions, which is the main reason for the interest in sequencing its genome. In this work, we describe the draft genome sequence of Be9, comprising 4,046,806 bp, with a G+C content of 68.10% and containing 3,947 protein-coding sequences. The preliminary genome annotation analysis identified some genes encoding for resistance to antibiotics and toxic compounds like heavy metals. This draft genome has been deposited at DDBJ/ENA/GenBank under the accession PRJNA590666.

**Keywords:** *Microbacterium*, Porewaters, Draft genome, Heavy metal, Uranium

## Data Description

*Microbacterium* spp. are Gram-positive, nonspore-forming and rod-shaped. Strains of the genus are distributed widely, such as in soil, water, dairy products or other living organisms (Kook et al., 2014; Lee et al., 2006; Yan et al., 2017).

**Table 1.** Project features and general information of *Microbacterium* sp. Be9 strain according to MIGS recommendations (Field et al. 2008). <sup>a</sup> Evidence codes - IDA: inferred from direct assay; TAS: traceable author statement (i.e., a direct report exists in the literature); NAS: non-traceable author statement (i.e., not directly observed for the living, isolated sample, but based on a generally accepted property for the species, or anecdotal evidence). These evidence codes are from the Gene Ontology project (Ashburner et al. 2000).

Property	Term	Evidence code <sup>a</sup>
Geographic location	Limousin/France	TAS
Latitude	46°5'49.09" N	TAS
Longitude	1°23'28.51" E	TAS
Depth	25 m	TAS
Time of sample collection	March 2012	TAS
Habitat	Groundwater	TAS
Number of replicons	-	-
Extrachromosomal elements	-	-
Reference for biomaterial	<a href="https://doi.org/10.1016/j.jenvrad.2016.03.016">dx.doi.org/10.1016/j.jenvrad.2016.03.016</a>	TAS
Source material identifiers	Still not deposited	-
Pathogenicity	Unknown	-
Biotic relationship	Free-living	TAS
Specific host	Environmental	TAS
Trophic level	Heterotroph	TAS
Oxygen requirement	Aerobic	TAS
Isolation and growth conditions	Isolated in R2A medium at 28°C	TAS
Nucleic acid preparation	Genomic DNA extraction (Martín-Platero et al., 2007)	IDA
Sequencing method	150bp paired-end sequencing reads	IDA
Assembly	<i>De novo</i> assembly, based on <i>de Bruijn</i> graphs (Phillip E. C. Compeau, Pavel A. Pevzner, 2015)	IDA
Finishing quality	Draft sequence	IDA
Sequencing platforms	Illumina Novaseq	IDA
Fold coverage	462x	IDA

*Microbacterium* sp. Be9 strain was isolated from porewaters sampled in mill tailings, located near Bessines-sur-Gartempe (Limousin, France). By a 16S rRNA gene sequence analysis (unpublished data), we classified Be9 within the genus *Microbacterium*. In

previous studies, isolate Be9 was evaluated and displayed high tolerance values for different metals/metalloids as U, Pb, Se or Zn (Sánchez-Castro et al., 2017), indicating that this strain may have a potential ability in bioremediation of heavy metals. Based on this fact and other previous experiments (unpublished data), we selected *Microbacterium* sp. Be9 for genome sequencing to identify genes potentially involved in its uranium removal ability (Table 1). The draft genome was comprised by 14 contigs, with 4,046,806 bp in length and N50 value of 1,332,702. The G+C content of the sequence was 68.10%. Main assembly statistics of the draft genome are shown in Table 2. Three copies of rRNA genes were predicted in the genome by using the RNAmmer V1.2 (Lagesen et al., 2007) while 50 copies of tRNA were anticipated by tRNAscan-SE v. 2.0 (Lowe and Chan, 2006).

**Table 2.** Main de novo assembly statistics of Be9 draft genome

<b>Feature</b>	<b>Value</b>
Contig count	14
Total contigs length (bp)	4,046,806
Total number of aligned bases (Mbp)	1,871
N50 (bp)	1,332,702
N75 (bp)	370,482
Maximum contig length (bp)	1,434,936
Average contig length (bp)	289,057
G+C content	68.10%
rRNA genes	3
tRNA genes	50

A total of 3947 protein-coding sequences were predicted using Rapid Annotation Subsystem Technology (RAST) (Brettin et al., 2015), where 1002 coding sequences (26%) were annotated as seed subsystem features and 2945 coding sequences (74%) as outside of the seed subsystem. Most of the annotated genes (Fig. 1) determined the synthesis of amino acids and derivatives (306), carbohydrates (206), protein metabolism (171) and cofactors, vitamins, prosthetic groups and pigments (148). As well, the strain Be9 possesses a substantial number of genes responsible for resistance to antibiotics and toxic compounds (36), membrane transport (78) and stress response (26). In the genome of *Microbacterium* sp. Be9 was uncovered the presence of *amt* gene, whose expression was regulated in

response to ammonium availability to ensure an adequate supply of nitrogen during in-situ uranium bioremediation (Mouser et al., 2009). Cobalt-zinc-cadmium resistance protein coding region (*CzcD*) was found in the draft genome of Be9 as well as in other *Microbacterium* species exposed to high metal concentrations, suggesting a relevant role implicated in its tolerance (Fierros-Romer et al., 2016). In addition, the Be9 genome annotation suggested the presence of ABC-type Fe<sup>3+</sup> siderophore transport proteins related to iron metabolism whose levels were increased under uranium stress as it was reported earlier (Gallois et al., 2018). Numerous genes involved in the interaction with metals/metalloids like copper (*CopC* and *CopD*), selenate and selenite (*DedA*), zinc (*YpfJ*) and arsenic (*ArsR*, *ArsB*, *ArsC* and *ACR3*) were also detected.

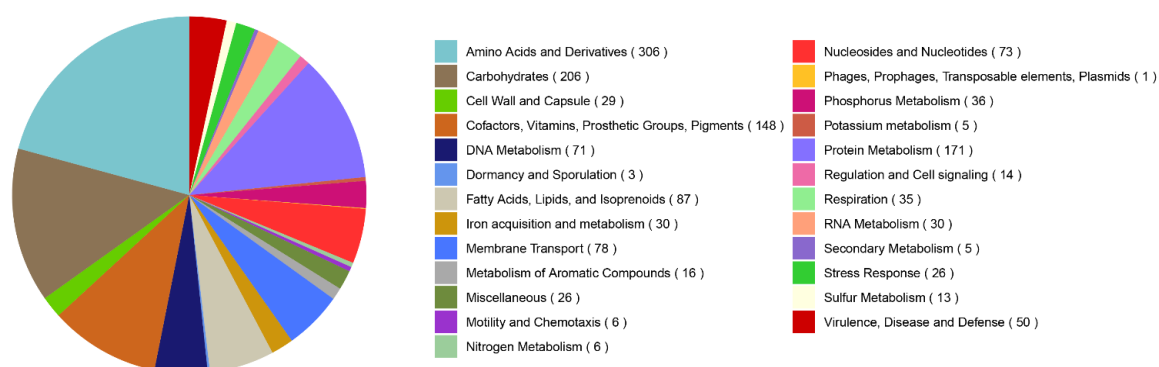


**Figure 1.** An overview of the subsystem categories assigned to the genome of *Microbacterium* sp. Be9 strain. Genome sequence was annotated using Rapid Annotation System Technology (RAST) server.

## Experimental Design, Materials, and Methods

### *Isolation of Microbacterium sp. Be9 strain*

*Microbacterium* sp. Be9 strain was isolated from uranium-containing porewaters of mill tailings, located near Bessines-sur-Gartempe (Limousin, France). These porewaters were collected from a monitoring well at 25 m depth, using an inertial water-pump (WaTerra Pumps Ltd.) and sterilized high-density polyethylene (HDPE) tubing and storing HDPE containers. At the time of sampling, pH and Eh of porewater were 6.25 and 161 mV/SHE respectively. The strain was isolated in R2A oligotrophic medium (low-nutrient medium) (Reasoner and Geldreich, 1985) and incubated at 28°C for 3 days.

### ***DNA isolation and sequencing***

Biomass of Be9 strain was grown in LB solid medium for 24h at 28°C, and genomic DNA extraction was performed as described by Martín-Platero (Martín-Platero et al., 2007). One µL of gDNA sample was used to test the integrity and purity by 1.5% agarose gel electrophoresis. Afterwards, the sample was quantified using the Qubit 3.0 Fluorometer (Life Technology) and used for library construction using the TruSeq DNA Whole genome library preparation kit (Illumina, USA). The generated DNA fragments (DNA libraries) were sequenced using the Illumina Novaseq platform, using 150bp paired-end sequencing reads. Low-quality reads were trimmed by CLC Genomics Workbench 12.0 to generate 14,144,710 reads with mean read length of 150bp.

### ***Genome assembly and annotation***

Quality-filtered reads were *de novo* assembled using an algorithm based on de Bruijn graphs performed by CLC Genomics Workbench 12.0 and resultant genome assemblies were evaluated with QUILT 5.0.2 (Gurevich et al., 2013). The final 4,046,806-bp-long genome assembly was functionally annotated through Rapid Annotation System Technology (RAST) server using the default RASTtk parameter (Brettin et al., 2015). Additionally, assembled sequence was uploaded to RNAmmer v1.2 (Lagesen et al., 2007) and tRNAscan-SE v. 2.0 (Lowe and Chan, 2006) to predict the rRNA and tRNA genes respectively.

### **Acknowledgments**

This paper comes from a Joint Research Project between Orano Mining R&D Department and the Department of Microbiology of the University of Granada. The authors thank Orano Mining for financial support.

### **References**

- Brettin, T., Davis, J.J., Disz, T., Edwards, R.A., Gerdes, S., Olsen, G.J., Olson, R., Overbeek, R., Parrello, B., Pusch, G.D., Shukla, M., Thomason, J.A., Stevens, R., Vonstein, V., Wattam, A.R., Xia, F., 2015. RASTtk: A modular and extensible implementation of the RAST algorithm for building custom annotation pipelines and annotating batches of genomes. *Sci Rep* 5. <https://doi.org/10.1038/srep08365>
- Dianawati, D., Mishra, V., Shah, N.P., 2016. Survival of Microencapsulated Probiotic Bacteria after Processing and during Storage: A Review. *Critical Reviews in Food Science and Nutrition* 56, 1685–1716. <https://doi.org/10.1080/10408398.2013.798779>
- Fierros-Romer, G., Gómez-Ramírez, M., Arenas-Isaac, G.E., Pless, R.C., Rojas-Avelizapa, N.G., 2016. Identification of *Bacillus megaterium* and *Microbacterium*

- liquefaciens* genes involved in metal resistance and metal removal. *Can J Microbiol* 62, 505–513. <https://doi.org/10.1139/cjm-2015-0507>
- Gallois, N., Alpha-Bazin, B., Ortet, P., Barakat, M., Piette, L., Long, J., Berthomieu, C., Armengaud, J., Chapon, V., 2018. Proteogenomic insights into uranium tolerance of a Chernobyl's *Microbacterium* bacterial isolate. *J Proteomics* 177, 148–157. <https://doi.org/10.1016/j.jprot.2017.11.021>
- Gurevich, A., Saveliev, V., Vyahhi, N., Tesler, G., 2013. QUASt: Quality assessment tool for genome assemblies. *Bioinformatics* 29, 1072–1075. <https://doi.org/10.1093/bioinformatics/btt086>
- Kook, M.C., Son, H.M., Yi, T.H., 2014. *Microbacterium kyungheense* sp. nov. and *Microbacterium jejuense* sp. nov., isolated from salty soil. *Int J Syst Evol Microbiol* 64, 2267–2273. <https://doi.org/10.1099/ijms.0.054973-0>
- Lagesen, K., Hallin, P., Rødland, E.A., Stærfeldt, H.H., Rognes, T., Ussery, D.W., 2007. RNAmmer: Consistent and rapid annotation of ribosomal RNA genes. *Nucleic Acids Res* 35, 3100–3108. <https://doi.org/10.1093/nar/gkm160>
- Lee, J.S., Lee, K.C., Park, Y.H., 2006. *Microbacterium koreense* sp. nov., from sea water in the South Sea of Korea. *Int J Syst Evol Microbiol* 56, 423–427. <https://doi.org/10.1099/ijms.0.63854-0>
- Lowe, T.M., Chan, P.P., 2006. tRNAscan-SE: Searching for tRNA Genes in Genomic Sequences 1962, 1–21.
- Martín-Platero, A.M., Valdivia, E., Maqueda, M., Martínez-Bueno, M., 2007. Fast, convenient, and economical method for isolating genomic DNA from lactic acid bacteria using a modification of the protein “salting-out” procedure. *Anal Biochem* 366, 102–104. <https://doi.org/10.1016/j.ab.2007.03.010>
- Mouser, P.J., N’Guessan, A.L., Elifantz, H., Holmes, D.E., Williams, K.H., Wilkins, M.J., Long, P.E., Lovley, D.R., 2009. Influence of heterogeneous ammonium availability on bacterial community structure and the expression of nitrogen fixation and ammonium transporter genes during in situ bioremediation of uranium-contaminated groundwater. *Environ Sci Technol* 43, 4386–4392. <https://doi.org/10.1021/es8031055>
- Phillip E. C. Campeau, Pavel A. Pevzner, G.T., 2015. Why are de Bruijn graphs useful for genome assembly? *Nat Biotechnology* 14, 871–882. <https://doi.org/10.1111/obr.12065>. Variation
- Reasoner, D.J., Geldreich, E.E., 1985. A new medium for the enumeration and subculture of bacteria from potable water. *Appl Environ Microbiol* 49, 1–7.
- Sánchez-Castro, I., Amador-García, A., Moreno-Romero, C., López-Fernández, M., Phrommavanh, V., Nos, J., Descostes, M., Merroun, M.L., 2017. Screening of bacterial strains isolated from uranium mill tailings porewaters for bioremediation purposes. *J Environ Radioact* 166, 130–141. <https://doi.org/10.1016/j.jenvrad.2016.03.016>
- Yan, Z.F., Lin, P., Won, K.H., Yang, J.E., Li, C.T., Kook, M.C., Wang, Q.J., Yi, T.H., 2017. *Microbacterium hibisci* sp. Nov., isolated from rhizosphere of mugunghwa (*Hibiscus syriacus* L.). *Int J Syst Evol Microbiol* 67, 3564–3569. <https://doi.org/10.1099/ijsem.0.002167>





## **CAPÍTULO II:**

### **Characterization and draft genome of *Stenotrophomonas* sp. Br8 strain, a bacterial isolate with high U-bioremediation capacity**

Pablo Martínez-Rodríguez<sup>1</sup>, Iván Sánchez-Castro<sup>1</sup>, Michael Descostes<sup>2,3</sup>, Mohamed L. Merroun<sup>1</sup>

<sup>1</sup> Department of Microbiology, University of Granada, Campus Fuentenueva s/n, 18071 Granada, Spain.

<sup>2</sup> ORANO Mining, Environmental R&D Department, 125 Avenue de Paris, 92330, Châtillon, France.

<sup>3</sup> PSL University/Mines ParisTech, Centre de Géosciences, 35 rue Saint-Honoré, 77305, Fontainebleau, France.

### **Abstract**

**S**tudies about microorganisms capable of immobilizing heavy metal are on the rise due to their potential use in bioremediation. The strain *Stenotrophomonas* sp. Br8 CECT 9810 is a gram negative and aerobic bacterium isolated from U tailing porewaters. The Br8 isolate has shown a high capacity for U phosphate biomineralization mediated by phosphatase activity. Here, its physiological, biochemical, and genomic characterization were carried out to better understand the U biomineralization potential of Br8. We report on the optimal growth conditions, cellular fatty acids and enzymatic activity of Br8. Phylogenetic analyses, conducted by Type Strain Genome Server and OAT Software, support the affiliation to *Stenotrophomonas* genus. U precipitation ability was demonstrated by STEM/HAADF microscopy. In addition to describing the draft genome sequence —containing 4,578,245 bp, and 4222 protein-coding sequences, as predicted in the genome annotation— we identify some specific genes related to U(VI) biomineralization (e.g., phosphatase-related coding regions). This draft genome has been deposited at NCBI GenBank under the accession code PRJNA649538.

**Keywords:** *Stenotrophomonas*; Draft genome; Genome annotation; Uranium; Biomineralization

## Introduction

Environmental contamination with radionuclides such as uranium (U) entails many ecological consequences as well as health issues. For this reason, the use of microorganisms as heavy metal bioremediation agents is a key research topic. Indigenous microbes from high radionuclide contaminated sites show higher tolerance to heavy metals and other toxic compounds (Lopez-Fernandez et al., 2021), and present different mechanisms to immobilize radionuclides. These microorganisms are therefore sound candidates for the design of efficient and eco-friendly strategies for uranium sequestration. Members of the genus *Stenotrophomonas* have an important ecological role in the biogeochemical cycle of different elements (Ryan et al., 2009) and reportedly exhibit resistance to various heavy metals. Diverse *Stenotrophomonas maltophilia* strains show tolerance to high concentrations of Cd, Se and Te (Pages et al., 2008), are Cu resistant (Ghosh and Saha, 2013) and can adapt to increased concentrations of Cu/Cd (Xiong et al., 2020). In particular, U-tolerance and different interaction mechanisms have been identified in *Stenotrophomonas* strains such as *Stenotrophomonas* sp. U18 and U22A (Islam and Sar, 2016), *Stenotrophomonas maltophilia* JG-2 (Merroun and Selenska-Pobell, 2008) or *Stenotrophomonas bentonitica* BII-R7 (Pinel-Cabello et al., 2021; Sánchez-Castro et al., 2017b).

*Stenotrophomonas* sp. Br8 strain is an aerobic bacterium, Gram negative, that forms small rods; it is motile by flagella and non-spore forming. In this case, it was isolated from porewaters sampled in U mill tailings located near Bessines-sur-Gartempe (Limousin, France). Recent studies indicate that the Br8 strain mediated a highly efficient process for soluble U(VI) immobilization in the presence of glycerol-2-phosphate (G2P) as organic phosphate substrate, able to tolerate and immobilize aerobically high U concentrations (Sánchez-Castro et al., 2020). Furthermore, Na alginate beads doped with Br8 cells were employed to remove U from complex mining waters, achieving a high rate of immobilization in the presence of G2P (Sánchez-Castro et al., 2021). The present study aimed to characterize the whole genome of the isolate Br8 to identify those genes potentially involved in U-tolerance and biomineralization capacity in U-contaminated environments. In addition, physiological, biochemical and phylogenetic analyses were performed to better characterize this isolate, determining the Br8 taxonomic classification and its physiological and biochemical properties.

### **Materials and methods**

#### ***Isolation of *Stenotrophomonas* sp. Br8 strain***

*Stenotrophomonas* sp. Br8 strain was isolated from uranium porewaters of mill tailings in Limousin, France (Sánchez-Castro et al., 2017a). The samples were collected from a monitoring well at 35 m depth, using an inertial water-pump (WaTerra Pumps Ltd.) and sterilized high-density polyethylene (HDPE) tubing, then stored in HDPE containers. At the time of sampling, the porewater pH and Eh values were, respectively, 5.80 and 250 mV/SHE. The strain was isolated in R2A oligotrophic medium (low-nutrient medium) (Reasoner and Geldreich, 1985) and incubated at 28°C for 3 days.

#### ***Physiology, chemotaxonomic and biochemical analyses***

*Stenotrophomonas* Br8 cells were grown on LB broth at 28°C for 24 h and observed by scanning electron microscopy (FEI Quanta-400 ESEM). Cell motility and presence of flagella were determined according to the method described by Clark (1976). The growth capacity at different pH values (4, 5, 10, ~11, ~13 and 14), NaCl concentrations (0.5, 1.5, 2.5 and 5%), and temperatures (4, 15, 28, 37 and 45°C) was tested in TSA culture medium during 48 h. Initial OD<sub>600nm</sub> of 0.1 and 0.2 were added in pH/salinity and temperature assays, respectively. Carbon source utilization, acid production from carbon sources, and enzymatic activities were respectively determined using the galleries API 20NE (48 h, 28°C), API 50CH (48 h, 28°C) and API ZYM (4 h, 28°C), according to the manufacturer's instructions (BioMérieux, France). Moreover, the oxidase activity (not included in the API galleries) was recorded by contacting the bacterial biomass with a 1% aqueous tetramethyl-p-phenylenediamine dihydrochloride solution. For the analysis of cellular fatty acid, Br8 and other five *Stenotrophomonas* strains biomass were grown on TSA at 28°C for 48 h and subsequently harvested. The analysis was performed as described by Kämpfer and Kroppenstedt (1996). Fatty acids were separated with a 5898A gas chromatograph (Hewlett Packard); the respective peaks were automatically integrated and fatty acid names and percentages were determined with the Sherlock MIDI software version 2.1 (TSBA v. 4.1).

### ***DNA isolation and sequencing***

Biomass of the Br8 strain was grown in LB solid medium for 24 h at 30°C, and genomic DNA extraction was performed as described by Martín-Platero et al. (2007). One  $\mu\text{L}$  of the gDNA sample served to test the integrity and purity by 1.5% agarose gel electrophoresis. Afterwards, the samples were quantified using the Qubit 3.0 Fluorometer (Life Technology). The libraries were constructed with the Illumina Novaseq platform, taking 150bp paired-end sequencing reads.

### ***Genome assembly, annotation and phylogenetic analysis***

Quality-filtered reads were *de novo* assembled using an algorithm based on de Bruijn graphs —performed by CLC Genomics Workbench 12.0— and resultant genome assemblies were evaluated with QUAST 5.0.2 (Gurevich et al., 2013). The final genome assembly was functionally annotated through the Rapid Annotation System Technology (RAST) server using the default RASTtk parameter (Brettin et al., 2015). Additionally, the assembled sequence was uploaded to RNAmmer v1.2 (Lagesen et al., 2007) and tRNAscan-SE v. 2.0 (Lowe and Chan, 2006) to predict the rRNA and tRNA genes, respectively. Phylogenetic analysis between Br8 and other *Stenotrophomonas* strains was generated by means of TYGS software (Meier-Kolthoff and Göker, 2019). Genome sequences of the 16 type species belonging to *Stenotrophomonas* genera were obtained from public databases. The sequences were uploaded on the TYGS server for a genome-based taxonomy classification and identification. Furthermore, analysis of the average nucleotide identity with respect to orthologous genes (Ortho-ANI; Lee et al., 2016) was carried out to compare all the genomes and unequivocally identify the Br8 strain.

### ***U removal potential of the strain Br8: Electron microscopy analysis***

Br8 cells were grown and incubated under 0.1 mM U and 5 mM G2P concentrations (as described in Sánchez-Castro et al., 2020) in order to investigate its U biomineralization ability. Br8 biomass exposed to U was harvested by centrifugation, washed twice with 0.9% NaCl and Na-cacodylate buffer (pH 7.2), fixed with glutaraldehyde in cacodylate buffer (4%), and stained with osmium tetroxide (1%, 1 h) in the same buffer before being dehydrated through graded alcohol followed by propylene oxide treatment. Finally, it was

embedded in epoxy resin. Ultrathin sections (0.1 mm) of the samples, obtained using an ultramicrotome, were loaded in a carbon-coated copper grid and analyzed by STEM-HAADF, conducted using a FEI TITAN G2 80-300.

## Results and discussion

### *Phenotypic characterization*

As observed by scanning electron microscopy (SEM), the bacterial cells of *Stenotrophomonas* sp. Br8 strain were Gram-negative, consisting of a short bacillus and motile rods (Figure 1A). Flagella were detected, as shown in figure 1B. Br8 growth took place between pH 5 and 10, but not at pH 4 or above ~11, at 4 to 45°C (optimum was 28°C) and with 0.5 to 2.5% NaCl, but not with 5% NaCl (Table 1). Enzymatic evaluation and carbon source assimilation results are also shown in Table 1.

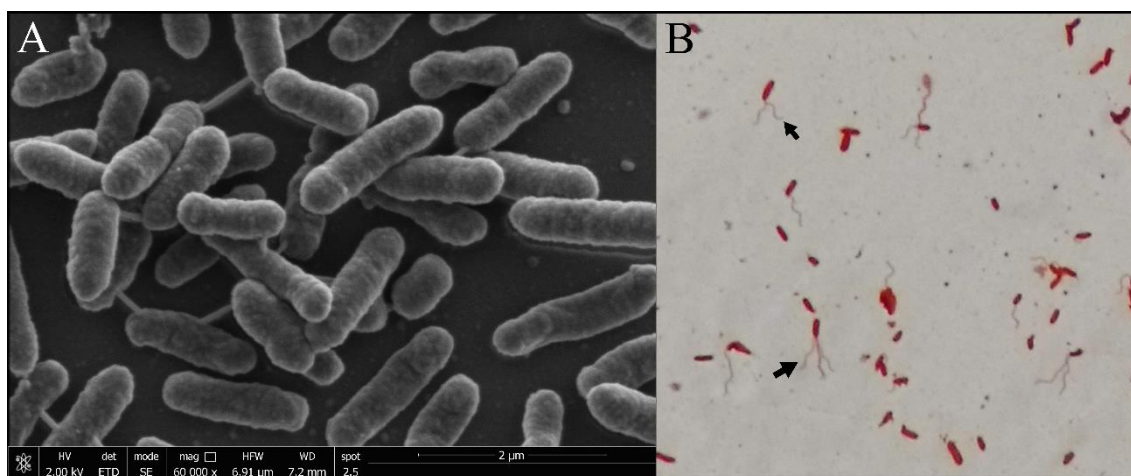


**Figure 1.** (A) SEM image of Br8 cells cultured in LB medium for 24 h at 28°C, and (B) flagella stain (black arrows) under optical microscopy.

**Table 1.** Phenotypic and biochemical characteristics of *Stenotrophomonas* Br8 strain. -, negative result; w, weakly positive; +, ++, +++ positive results with increasing intensity.

Characteristics	<i>Stenotrophomonas</i> Br8 strain
Growth at/with:	
pH 4	-
pH 5	+++
pH 10	++
pH 11	-
pH 13	-
pH 14	-
0.5% NaCl	+++
1.5% NaCl	+++
2.5% NaCl	++
5% NaCl	-
4°C	++
15°C	+++
28°C	+++
37°C	++
45°C	++
Enzymatic activity:	
Alkaline phosphatase	+++
Acid phosphatase	+++
Esterase lipase (C8)	++
Lipase (C-++)	-
Leucine arylamidase	+
Valine arylamidase	-
Cystine arylamidase	-
Trypsin	-
a-Chymotrypsin	-
Esterase (C++)	++
Naphthol-AS-BI-phosphohydrolase	++
a-Galactosidase	-
b-Galactosidase	-
b-Glucuronidase	-
a-Glucosidase	-
b-Glucosidase	-
N-acetyl-b-glucosaminidase	-
a-Mannosidase	-
a-Fucosidase	-
Arginine dihydrolase	-
Urease	-
Protease	+
Cytochrome oxidase	-
Assimilation of:	
Glucose	-
Arabinose	-
Mannose	w
Mannitol	-
N-acetyl-glucosamine	+
Maltose	-
Potassium gluconate	-
Capric acid	-
Adipic acid	-
Malate	+
Trisodium citrate	+
Phenylacetic acid	-



The presence of enzymatic activity in Br8 strain provides valuable information regarding the ability of metal immobilization, in particular of U. Esterase, esterase lipase and naphthol-AS-BI-phosphohydrolase activity were detected. In addition, alkaline/acid phosphatase activity displayed a positive result, as demonstrated in previous work (Sánchez-Castro et al., 2021, 2020). This finding confirms the potential for U phosphate biomineralization mediated by phosphatase enzymes from the *Stenotrophomonas* Br8 strain. Thus, this strain could remove soluble and toxic U species as U phosphate mineral phases, under both acidic and alkaline conditions, proving relevant for U contaminated sites, in addition to the summative effect detected previously under circumneutral pH and U presence (Sánchez-Castro et al., 2020). The fatty acid profile of Br8 strain was found to be consistent with the profiles described for related *Stenotrophomonas* strains (Table 2). Unsaturated fatty acids such as anteiso-C15:0 and iso-C15:0, and a variety of iso-branched hydroxyls, were predominant in Br8 strain and can be considered representative of the genus *Stenotrophomonas*.

**Table 2.** Fatty acid compositions of Br8 and other members of the genus *Stenotrophomonas* strains: 1, Br8<sup>T</sup>; 2, BII-R7; 3, *S. rhizophila* DSM 14405<sup>T</sup>; 4, *S. pavanii* DSM 25135<sup>T</sup>; 5, *S. maltophilia* DSM 50170<sup>T</sup>; 6, *S. chelatophaga* DSM 21508<sup>T</sup>. All data from this study. Summed feature 3: 16:1 w7c/15:0 iso 2-OH. -, Not detected.

Fatty acid	1	2	3	4	5	6
C <sub>10:0</sub>	0.7	-	0.6	0.6	0.9	2.0
C <sub>11:0</sub> ISO	3.2	3.7	3.0	3.3	3.0	4.2
Unknown 11.799	1.5	1.0	0.7	1.3	1.5	1.6
C <sub>11:0</sub> ISO 3-OH	1.3	2.0	1.6	1.4	1.8	2.9
C <sub>13:0</sub> Iso	-	-	-	-	-	2.2
C <sub>13:0</sub> Anteiso	0.7	-	-	-	-	2.0
C <sub>12:0</sub> Iso 3-OH	0.7	-	0.4	-	-	1.1
C <sub>12:0</sub> 3-OH	3.0	3.6	2.0	1.6	4.1	4.3
C <sub>14:0</sub> Iso	3.2	1.4	1.0	0.8	-	4.0
C <sub>14:0</sub>	4.2	2.3	1.0	1.9	2.5	15.8
C <sub>13:0</sub> Iso 3-OH	2.5	3.2	1.8	3.4	3.3	1.9
C <sub>13:0</sub> 2-OH	2.0	1.7	0.9	0.9	-	1.6
C <sub>15:1</sub> IsoF	0.7	1.1	1.6	-	-	6.3
C <sub>15:0</sub> Iso	24.3	23.8	17.9	30.1	29.4	10.6
C <sub>15:0</sub> Anteiso	27.7	19.4	22.2	23.3	13.3	10.8
Unknown 14.959	0.7	-	-	-	-	-
C <sub>15:0</sub>	0.9	0.9	0.7	-	-	1.4
C <sub>16:0</sub> Iso	2.7	4.0	3.7	1.9	-	1.1
C <sub>16:1</sub> ω9c	2.1	2.3	3.2	2.2	4.2	3.9
Summed feature 3	4.8	9.2	8.4	6.1	8.3	13.7
C <sub>16:0</sub>	4.5	9.4	8.6	7.0	13.7	7.4
Iso C <sub>17:1</sub> ω9c	1.5	7.5	10.0	4.0	3.9	1.5
C <sub>15:0</sub> 3-OH	0.8	-	-	-	-	-
C <sub>17:0</sub> Iso	1.1	2.8	4.8	4.2	4.7	-
C <sub>17:0</sub> Anteiso	-	-	0.9	1.0	-	-
C <sub>17:1</sub> ω8c	-	-	0.7	-	-	-
C <sub>17:0</sub> Cyclo	4.5	1.7	1.6	2.4	-	-
C <sub>18:1</sub> ω9c	-	-	1.0	1.7	2.2	-
C <sub>18:1</sub> ω7c	0.7	-	1.4	0.9	1.7	-

### ***General genomic features***

Low-quality reads were trimmed by CLC Genomics Workbench 12.0 to generate 16,919,206 reads with a mean read length of 150bp. The draft genome comprised 30 contigs, with 4,578,245 bp length and a N50 value of 254,102. The G+C content of the sequence was 66.1%. Four copies of rRNA genes were predicted in the genome (two copies of 5S and one copy each of 16S and 23S) by the RNAmmer V1.2 (Lagesen et al., 2007), while 71 copies of tRNA were anticipated by tRNAscan-SE v. 2.0 (Lowe and Chan, 2006). The draft genome of Br8 strain has been deposited at GenBank under the accession JACGTN000000000 with BioProject number PRJNA649538. The version described in this paper is version JACGTN010000000.

### ***Phylogenetic analysis***

The phylogenomic classification of *Stenotrophomonas* sp. Br8 was carried out with a Genome-Blast Distance Phylogeny (GBDP) tree (Figure 2) inferred with the Type Strain Genome Server (Meier-Kolthoff and Göker, 2019) (TYGS; <https://tygs.dsmz>). Analyses confirmed the taxonomical affiliation of the bacterial strain Br8 to the genus *Stenotrophomonas* and provided comparative data on the protein count and G+C percentage between selected *Stenotrophomonas* species (data not shown). The whole-genome sequence-based tree from TYGS indicated that Br8 is closely related to *Stenotrophomonas lactitubi* M15 and *Stenotrophomonas indicatrix* WS40 strains (Weber et al., 2018), being consistent with a 16S rDNA gene sequence-based tree (Figure 3);  $\delta$  values were low in both trees (0.136 and 0.288, respectively), meaning a high phylogenetic accuracy in terms of tree-likeness.

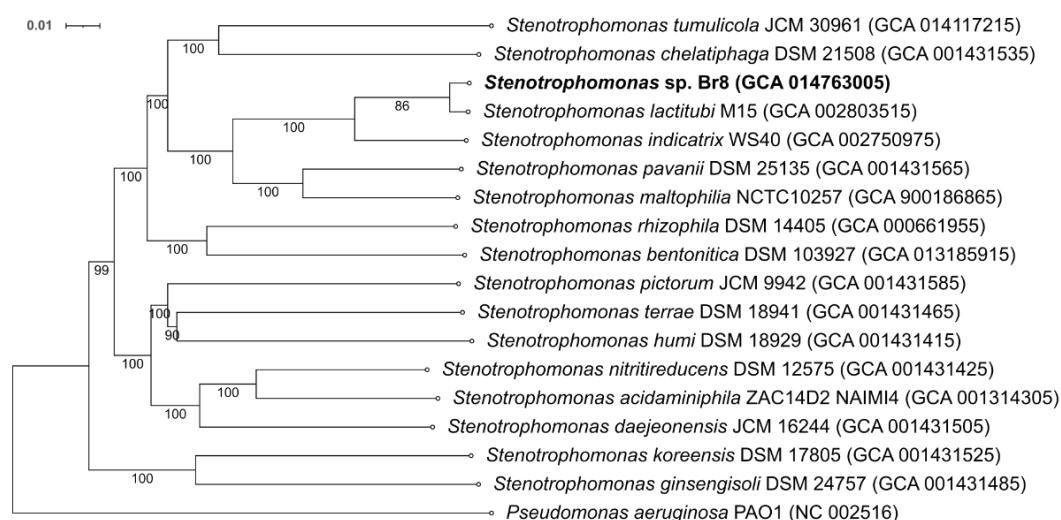


**Figure 2.** Genome-Blast Distance Phylogeny (GBDP) tree inferred with Type Strain Genome Server (TYGS; <https://tygs.dsmz>) from GBDP distances calculated from genome sequences. The branch lengths are scaled in terms of GBDP distance formula  $d_5$ . The numbers above branches are GBDP pseudo-bootstrap support values >86 % from 100 replications, with an average branch support of 98.3%. GenBank accession codes are shown in parentheses after the species name. *Pseudomonas aeruginosa* was used as outgroup.

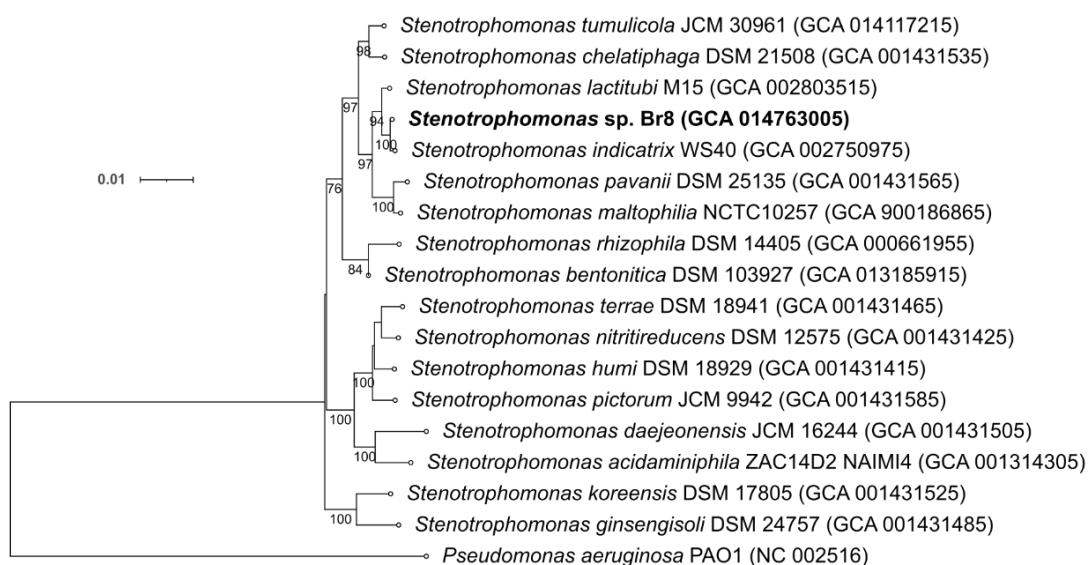


**Figure 3.** Tree inferred with Type Strain Genome Server (TYGS; <https://tygs.dsmz>) from GBDP distances calculated from 16S rDNA gene sequences. The branch lengths are scaled in terms of GBDP distance formula  $d_5$ . The numbers above branches are GBDP pseudo-bootstrap support values >75 % from 100 replications, with an average branch support of 86.5%. GenBank accession codes are shown in parentheses after the species name. *Pseudomonas aeruginosa* was used as outgroup.

To unequivocally classify the strain Br8 within the genus *Stenotrophomonas*, a full ANI analysis including all genomes of the genus was performed (Table 3). Based on this algorithm, similarity between the Br8 strain and *Stenotrophomonas lactitubi* is over the proposed 95-96% threshold for the species boundary (Richter and Rosselló-Móra, 2009), hence the Br8 strain is *S. lactitubi*.

**Table 3.** Genome-based comparisons of *Stenotrophomonas* sp. Br8 and other type strains from the genus *Stenotrophomonas*. Ortho-ANI values were obtained by OAT software (Lee et al., 2016). Digital DDH values and G+C content differences were calculated with Type Strain Genome Server (TYGS; <https://tygs.dsmz>).

Reference strain	Ortho-ANI (%)	dDDH ( $\delta 4$ , %)	G+C content difference (%)
<i>Stenotrophomonas lactitubi</i> M15	98.9	90	0.22
<i>Stenotrophomonas maltophilia</i> NCTC10257	87.0	32	0.03
<i>Stenotrophomonas nitritireducens</i> DSM 12575	80.0	23.5	2.25
<i>Stenotrophomonas pavanii</i> DSM 25135	87.4	32.3	1.3
<i>Stenotrophomonas pictorum</i> JCM 9942	79.1	22.3	0.08
<i>Stenotrophomonas rhizophila</i> DSM 14405	81.5	24.6	1.21
<i>Stenotrophomonas terrae</i> DSM 18941	78.7	22.7	2.20
<i>Stenotrophomonas tumulicola</i> JCM 30961	81.8	25.1	0.48
<i>Stenotrophomonas acidaminiphila</i> ZAC14D2_NAIMI4	79.7	23.2	2.39
<i>Stenotrophomonas bentonitica</i> DSM 103927	81.6	24.8	0.38
<i>Stenotrophomonas chelatiphaga</i> DSM 21508	82.3	25.6	0.75
<i>Stenotrophomonas daejeonensis</i> JCM 16244	80.1	23.5	2.47
<i>Stenotrophomonas ginsengisoli</i> DSM 24757	76.4	20.7	0.20
<i>Stenotrophomonas humi</i> DSM 18929	78.4	22.3	2.05
<i>Stenotrophomonas indicatrix</i> WS40	93.5	52.4	0.32
<i>Stenotrophomonas koreensis</i> DSM 17805	76.5	21	0.02

The Rapid Annotation Subsystem Technology (RAST) server annotation (Brettin et al., 2015) (<https://rast.nmpdr.org/>) of the Br8 draft genome predicted a total of 4222 protein-coding sequences. The subsystem categorical distribution of the annotated genes is represented in Figure 4. Most of the genes identified were involved in the synthesis of amino acids and derivatives (257), protein metabolism (155), and membrane transport

(152). Likewise, the strain Br8 possesses a substantial number of genes responsible for carbohydrate metabolism (146), cofactors, vitamins, prosthetic groups and pigment metabolism (139), resistance to antibiotics and toxic compounds (18), and stress response (66). In Br8 strain, genome annotation of the protein-coding region marks the presence of alkaline phosphatase (EC 3.1.3.1), exopolyphosphatase (EC 3.6.1.11) and inorganic pyrophosphatase (EC 3.6.1.1), thus supporting the phosphatase enzyme-mediated biomineralization of soluble U shown previously by Sánchez-Castro et al. (2020). The draft genome also presented protein-coding regions for ABC-type glycerol-3-phosphate transport and glycerol-3-phosphate acyltransferase, which were reported to have an elevated expression under uranium stress conditions (Gallois et al., 2018). Moreover, *phoU*, *phoB* and *phoR* genes are present in the Br8 genome, whose modulating function in P uptake under phosphate-limiting conditions (Hirota et al., 2010) could be involved in the U(VI) biomineralization process stated above. The Br8 genome was found to possess numerous genes related to superoxide dismutase, glutathione synthetase and glutaredoxins, enzymes with a defensive role against oxidative stress likely produced in the microbes by elevated U concentrations (Dekker et al., 2016; Orellana et al., 2014). Coding regions related to iron homeostasis —e.g. TonB-dependent receptor, TonB-dependent siderophore receptor, and TPR domain— associated with expressed genes in different microbes in the presence of U(VI) (Khare et al., 2020) and Cr(VI) (Gao et al., 2020) were also found in the Br8 annotated genome. In addition, it showed the presence of copper-translocating P-type ATPase, whose expression was previously detected under the effect of metals as U, Cd and Zn (Khare et al., 2020).

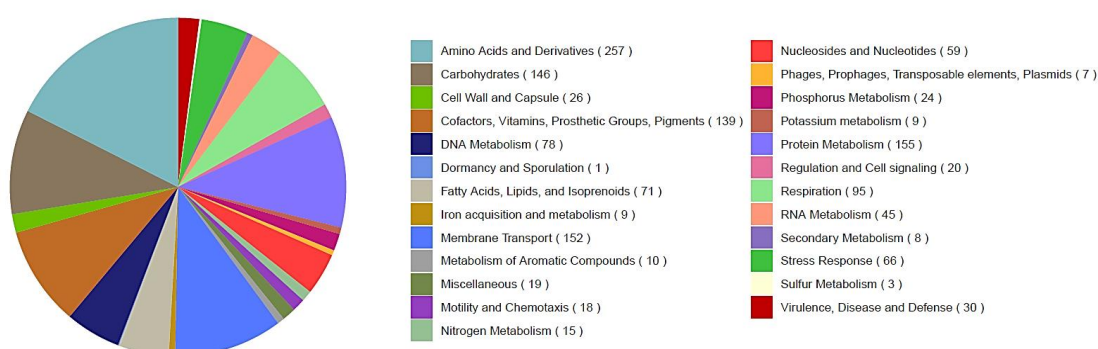


**Figure 4.** An overview of the subsystem categories assigned to the genome of *Stenotrophomonas* sp. Br8 strain. (<https://rast.nmpdr.org/>).

**STEM-HAADF/EDX analysis**

Electron microscopy was performed to confirm the U precipitation capacity of *Stenotrophomonas* Br8 strain. The micrographs of ultrathin sections (Figure 5A) with metal-treated cells revealed U precipitates localized around the cells and extracellularly. No intracellular accumulates were detected. Element mapping analysis (Figures 5B and 5C) showed that precipitates were composed by P and U. Extracellular and surface-level U phosphate precipitates indicate that Br8 copes with metal toxicity, preventing the intracellular accumulation of U (Sánchez-Castro et al., 2020). Indeed, U phosphate biomineralization is considered as the most efficient and stable long-term strategy for U bioremediation under aerobic conditions.

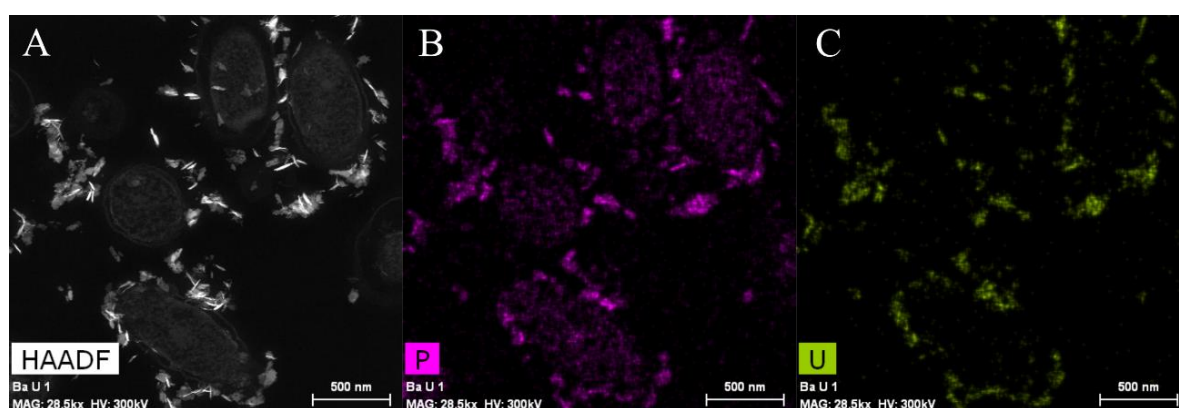


**Figure 5.** (A) HAADF-STEM image of Br8 cells after incubation under U presence; EDX element mapping for P (B) and U (C).

**Statements & Declarations****Funding**

This work was supported by ORANO Mining (France) [collaborative research contract n° 3022 OTRI-UGR]. The paper comes from a Joint Research Project between Orano Mining R&D Department and the Department of Microbiology of the University of Granada. The authors thank Orano Mining for financial support.

**Data Availability**

*Stenotrophomonas* sp. Br8 draft genome has been deposited at NCBI GenBank under the accession code PRJNA649538

[[https://www.ncbi.nlm.nih.gov/assembly/GCF\\_014763005.1](https://www.ncbi.nlm.nih.gov/assembly/GCF_014763005.1)].

## References

- Brettin, T., Davis, J.J., Disz, T., Edwards, R.A., Gerdes, S., Olsen, G.J., Olson, R., Overbeek, R., Parrello, B., Pusch, G.D., Shukla, M., Thomason, J.A., Stevens, R., Vonstein, V., Wattam, A.R., Xia, F., 2015. RASTtk: A modular and extensible implementation of the RAST algorithm for building custom annotation pipelines and annotating batches of genomes. *Sci. Rep.* 5. <https://doi.org/10.1038/srep08365>
- Clark, W.A., 1976. A Simplified Leifson Flagella Stain. *J. Clin. Microbiol.* 3, 632–634.
- Dekker, L., Arsène-Ploetze, F., Santini, J.M., 2016. Comparative proteomics of *Acidithiobacillus ferrooxidans* grown in the presence and absence of uranium. *Res. Microbiol.* 167, 234–239. <https://doi.org/10.1016/j.resmic.2016.01.007>
- Gallois, N., Alpha-Bazin, B., Ortet, P., Barakat, M., Piette, L., Long, J., Berthomieu, C., Armengaud, J., Chapon, V., 2018. Proteogenomic insights into uranium tolerance of a Chernobyl's *Microbacterium* bacterial isolate. *J. Proteomics* 177, 148–157. <https://doi.org/10.1016/j.jpro.2017.11.021>
- Gao, J., Wu, Shimin, Liu, Y., Wu, Shanghua, Jiang, C., Li, X., Wang, R., Bai, Z., Zhuang, G., Zhuang, X., 2020. Characterization and transcriptomic analysis of a highly Cr(VI)-resistant and -reductive plant-growth-promoting rhizobacterium *Stenotrophomonas rhizophila* DSM14405T. *Environ. Pollut.* 263, 114622. <https://doi.org/10.1016/j.envpol.2020.114622>
- Ghosh, A., Saha, P. Das, 2013. Optimization of copper bioremediation by *Stenotrophomonas maltophilia* PD2. *J. Environ. Chem. Eng.* 1, 159–163. <https://doi.org/10.1016/j.jece.2013.04.012>
- Gurevich, A., Saveliev, V., Vyahhi, N., Tesler, G., 2013. QUAST: Quality assessment tool for genome assemblies. *Bioinformatics* 29, 1072–1075. <https://doi.org/10.1093/bioinformatics/btt086>
- Hirota, R., Kuroda, A., Kato, J., Ohtake, H., 2010. Bacterial phosphate metabolism and its application to phosphorus recovery and industrial bioprocesses. *J. Biosci. Bioeng.* 109, 423–432. <https://doi.org/10.1016/j.jbiosc.2009.10.018>
- Islam, E., Sar, P., 2016. Diversity, metal resistance and uranium sequestration abilities of bacteria from uranium ore deposit in deep earth stratum. *Ecotoxicol. Environ. Saf.* 127, 12–21. <https://doi.org/10.1016/j.ecoenv.2016.01.001>
- Kämpfer, P., Kroppenstedt, R.M., 1996. Numerical analysis of fatty acid patterns of coryneform bacteria and related taxa. *Can. J. Microbiol.* 42, 989–1005. <https://doi.org/10.1139/m96-128>
- Khare, D., Kumar, R., Acharya, C., 2020. Genomic and functional insights into the adaptation and survival of *Chryseobacterium* sp. strain PMSZPI in uranium enriched environment. *Ecotoxicol. Environ. Saf.* 191, 110217. <https://doi.org/10.1016/j.ecoenv.2020.110217>
- Lagesen, K., Hallin, P., Rødland, E.A., Stærfeldt, H.H., Rognes, T., Ussery, D.W., 2007. RNAmmer: Consistent and rapid annotation of ribosomal RNA genes. *Nucleic Acids Res.* 35, 3100–3108. <https://doi.org/10.1093/nar/gkm160>
- Lee, I., Kim, Y.O., Park, S.C., Chun, J., 2016. OrthoANI: An improved algorithm and software for calculating average nucleotide identity. *Int. J. Syst. Evol. Microbiol.* 66, 1100–1103. <https://doi.org/10.1099/ijsem.0.000760>
- Lopez-Fernandez, M., Jroundi, F., Ruiz-Fresneda, M.A., Merroun, M.L., 2021. Microbial interaction with and tolerance of radionuclides: underlying mechanisms and biotechnological applications. *Microb. Biotechnol.* 14, 810–828. <https://doi.org/10.1111/1751-7915.13718>
- Lowe, T.M., Chan, P.P., 2006. tRNAscan-SE: Searching for tRNA Genes in Genomic Sequences 1962, 1–21.
- Martín-Platero, A.M., Valdivia, E., Maqueda, M., Martínez-Bueno, M., 2007. Fast, convenient, and economical method for isolating genomic DNA from lactic acid bacteria using a modification of the protein “salting-out” procedure. *Anal. Biochem.* 366, 102–104.

- <https://doi.org/10.1016/j.ab.2007.03.010>
- Meier-Kolthoff, J.P., Göker, M., 2019. TYGS is an automated high-throughput platform for state-of-the-art genome-based taxonomy. *Nat. Commun.* 10. <https://doi.org/10.1038/s41467-019-10210-3>
- Merroun, M.L., Selenska-Pobell, S., 2008. Bacterial interactions with uranium: An environmental perspective. *J. Contam. Hydrol.* 102, 285–295. <https://doi.org/10.1016/j.jconhyd.2008.09.019>
- Orellana, R., Hixson, K.K., Murphy, S., Mester, T., Sharma, M.L., Lipton, M.S., Lovley, D.R., 2014. Proteome of *Geobacter sulfurreducens* in the presence of U(VI). *Microbiol. (United Kingdom)* 160, 2607–2617. <https://doi.org/10.1099/mic.0.081398-0>
- Pages, D., Rose, J., Conrod, S., Cuine, S., Carrier, P., Heulin, T., Achouak, W., 2008. Heavy metal tolerance in *Stenotrophomonas maltophilia*. *PLoS One* 3. <https://doi.org/10.1371/journal.pone.0001539>
- Pinel-Cabello, M., Jroundi, F., López-Fernández, M., Geffers, R., Jarek, M., Jauregui, R., Link, A., Vílchez-Vargas, R., Merroun, M.L., 2021. Multisystem combined uranium resistance mechanisms and bioremediation potential of *Stenotrophomonas bentonitica* BII-R7: Transcriptomics and microscopic study. *J. Hazard. Mater.* 403. <https://doi.org/10.1016/j.jhazmat.2020.123858>
- Reasoner, D.J., Geldreich, E.E., 1985. A new medium for the enumeration and subculture of bacteria from potable water. *Appl. Environ. Microbiol.* 49, 1–7.
- Richter, M., Rosselló-Móra, R., 2009. Shifting the genomic gold standard for the prokaryotic species definition. *Proc. Natl. Acad. Sci. U. S. A.* 106, 19126–19131. <https://doi.org/10.1073/pnas.0906412106>
- Ryan, R.P., Monchy, S., Cardinale, M., Taghavi, S., Crossman, L., Avison, M.B., Berg, G., van der Lelie, D., Dow, J.M., 2009. The versatility and adaptation of bacteria from the genus *Stenotrophomonas*. *Nat. Rev. Microbiol.* 7, 514–525. <https://doi.org/10.1038/nrmicro2163>
- Sánchez-Castro, I., Amador-García, A., Moreno-Romero, C., López-Fernández, M., Phrommavanh, V., Nos, J., Descostes, M., Merroun, M.L., 2017a. Screening of bacterial strains isolated from uranium mill tailings porewaters for bioremediation purposes. *J. Environ. Radioact.* 166, 130–141. <https://doi.org/10.1016/j.jenvrad.2016.03.016>
- Sánchez-Castro, I., Martínez-Rodríguez, P., Abad, M.M., Descostes, M., Merroun, M.L., 2021. Uranium removal from complex mining waters by alginate beads doped with cells of *Stenotrophomonas* sp. Br8: Novel perspectives for metal bioremediation. *J. Environ. Manage.* 296, 1–10. <https://doi.org/10.1016/j.jenvman.2021.113411>
- Sánchez-Castro, I., Martínez-Rodríguez, P., Jroundi, F., Lorenzo, P., Descostes, M., L. Merroun, M., 2020. High-efficient microbial immobilization of solved U(VI) by the *Stenotrophomonas* strain Br8. *Water Res.* 183. <https://doi.org/10.1016/j.watres.2020.116110>
- Sánchez-Castro, I., Ruiz-Fresneda, M.A., Bakkali, M., Kämpfer, P., Glaeser, S.P., Busse, H.J., López-Fernández, M., Martínez-Rodríguez, P., Merroun, M.L., 2017b. *Stenotrophomonas bentonitica* sp. nov., isolated from bentonite formations. *Int. J. Syst. Evol. Microbiol.* 67, 2779–2786. <https://doi.org/10.1099/ijsem.0.002016>
- Weber, M., Schünemann, W., Fuß, J., Kämpfer, P., Lipski, A., 2018. *Stenotrophomonas lactitubi* sp. nov. and *Stenotrophomonas indicatrix* sp. nov., isolated from surfaces with food contact. *Int. J. Syst. Evol. Microbiol.* 68, 1830–1838. <https://doi.org/10.1099/ijsem.0.002732>
- Xiong, W., Yin, C., Wang, Y., Lin, S., Deng, Z., Liang, R., 2020. Characterization of an efficient estrogen-degrading bacterium *Stenotrophomonas maltophilia* SJTH1 in saline-, alkaline-, heavy metal-contained environments or solid soil and identification of four 17 $\beta$ -estradiol-oxidizing dehydrogenases. *J. Hazard. Mater.* 385, 121616. <https://doi.org/10.1016/j.jhazmat.2019.121616>



## CAPÍTULO II

## CAPÍTULO III:

### **Effect of different phosphate sources on uranium biomineralization by the *Microbacterium* sp. Be9 strain: a multidisciplinary approach study**

Pablo Martínez-Rodríguez<sup>1\*</sup>, Iván Sánchez-Castro<sup>1</sup>, Jesús J. Ojeda<sup>2</sup>, María M. Abad<sup>3</sup>,  
Michael Descostes<sup>4,5</sup>, Mohamed Larbi Merroun<sup>1</sup>

<sup>1</sup> Department of Microbiology, University of Granada, Campus Fuentenueva s/n, 18071, Granada, Spain.

<sup>2</sup> Department of Chemical Engineering, Faculty of Science and Engineering, Swansea University, Swansea SA1 8EN, UK

<sup>3</sup> Centro de Instrumentación Científica (CIC), University of Granada, Campus Fuentenueva, Granada, Spain

<sup>4</sup> Environmental R&D Department, ORANO Mining, 92320 Chatillon, France.

<sup>5</sup> Centre de Géosciences, MINES Paris, PSL University, 35 rue St Honoré, 77300 Fontainebleau, France

This chapter has been accepted in *Frontiers in Microbiology*:

Pablo Martínez-Rodríguez, Iván Sánchez-Castro, Jesús J. Ojeda, María M. Abad, Michael Descostes, Mohamed Larbi Merroun, 2022. Effect of different phosphate sources on uranium biomineralization by the *Microbacterium* sp. Be9 strain: a multidisciplinary approach study. *Frontiers in Microbiology*, doi: 10.3389/fmicb.2022.1092184



### **Abstract**

Industrial activities related with the uranium industry are known to generate hazardous waste which must be managed adequately. Amongst the remediation activities available, eco-friendly strategies based on microbial activity have been investigated in depth in the last decades and biomineralization-based methods, mediated by microbial enzymes (e.g. phosphatase), have been proposed as a promising approach. However, the presence of different forms of phosphates in these environments plays a complicated role which must be thoroughly unravelled to optimize results when applying this remediation process. In this study, we have looked at the effect of different phosphate sources on the uranium (U) biomineralization process mediated by *Microbacterium* sp. Be9, a bacterial strain previously isolated from U mill tailings. We applied a multidisciplinary approach (cell surface characterization, phosphatase activity, inorganic phosphate release, cell viability, microscopy, etc.). It was clear that the U removal ability and related U interaction mechanisms by the strain depend on the type of phosphate substrate. In the absence of exogenous phosphate substrate, the cells interact with U through U phosphate biomineralization with a 98% removal of U within the first 48h. However, the U solubilization process was the main U interaction mechanism of the cells in the presence of inorganic phosphate, demonstrating the phosphate solubilizing potential of the strain. These findings show the biotechnological use of this strain in the bioremediation of U as a function of phosphate substrate: U biomineralization (in a phosphate free system) and indirectly through the solubilization of orthophosphate from phosphate (P) containing waste products needed for U precipitation.

**Keywords:** *Microbacterium*, uranium, phosphate source, bioprecipitation, solubilization, PSB

## Introduction

Uranium is a naturally occurring element that is ubiquitous in the Earth's crust (e.g. soil and water). However, anthropogenic activities related to uranium mining, the nuclear energy industry, or weapon manufacturing may involve the redistribution of this element in the environment, sometimes resulting in locally high U concentrations (Kolhe et al., 2018). Due to U radiological and chemical toxicity, remediation strategies are highly recommended to prevent the potentially harmful effects for the environment and health.

Several remediation approaches have been proposed to remove inorganic contaminants from polluted sites leading to a decrease in their associated risks (Gavrilescu et al. 2009). Traditional strategies based on physico-chemical methods, such as precipitation, evaporation, or extraction amongst others, have been used to treat heavy-metal contaminated sites (Selvakumar et al., 2018). However, these approaches are known to be costly at environmental level in comparison with biologically based remediation. Both types of techniques are often additionally used for more efficient and economical rehabilitation of contaminated areas (Khalid et al., 2017). In recent years, a wide range of microorganisms isolated from contaminated sites (such as mining areas) have been shown to possess the ability to immobilize U (Banala et al., 2021). The main strategies which have been adopted by microorganisms to avoid U cytotoxic effects are based on different mechanisms such as U biosorption at the cell surface (Merroun et al., 2006), U biomineralization (Beazley et al., 2007; Lopez-Fernandez et al., 2021; Macaskie et al., 2000), U intracellular accumulation (Gerber et al., 2016; Merroun et al., 2003) and U biotransformation, either by reduction (Lovley et al., 1991; Williams et al., 2013) or by oxidation (DiSpirito and Tuovinen, 1982). In particular, one of the most promising approaches consists of U-biomineralization under aerobic conditions (Beazley et al., 2011; Sánchez-Castro et al., 2020; Tu et al., 2019).

The uranium biomineralization process probably occurs in the presence of ligands such as carbonates, phosphates and hydroxides, which act as nucleation sites generated by microbial activity (Lloyd and Macaskie, 2000; Wufuer et al., 2017). Amongst the different mineralization processes, U-phosphate precipitation has been well documented in recent years by numerous studies (Zhang et al., 2020). They are generally bi-phasic processes based on passive U binding at the cell surface through phosphate and/or carboxyl groups and a metabolism-dependent release of orthophosphates from organic phosphate substrates

(e.g. glycerol-2-phosphates (G2P), glycerol-3-phosphates (G3P)) mediated by phosphatase activity (Lopez-Fernandez et al., 2021). The resulting orthophosphates interact with uranyl ion ( $\text{UO}_2^{2+}$ ), the most common soluble form of environmental U, making it immobile and consequently less toxic. Specifically, meta-autunite-like U phosphate forms have been widely studied due to their long-term stability under different physico-chemical conditions (Beazley et al., 2009). These U-phosphate compounds are attractive for bioremediation purposes rather than the uraninite forms produced during bioreduction processes which are known to be less stable and easily oxidized (Wang et al., 2013). Previous studies have reported the formation of U phosphates in presence of determined microbial strains and organic phosphate sources such as G3P (Beazley et al., 2011) or G2P (Macaskie et al., 2000; Newsome et al., 2015; Sánchez-Castro et al., 2020), as well as inorganic phosphates (Pi). The microbial-mediated formation of U phosphates is known to be affected by different physico-chemical factors such as pH (Zheng et al., 2018), redox conditions (Salome et al., 2013), co-existing cations/anions (Wei et al., 2019) and humic substances (Boiteau et al., 2018), which may decrease the bioprecipitation efficiency. However, to the best of our knowledge, no studies on the impact of different forms of phosphates (organic/inorganic) on U biomineralization have been conducted so far. The presence of different phosphate forms should be considered, especially when phosphate solubilizing bacteria (PSB) are used as bioremediation agents or are present in the medium. PSB are known to play a major role in enhancing phosphate-induced immobilization of heavy metals such as U for bioremediation purposes (Sowmya et al., 2014). However, eutrophication issues should be contemplated since there is a limit on the amount of phosphate which can be added to the environment (Park et al., 2011). Therefore, the use of PSB (e.g., the species of the genus *Microbacterium*) in the bioremediation of heavy metals could contribute to the circular economy by using cheap and readily available material which is rich in insoluble phosphates.

This study addresses the impact of phosphate forms (organic/inorganic) in U biomineralization by *Microbacterium* sp. Be9, a bacterial strain isolated from U mill tailings. In previous studies, this bacterium showed high tolerance to different heavy metals (Sánchez-Castro et al., 2017). Moreover, members of the *Microbacterium* genus have been described for their potential role in uranium-contaminated water remediation. They have been shown to accumulate uranium both at cell surface level and also extracellularly as uranium phosphates at pH 4.5 (Nedelkova et al., 2007) displaying multiple detoxification

mechanisms involving phosphates (Theodorakopoulos et al., 2015). According to the latter works, *Microbacterium* sp. strain Be9 would display similar U interaction mechanisms mediated by different enzymatic activities upon phosphate source (phosphatase in presence of organic phosphates and polyphosphatase in a free phosphate system) leading to the biomineralization of U as U phosphate mineral phases. Thus, Be9 could precipitate U under the presence of organic phosphates. Bacterial strains with phosphatase activity are capable of releasing orthophosphates from organophosphate sources in order to avoid the stress caused by U. In presence of inorganic phosphates, most of the U should remain in the insoluble form. In our study, systems with three different sources of phosphate were assayed (no-phosphate, organic and inorganic phosphates) to investigate the mechanisms displayed by the Be9 strain under U presence. We have used a multidisciplinary approach combining colorimetric methods for measuring residual uranium and inorganic-phosphate release, as well as flow cytometry to assess bacterial activity and viability. A characterization of Be9 membrane surface was determined by potentiometric titrations and X-ray photoelectron spectroscopy (XPS) analysis. Moreover, we also used microscopic and spectroscopic techniques (Scanning Transmission Electron Microscopy-High Angle Annular Dark-Field (STEM-HAADF) and X-ray Diffraction (XRD) to localize at cellular level the U precipitates obtained and to analyse their composition.

## **Material and Methods**

### ***Bacterial culture***

*Microbacterium* sp. strain Be9 was isolated from mill-tailing repository sites, located near Bessines-sur-Gartempe (Limousin, France) (Sánchez-Castro et al., 2017). The cultures were maintained and grown in a solid/liquid Lysogeny broth (LB) medium (tryptone 10 g/L, yeast extract 5 g/L and NaCl 10 g/L, pH  $7.0 \pm 0.2$ ) at 28°C with shaking at 160 rpm. For long-term storage, the cultures were stored at  $-80^{\circ}\text{C}$  in 50% glycerol.

### ***Potentiometric titrations***

Potentiometric titrations were carried out to determine the chemical properties of *Microbacterium* sp. Be9 cell surface. An amount of live bacteria equivalent to 0.14 – 0.19 g of dry biomass (washed four times with  $\text{NaClO}_4$ ) was suspended in a vessel with 20 mL

of 0.1 M NaClO<sub>4</sub>. The suspension was titrated with 0.1 M HCl to pH 3.5 followed by 0.1 M NaOH to pH 10.0. To test the reversibility of the protonation–deprotonation behaviour, the suspension was back-titrated with 0.1 M HCl from pH 10.0 to 3.5. HCl and NaOH solutions were previously calibrated against primary standards. All the titrations were performed using a Metrohm® *Titrand* 906 automatic titrator (Metrohm, UK) at 25°C. The temperature was kept constant and continuously monitored during the titration. To calculate the acidity constant (pK<sub>a</sub>) values and the corresponding total concentration of the binding sites for Be9 cells, data from three replicates of each titration curve were fitted using the program Prototit 2.1 rev1 (Turner and Fein, 2006) using a Non-Electrostatic Model (NEM).

### ***X-ray photoelectron spectroscopy (XPS)***

To characterize the elemental composition of the near-cell surface of Be9 strain (2 – 5 nm penetration depth), the X-ray photoelectron spectroscopy technique was used. Be9 pellets were freeze-dried and the obtained powder was mounted on standard studs using double-sided adhesive tape. XPS measurements were made on a Kratos Supra photoelectron spectrometer at 10 kV and 20 mA using a monochromatic Al K $\alpha$  X-ray source (1486.6 eV). The take-off angle was fixed at 90°. For each sample the data were collected from three randomly selected locations, and the area corresponding to each acquisition was 400  $\mu$ m in diameter. Each analysis consisted of a wide survey scan (pass energy 160 eV, 1.0 eV step size) and high-resolution scan (pass energy 20 eV, 0.1 eV step size) for component speciation. The binding energies of the peaks were determined using the C<sub>1s</sub> peak at 284.5 eV. To fit the XPS spectra peaks CasaXPS software (version 2.3.22PR1.0; <http://www.casaxps.com/>) was used (Fairley, 2020).

### ***Uranium speciation modelling***

Uranium speciation in different assayed media (organic and inorganic phosphate sources) was determined by Visual MINTEQ version 3.1 (<https://vminteq.lwr.kth.se/>) and PhreeQC software (calculated using PRODATA thermodynamic database). The initial conditions of temperature, pH and U concentration were incorporated into the model as 28°C, 6.6 and 100  $\mu$ M respectively.

***Phosphate impact on U biomineralization: experimental design***

The *Microbacterium* sp. strain Be9 was grown in liquid LB medium in continuous shaking (160 rpm) at 28°C for 24 h. The cells were harvested by centrifugation for 5 min at 10,000 × g and washed twice with 0.9% NaCl solution to remove the interfering elements of the growth medium. In all cases, the acid-washed glass Erlenmeyer flasks were filled with the corresponding incubation solution. In treatments including the Be9 cells, an initial optical density (O.D.) of 0.7 (at 600 nm) was used. All the flasks were incubated under controlled temperature (28°C) with shaking (160 rpm) for 48 h. Uranium-free, no-bacteria and heat-killed-bacteria (incubated at 80°C for 1 h) flasks were considered as control treatments.

Potential U-bioprecipitation in presence of Be9 cells and organic and inorganic phosphate sources were investigated with the following conditions: i) exogenous phosphate-free system (MOPS buffer + Be9 + U), labelled as MC1, ii) organic phosphate (G2P) supplemented system (MOPS buffer + Be9 + G2P + U), labelled as MC2, and iii) inorganic phosphate supplemented system (low phosphate medium, LPM + Be9 + U), labelled as MC3. Uranium was added as uranyl nitrate  $\text{UO}_2(\text{NO}_3)_2 \cdot 6\text{H}_2\text{O}$  from a 0.1 M stock solution to a final concentration of 100 µM, with the exception of the MC3 condition. In this case, the U concentration was increased to 0.5 and 1 mM due to the estimated presumption of abiotic U precipitation. To investigate the effect of the organic-phosphate source, flasks were filled with 20 mM 3-(N-Morpholino)propanesulfonic acid (MOPS; Sigma Aldrich) buffered at pH 6.5, and supplemented with 5 mM G2P (Sigma Aldrich). Control flasks without G2P were also tested. In the case of inorganic-phosphate sources, the culture medium LPM (Supplementary Table 1) at pH 7.5 was prepared as described in Lopez-Fernandez et al. (2018). In this condition, control flasks including reduced phosphate concentration (0.2 mg/L peptone) were also considered. Once the incubations were completed, aliquots from all the flasks were centrifuged at 10,000 × g for 10 min at 4°C, and the supernatants and solid pellets were analysed separately. All the treatments were conducted in triplicate and the subsequent analyses used all the replicate data from each respective treatment for statistics.

***Uranium removal quantification***

Uranium concentrations in recovered supernatants were analysed spectro-photometrically using the Arsenazo III method (Jauberty et al., 2013). The reagent was prepared by



## CAPÍTULO III

dissolving 70 mg of 2,7-bis(2-arsenophenylazo)-1,8-dihydroxynaphthalene-3,6-disulfonic acid (Arsenazo-III) into 1 L of 3 M HClO<sub>4</sub>. Then, 250 µl from each sub-sample were mixed with 1 mL of reagent. Absorbance was measured at 651 nm with Thermo Scientific™ GENESYS 10S UV-Vis spectrophotometer. Uranium removal in treatments was calculated as the difference between the initial and final U concentrations.

### ***Inorganic phosphate quantification***

After incubation, inorganic phosphate (Pi) concentration in supernatants was quantified by the ammonium-molybdate and ascorbic acid method (Murphy and Riley, 1962). This colorimetric procedure is based on the reaction of the orthophosphate ions with ammonium-molybdate in an acidic solution forming phosphomolybdic acid. After reduction with ascorbic acid, the resultant compound shows an intensely blue complex measurable at 850 nm after exactly 30 min.

### ***Phosphatase activity***

Phosphatase activity determination was carried out using Methylumbelliferyl (MUB)-linked phosphate as optimized and described German et al. (2011). Be9 cells samples from different assays were dissolved in sodium perchlorate buffer (pH 5) and MUB standards (0.16 µM, 0.625 µM, 1.25 µM and 2.50 µM) in order to calculate the emission and quench coefficients using an automatic fluorometer NanoQuant Infinite 200 PRO (Tecan). Enzyme activity calculations were performed following German et al. (2011).

### ***Bacterial viability and cell membrane potential***

The cell viability and the cell membrane potential of *Microbacterium* sp. strain Be9 in the presence of U were determined through the flow cytometry technique. The cultures were prepared as stated above with an initial concentration of U of 100 µM. After 1 h, 24 h, and 48 h of incubation for viability, and 24 h and 48 h for cell membrane potential, the cells were collected by centrifugation at 11,000 × g and 4°C for 10 min. The resultant pellet was washed three times and dissolved in phosphate buffered saline solution at pH 7. For the cell viability test, fluorescein diacetate and propidium iodide were added to each sample to a

final concentration of 20  $\mu\text{L}/\text{mL}$  and 2  $\mu\text{L}/\text{mL}$ , respectively. In the case of cell membrane potential, 3,3'-dihexyloxacarbocyanine iodide was used at a final concentration of 20  $\mu\text{L}/\text{mL}$ . Finally, all the samples were analysed by Forward Scatter using a FACSCanto II™ cytometer (Becton Dickinson, San Jose, CA, USA).

#### ***Microscopy analysis (STEM/HAADF)***

Uranium-treated Be9 cells were harvested as described above, washed twice with 0.9% NaCl and sodium cacodylate buffer (pH 7.2), fixed with glutaraldehyde in a cacodylate buffer (4%) and stained with osmium tetroxide (1%, for 1 h) in the same buffer before being dehydrated through graded alcohol followed by propylene oxide treatment and finally embedded in epoxy resin. TEM specimen holders were cleaned by plasma prior to STEM analysis to minimize contamination. Ultrathin sections (0.1  $\mu\text{m}$ ) of the samples, obtained using an ultra-microtome, were loaded in a carbon coated copper grid. The samples obtained were observed by high-angle annular dark field scanning transmission electron microscope (HAADF-STEM), conducted using a FEI TITAN G2 80-300.

#### ***Statistical analysis***

All the data were performed by GraphPad Prism version 8.0.0 for Windows (GraphPad Software, California, USA) and presented as averages and standard deviations for at least three replicates per experimental condition tested.

### **Results**

#### ***Chemical characterization of the *Microbacterium* sp. Be9 cell surface***

##### *Potentiometric titrations*

Potentiometric titration curves of *Microbacterium* sp. Be9 are presented in Figure 1. The concentration of deprotonated sites is standardized per mass of dry biomass (mol/g) and calculated according to Fein et al. (1997). Titrated bacterial suspension exhibited a protonation-deprotonation behaviour over the whole pH range studied. During the titration, no evidence of saturation was observed with respect to proton adsorption. The intersection

point at zero charge appears between pH 6.48 – 6.77, being consistent with the experimental pH of zero proton charge ( $\text{pH}_{zpc}$ ) set by Protokit 2.1 rev1 ( $6.61 \pm 0.07$ ). The obtained  $\text{pH}_{zpc}$  value indicated that Be9 strain exhibited a net negative charge at circumneutral pH which could bind positively charged metal species such as uranium and other heavy metals. Supplementary Table 2 summarizes the deprotonation constants and surface concentrations values of *Microbacterium* sp. Be9 and that of other bacterial strains for comparison purposes. The obtained pKa values are representative of carboxylic groups for  $\text{pK}_1$  (4.38), phosphate groups for  $\text{pK}_2$  (6.07) and amine and hydroxyl groups for  $\text{pK}_3$  (9.82). The results of potentiometric titration experiments showed that the cell surface functional groups with metal binding potential are carboxyl groups ( $\text{pK}_1$  around 4.3), phosphate groups ( $\text{pK}_2$  around 6), and hydroxyl and amine groups ( $\text{pK}_3$  around 9.8). These findings are in agreement with previous studies on bacterial surfaces (Haas et al., 2001; Merroun et al., 2011; Moll et al., 2014; Ruiz-Fresneda et al., 2020; Yu et al., 2014).

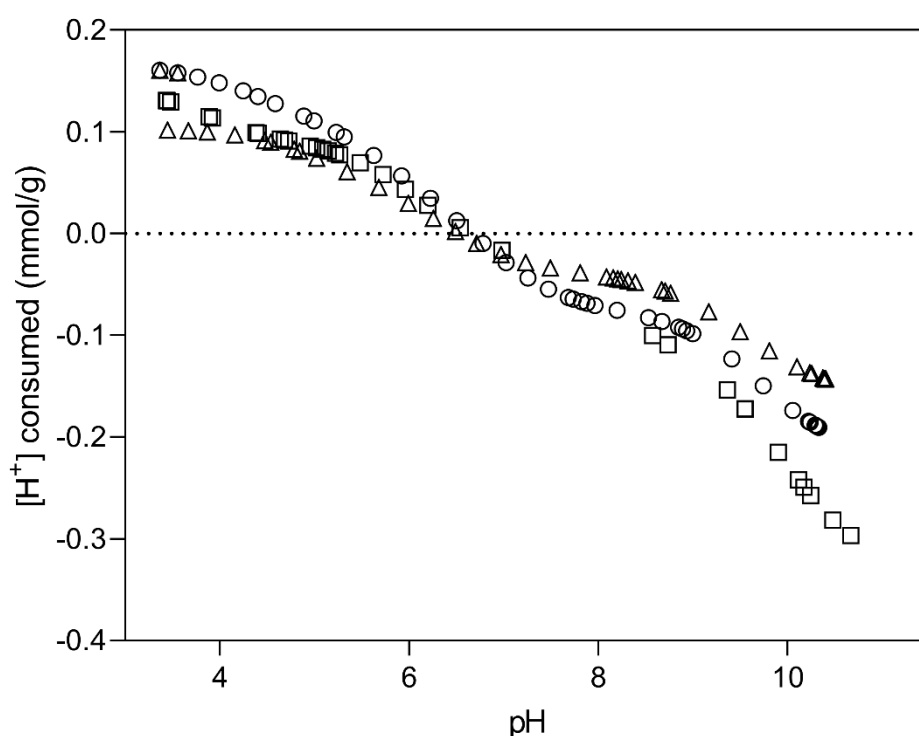


**Figure 1.** Potentiometric titration curves of Be9 strain in of 0.1 M  $\text{NaClO}_4$  at 25 °C. The symbols refer to experimental replicates of each titration curve.

Surface site concentrations obtained were normalized to the dry mass of bacteria, resulting  $0.45 \pm 0.006 \text{ mol/g} \times 10^{-4}$  for acidic sites,  $0.76 \pm 0.015 \text{ mol/g} \times 10^{-4}$  for neutral sites and 1.19

$\pm 0.061 \text{ mol/g} \times 10^{-4}$  for basic sites. The surface of Be9 cells exhibit low concentrations of phosphates ( $0.76 \pm 0.015 \times 10^{-4} \text{ mol/g}$ ) compared to those of other bacterial species (Supplementary Table 2) such as *Stenotrophomonas bentonitica* ( $10.78 \pm 0.31 \times 10^{-4} \text{ mol/g}$ ) (Ruiz-Fresneda et al., 2020), *Sporomusa* sp. MT-2.99 ( $5.30 \pm 0.8 \times 10^{-4} \text{ mol/g}$ ) (Moll et al., 2014), *Sphingomonas* sp. S15–S1 ( $3.16 \pm 0.56 \times 10^{-4} \text{ mol/g}$ ) (Merroun et al., 2011), or *Bacillus sphaericus* JG-7B ( $2.19 \pm 0.25 \times 10^{-4} \text{ mol/g}$ ) (Merroun et al., 2011). Similarly, the concentrations of carboxyl and hydroxyl/amine groups are also lower than those described above for other bacterial strains. However, strains such as *Shewanella putrefaciens* (Haas et al., 2001) or *Bacillus licheniformis* (Yu et al., 2014) have shown comparable values to Be9 strain.

#### *X-ray Photoelectron Spectroscopy (XPS)*

In order to identify the elemental composition and estimate the concentration of main constituents of the *Microbacterium* sp. Be9 cell surface, XPS analysis was carried out using an X-ray photoelectron spectrometer (Kratos Axis Supra XPS). Binding energy curves of viable Be9 cells as a wide scan is shown in Figure 2A. A phosphorous peak appeared at a binding energy of 134.02 eV, and was attributed to phosphate groups (Ahimou et al., 2007; Ojeda et al., 2008), and the nitrogen peak at 400.02 eV attributable to amine or amide groups present in proteins (Kjærviik et al., 2018; Ojeda et al., 2008). Carbon and oxygen peaks were detected around 285 and 532 eV respectively (Kjærviik et al., 2018; Leone et al., 2006; Ojeda et al., 2008) and analysed at high resolution and deconvoluted to assess the contributions from each element (Figs. 2B and 2C). The carbon peak was fit into four components: carbon bound to carbon or hydrogen [C–(C, H)], at 284.52 eV; carbon bound to nitrogen or hydroxyl group from amines, amides and/or alcohols [C–OH, N] at 285.89 eV; carbon doubly bound to oxygen from esters, acetals, carbonyls or carboxylates [C=O], at 287.46 eV; and carbon from carboxyl group [COOH], at 288.51 eV. The oxygen peak was decomposed into two components: oxygen double bound to carbon or phosphorous constituted in esters, carbonyls, amides, carboxylic acids, carboxylates or phosphoryl groups [C=O, P=O], at 528.89 eV; and oxygen present in phosphate, acetal, hemiacetal or hydroxide groups [P–OH, C–O–C and C–OH], at 530.27 eV.

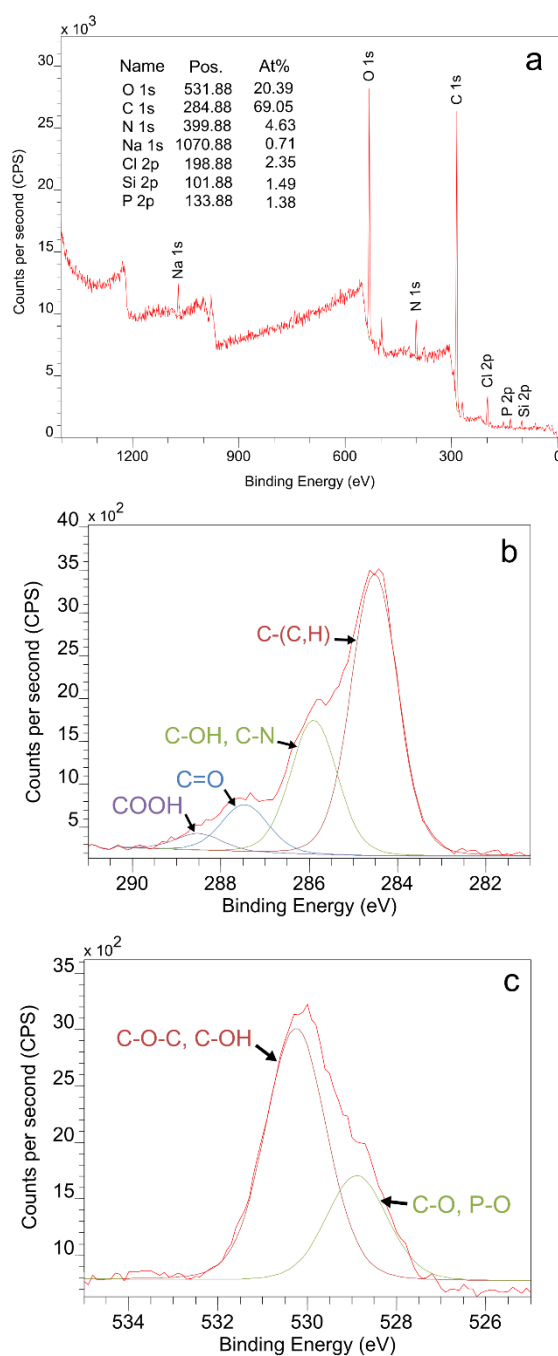


**Figure 2.** (A) XPS survey spectrum collected from viable cells of *Microbacterium* sp. Be9 as a wide scan. The peaks of carbon (B) and oxygen (C) were scanned at high resolution and deconvoluted to assess the local chemical environment of these two elements.

The elemental concentration was estimated assuming polysaccharides, peptides and hydrocarbon-like products (such as lipids) as the main constituents on the bacterial surface. Based on previous studies (Dufrière et al., 1997; Rouxhet et al., 1994; Van Der Mei et al., 2000), the molecular composition has been calculated by comparing the carbon

concentration (in mmol/g) and the atomic concentration ratio of nitrogen and oxygen with respect to carbon for glucan  $(C_6H_{10}O_5)_n$  for polysaccharides, the major outer membrane protein of *Pseudomonas fluorescens* OE 28.3 for peptides and using  $C-(C,H)/C=1.000$  from  $(CH_2)_n$  for hydrocarbon-like products. Considering those compositions, a set of three equations can be provided:

$$\frac{O}{C} = 0.325 \left( \frac{CPEP}{C} \right) + 0.833 \left( \frac{CPS}{C} \right) \quad (1)$$

$$\frac{N}{C} = 0.279 \left( \frac{CPEP}{C} \right) \quad (2)$$

$$1 = \left( \frac{CPEP}{C} \right) + \left( \frac{CPS}{C} \right) + \left( \frac{CHC}{C} \right) \quad (3)$$

*Microbacterium* sp. Be9 proportions for each constituent were  $CPEP/C = 0.52$ ,  $CPS/C = 0.75$  and  $CHC/C = 0.69$ . Thus, the estimated concentrations of main constituents in the Be9 cell surface are 26.7% peptides, 38.2% polysaccharides and 35.1% hydrocarbon-like compounds.

### ***U chemical speciation***

The chemical speciation of 100  $\mu$ M U in MOPS buffer [in the absence of G2P (MC1) and with the addition of G2P (MC2)] and in LPM (MC3) at pH 6.6 were determined using Visual MINTEQ 3.1 software (Gustafsson, 2020) and PhreeqC software (calculated using PRODATA thermodynamic database; Reiller and Descostes, 2020), respectively (Supplementary Table 3). In MC1/MC2 systems, the presence/absence of G2P showed no differences in the U speciation, dominated by hydroxo-uranyl complexes as  $(UO_2)_3(OH)^{5+}$  (78.3% – 78.5%) and  $(UO_2)_4(OH)^{7+}$  (19.5% – 19.2%). In contrast, U speciation in MC3 medium showed the presence of hydroxo-uranyl complexes [ $(UO_2)_3(OH)^{5+}$  (48.6%) and  $(UO_2)_4(OH)^{7+}$  (25.1%)] and U hydroxy-carbonates ( $(UO_2)_2(OH)_3CO_3^-$ ) (24.2%). In addition, U phosphate ( $UO_2PO_4^-$ ) was also identified (0.38%). In this case, a high positive saturation index was calculated, indicating a probable precipitation of inorganic uranyl orthophosphate  $(UO_2)_3(PO_4)_2 \cdot 4H_2O$ .

### ***Effect of different phosphate species on Be9-U interactions***

Our study aimed to investigate the effect of phosphates on the performance of the U biomineralization mediated by cells of *Microbacterium* sp. Be9. Three specific conditions using different phosphate sources were assayed (see above). A combination of wet

chemistry (U removal kinetics, orthophosphate release monitoring), flow cytometry (cell viability assays), biochemical (phosphatase activity) and microscopic techniques were applied.

#### *Phosphate free system (MC1)*

Uranium removal kinetics by Be9 cells under absence of exogenous phosphates was determined by measuring residual U in the supernatants. The results indicated that the cells removed 60% and 88% of the initially added U within the first minutes and after 48 h of incubation, respectively (Fig. 3). Abiotic controls consisting of U added to MOPS buffer showed that metal removal only reached up to 13% after 48 h of exposure, supporting the key biotic role in the high precipitation of U detected. To investigate whether phosphatases are involved in the U removal process, the activity of these enzymes and the associated orthophosphate released during the experiment were determined. The results showed no phosphatase activity in the U treated cells (Supplementary Fig. 1). A very low release of inorganic phosphates was detected in this assay (2.21 mg/ml; Supplementary Fig. 2A), coinciding with a non-significant phosphatase activity.

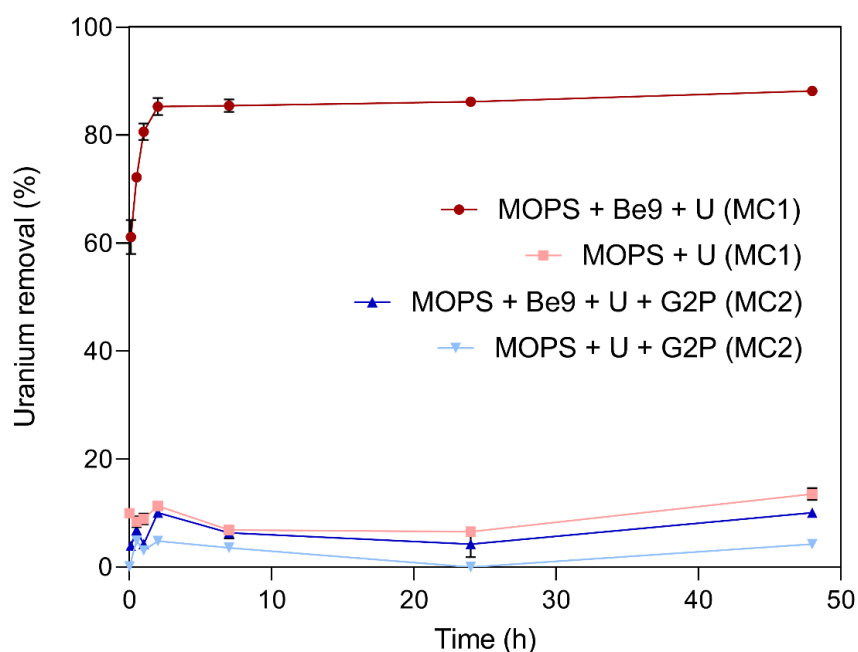


**Figure 3:** Uranium removal efficiency (%) kinetics during MC1 and MC2 conditions assayed. Abiotic treatments were used as control in both conditions. Data are shown as the mean and error bars represent standard error of three independent measurements.

STEM micrographs of U-treated cells at 48 h showed that this radionuclide is mainly located intracellularly as needle-like fibrils (Supplementary Fig. 3). The number of intracellular accumulates apparently increased according to the incubation time. No extracellular U precipitates were observed. Elemental mapping analysis illustrated in Figure 4 shows that the U precipitates were composed of U and P, probably revealing a biomineralization of the U phosphates.

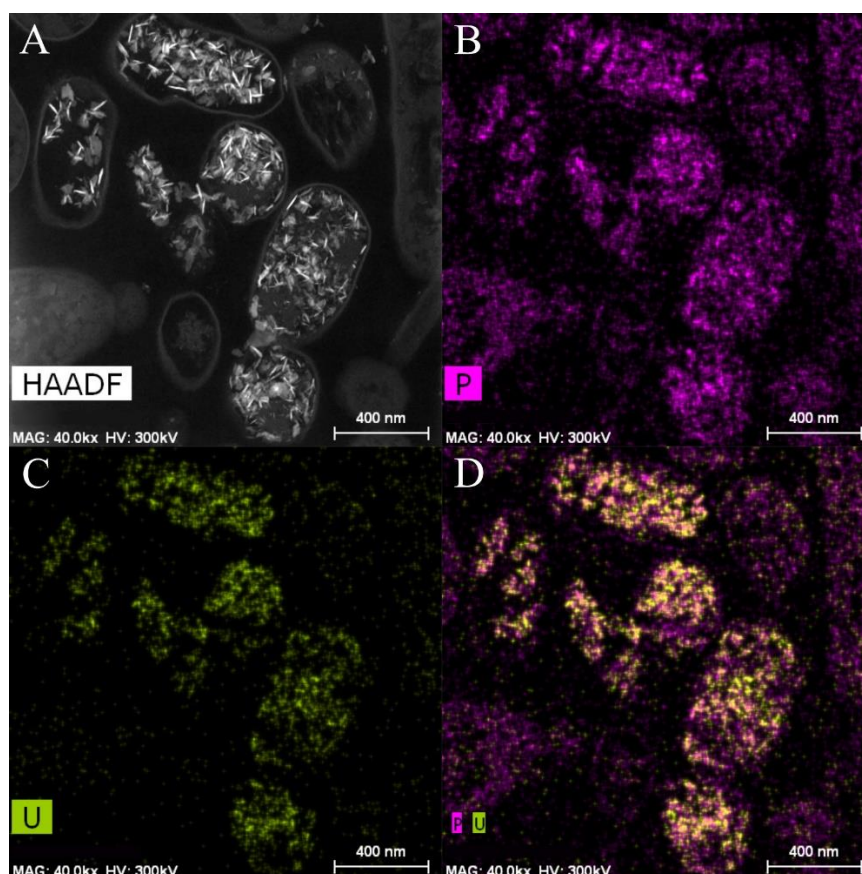


**Figure 4.** HAADF-STEM image of *Microbacterium* sp. Be9 cells after incubation under MC1 condition; EDX element mapping for P (B), U (C) and P-U combined (D).

We used flow cytometry technique based on live/dead staining to investigate the effect of U in the cell viability and cell membrane potential. 100% of untreated (control treatment) and U-treated Be9 cell populations remained viable and metabolically active for the first 24 h. The results suggest that the intracellular accumulation of U at 24 h (86% of accumulated U) and the consequent biomineralization of U phosphates is a metabolically active process associated with biological activity of the strain Be9. However, at 48 h, the



viability of the U-treated cells decreased to 18% and the membrane potential of the cells was markedly reduced to 0% (Supplementary Table 4).

#### *System amended with organic phosphates (MC2)*

We investigated the effect of an exogenous organic phosphate substrate (G2P) in the U biomineralization. When G2P was added, U-removal by Be9 cells was about 10% after 48 h (Fig. 3), significantly lower than that in phosphate-free system (MC1 system) (see above). In the abiotic control treatments, consisting of the MOPS buffer treated with G2P and U, the removal rate was only 4.3% of the initial U concentration. At the end of the experiment, the results indicated that, in the presence of organic phosphates, bacterial cells play a minor role in U removal. Despite the addition of G2P, low levels of Pi were released, in accordance with the weak acid phosphatase displayed (Supplementary Fig. 2A). Considering that the added G2P concentration (5 mM) was equivalent to 475 mg/L of Pi, the amount of Pi released to the supernatant was low (10.59 mg/L), similar to the MC1 condition shown above (Supplementary Fig. 2A). In the presence of G2P an increase in Be9 cell viability was measured from 24 h (61.03% viable cells) to 48 h (85.14% viable cells), but their cell membrane potential at 48 h was reduced in comparison with the non-G2P treatment (Table Supplementary 4). STEM micrographs of thin sections of U-treated cells in the presence of G2P showed a few U intracellular accumulates (Figs. Supplementary 4 and 5). These U accumulates appeared as needle fibrils as well as immobilized within the granules of the phosphates. The detection of a low number of U accumulates are in line with the low levels of U removal (10%). Elemental mapping analysis of certain Be9 cells that showed precipitation revealed that U appeared co-localised with P (Fig. 5), as in the phosphate-free system (MC1).

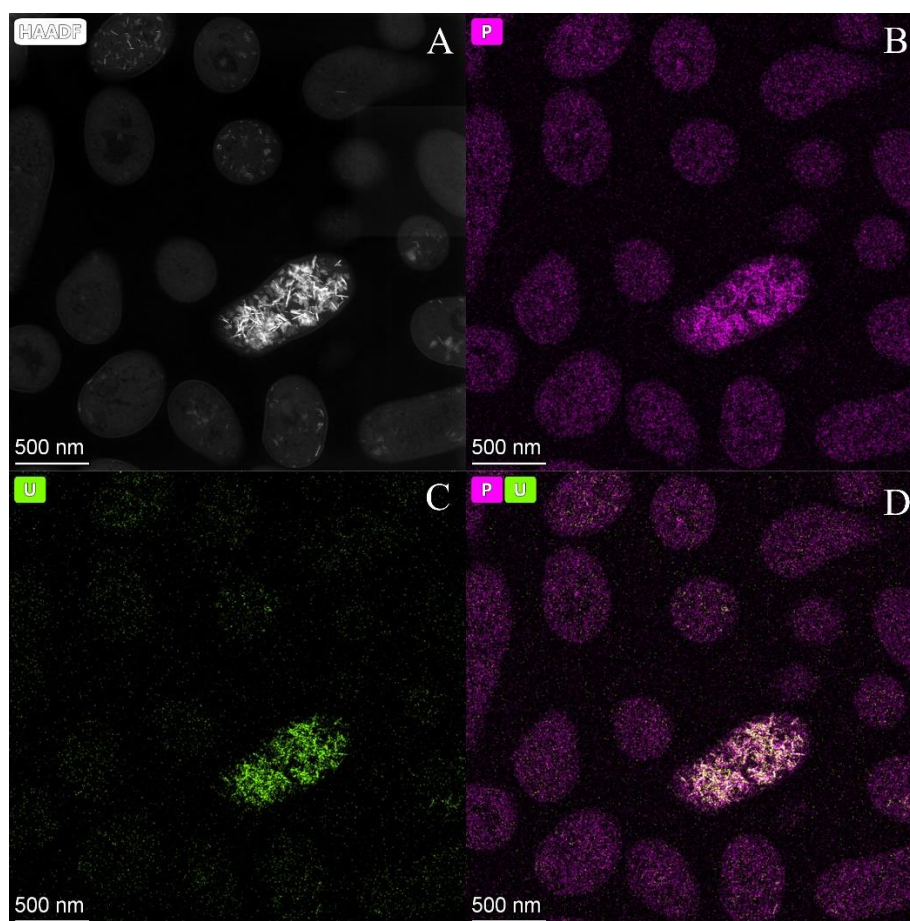


**Figure 5.** HAADF-STEM image of *Microbacterium* sp. Be9 cells after incubation under MC2 condition (A); EDX element mapping for P (B), U (C) and P-U combined (D).

#### *Effect of inorganic phosphates in U biomineralization (MC3)*

We studied the effect of inorganic phosphates in the U interaction by the strain Be9 using low phosphate medium (LPM) at two U concentrations (0.5 and 1 mM). Peptone was used as source of phosphate at different concentrations (100 and 0.2 mg/L) in order to consider the theoretical abiotic precipitation of U according to the speciation analysis previously presented (Table Supplementary 3). Under abiotic conditions, almost all the U was removed from the solution (93 – 99%) (Fig. 6), supporting the precipitation of the metal as indicated by U chemical speciation studies. However, in the treatments with Be9 strain and LPM supplemented with U, the elimination was 13% and 23% of U at 0.5 and 1 mM metal concentration, respectively, after 48 h (Fig. 8). Moreover, when the Be9 cells were inoculated in low-peptone LPM (0.2 mg/L) supplemented with 0.5 and 1 mM U, non-metal removal was observed, with 100% of the U remaining in the soluble form.

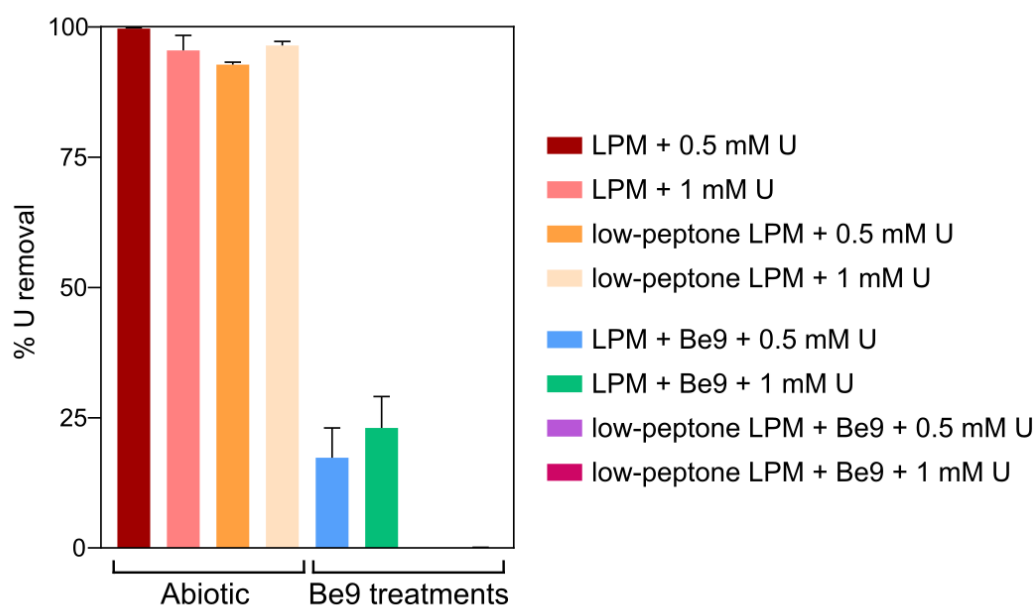


**Figure 6.** U removal after the incubation under different phosphate and U concentrations in the presence and absence of *Microbacterium* sp. Be9 cells. Peptone reduction (0.2 mg/L) is labelled as low-peptone LPM. Data are shown as the mean and the error bar

Phosphatase activity of the Be9 strain was only detected after incubation in the LPM medium under 0.5 and 1 mM U concentrations (Supplementary Fig. 1), whilst the low-peptone condition assays exhibited no enzyme activity. Measurements of the released Pi (Supplementary Fig. 2B) revealed that the cells were able to solubilize 20 and 25 mg/L of orthophosphates from the solution supplemented with 0.5 and 1 mM U, respectively. Under peptone-reduced treatments with 0.5 and 1 mM U concentrations, the Be9 strain also released similar amounts to before (27 and 24 mg/L, respectively). The Pi concentration detected after incubation in abiotic control treatments was around 0.02 – 3 mg/L due to its interaction with U, except at 0.5 mM U concentration, which was 47.40 mg/L. Be9 cell viability and activity in the LPM medium remained over 98% for 48 h under phosphate reduction and both U concentrations tested (Table Supplementary 4). STEM-HAADF micrographs of U precipitates formed abiotically in LPM (100 and 0.2 mg/L peptone concentration) supplemented with 0.5 and 1 mM U for 48 h revealed the presence of solid phases with different sizes and morphology (aggregates, needle-like fibrils, etc.) (Supplementary Fig. 5). In the presence of the Be9 strain, STEM micrographs did not show any U precipitates (Supplementary Fig. 6), according to the U removal levels measured before. Only some U precipitates were detected in the extracellular space which could

correspond to abiotic U precipitates. Elemental mapping analysis showed that these extracellular precipitates were mainly composed of U and P indicating the precipitation of the abiotic U phosphates (Fig. 7).

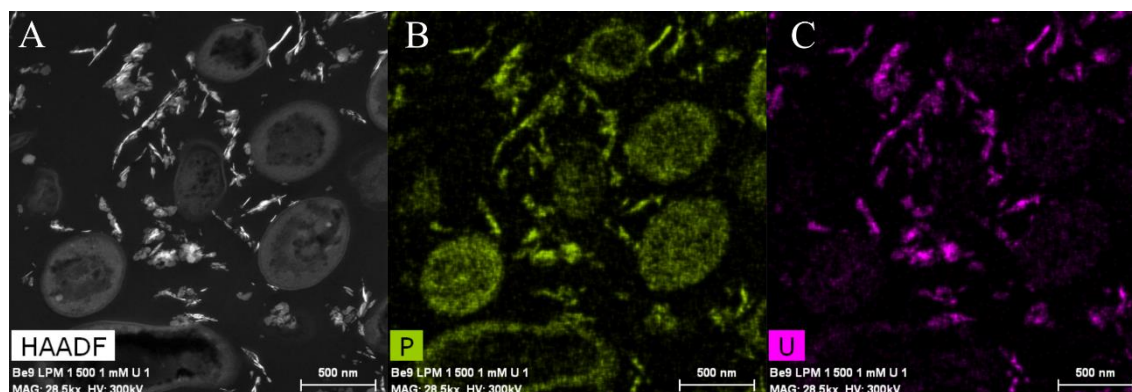


**Figure 7.** HAADF-STEM image of *Microbacterium* sp. Be9 cells after incubation under MC3 treatment (0.2 mg/L peptone concentration and 1 mM U) (A); EDX element mapping for P (B) and U (C).

#### *Uranium solubilization kinetic assay*

It is well known that *Microbacterium* species from diverse natural environments are classified within the group of PSB (Panda et al., 2016; Zhang et al., 2017). Therefore, we further studied the uranium solubilization process detected through a kinetic assay using living and heat-killed Be9 cells. Abiotic U-phosphate precipitates recovered from LPM supplemented with 0.5 mM U for 48 h (as detected previously), were inoculated with active and heat-killed cells of Be9 strain. In addition, LPM supplemented with 0.5 mM U was also considered as an abiotic control. In the presence of active cells, the solubilization of U phosphates increased gradually throughout the incubation time, reaching around 25% of U immobilized at 24 h and 5% at 48 h (Fig. 8). In heat-killed cells and abiotic control treatments, 90% of the U amended phosphates remained intact within the 48 h of exposure. These results indicate that the biological activity of the strain *Microbacterium* sp. Be9 was directly involved in the U solubilization.

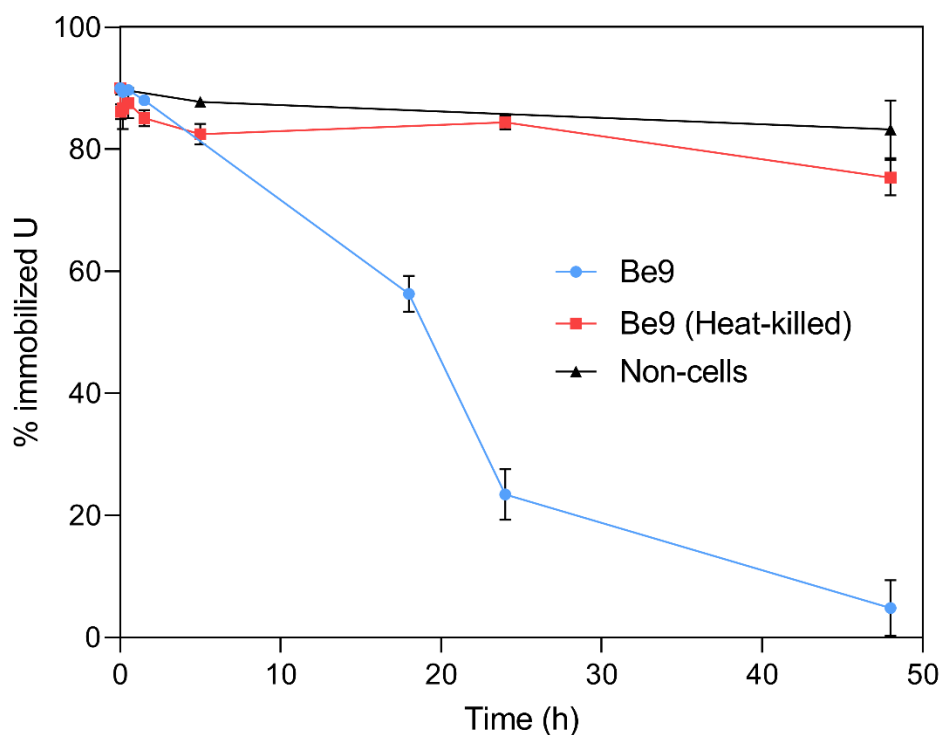


**Figure 8.** U solubilization kinetics assay (%) during the incubation of *Microbacterium* sp. Be9 cells with U-phosphate precipitates. Flasks without cells and including heat-killed bacterial cells were used as control treatments. Data are shown as the mean and the error bars represent the standard error of at least three independent measurements.

## Discussion

The main objective of this study is to investigate the effect of phosphates in the biomineralization of U (VI) by *Microbacterium* sp. Be9, a uranium mill tailings porewater isolate. To the best of our knowledge, this is the first study determining the effect of organic and inorganic phosphates in the U phosphate biomineralization process. Previously, environmental factors such as pH (Beazley et al., 2007; Chandwadkar et al., 2018; Zhang et al., 2018), temperature (Li et al., 2013), the presence of carbonates (Wei et al., 2019),  $\text{NH}_4^+$  incorporation (Yong and Macaskie, 1995) and organic matter (Boiteau et al., 2018; Medina et al., 2017) have been described to affect the U phosphate biomineralization. Our experiments have shown that the U biomineralization ability by the Be9 strain is drastically reduced by both organic and inorganic phosphates. However, in an exogenous phosphate-free system, the cells removed up to 88% U within 24 h (Fig. 3) through intracellular U phosphate biomineralization. In addition, as a result of the kinetic studies, we can confirm

that in the presence of previously abiotically precipitated U phosphates, the Be9 cells were able to solubilize this radionuclide (Fig. 8) through a metabolism-dependent process.

The first step in this microbial U biomineralization process by the Be9 strain appears to be surface biosorption. Bacterial surfaces act as nucleation sites for the formation of biogenic U(VI)-phosphates through combined surface sorption of this radionuclide and phosphatase-mediated U biomineralization (Pan et al., 2015; Theodorakopoulos et al., 2015). Membranes play a major role in sorption of metals where electrostatic interactions between positively charged metal species and negatively charged functional groups (e.g. phosphates, carboxyles) occur. Gram-positive bacteria (such as the Be9 strain) exhibit greater biosorption capacity than Gram-negative bacteria due to their cell envelope components (Hufton et al., 2021). Liu et al., (2015) demonstrated the role of carboxyl, phosphoryl, and amino functional groups of *Synechococcus* sp. PCC 7002 cells as metal surface ligands by means of potentiometric titrations. Therefore, in our study, the chemical properties of the cell surface of Be9 strain were characterized using potentiometric titration and XPS analysis. The pH zero proton charge ( $\text{pH}_{\text{zpc}}$ ) around  $6.61 \pm 0.07$  (Supplementary Table 2) indicated that Be9 cells developed a negative net charge at the pH value we studied. These data show that electrostatic attraction of negatively ionizing groups (e.g. carboxyl, phosphoryl and hydroxyl groups) with positively charged U species (e.g.  $\text{UO}_2)_3(\text{OH})^{5+}$  and  $(\text{UO}_2)_4(\text{OH})^{7+}$ ) is favourable. Thermodynamic calculation showed that under phosphate free system and in presence of G2P, these favourable compounds as  $(\text{UO}_2)_3(\text{OH})^{5+}$  and  $(\text{UO}_2)_4(\text{OH})^{7+}$  represented 78% and 20% species of U (Supplementary Table 3). In the case of phosphate-free system, the negatively ionizing groups of the cell wall could sorb 70% of positively charged U species in the first 10 min as was shown by the U removal kinetics studies (Fig. 3). XPS analysis exhibited a high proportion of polysaccharides in the Be9 cell surface. Polysaccharides have been described as playing an important role in enhancing the tolerance of microorganisms under metal stress (Sun et al., 2020). In the cell surfaces of *Pseudomonas putida* similar percentages of peptides were obtained and were involved in the interaction with nZVI/Pd particles (Lv et al., 2017).

Under the absence of phosphates (MC1 system), a metabolism dependant precipitation of U intracellular phosphates seemed to take place after the surface sorption. The U removal capacity increased slowly throughout the time, without any significant differences between 24 h and 48 h. These results show that U removal by this strain is a biphasic process with a fast first phase mediated by a passive process (e.g. sorption at cell surfaces) and a slow

second phase driven by metabolically active processes (e.g. intracellular accumulation, biomineralization, etc.). However, in comparison to other bacterial strains, Be9 showed low concentrations of phosphate or carboxyl groups at the cell surface (Supplementary Table 2) which could probably explain why U is mainly accumulated intracellularly as was demonstrated by electron microscope analysis. Previous studies showed a strong correlation between the concentration of phosphates and carboxyl groups of the cell wall and cellular localization of the metal of some bacterial strains such *S. bentonitica* BII-R7 (Sánchez-Castro et al., 2020). The latter strain exhibited 12 and 10 orders of magnitude of phosphate and carboxyl groups (Ruiz-Fresneda et al., 2020) higher than the Be9 strain, and high capability to bind and biomineralize U at the cell surface (Sanchez-Castro et al., 2020). However, in spite of the low amount of phosphate and carboxyl groups, seems to be sufficient to act as a first passive sorption step followed by intracellular precipitation of uranium.

Biphasic U removal process has also been reported by other authors in different bacteria such as *Acidovorax facilis* (Gerber et al., 2016), *Stenotrophomonas bentonitica* BII-R7 (Pinel-Cabello et al., 2021) and *Microbacterium* sp. A9 (Theodorakopoulos et al., 2015). Flow cytometry studies revealed that 100% of the cells were viable and metabolically active during the first 24 h, supporting the involvement of a metabolic-dependent process in the interaction with U besides biosorption. A decrease in cell viability at 48 h seems to be clearly related to the high U-bioprecipitation inside the cells. In the case of uranium, numerous studies have reported the immobilization of this radionuclide by intracellular polyphosphate bodies through different analyses as TEM and EDX (Li et al., 2016; Merroun et al., 2006, 2003; Suzuki and Banfield, 2004). The low concentrations of phosphate and carboxyl groups at the Be9 cell surface indicated by potentiometric titration studies (Supplementary Table 2) could explain the low U amount bound to the surface. However, in spite of the low amount of phosphate and carboxyl groups, seems to be sufficient to act as a first passive sorption. In our study, the presence of U in the cells is speculated to induce the activity of enzymes such as exopolyphosphatase to degrade polyphosphate, thus releasing orthophosphates for the biomineralization of U. Theodorakopoulos et al., (2015) proposed an induction of enzymatic pathways from a *Microbacterium* strain which causes bound breakage of polyphosphate granules in the cytoplasm for the biomineralization of U intracellularly. However, the intracellular biomineralization of U associated with degradation of polyphosphates require the U uptake

by the cells. For metal uptake in microorganisms, two main mechanisms were described: first, an active process through metal transporters for essential metals, and then, a passive process by an increase of cell membrane permeability due to damage for toxic metals (Suzuki and Banfield, 1999). In the case of *Microbacterium*, it has been demonstrated that iron transportation proteins are involved in the uranium uptake by *Microbacterium oleivorans* A9 (Gallois et al., 2018). A recent study about different *Microbacterium* strains revealed a transmembrane protein with binding affinity for  $\text{UO}_2^{2+}$  and  $\text{Fe}^{3+}$  specific to U-tolerant strains (Gallois et al., 2022). Regarding to the Be9 strain, in a previous study, its genome was annotated and ABC-type  $\text{Fe}^{3+}$  siderophore transport proteins, which may be involved in U uptake, were identified (Martínez-Rodríguez et al., 2020). Transcriptomics and proteomics studies are needed to further address the nature of transporters used for U intracellular accumulation in the strain Be9.

STEM micrographs of Be9 cells showed a gradual formation of needle-like structures composed of U and P in the cytoplasm over time. The U phosphate nature of similar needle-like structures was confirmed in the literature by the use of different spectroscopic techniques such as EXAFS, TRLS, etc. (Lopez-Fernandez et al., 2018), also in *Microbacterium* genus (Theodorakopoulos et al., 2015). Microbes are able to precipitate U phosphate phases with different structures (e.g. autunite, chernikovite, etc.) through phosphatase activity which degrade organic phosphates (e.g. glycerol phosphates) and release orthophosphates (Merroun et al., 2011; Sánchez-Castro et al., 2020; Skouri-Panet et al., 2018). In our study, although phosphatase activity was not detected, U phosphates were evidenced in the cells treated with U. Thus, the U phosphate biomineralization induced by this strain is probably not associated with phosphatase activity. Similarly, other U-tolerant *Microbacterium* strains showed a very low abundance of acid and alkaline phosphatase activity in their proteome (Gallois et al., 2022). The needle-like structures identified in STEM micrographs could be raised from the interaction of U species with existent orthophosphates in intracellular polyphosphates since no exogenous phosphate substrate was added. Previous studies have reported some bacterial strains capable of precipitating U into uramphite without additional phosphorous sources (Pan et al., 2015; Zhang et al., 2018). Polyphosphates (polyPs) granules are ubiquitous polymers occurring in many microorganisms (Seufferheld et al., 2008). They contain a high number of orthophosphate residues that are linked to phosphoanhydride bonds to form linear polymers (Mandala et al., 2020). However, a recent study described the existence of small



metaphosphates, cyclic oligomers of  $[\text{PO}_3]^{(-)}$  made up of 3 to 8 phosphate groups (Mandala et al., 2020) as a candidate for precipitation of positively charged U species. Polyphosphate bodies possess various biological functions including phosphate removal, metal chelation, stress response, etc. (Achbergerová and Nahálka, 2011). Previous studies have demonstrated the role of bacterial polyphosphates in the accumulation of heavy metals and radionuclides (Acharya and Apte, 2013; Brim et al., 2000; Villagrasa et al., 2020). Be9 whole genome sequence analysis indicated the presence of genes codifying for enzymes involved in the synthesis (e.g. polyphosphate kinase) and degradation (e.g. exopolyphosphatase) of polyphosphates (Martínez-Rodríguez et al., 2020). In addition, *Microbacterium* spp are well documented as potential polyphosphate accumulating microorganisms (Suzina et al., 2022; Theodorakopoulos et al., 2015). Therefore, the results obtained are in agreement with the expected hypothesis, where Be9 cells are able to release orthophosphates for the U biomineralization through polyphosphatase activity on intracellular polyphosphate granules. No phosphatase activity was involved in this metal/bacteria interaction process.

Surprisingly, in MC2 system (G2P presence), Be9 cells exhibited low U removal capacity contrary to expected, as compared to free phosphate system. In addition, no phosphatase activity was detected. Microbial phosphatase enzymes (acid and alkaline) catalyse the hydrolysis of G2P into glycerol and orthophosphates which lead to the precipitation of U phosphates with different structures such as efficient strategy for U bioremediation (Beazley et al., 2011; Liang et al., 2016; Merroun et al., 2011; Sánchez-Castro et al., 2021, 2020). However, although no phosphatase activity was measured, a certain concentration of orthophosphates was detected under these conditions. Thus, since G2P is not degraded extracellularly, it is probably transported intracellularly to be used as an organic carbon source for the metabolism of carbohydrates and lipids. This hypothesis is supported by the fact that the whole genome sequence of Be9 exhibited genes codifying for proteins for the uptake and utilization of G3P and glycerol (glycerol-3-phosphate ABC transporter, ATP-binding protein UgpC, glycerol-3-phosphate dehydrogenase, glycerophosphoryl diester phosphodiesterase). Gallois et al. (2018) reported the upregulation of proteins involving transport of glycerol-3-phosphate in the cells of *Microbacterium oleivorans* A9 treated with uranium. In contrast with the previous conditions (phosphate-free system), cell viability under the presence of U and G2P increased from 24 to 48 h of incubation, which supports the assumption that G2P is used by Be9 cells as a carbon or phosphorus source. Tu et al.

(2019) described that strong organic-ligands such as oxalate and citrate competed with biotic  $\text{PO}_4^{3-}$  for uranyl, inhibiting the U-phosphate biomineralization by the cells of *Bacillus* sp. dw-2. Speciation of U in MC2 system (Supplementary Table 3) was dominated by hydroxo-uranyl complexes as  $(\text{UO}_2)_3(\text{OH})^{5+}$  (78.51%) and  $(\text{UO}_2)_4(\text{OH})^{7+}$  (19.22%) and no G2P-U complexes were expected. However, the mechanisms responsible for the decrease of U removal and biomineralization rate remains unclear.

Finally, we used the culture medium LPM in different treatments (MC3 system) to induce abiotic precipitation of U phosphates. As expected, the chemical speciation of U (at 0.5 and 1 mM) in this medium and in its diluted form (0.2 mg/L peptone concentration) resulted in a high positive saturation index (Supplementary Table 3), predicting the precipitation of various uranyl compounds including U phosphates. These results were confirmed by abiotic precipitation experiments where U precipitation reached high values after 48 h (Fig. 6). Numerous amorphous structures such as U-phosphates and U-carbonates were identified in HR-TEM micrographs by EDX analysis (Supplementary Fig. 7). However, in presence of Be9 cells, 94.5% of U was re-solubilized from abiotically precipitated U phosphates. Under this U concentration, the Be9 cells remained viable until 48 h, reacting with the precipitated U species, mainly U inorganic phosphates. Thus, contrary to the expected hypothesis, the obtained results demonstrated the *Microbacterium* sp. strain Be9 capacity of U phosphate solubilization, due to its belonging to PSB group. The cells seemed to display active mechanisms to solubilize this radionuclide. Microorganisms known as PSBs are able to solubilize both organic and inorganic phosphorus from insoluble compounds. Recently, numerous U-tolerant PSB strains have been isolated from mining sites of this radionuclide (Lv et al., 2022; Sowmya et al., 2020, 2014). Mechanisms of phosphate solubilization by PSB strains involve hydroxyl and carboxyl groups present in the cells or in released organic acids (Chen et al., 2006). In addition, a number of genes encoding enzymes responsible for P solubilization (e.g. encoding quinoprotein glucose dehydrogenase (*gcd*), phnP C-P lyase subunit (*phnP*), *phoA* alkaline phosphatase (*phoA*), *phoD* alkaline phosphatase (*phoD*), and *phoN* acid phosphatase (*phoN*)) have been reported (Rawat et al., 2021). In our study, we detected the U-mobilization activity by the Be9 strain reacting with inorganic phosphates. This fact indicates that this behaviour may involve the solubilization of U from precipitated U-phosphates. In this way, bonded heavy metals (such as U) could be released in a soluble and toxic form to the environment. However, some bioremediation strategies require interaction with an available form of the metal to facilitate

its removal. To this aim, the Be9 solubilization behaviour could be applied in combined U remediation technologies.

### **Conclusions**

In this study we have demonstrated that the *Microbacterium* sp. strain Be9 possesses a dual behaviour towards U and is capable of precipitating and solubilizing this radionuclide under different conditions. In addition, the presence or absence of different phosphate sources had an influence on the U biomineralization ability of the Be9 strain. Therefore, this strain could be used as U bioremediation agent in a free exogenous phosphate system. And due to its potential in the solubilization of phosphates from organic and inorganic P sources, this strain could contribute indirectly to providing this inorganic anion for the precipitation of this radionuclide. Thus, our results provide new insights into the impact of microbes on the biogeochemical cycle of U in the presence of different forms of phosphates. This information leads to the understanding of the conditions regarding biogenic U (VI) phosphate mineral formation and the physico-chemical parameters which hinder biomineralization and remediation strategies in oxidizing conditions. The correct selection of the supplemented organic phosphate donor could be crucial depending on the microorganism used. Therefore, the importance of gaining knowledge about microbial diversity and its role with the target metal is crucial to achieve the correct application of selected bioremediation technologies.

### **Conflict of Interest**

The authors declare that the research was conducted in the absence of any commercial or financial relationships that could be construed as a potential conflict of interest.

### **Acknowledgments**

This work was supported by ORANO Mining (France) [collaborative research contract n° 3022 OTRI-UGR]. The authors acknowledge the *Centro de Instrumentación Científica* within the University of Granada (Spain) for TEM measurements and sample preparation

(Concepción Hernández Castillo). The authors would like to acknowledge Angela Tate for language editing of the original and revised versions of the article.

## References

- Acharya, C., Apte, S.K., 2013. Novel surface associated polyphosphate bodies sequester uranium in the filamentous, marine cyanobacterium, *Anabaena torulosa*. *Metallomics* 5, 1595–1598. <https://doi.org/10.1039/c3mt00139c>
- Achbergerová, L., Nahálka, J., 2011. Polyphosphate - an ancient energy source and active metabolic regulator. *Microb. Cell Fact.* 10, 1–14. <https://doi.org/10.1186/1475-2859-10-63>
- Ahimou, F., Boonaert, C.J.P., Adriaensen, Y., Jacques, P., Thonart, P., Paquot, M., Rouxhet, P.G., 2007. XPS analysis of chemical functions at the surface of *Bacillus subtilis*. *J. Colloid Interface Sci.* 309, 49–55. <https://doi.org/10.1016/j.jcis.2007.01.055>
- Banala, U.K., Das, N.P.I., Toleti, S.R., 2021. Microbial interactions with uranium: Towards an effective bioremediation approach. *Environ. Technol. Innov.* 21, 101254. <https://doi.org/10.1016/j.eti.2020.101254>
- Beazley, M.J., Martinez, R.J., Sobecky, P.A., Webb, S.M., Taillefert, M., 2009. Nonreductive biomineralization of uranium(VI) phosphate via microbial phosphatase activity in anaerobic conditions. *Geomicrobiol. J.* 26, 431–441. <https://doi.org/10.1080/01490450903060780>
- Beazley, M.J., Martinez, R.J., Sobecky, P.A., Webb, S.M., Taillefert, M., 2007. Uranium biomineralization as a result of bacterial phosphatase activity: Insights from bacterial isolates from a contaminated subsurface. *Environ. Sci. Technol.* 41, 5701–5707. <https://doi.org/10.1021/es070567g>
- Beazley, M.J., Martinez, R.J., Webb, S.M., Sobecky, P.A., Taillefert, M., 2011. The effect of pH and natural microbial phosphatase activity on the speciation of uranium in subsurface soils. *Geochim. Cosmochim. Acta* 75, 5648–5663. <https://doi.org/10.1016/j.gca.2011.07.006>
- Boiteau, R.M., Shaw, J.B., Pasa-Tolic, L., Koppelaar, D.W., Jansson, J.K., 2018. Micronutrient metal speciation is controlled by competitive organic chelation in grassland soils. *Soil Biol. Biochem.* 120, 283–291. <https://doi.org/10.1016/j.soilbio.2018.02.018>
- Brim, H., McFarlan, S.C., Fredrickson, J.K., Minton, K.W., Zhai, M., Wackett, L.P., Daly, M.J., 2000. Engineering *Deinococcus radiodurans* for metal remediation in radioactive mixed waste environments. *Nat. Biotechnol.* 18, 85–90. <https://doi.org/10.1038/71986>
- Chandwadkar, P., Misra, H.S., Acharya, C., 2018. Uranium biomineralization induced by a metal tolerant: *Serratia* strain under acid, alkaline and irradiated conditions. *Metallomics* 10, 1078–1088. <https://doi.org/10.1039/c8mt00061a>
- Chen, Y.P., Rekha, P.D., Arun, A.B., Shen, F.T., Lai, W., Young, C.C., 2006. Phosphate solubilizing bacteria from subtropical soil and their tricalcium phosphate solubilizing abilities. *Applied Soil Ecology* 34, 33–41. <https://doi.org/10.1016/j.apsoil.2005.12.002>
- DiSpirito, A.A., Tuovinen, O.H., 1982. Uranous ion oxidation and carbon dioxide fixation by *Thiobacillus ferrooxidans*. *Archives of Microbiology* 133, 28–32.
- Dufrêne, Y.F., Van der Wal, A., Norde, W., Rouxhet, P.G., 1997. X-ray photoelectron spectroscopy analysis of whole cells and isolated cell walls of gram-positive bacteria: Comparison with biochemical analysis. *J. Bacteriol.* 179, 1023–1028. <https://doi.org/10.1128/jb.179.4.1023-1028.1997>

### CAPÍTULO III

- Fairley, N., 2020. CasaXPS: Processing Software for XPS, AES, SIMS and More. <http://www.casaxps.com/>
- Fein, J.B., Daughney, C.J., Yee, N., Davis, T.A., 1997. A chemical equilibrium model for metal adsorption onto bacterial surfaces. *Geochim. Cosmochim. Acta* 61, 3319–3328. [https://doi.org/10.1016/S0016-7037\(97\)00166-X](https://doi.org/10.1016/S0016-7037(97)00166-X)
- Gallois, N., Alpha-Bazin, B., Bremond, N., Ortet, P., Barakat, M., Piette, L., Mohamad Ali, A., Lemaire, D., Legrand, P., Theodorakopoulos, N., Floriani, M., Février, L., Den Auwer, C., Arnoux, P., Berthomieu, C., Armengaud, J., Chapon, V., 2022. Discovery and characterization of UipA, a uranium- and iron-binding PepSY protein involved in uranium tolerance by soil bacteria. *ISME J.* 16, 705–716. <https://doi.org/10.1038/s41396-021-01113-7>
- Gallois, N., Alpha-Bazin, B., Ortet, P., Barakat, M., Piette, L., Long, J., Berthomieu, C., Armengaud, J., Chapon, V., 2018. Proteogenomic insights into uranium tolerance of a Chernobyl's *Microbacterium* bacterial isolate. *J. Proteomics* 177, 148–157. <https://doi.org/10.1016/j.jprot.2017.11.021>
- Gavrilescu, M., Pavel, L.V., Cretescu, I., 2009. Characterization and remediation of soils contaminated with uranium. *J. Hazard. Mater.* 163, 475–510. <https://doi.org/10.1016/j.jhazmat.2008.07.103>
- Gerber, U., Zirnstein, I., Krawczyk-bärsch, E., Lünsdorf, H., Arnold, T., Merroun, M.L., 2016. Combined use of flow cytometry and microscopy to study the interactions between the gram-negative betaproteobacterium *Acidovorax facilis* and uranium(VI). *J. Hazard. Mater.* 317, 127–134. <https://doi.org/10.1016/j.jhazmat.2016.05.062>
- German, D.P., Weintraub, M.N., Grandy, A.S., Lauber, C.L., Rinkes, Z.L., Allison, S.D., 2011. Optimization of hydrolytic and oxidative enzyme methods for ecosystem studies. *Soil Biol. Biochem.* 43, 1387–1397. <https://doi.org/10.1016/j.soilbio.2011.03.017>
- Gustafsson, J.P., 2020. Visual MINTEQ, version 3.1. KTH Royal Institute of Technology, Stockholm, Sweden.
- Haas, J.R., Dichristina, T.J., Wade, R., 2001. Thermodynamics of U(VI) sorption onto *Shewanella putrefaciens*. *Chem. Geol.* 180, 33–54. [https://doi.org/10.1016/S0009-2541\(01\)00304-7](https://doi.org/10.1016/S0009-2541(01)00304-7)
- Hufton, J., Harding, J., Smith, T., Romero-González, M.E., 2021. The importance of the bacterial cell wall in uranium(vi) biosorption. *Phys. Chem. Chem. Phys.* 23, 1566–1576. <https://doi.org/10.1039/d0cp04067c>
- Jauberty, L., Drogat, N., Decossas, J.L., Delpech, V., Gloaguen, V., Sol, V., 2013. Optimization of the arsenazo-III method for the determination of uranium in water and plant samples. *Talanta* 115, 751–754. <https://doi.org/10.1016/j.talanta.2013.06.046>
- Khalid, S., Shahid, M., Niazi, N.K., Murtaza, B., Bibi, I., Dumat, C., 2017. A comparison of technologies for remediation of heavy metal contaminated soils. *J. Geochemical Explor.* 182, 247–268. <https://doi.org/10.1016/j.gexplo.2016.11.021>
- Kjærøvik, M., Schwibbert, K., Dietrich, P., Thissen, A., Unger, W.E.S., 2018. Surface characterisation of *Escherichia coli* under various conditions by near-ambient pressure XPS. *Surf. Interface Anal.* 50, 996–1000. <https://doi.org/10.1002/sia.6480>
- Kolhe, N., Zinjarde, S., Acharya, C., 2018. Responses exhibited by various microbial groups relevant to uranium exposure. *Biotechnol. Adv.* 36, 1828–1846. <https://doi.org/10.1016/j.biotechadv.2018.07.002>
- Leone, L., Loring, J., Sjöberg, S., Persson, P., Shchukarev, A., 2006. Surface characterization of the Gram-positive bacteria *Bacillus subtilis*-an XPS study. *Surf. Interface Anal.* 38, 1380–1385. <https://doi.org/10.1002/sia>
- Li, P., Liu, W., Gao, K., 2013. Effects of temperature, pH, and UV radiation on alkaline phosphatase activity in the terrestrial cyanobacterium *Nostoc flagelliforme*. *J. Appl. Phycol.* 25, 1031–

1038. <https://doi.org/10.1007/s10811-012-9936-8>
- Li, X., Ding, C., Liao, J., Du, L., Sun, Q., Yang, J., Yang, Y., Zhang, D., Tang, J., Liu, N., 2016. Bioaccumulation characterization of uranium by a novel *Streptomyces sporoverrucosus* dwc-3. *J. Environ. Sci. (China)* 41, 162–171. <https://doi.org/10.1016/j.jes.2015.06.007>
- Liang, X., Csetenyi, L., Gadd, G.M., 2016. Uranium bioprecipitation mediated by yeasts utilizing organic phosphorus substrates. *Appl. Microbiol. Biotechnol.* 100, 5141–5151. <https://doi.org/10.1007/s00253-016-7327-9>
- Liu, Y., Alessi, D.S., Owtrim, G.W., Petrash, D.A., Mloszewska, A.M., Lalonde, S. V., Martinez, R.E., Zhou, Q., Konhauser, K.O., 2015. Cell surface reactivity of *Synechococcus* sp. PCC 7002: Implications for metal sorption from seawater. *Geochim. Cosmochim. Acta* 169, 30–44. <https://doi.org/10.1016/j.gca.2015.07.033>
- Lloyd, J.R., Macaskie, L.E., 2000. Bioremediation of Radionuclide-Containing Wastewaters, in: *Environmental Microbe-Metal Interactions*. pp. 277–327. <https://doi.org/10.1128/9781555818098.ch13>
- Lopez-Fernandez, M., Jroundi, F., Ruiz-Fresneda, M.A., Merroun, M.L., 2021. Microbial interaction with and tolerance of radionuclides: underlying mechanisms and biotechnological applications. *Microb. Biotechnol.* 14, 810–828. <https://doi.org/10.1111/1751-7915.13718>
- Lopez-Fernandez, M., Romero-González, M., Günther, A., Solari, P.L., Merroun, M.L., 2018. Effect of U(VI) aqueous speciation on the binding of uranium by the cell surface of *Rhodotorula mucilaginosa*, a natural yeast isolate from bentonites. *Chemosphere* 199, 351–360. <https://doi.org/10.1016/j.chemosphere.2018.02.055>
- Lovley, D.R., Phillips, E.J.P., Gorby, Y.A., Landa, E.R., 1991. Microbial reduction of uranium. *Nature* 350, 413–416. <https://doi.org/10.1038/350413a0>
- Lv, Y., Niu, Z., Chen, Y., Hu, Y., 2017. Bacterial effects and interfacial inactivation mechanism of nZVI/Pd on *Pseudomonas putida* strain. *Water Res.* 115, 297–308. <https://doi.org/10.1016/j.watres.2017.03.012>
- Lv, Y., Tang, C., Liu, X., Chen, B., Zhang, M., Yan, X., Hu, X., Chen, S., Zhu, X., 2022. Stabilization and mechanism of uranium sequestration by a mixed culture consortia of sulfate-reducing and phosphate-solubilizing bacteria. *Sci. Total Environ.* 827, 154216. <https://doi.org/10.1016/j.scitotenv.2022.154216>
- Macaskie, L.E., Bonthron, K.M., Yong, P., Goddard, D.T., 2000. Enzymically mediated bioprecipitation of uranium by a *Citrobacter* sp.: A concerted role for exocellular lipopolysaccharide and associated phosphatase in biomineral formation. *Microbiology* 146, 1855–1867. <https://doi.org/10.1099/00221287-146-8-1855>
- Mandala, V.S., Loh, D.M., Shepard, S.M., Geeson, M.B., Sergeev, I. V., Nocera, D.G., Cummins, C.C., Hong, M., 2020. Bacterial phosphate granules contain cyclic polyphosphates: Evidence from <sup>31</sup>P solid-state NMR. *J. Am. Chem. Soc.* 142, 18407–18421. <https://doi.org/10.1021/jacs.0c06335>
- Martínez-Rodríguez, P., Sánchez-Castro, I., Descostes, M., Merroun, M.L., 2020. Draft genome sequence data of *Microbacterium* sp. strain Be9 isolated from uranium-mill tailings porewaters. *Data Br.* 31, 10–14. <https://doi.org/10.1016/j.dib.2020.105732>
- Medina, J., Monreal, C., Chabot, D., Meier, S., González, M.E., Morales, E., Parillo, R., Borie, F., Cornejo, P., 2017. Microscopic and spectroscopic characterization of humic substances from a compost amended copper contaminated soil: main features and their potential effects on Cu immobilization. *Environ. Sci. Pollut. Res.* 24, 14104–14116. <https://doi.org/10.1007/s11356-017-8981-x>
- Merroun, M., Nedelkova, M., Rossberg, A., Hennig, C., Selenska-Pobell, S., 2006. Interaction mechanisms of bacterial strains isolated from extreme habitats with uranium. *Radiochim. Acta* 94, 723–

729.  
<https://doi.org/10.1524/ract.2006.94.9-11.723>
- Merroun, M.L., Geipel, G., Nicolai, R., Heise, K.H., Selenska-Pobell, S., 2003. Complexation of uranium (VI) by three eco-types of *Acidithiobacillus ferrooxidans* studied using time-resolved laser-induced fluorescence spectroscopy and infrared spectroscopy. *BioMetals* 16, 331–339.  
<https://doi.org/10.1023/A:1020612600726>
- Merroun, M.L., Nedelkova, M., Ojeda, J.J., Reitz, T., Fernández, M.L., Arias, J.M., Romero-González, M., Selenska-Pobell, S., 2011. Bio-precipitation of uranium by two bacterial isolates recovered from extreme environments as estimated by potentiometric titration, TEM and X-ray absorption spectroscopic analyses. *J. Hazard. Mater.* 197, 1–10.  
<https://doi.org/10.1016/j.jhazmat.2011.09.049>
- Moll, H., Lütke, L., Bachvarova, V., Cherkouk, A., Selenska-Pobell, S., Bernhard, G., 2014. Interactions of the Mont Terri Opalinus Clay Isolate *Sporomusa* sp. MT-2.99 with Curium(III) and Europium(III). *Geomicrobiol. J.* 31, 682–696.  
<https://doi.org/10.1080/01490451.2014.889975>
- Murphy, J., Riley, J.P., 1962. Determination Single Solution Method For The In Natural Waters. *Anal. Chim. Act* 27, 31–36.
- Nedelkova, M., Merroun, M.L., Rossberg, A., Hennig, C., Selenska-Pobell, S., 2007. *Microbacterium* isolates from the vicinity of a radioactive waste depository and their interactions with uranium. *FEMS Microbiol. Ecol.* 59, 694–705.  
<https://doi.org/10.1111/j.1574-6941.2006.00261.x>
- Newsome, L., Morris, K., Trivedi, D., Bewsher, A., Lloyd, J.R., 2015. Biostimulation by glycerol phosphate to precipitate recalcitrant uranium(IV) phosphate. *Environ. Sci. Technol.* 49, 11070–11078.  
<https://doi.org/10.1021/acs.est.5b02042>
- Ojeda, J.J., Romero-González, M.E., Bachmann, R.T., Edyvean, R.G.J., Banwart, S.A., 2008. Characterization of the cell surface and cell wall chemistry of drinking water bacteria by combining XPS, FTIR spectroscopy, modeling, and potentiometric titrations. *Langmuir* 24, 4032–4040.  
<https://doi.org/10.1021/la702284b>
- Pan, X., Chen, Z., Chen, F., Cheng, Y., Lin, Z., Guan, X., 2015. The mechanism of uranium transformation from U(VI) into nano-uramphite by two indigenous *Bacillus thuringiensis* strains. *J. Hazard. Mater.* 297, 313–319.  
<https://doi.org/10.1016/j.jhazmat.2015.05.019>
- Panda, B., Rahman, H., Panda, J., 2016. Rhizosphere Phosphate solubilizing bacteria from the acidic soils of Eastern Himalayan region and their antagonistic effect on fungal pathogens. *Rhizosphere* 2, 62–71.  
<https://doi.org/10.1016/j.rhisph.2016.08.001>
- Park, J.H., Bolan, N., Megharaj, M., Naidu, R., 2011. Isolation of phosphate solubilizing bacteria and their potential for lead immobilization in soil. *J. Hazard. Mater.* 185, 829–836.  
<https://doi.org/10.1016/j.jhazmat.2010.09.095>
- Pinel-Cabello, M., Jroundi, F., López-Fernández, M., Geffers, R., Jarek, M., Jauregui, R., Link, A., Vílchez-Vargas, R., Merroun, M.L., 2021. Multisystem combined uranium resistance mechanisms and bioremediation potential of *Stenotrophomonas bentonitica* BII-R7: Transcriptomics and microscopic study. *J. Hazard. Mater.* 403, 123858.  
<https://doi.org/10.1016/j.jhazmat.2020.123858>
- Rawat, P., Das, S., Shankhdhar, D., Shankhdhar, S.C., 2021. Phosphate-solubilizing microorganisms: mechanism and their role in phosphate solubilization and uptake. *J. Soil Sci. Plant Nutr.* 21, 49–68.  
<https://doi.org/10.1007/s42729-020-00342-7>
- Reiller, P.E., Descostes, M., 2020. Development and application of the thermodynamic database PRODATA dedicated to the monitoring of mining activities from exploration to remediation. *Chemosphere* 251.  
<https://doi.org/10.1016/j.chemosphere.2020.126301>

- Rouxhet, P.G., Mozes, N., Dengis, P.B., Dufrêne, Y.F., Gerin, P.A., Genet, M.J., 1994. Application of X-ray photoelectron spectroscopy to microorganisms. *Colloids Surfaces B Biointerfaces* 2, 347–369. [https://doi.org/10.1016/0927-7765\(94\)80049-9](https://doi.org/10.1016/0927-7765(94)80049-9)
- Ruiz-Fresneda, M.A., Lopez-fernandez, M., Martinez-moreno, M.F., Cherkouk, A., Ju-nam, Y., Ojeda, J.J., Moll, H., Merroun, M.L., 2020. Molecular binding of Eu III / Cm III by *Stenotrophomonas bentonitica* and its impact on the safety of future geodisposal of radioactive waste. *Environ. Sci. Technol.* 54, 15180–15190. <https://doi.org/10.1021/acs.est.0c02418>
- Salome, K.R., Green, S.J., Beazley, M.J., Webb, S.M., Kostka, J.E., Taillefert, M., 2013. The role of anaerobic respiration in the immobilization of uranium through biomineralization of phosphate minerals. *Geochim. Cosmochim. Acta* 106, 344–363. <https://doi.org/10.1016/j.gca.2012.12.037>
- Sánchez-Castro, I., Amador-García, A., Moreno-Romero, C., López-Fernández, M., Phommavanh, V., Nos, J., Descostes, M., Merroun, M.L., 2017. Screening of bacterial strains isolated from uranium mill tailings porewaters for bioremediation purposes. *J. Environ. Radioact.* 166, 130–141. <https://doi.org/10.1016/j.jenvrad.2016.03.016>
- Sánchez-Castro, I., Martínez-Rodríguez, P., Abad, M.M., Descostes, M., Merroun, M.L., 2021. Uranium removal from complex mining waters by alginate beads doped with cells of *Stenotrophomonas* sp. Br8: Novel perspectives for metal bioremediation. *J. Environ. Manage.* 296, 1–10. <https://doi.org/10.1016/j.jenvman.2021.113411>
- Sánchez-Castro, I., Martínez-Rodríguez, P., Jroundi, F., Lorenzo, P., Descostes, M., L. Merroun, M., 2020. High-efficient microbial immobilization of solved U(VI) by the *Stenotrophomonas* strain Br8. *Water Res.* 183, 116110. <https://doi.org/10.1016/j.watres.2020.116110>
- Selvakumar, R., Ramadoss, G., Mridula, P.M., Rajendran, K., Thavamani, P., Ravi Naidu, Megharaj, M., 2018. Challenges and complexities in remediation of uranium contaminated soils: A review. *J. Environ. Radioact.* 192, 592–603. <https://doi.org/10.1016/j.jenvrad.2018.02.018>
- Seufferheld, M.J., Alvarez, H.M., Farias, M.E., 2008. Role of polyphosphates in microbial adaptation to extreme environments. *Appl. Environ. Microbiol.* 74, 5867–5874. <https://doi.org/10.1128/AEM.00501-08>
- Skouri-Panet, F., Benzerara, K., Cosmidis, J., Féraud, C., Caumes, G., De Luca, G., Heulin, T., Duprat, E., 2018. In vitro and in silico evidence of phosphatase diversity in the biomineralizing bacterium *Ramlibacter tataouinensis*. *Front. Microbiol.* 8, 2592. <https://doi.org/10.3389/fmicb.2017.02592>
- Sowmya, S., Rekha, P.D., Arun, A.B., 2014. Uranium(VI) bioprecipitation mediated by a phosphate solubilizing *Acinetobacter* sp: YU-SS-SB-29 isolated from a high natural background radiation site. *Int. Biodeterior. Biodegrad.* 94, 134–140. <https://doi.org/10.1016/j.ibiod.2014.07.009>
- Sowmya, S., Rekha, P.D., Yashodhara, I., Karunakara, N., Arun, A.B., 2020. Uranium tolerant phosphate solubilizing bacteria isolated from Gogi, a proposed uranium mining site in South India. *Appl. Geochemistry* 114, 104523. <https://doi.org/10.1016/j.apgeochem.2020.104523>
- Sun, H., Meng, M., Wu, L., Zheng, X., Zhu, Z., Dai, S., 2020. Function and mechanism of polysaccharide on enhancing tolerance of *Trichoderma asperellum* under Pb<sup>2+</sup> stress. *Int. J. Biol. Macromol.* 151, 509–518. <https://doi.org/10.1016/j.ijbiomac.2020.02.207>
- Suzina, N.E., Machulin, A. V., Sorokin, V. V., Polivtseva, V.N., Esikova, T.Z., Shorokhova, A.P., Delegan, Y.A., Abashina, T.N., 2022. Capture of essential trace elements and phosphate accumulation as a basis for the antimicrobial activity of a new ultramicrobacterium—*Microbacterium lacticum* Str. F2E. *Microorganisms* 10, 128.



- <https://doi.org/10.3390/microorganisms10010128>
- Suzuki, Y., Banfield, J.F., 2004. Resistance to, and accumulation of, uranium by bacteria from a uranium-contaminated site. *Geomicrobiol. J.* 21, 113–121. <https://doi.org/10.1080/01490450490266361>
- Suzuki, Y., Banfield, J.F., 1999. Chapter 8 - Geomicrobiology of Uranium. Uranium: Mineralogy, geochemistry, and the environment. Editors: Peter C. Burns and Robert J. Finch. De Gruyter, Berlin, Boston, pp. 393–432. <https://doi.org/https://doi.org/10.1515/9781501509193-013>
- Theodorakopoulos, N., Chapon, V., Coppin, F., Floriani, M., Vercouter, T., Sergeant, C., Camilleri, V., Berthomieu, C., Février, L., 2015. Use of combined microscopic and spectroscopic techniques to reveal interactions between uranium and *Microbacterium* sp. A9, a strain isolated from the Chernobyl exclusion zone. *J. Hazard. Mater.* 285, 285–293. <https://doi.org/10.1016/j.jhazmat.2014.12.018>
- Tu, H., Yuan, G., Zhao, C., Liu, J., Li, F., Yang, J., Liao, J., Yang, Y., Liu, N., 2019. U-phosphate biomineralization induced by *Bacillus* sp. dw-2 in the presence of organic acids. *Nucl. Eng. Technol.* 51, 1322–1332. <https://doi.org/10.1016/j.net.2019.03.002>
- Turner, B.F., Fein, J.B., 2006. Protomit: A program for determining surface protonation constants from titration data. *Comput. Geosci.* 32, 1344–1356. <https://doi.org/10.1016/j.cageo.2005.12.005>
- Van Der Mei, H.C., De Vries, J., Busscher, H.J., 2000. X-ray photoelectron spectroscopy for the study of microbial cell surfaces. *Surf. Sci. Rep.* 39, 1–24. [https://doi.org/10.1016/S0167-5729\(00\)00003-0](https://doi.org/10.1016/S0167-5729(00)00003-0)
- Villagrasa, E., Egea, R., Ferrer-Miralles, N., Solé, A., 2020. Genomic and biotechnological insights on stress-linked polyphosphate production induced by chromium(III) in *Ochrobactrum anthropi* DE2010. *World J. Microbiol. Biotechnol.* 36, 1–10. <https://doi.org/10.1007/s11274-020-02875-6>
- Wang, Y., Frutschi, M., Suvorova, E., Phrommavanh, V., Descostes, M., Osman, A.A.A., Geipel, G., Bernier-Latmani, R., 2013. Mobile uranium(IV)-bearing colloids in a mining-impacted wetland. *Nat. Commun.* 4, 1–9. <https://doi.org/10.1038/ncomms3942>
- Wei, Y., Chen, Z., Song, H., Zhang, J., Lin, Z., Dang, Z., Deng, H., 2019. The immobilization mechanism of U(VI) induced by *Bacillus thuringiensis* 016 and the effects of coexisting ions. *Biochem. Eng. J.* 144, 57–63. <https://doi.org/10.1016/j.bej.2019.01.013>
- Williams, K.H., Bargar, J.R., Lloyd, J.R., Lovley, D.R., 2013. Bioremediation of uranium-contaminated groundwater: A systems approach to subsurface biogeochemistry. *Curr. Opin. Biotechnol.* 24, 489–497. <https://doi.org/10.1016/j.copbio.2012.10.008>
- Wufuer, R., Wei, Y., Lin, Q., Wang, H., Song, W., Liu, W., Zhang, D., Pan, X., Gadd, G.M., 2017. Chapter Four - Uranium Bioreduction and Biomineralization, in: Sariaslani, S., Gadd, G.M.B.T.-A. in A.M. (Eds.), Academic Press, pp. 137–168. <https://doi.org/10.1016/bs.aambs.2017.01.003>
- Yong, P., Macaskie, L.E., 1995. Enhancement of uranium bioaccumulation by a *Citrobacter* sp. via enzymically-mediated growth of polycrystalline NH<sub>4</sub>UO<sub>2</sub>PO<sub>4</sub>. *J. Chem. Technol. Biotechnol.* 63, 101–108. <https://doi.org/10.1002/jctb.280630202>
- Yu, Q., Szymanowski, J., Myneni, S.C.B., Fein, J.B., 2014. Characterization of sulfhydryl sites within bacterial cell envelopes using selective site-blocking and potentiometric titrations. *Chem. Geol.* 373, 50–58. <https://doi.org/10.1016/j.chemgeo.2014.02.027>
- Zhang, B.H., Salam, N., Cheng, J., Li, H.Q., Yang, J.Y., Zha, D.M., Guo, Q.G., Li, W.J., 2017. *Microbacterium lacusdiani* sp. nov., a phosphate-solubilizing novel actinobacterium isolated from mucilaginous sheath of *Microcystis*. *J. Antibiot. (Tokyo)*. 70, 147–151. <https://doi.org/10.1038/ja.2016.125>

- Zhang, D., Chen, X., Larson, S.L., Ballard, J.H., Knotek-Smith, H.M., Ding, D., Hu, N., Han, F.X., 2020. Uranium biomineralization with phosphate - biogeochemical process and its application. *ACS Earth Sp. Chem.* 4, 2205–2214. <https://doi.org/10.1021/acsearthspacechem.0c00252>
- Zhang, J., Song, H., Chen, Z., Liu, S., Wei, Y., Huang, J., Guo, C., Dang, Z., Lin, Z., 2018. Biomineralization mechanism of U(VI) induced by *Bacillus cereus* 12-2: The role of functional groups and enzymes. *Chemosphere* 206, 682–692. <https://doi.org/10.1016/j.chemosphere.2018.04.181>
- Zheng, X.Y., Shen, Y.H., Wang, X.Y., Wang, T.S., 2018. Effect of pH on uranium(VI) biosorption and biomineralization by *Saccharomyces cerevisiae*. *Chemosphere* 203, 109–116. <https://doi.org/10.1016/j.chemosphere.2018.03.165>

## Supplementary data

**Table Supplementary 1.** Low Phosphate Medium composition.

*Saline solution10x, pH 7.2 100 ml/l	
<u>*Saline solution10X, pH 7.2, composition</u>	
NaCl	46.8 g/l
KCl	14.9 g/l
NH <sub>4</sub> Cl	10.7 g/l
(NH <sub>4</sub> ) <sub>2</sub> SO <sub>4</sub>	4.3 g/l
MgCl <sub>2</sub>	10 ml/l
ZnSO <sub>4</sub>	2.7 mg/l
Tris-base	143.3 g/l
Glycerol	5 ml/l
Tiamine (50 mg/ml)	0.4 ml/l
Peptone 10%	100 ml/l
CaCl <sub>2</sub> (100 mM)	1 ml/l
Destillated water	793.6 ml/l

**Table Supplementary 2.** Comparison of deprotonation constants and surface site concentrations between *Microbacterium* Be9 and other six bacterial species from different studies.

Species	pK1	pK2	pK3	C <sub>1</sub> (x10 <sup>-4</sup> mol/g)	C <sub>2</sub> (x10 <sup>-4</sup> mol/g)	C <sub>3</sub> (x10 <sup>-4</sup> mol/g)	pH <sub>zpc</sub>	Reference
Be9 strain	4.38 ± 0.67	6.07 ± 0.37	9.82 ± 0.12	0.45 ± 0.006	0.76 ± 0.015	1.19 ± 0.061	6.61 ± 0.07	This study
<i>S. bentonitica</i>	4.97 ± 0.08	6.88 ± 0.02	9.43± 0.02	5.05 ± 0.31	10.78 ± 0.31	16.93 ± 1.45	5.7	(Ruiz-fresneda et al., 2020)
<i>Sporomusa</i> sp. MT - 2.99	4.8 ± 0.06	6.68 ± 0.06	9.01 ± 0.08	5.3 ± 0.8	3.5 ±0.3	4.8 ± 0.5	-	(Moll et al., 2014)
<i>Bacillus</i> <i>licheniformis</i>	3.7 ± 0.2	5.5 ± 0.3	9.4 ± 0.3	0.59 ± 0.3	0.34 ± 4.9	0.50 ± 11.0	-	(Yu et al., 2014)
<i>S. putrefaciens</i>	5.16 ± 0.04	7.22 ± 0.15	10.04 ± 0.67	0.32 ± 0.02	0.09 ± 0.01	0.38 ± 0.01	-	(Haas et al., 2001)
<i>Sphingomonas</i> sp. S15-S1	4.27 ± 0.45	7.03 ± 0.86	9.92 ± 0.32	4.91 ± 1.04	3.16 ± 0.56	9.24 ± 2.97	5.8	(Merroun et al., 2011)
<i>B. sphaericus</i> JG-7B	4.37 ± 0.27	6.37 ± 0.31	9.95 ± 0.16	4.70 ± 0.55	2.19 ± 0.25	4.56 ± 0.77	5.5	(Merroun et al., 2011)

**Table Supplementary 3.** U speciation (0.1 mM) in MC1 (MOPS+U), MC2 (MOPS+U+G2P) and MC3 (LPM + U) treatments, as predicted by Visual MINTEQ software 3.1 and PhreeqC software.<sup>a</sup> aq, aqueous.

U Species	% of total concentration		
	MC1	MC2	MC3
UO <sub>2</sub> <sup>2+</sup>	0.05	0.06	0.02
UO <sub>2</sub> OH <sup>+</sup>	1.10	1.14	0.64
(UO <sub>2</sub> ) <sub>2</sub> (OH) <sub>2</sub> <sup>2+</sup>	0.17	0.20	0.09
(UO <sub>2</sub> ) <sub>3</sub> (OH) <sub>5</sub> <sup>+</sup>	78.31	78.51	48.59
(UO <sub>2</sub> ) <sub>2</sub> (OH) <sub>3</sub> CO <sub>3</sub> <sup>3-</sup>	-	-	24.25
(UO <sub>2</sub> ) <sub>4</sub> (OH) <sub>7</sub> <sup>+</sup>	19.52	19.22	25.14
UO <sub>2</sub> PO <sub>4</sub> <sup>+</sup>	-	-	0.38
UO <sub>2</sub> HPO <sub>4</sub>	-	-	0.07
UO <sub>2</sub> CO <sub>3</sub>	-	-	0.04
(UO <sub>2</sub> ) <sub>3</sub> (OH) <sub>7</sub> <sup>-</sup>	0.05	0.05	0.12
(UO <sub>2</sub> ) <sub>3</sub> (OH) <sub>4</sub> <sup>2+</sup>	0.10	0.12	0.05
UO <sub>2</sub> (OH) <sub>3</sub> <sup>3-</sup>	0.03	0.03	0.06
UO <sub>2</sub> (OH) <sub>2</sub> (aq) <sup>a</sup>	0.68	0.67	0.55

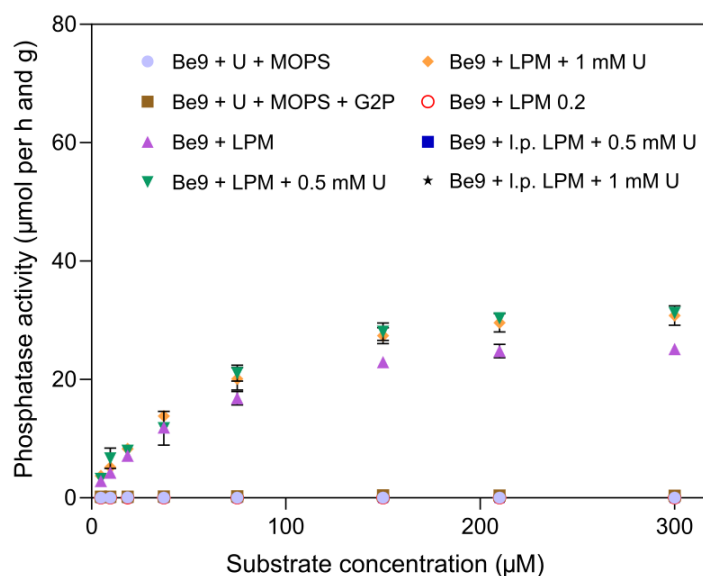


**Figure Supplementary 1.** Phosphatase activity (measured as  $\mu\text{mol}$  released per h and g at different substrate concentrations) of Be9 cells after incubation in the different conditions (MC1, MC2 and MC3). Peptone reduction (0.2 mg/L) is labelled as l.p. LPM (low-peptone LPM). Data are showed as the mean and error bars represent the standard error of at least three independent measurements.

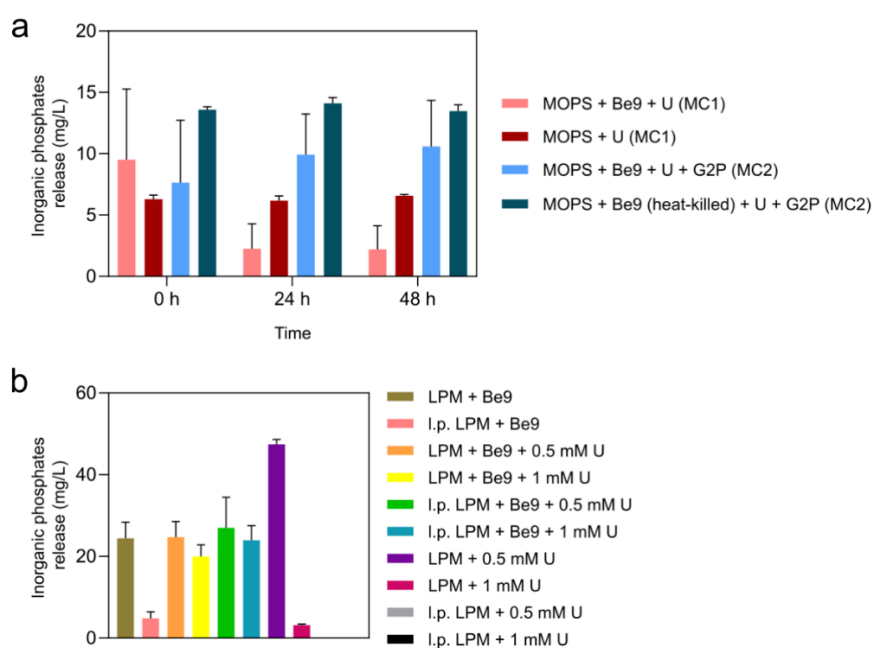


**Figure Supplementary 2.** Inorganic phosphates in solution (mg/L) detected during (A) MC1 and MC2 treatments incubation at different times (0, 24 and 48 h), and (B) MC3 treatment incubations at 48 h. Flasks without Be9 cells and heat-killed Be9 cells were used as control treatments. Data are showed as the mean  $\pm$ SD of at least three independent measurements.

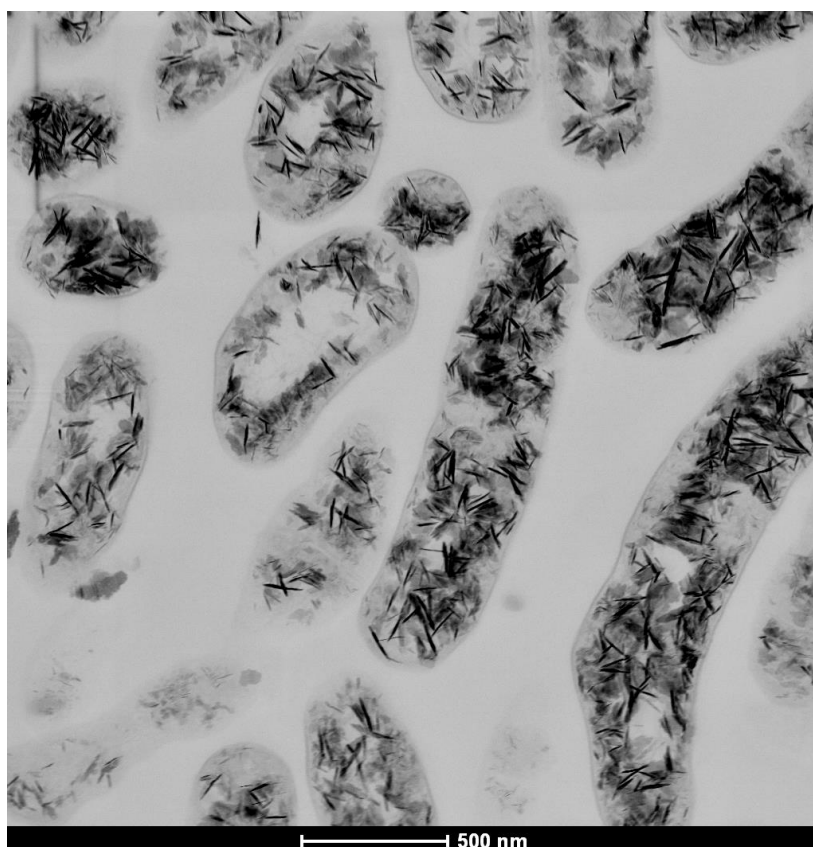


**Figure Supplementary 3.** HAADF-STEM image of a thin section of *Microbacterium* sp. Be9 cells recovered after their incubation in MOPS solution (5 mM) amended with U (0.1 mM). Intracellular U-precipitates are showed as condensed dark accumulations.

**Table Supplementary 4.** Cell viability and membrane potential of Be9 after 24 h and 48 h at different uranium concentrations. Data are showed as the mean and standard deviation is included as  $\pm$  SD.

Conditions	Cell viability-24h		Cell viability-48h		Membrane potential-24h		Membrane potential-48h	
	Alive (%)	Dead (%)	Alive (%)	Dead (%)	Active (%)	Non active (%)	Active (%)	Non active (%)
0 mM U	99.22 $\pm$ 0.22	0.78 $\pm$ 0.22	85.95 $\pm$ 0.26	14.05 $\pm$ 0.26	99.18 $\pm$ 0.07	0.82 $\pm$ 0.07	99.00 $\pm$ 0.00	1.00 $\pm$ 0.00
0.1 mM U	100 $\pm$ 0.18	0.00 $\pm$ 0.18	18.42 $\pm$ 0.00	81.58 $\pm$ 0.00	97.10 $\pm$ 0.08	2.90 $\pm$ 0.08	0.00 $\pm$ 0.00	100 $\pm$ 0.00



**Figure Supplementary 4.** HAADF-STEM image of a thin section of *Microbacterium* sp. Be9 cells recovered after their incubation in MOPS solution (5 mM) amended with U (0.1 mM) and G2P (5 mM). Intracellular U-precipitates are showed as condensed dark accumulations.

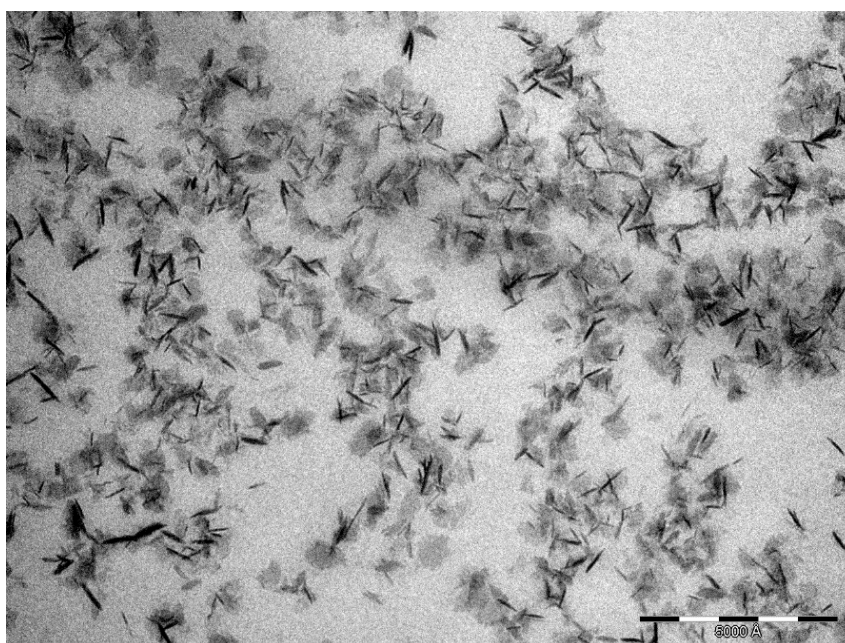


**Figure Supplementary 5.** HAADF-STEM image of U-precipitates formed abiotically after their incubation (48 h) in LPM amended with U (1 mM). U-precipitates are showed as condensed dark aggregates and needle-like fibrils.

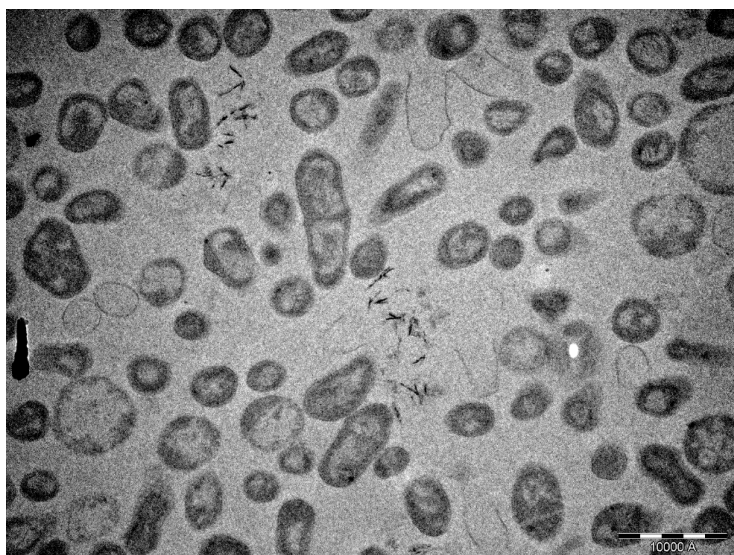


**Figure Supplementary 6.** HAADF-STEM image of a thin section of *Microbacterium* sp. Be9 cells recovered after their incubation during 48 h in LPM amended with U (1 mM). Extracellular U-precipitates are showed as condensed dark accumulations.

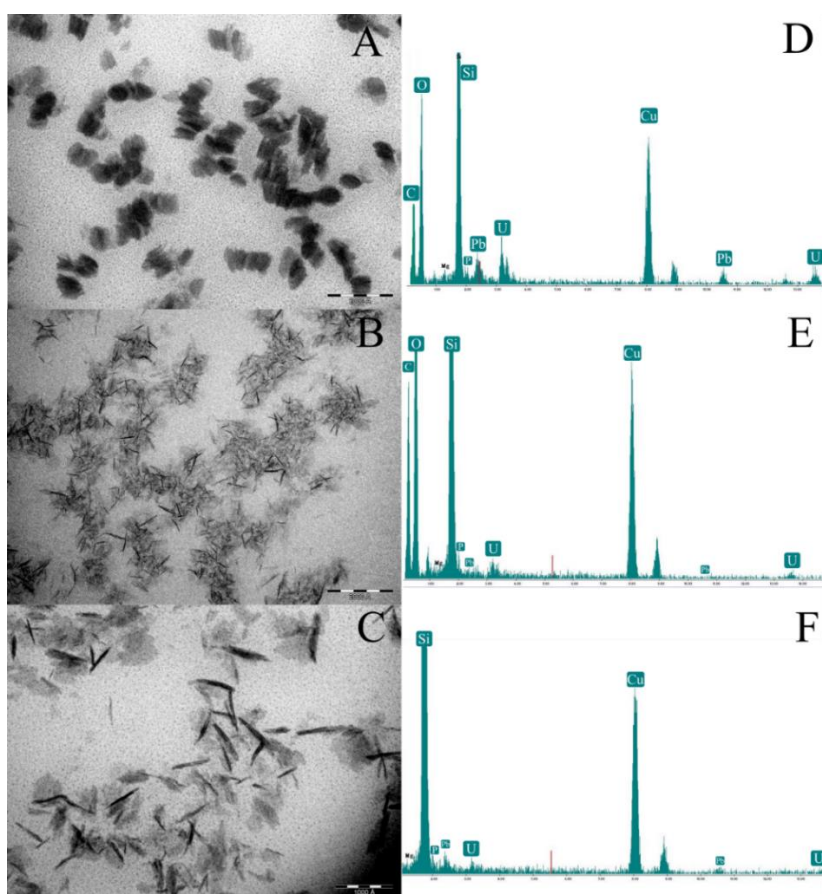


**Figure Supplementary 7.** HR-TEM images of (A) U (1 mM) amended abiotic low-peptone LPM sample, (B) U (0.1 mM) amended abiotic LPM sample, (C) U (1 Mm) amended abiotic LPM sample, and their respectively EDX analysis spectrum (D, E and F).

## CAPÍTULO IV:

### **High-efficient microbial immobilization of solved U(VI) by the *Stenotrophomonas* strain Br8**

Iván Sánchez-Castro<sup>1</sup>, Pablo Martínez-Rodríguez<sup>1</sup>, Fadwa Jroundi<sup>1</sup>, Pier Lorenzo Solari<sup>2</sup>,  
Michael Descostes<sup>3,4</sup>, Mohamed Larbi Merroun<sup>1</sup>

<sup>1</sup> Department of Microbiology, University of Granada, Campus Fuentenueva s/n, 18071 Granada, Spain.

<sup>2</sup> Synchrotron SOLEIL, MARS beamline, L'Orme des Merisiers, Saint-Aubin BP 48, 91192 Gif-sur-Yvette Cedex, France

<sup>3</sup> ORANO Mining, Environmental R&D Department, 125 Avenue de Paris, 92330, Châtillon, France.

<sup>4</sup> PSL University/Mines ParisTech, Centre de Géosciences, 35 rue Saint-Honoré, 77305, Fontainebleau, France.

Este capítulo ha sido publicado en la revista Water Research:

Sánchez-Castro, I., Martínez-Rodríguez, P., Jroundi, F., Lorenzo, P., Descostes, M., L. Merroun, M., 2020. High-efficient microbial immobilization of solved U(VI) by the *Stenotrophomonas* strain Br8. Water Res. 183. <https://doi.org/10.1016/j.watres.2020.116110>





**Abstract**

The environmental impact of uranium released during nuclear power production and related mining activity is an issue of great concern. Innovative environmental-friendly water remediation strategies, like those based on U biomineralization through phosphatase activity, are desirable. Here, we report the great U biomineralization potential of *Stenotrophomonas* sp. Br8 CECT 9810 over a wide range of physicochemical and biological conditions. Br8 cells exhibited high phosphatase activity which mediated the release of orthophosphate in the presence of glycerol-2-phosphate around pH 6.3. Mobile uranyl ions were bioprecipitated as needle-like fibrils at the cell surface and in the extracellular space, as observed by Scanning Transmission Electron Microscopy (STEM). Extended X-Ray Absorption Fine Structure (EXAFS) and X-Ray Diffraction (XRD) analyses showed the local structure of biogenic U precipitates to be similar to that of meta-autunite. In addition to the active U phosphate biomineralization process, the cells interact with this radionuclide through passive biosorption, removing up to 373 mg of U per g of bacterial dry biomass. The high U biomineralization capacity of the studied strain was also observed under different conditions of pH, temperature, etc. Results presented in this work will help to design efficient U bioremediation strategies for real polluted waters.

**Keywords:** Porewaters; Bioremediation; Biomineralization; Uranium; EXAFS; Bacteria

## Introduction

Uranium (U) is intensively exploited and widely used for nuclear power production. Radioactive wastes generated during these operations, including spent nuclear fuel, may lead to the release of U to adjacent soils and groundwater (Gavrilescu et al., 2009) provoking deleterious side effects that are a major environmental concern. Both the mobility and the solubility of released U in nature are known to be governed by its oxidation state and chemical speciation, which in turn are controlled by biotic and abiotic processes (Suzuki and Banfield, 1999). Main primary U oxidation states are U(IV), stable as uraninite ( $\text{UO}_2$ ) in anaerobic conditions, and U(VI), dominating in oxidizing conditions as the extremely soluble and stable linear uranyl ion ( $\text{UO}_2^{2+}$ ) (Langmuir 1978). The solid mineral uraninite is very sensitive to dissolved  $\text{O}_2$  exposition which oxidizes this compound to more mobile U(VI) forms like uranyl ion. In addition, the chemical speciation of U(VI) in natural systems is highly dependent on pH. Under acidic conditions, U(VI) is likely to be adsorbed by mineral surfaces, complexed by organic matter or precipitated, forming insoluble phosphate minerals as autunite ( $\text{Ca}(\text{UO}_2)_2(\text{PO}_4)_2$ ) (Kolhe et al., 2018). However, alkaline conditions may favor the formation of soluble uranyl compounds, such as carbonate complexes (Hsi and Langmuir, 1985; Waite et al., 1994), potentially mobile in aqueous systems. In this sense, it is well known that toxicity of uranium depends mainly on its oxidation state (U(VI)/U(IV)), being the most systemic toxicants those compounds showing highest solubility (mainly U(VI) forms like uranyl complexes). In the case of low-solubility compounds (mainly U(IV) species as uraninite,  $\text{UO}_2$ ), they present low environmental and human health toxicity. The US Environmental Protection Agency and the World Health Organization have set the maximum uranium concentration level in drinking water at 30  $\mu\text{g/L}$ , classifying this radionuclide as a human carcinogen (Group A).

Application of sustainable management programs, including well-designed, -operated, and -remediated mining operations, is deemed necessary to minimize U-linked environmental impacts. The inherent complexity of subsurface environments, due to changing redox conditions and diverse biogeochemical processes occurring underground, makes it essential to search for innovative remediation approaches. Standard pump-and-treat and excavation-and-removal remediation approaches are costly and inefficient in extensive areas co-contaminated with radionuclides and heavy metals. Among alternative strategies, those based on microbial processes promoting U precipitation are considered environmentally

friendly, cost-effective and highly efficient (Acharya, 2015), and are therefore gaining attention in recent years.

Previous evaluation of the effects and consequences of these microbe-U interactions comes to confirm the capacity of indigenous bacteria to mediate U immobilization and thereby reduce its toxicity, suggesting applicability for bioremediation purposes (reviewed in Kolhe et al., 2018, and Merroun and Selenska-Pobell, 2008). In this context, the two microbial processes most investigated thus far are the enzymatically-catalyzed reductive precipitation of U(VI) to U(IV) and the bioprecipitation of U(VI) with ligands such as inorganic phosphates. First proposed by Lovley et al. (1991), the strategies based on U(VI) enzymatic reduction, performed by dissimilatory metal-reducing bacteria and sulfate-reducing bacteria, have been successfully applied on several occasions under laboratory conditions (Lovley and Phillips, 1992; Lovley, 2001; Xie et al., 2018) as well as at field scale in Oak Ridge site (USA) where U concentration was up to 10-60 mg/L (Wu et al., 2006 and 2007). This approach entails some limitations, however, including the poor stability of bio-reduced U in the presence of oxidizing agents like O<sub>2</sub> or compounds such as nitrates or bicarbonates, along with Fe or Mn species (Wan et al., 2005, 2008; Wu et al., 2010; Spycher et al., 2011; Watson et al., 2013). The high solubility of resulting uraninite nanoparticles as well as other U(IV)-bearing colloids has also been reported (Bargar et al., 2008; Wang et al., 2013; Schindler et al., 2017; Neill et al., 2018).

Overall, recent research interests have switched to a second approach based on U biomineralization by aerobic or facultative bacteria exhibiting phosphatase (P-ase) enzymatic activity. Phosphohydrolases (EC 3.1.3), also known as phosphatases, are broadly categorized as acid or alkaline phosphatases, based on the pH required for their optimum activity. They are either released outside the plasma membrane or embedded as membrane components. Since free orthophosphate is rarely found in certain environments, the main role of phosphatases is supporting microbial nutrition by releasing assimilable orthophosphates from organic sources, which should be amended in case they are not naturally present. These inorganic phosphates may also act as ligands in the presence of cations, such as uranyl ion (UO<sub>2</sub><sup>2+</sup>), inducing the bioprecipitation of U(VI) as a protective strategy for bacteria. This mechanism is the basis of promising research efforts, aiming at U precipitation by applying members of various genera like *Citrobacter*, *Pseudomonas*, *Bacillus*, *Pelosinus*, *Sphingomonas* or *Rahnella*, over a wide pH range and under aerobic and anaerobic conditions (Beazley et al., 2011; Merroun et al., 2011; Newsome et al., 2015;

Bader et al., 2017; Shen et al., 2018; Kong et al., 2020). The formation of low solubility U-containing minerals like  $(\text{H}_3\text{O})_2(\text{UO}_2)_2(\text{PO}_4)_2 \cdot 6\text{H}_2\text{O}$  (Yong and Macaskie, 1995),  $(\text{NH}_4)(\text{UO}_2)(\text{PO}_4) \cdot 3\text{H}_2\text{O}$  (Wall and Krumholz, 2006) and  $\text{Ca}(\text{UO}_2)_2(\text{PO}_4)_2 \cdot x\text{H}_2\text{O}$  (Mehta et al., 2013; Krawczyk-Bärsch et al., 2018), stable across a wide range of redox and pH conditions, makes this remediation alternative even more attractive.

The current work emerges as the result of a multi-criteria screening process where a significant number of bacterial isolates, recovered from rarely studied uranium mill tailing porewaters, were thoroughly analyzed at different levels (results partially published in Sánchez-Castro et al., 2017a). After the screening pipeline applied, which included molecular analyses (16S rDNA taxonomic identification), physiological tests (metals/metalloid tolerance) and microscopic observations (Scanning Transmission Electron Microscopy with High-Angle Annular Dark-Field, STEM-HAADF; Energy Dispersive X-Ray, EDX, element-distribution maps), the bacterial strain Br8 was found to be the most promising candidate. A series of assays were conducted to explore the P-ase-based U immobilization in the presence of Br8 and an organophosphate compound. Characterization of the chemical nature and localization of the U precipitates formed during biomineralization were also addressed through microscopic techniques such as STEM-HAADF and spectroscopic measurements through Extended X-Ray Absorption Fine Structure (EXAFS) spectroscopy and X-Ray Diffraction (XRD). Moreover, a thorough experimental design was developed to evaluate the influence of several parameters (time, temperature, pH and biomass concentration) on the performance of the Br8-mediated U removal process. These results are expected to provide key information for understanding the U biogeochemical cycle in subsurface environment as well as to determine the optimal conditions for the future application of this innovative strategy, under oxidizing conditions in real polluted waters, by immobilizing Br8 bacterial cells.

## **Materials and methods**

### ***Bacterial strain isolation and molecular identification***

The bacterial strain used in this work (*Stenotrophomonas* sp. Br8 CECT 9810; 16S rRNA accession number HG798865) was previously isolated from U mill tailing porewaters and identified by 16S rDNA phylogeny, as described by Sánchez-Castro et al. (2017a).

Physicochemical characterization of this water sample is published in Sánchez-Castro et al. (2017a).

### ***Determination of metals' Minimum Inhibitory Concentration for bacterial growth***

Filtered-sterilized stock solutions (0.1 M) of  $\text{UO}_2(\text{NO}_3)_2 \cdot 6\text{H}_2\text{O}$ ,  $\text{Cr}(\text{NO}_3)_3 \cdot 9\text{H}_2\text{O}$ ,  $\text{Pb}(\text{NO}_3)_2$ ,  $\text{LaN}_3\text{O}_9 \cdot 6\text{H}_2\text{O}$ ,  $\text{Cd}(\text{NO}_3)_2 \cdot 4\text{H}_2\text{O}$ ,  $\text{Ni}(\text{NO}_3)_2 \cdot 6\text{H}_2\text{O}$ ,  $\text{ZnSO}_4 \cdot 7\text{H}_2\text{O}$ ,  $\text{Na}_2\text{MoO}_4 \cdot 2\text{H}_2\text{O}$ ,  $\text{VOSO}_4$ ,  $\text{Eu}_2\text{O}_3$ , and  $\text{Cu}(\text{NO}_3)_2 \cdot 3\text{H}_2\text{O}$  were prepared by dissolving appropriate quantities of these metal salts in 0.1 M  $\text{NaClO}_4$ . In the case of Ag and Se, 1-M stock solutions of  $\text{AgNO}_3$  and  $\text{Na}_2\text{SeO}_3$  were prepared by dissolving the appropriate quantity in distilled water. To evaluate the tolerance of strain Br8 to these metals, the Minimum Inhibitory Concentration (MIC) method was applied as previously described (Sánchez-Castro et al., 2017a). This standard method is used to determine the tolerance level of a bacterium in the presence of heavy metals or other constraining agents.

### ***Uranium immobilization assay***

The ability of Br8 cells to immobilize U was studied by monitoring the removal of dissolved U(VI) as a function of U concentration in an incubation medium containing an organic phosphate source (glycerol-2-phosphate, G2P). For this purpose, MOPS-buffered (20 mM) distilled water was added to acid-washed glass Erlenmeyer flasks. Br8 cells were grown in LB broth (rich-nutrient medium; Scharlau Chemie SA, Barcelona, Spain) at 28 °C and 160 rpm for 20-24 h. Subsequently, mid-exponential growth phase cells were washed twice with 0.9% NaCl solution and inoculated, when applicable, to a final concentration of 0.5 mg dry Br8 biomass per mL of medium (equivalent optical density at 600 nm [OD<sub>600</sub>], ≈0.5). Four U(VI) concentrations (0.01, 0.1, 0.5 and 1 mM), provided as uranyl nitrate, and/or 5 mM G2P (Sigma Aldrich), as the sole organic phosphates source, were tested. Initial pH was 6.3 in all cases and potential changes were determined by measuring the pH at the end of each assay. Flasks including no-uranium, heat-killed bacterial cells, and no-bacteria were assayed as controls. For the heat-killed cell control, the recovered Br8 biomass was exposed to 80 °C pre-incubation for 1h. Incubation of all samples was conducted at 28 °C for 48 h and under continuous shaking (165 rpm).

Once incubations were completed, aliquots from all replicate liquid samples were centrifuged at 10,000 g for 10 min at 4 °C. The supernatants and solid pellets were analyzed separately by using different techniques described below. Solid phase precipitates recovered were washed twice with 0.9% NaCl to remove the interfering elements of the incubating solution.

#### ***Quantification of phosphatase enzymatic activity***

Determination of the activity of P-ase enzyme (EC 3.1.3) was based on the procedure of German et al. (2011) using the substrate 4-MUB (methylumbelliferone)-phosphate. MUB standards (0.16  $\mu$ M, 0.625  $\mu$ M, 1.25  $\mu$ M and 2.5  $\mu$ M) dissolved in Na-perchlorate buffer (pH 5) and cell suspensions were used to calculate the emission and quench coefficients for each sample using an automatic fluorometer NanoQuant equipment (TECAN, Mannedorf, Switzerland). Enzyme activity was calculated following German et al. (2011). P-ase activity was expressed as  $\mu$ moles of inorganic phosphates released per hour and gram of substrate.

#### ***Determination of inorganic phosphates released***

In order to calculate the inorganic phosphates concentration in solution after the incubation period, the “ammonium-molybdate method” (Murphy and Riley, 1962) based on colorimetric measurements was employed. This technique is based on the reaction of orthophosphate ions with ammonium-molybdate in acidic solution, forming phosphomolybdic acid. This compound produces an intensely blue complex upon reduction with ascorbic acid. Antimony potassium tartrate is added to increase the rate of reduction.

#### ***Quantification of uranium removal***

The final concentration of U(VI) remaining in solution was determined by inductively-coupled plasma mass spectrometry (ICP-MS) with a NexION 300d (Perkin Elmer) system after HNO<sub>3</sub> acidification using multi-element standard solutions for calibration. The concentration of U removed from solution by the cells was calculated as the difference between the initial and final U concentrations.

### ***Cellular localization of uranium precipitates: STEM-HAADF and HRTEM/EDX analysis***

Cells exposed to uranium for 48 h were harvested by centrifugation, washed twice with 0.9% NaCl and Na-cacodylate buffer (pH 7.2), fixed with glutaraldehyde in cacodylate buffer (4%) and stained with osmium tetroxide (1%, 1 h) in the same buffer before being dehydrated through graded alcohol followed by propylene oxide treatment, and finally were embedded in epoxy resin. Ultrathin sections (0.1  $\mu\text{m}$ ) of the samples, obtained using an ultra-microtome, were loaded in a carbon coated copper grid and analyzed by STEM-HAADF, conducted using a FEI TITAN G2 80-300. The TEM specimen holders were cleaned by plasma prior to STEM analysis to minimize contamination. The high resolution STEM is equipped with a HAADF detector and EDX energy dispersive X-ray detector, thus providing elemental information via the analysis of X-ray emissions caused by a high-energy electron beam.

### ***Characterization of uranium solid phase precipitated by the cells***

In order to characterize the uranium solid phases precipitated during assays, EXAFS spectroscopy and XRD were applied.

### ***Extended X-Ray Absorption Fine Structure (EXAFS) spectroscopy***

EXAFS analyses were performed in the SOLEIL synchrotron (Paris, France). This facility is a medium energy third-generation synchrotron optimized for the production of vacuum-ultraviolet (VUV) and soft X-ray light, and operated with electrons at energy of 2.75 GeV. In particular, the measurements were performed on the MARS beamline which is dedicated to the study of radioactive samples (Sitaud et al., 2012). The beamline was built on a 1.71 T bending magnet port of the SOLEIL storage ring and operates in the hard X-ray regime from 3.5 to 35 keV with a critical energy of 8.6 keV.

EXAFS samples were prepared as previously described in Merroun et al. (2005). After incubation, cells were harvested and washed with 0.1 M NaClO<sub>4</sub>, pH 7. Briefly, the pellets were dried in an oven at 30 °C for 24 h and subsequently powdered. Data were collected in

fluorescence mode using a 13-element Ge detector (EG & G ORTEC, USA) and processed using the ATHENA code (Ravel and Newville, 2005). FEFF is an automated program for ab initio multiple scattering calculations of EXAFS, X-ray Absorption Near-Edge Structure (XANES) and various other spectra for clusters of atoms. Background removal was performed by means of a pre-edge linear function. Atomic absorption was simulated with a square-spline function. The theoretical phase and amplitude functions used in data analysis were calculated with FEFF8 (Ankudinov et al., 1998) using the crystal structure of meta-autunite,  $\text{Ca}(\text{UO}_2)_2(\text{PO}_4)_2 \cdot 6\text{H}_2\text{O}$  (Makarov and Ivanov, 1960) as a model. All fits were performed with the ARTEMIS code (Ravel and Newville, 2005). They included the four-legged multiple scattering (MS) path of the uranyl group, U-Oax-U-Oax. The coordination number (N) of this MS path was linked to N of the single-scattering (SS) path U-Oax. The radial distance (R) and Debye-Waller factor ( $\sigma^2$ ) of the MS path were respectively linked at twice the R and  $\sigma^2$  of the SS path U-Oax (Hudson et al., 1996). During the fitting procedure, N of the U-Oax SS path was held constant at two. The amplitude reduction factor (S02) was held constant at 1.0 for the FEFF8 calculation and EXAFS fits. The shift in threshold energy,  $\Delta E_0$ , was varied as a global parameter in the fits.

### ***X-Ray Diffraction***

For XRD analyses, U treated cells of Br8 were dried in an oven at 70 °C for 6 h. The dried pellet was scraped and crushed into a fine powder that was analyzed using a X'Pert PRO (PANalytical B.V.) equipped with Cu-K $\alpha$  radiation; Ni filter; 45 kV voltage; 40 mA intensity; exploration range of 3° to 60° 2 $\theta$ ; and goniometer speed of 0.05° 2 $\theta$  s<sup>-1</sup>. Previously, samples were thoroughly homogenized and crushed with an agate mortar and pestle. Patterns obtained were analyzed with X Powder software.

### ***Effect of physicochemical and biological parameters in U biomineralization***

Additional assays modifying certain experimental parameters were performed to ascertain the most favorable conditions for P-ase activity and subsequent U removal. Time-dependent experiments considered different sampling points (0, 10 min, 30 min, 1 h, 3 h, 7 h, 24 h, 48 h and 72 h) in order to study the kinetics of the U immobilization process. The



effects of different physicochemical and biological parameters including temperature (15 °C and 37 °C), pH (5 and 8) and biomass concentration (0.25 and 1 mg dry Br8 biomass per mL) were investigated to determine optimal U removal conditions. With the exception of the tested parameter and U concentration (0.1, 0.5 and 1 mM in pH tests and 0.5 mM for the rest), the experimental conditions were maintained as stated above (5 mM G2P; pH 6.3; incubation at 28 °C, 48 h, 165 rpm).

### ***Statistical analysis and thermodynamic modeling***

Data in this manuscript are presented as averages and standard deviations for three replicates per experimental condition tested. All statistical analyses were carried out using Microsoft Office Excel 2010. Aqueous U speciation under GC1 or GC2 was determined using Visual MINTEQ version 3.1 (<http://vminteq.lwr.kth.se/download/>) (VanEngelen et al., 2010).

## **Results and discussion**

### ***Br8 bacterial strain identification and heavy metal tolerance studies***

Based on 16S rRNA gene analysis, the bacterial strain Br8 was found to be affiliated to the genus *Stenotrophomonas* (Fig. S-1). Members of this genus are known to play an essential role in elements' biogeochemical cycles in nature, as is the case for sulfur (Ikemoto et al., 1980; Banerjee and Yesmin, 2002) or nitrogen (Park et al., 2005), presenting also high biotechnological potential as bioremediation agents (reviewed in Ryan et al., 2009, Ruiz-Fresneda et al., 2018, 2019). However, few *Stenotrophomonas* strains (*S. maltophilia* JG-2, *S. maltophilia* P-8-1 and P-8-3c, and *Stenotrophomonas* sp. U18) have been distinguished for their U immobilization ability (Merroun and Selenska-Pobell, 2008; Nazina et al., 2010; Islam and Sar, 2016).

The MIC of different metals for the growth of this strain was also determined for assessing tolerance of Br8 to these inorganic contaminants (Table 1). Although this method is standardly used (Wiegand et al., 2008; Sánchez-Castro et al., 2017a, Li et al., 2019), it should be noted that a minimum part of the metal assayed might be un-bioavailable due to

abiotic interactions with medium components. Silver appears to be the most toxic, since no growth was detected for all tested concentrations (the minimum being 0.25 mM). Selenium, on the other hand, was found to be the least toxic. In this case, the MIC was not reached since growth was observed at the maximum concentration tested (100 mM). The formation of red color precipitates in the bacterial colonies revealed the reduction of Se(IV) and formation of elemental selenium. A phylogenetically similar bacterial strain (*S. bentonitica* BII-R7; Sánchez-Castro et al., 2017b) has recently been shown to induce the reduction of Se(IV) to Se(0), forming low-solubility trigonal Se nanostructures (Ruiz-Fresneda et al., 2018), which could explain the high tolerance of *Stenotrophomonas* strains to this element. Likewise in the case of U, MIC was not determined since the maximum concentration tested (4 mM) did not limit the cell growth. No further concentrations were tested, since heavy metals levels reported for real polluted scenarios were much lower than the concentrations assayed in the present study. The maximum tolerated U concentration for the above mentioned strain BII-R7 was 6 mM (López-Fernández et al., 2014). Such high levels of tolerance to heavy metals (e.g. U) and antibiotics in members of this genus have been underlined in other studies (reviewed in Page et al., 2008; Ryan et al., 2009; Nazina et al., 2010; Islam and Sar, 2011, 2016). It may be that a cluster of genes is involved in antibiotic and heavy metal resistance, typically from gram-positive bacteria, as found for *S. maltophilia* D457R (Alonso et al., 2000).

**Table 1.** Heavy metals/metalloids minimum inhibitory concentration (MIC), in milliMolar (mM), of the bacterial isolate Br8.

Metal	Cr	Pb	La	Cd	Ni	Zn	Se	Mo	Va	Eu	Cu	Ag	U
mM	≥16	≥16	≥16	≥2	8	≥8	≥100*	≥8	≥8	≥4	8	<0.25	≥4

Due to possible abiotic HMMs precipitation, it was impossible to reach the final MIC value in most cases

\* 100 mM was used instead of 128 mM to avoid abiotic precipitation of the metal

### ***Bacterial immobilization of uranium***

The U removal capacity of the strain Br8 was determined by means of ICP-MS. In the presence of Br8 cells and G2P (5 mM), U removal rates around 90% (maximum of 94.7%) were observed for all U concentrations tested (0.01, 0.1, 0.5 and 1 mM) at 48 h (pH 6.3, 28 °C, 165 rpm) (Fig. 1). Although no variation was detected in pH level during the incubation, abiotic controls showed U immobilization values between 10% and 30%, except at the lowest U concentration (0.01 mM), where abiotic precipitation accounted for 60% of the

total U removal (Fig. 1). Heat-killed biomass controls exhibited 11% and 54% U removal in the presence of 1 mM and 0.1 mM U, respectively (Fig. 1). Although for 0.1 mM the removal rate was much higher with inactive cells than with no cells, in the case of 1 mM U no significant differences were observed for the two treatments. These results suggest that the cells of this strain interact with U through active (e.g. biomineralization) and passive (e.g. biosorption) mediated processes, as was confirmed by U kinetics studies (see results below).

The combination of different interaction mechanisms for U immobilization seems reasonable when a bacterial consortium is occurring, but numerous studies confirmed also this ability for single microbial strains (Song et al., 2019). Regarding U immobilization efficiency, a limited number of studies have reported removal rates similar to those presented here, in the presence of such high U concentrations and G2P (e.g. 95% removal for 0.5 mM initial U concentration). When considering lower initial U concentrations, bacterial strains like *Rahnella* sp. Y9602, *Leifsonia* sp. J5, or *Serratia* sp. OT-II-7, all isolated from U-rich environments, also showed U immobilization rates over 90% under different incubation conditions (Beazley et al., 2007; Chandwadkar et al., 2018; Ding et al., 2018). Moreover, three *Xanthomonadales* isolates (*Stenotrophomonas maltophilia* P-8-1 and P-8-3c, and *Rhodanobacter* sp. A2-61), likewise recovered from mining or waste disposal sites, showed much lower immobilization rates (Nazina et al., 2010; Sousa et al., 2013).

Regarding the U removal capacity of *Stenotrophomonas* sp. Br8 expressed by dry biomass weight, it was observed that 1 g of this bacterium was able to immobilize 373 mg of U after 48 h at 28 °C from a solution containing U (0.5 mM) and G2P (5 mM) at pH 6.3. Although most of previous studies report lower or similar values, e.g. *Bacillus cereus* 12-2 at pH 5 (448 mg U/g dry biomass; Zhang et al., 2018), *Paenibacillus* sp. JG-TB8 under anoxic conditions (138 mg U/g dry biomass; Reitz et al., 2014), or *B. thuringiensis* strains (400 mg U/g dry biomass; Pan et al., 2015), extreme loading capacity was observed in the engineered bacterial strain *Deinococcus radiodurans*-PhoK at 10 mM U (10700 mg U/g dry biomass; Kulkarni et al., 2013).

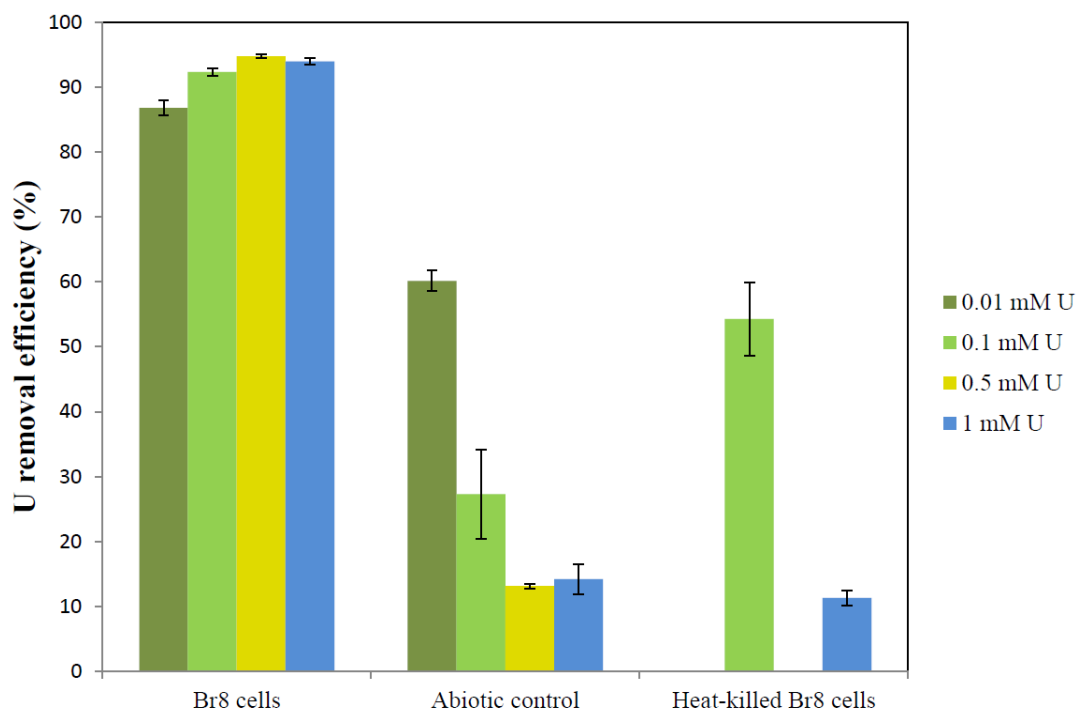


**Figure 1.** Uranium removal efficiency (%) after incubation (48h; 28°C; 165 rpm) of MOPS-buffered (20 mM) distilled water (pH 6.3) amended with G2P (5 mM) and various U concentrations (0.01, 0.1, 0.5 and 1 mM) in presence of *Stenotrophomonas* sp. Br8 cells (0.5 mg dry biomass per ml of medium, equivalent OD<sub>600nm</sub> ≈ 0.5). Flasks without cells and including heat-killed bacterial cells were used as control treatments. The data are showed as the mean ± SD of at least three independent measurements.

### *Phosphatase activity and inorganic phosphate release*

*Stenotrophomonas* species are known to express P-ase activity (Sánchez-Castro et al., 2017b; Weber et al., 2018). Therefore, the role of this enzyme in the removal of U by its precipitation as U phosphates was investigated for other bacterial strains (Kulkarni et al., 2016; Chandwadkar et al., 2018; Zhang et al., 2018; Shukla et al., 2019). The P-ase activity of Br8-strain cells exposed to different U concentrations (0.01, 0.1, 0.5 and 1 mM) for 48 h, in presence of G2P, was assessed. Results showed that the enzymatic activity depends upon U concentration, being twice as high at 0.1 and 0.5 mM U concentration than at 1 mM U (Fig. 2). Although the presence of U may enhance microbial P-ase activity as a protective strategy against the U toxicity, certain concentrations of this metal seem to hinder this defense mechanism, as previously reported for uranyl ion (Macaskie et al., 2000) and other heavy metal ions such as VO<sub>4</sub><sup>3-</sup>, Hg<sup>2+</sup> and Mg<sup>2+</sup> (Swarup et al., 1982; Tabaldi et al., 2007; Xu et al., 2018). In addition, low P-ase activity was exhibited by heat-killed cells, U untreated cells and low-U concentration (0.01 mM) treated cells (Fig. 2).

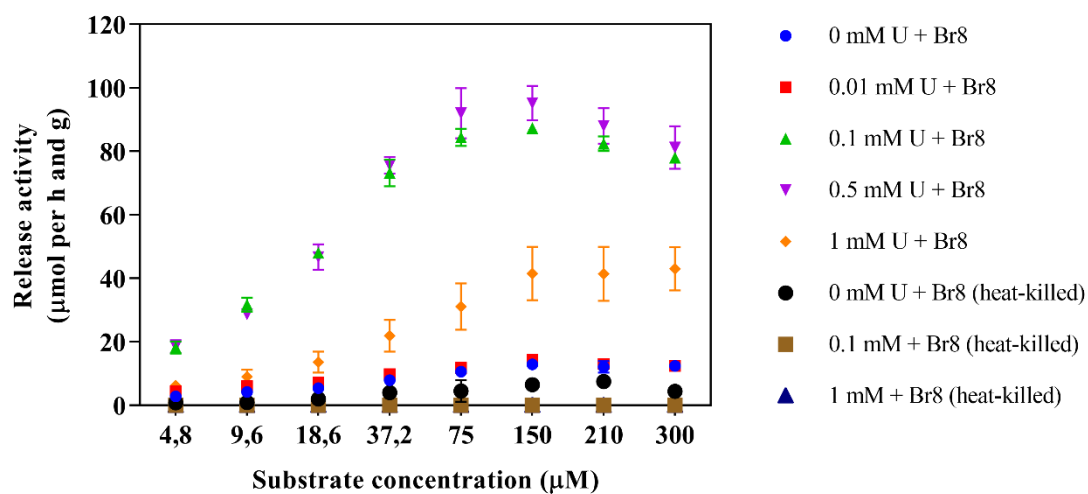


**Figure 2.** Phosphatase activity (measured as  $\mu\text{mol}$  released per h and g at different substrate concentrations) of Br8 cells (0.5 mg dry biomass per ml of medium, equivalent  $\text{OD}_{600\text{nm}} \approx 0.5$ ) after incubation (48h;  $28^\circ\text{C}$ ; 165 rpm) in MOPS-buffered (20 mM) distilled water (pH 6.3) amended with G2P (5 mM) and various U concentrations (0, 0.01, 0.1, 0.5 and 1 mM). Flasks with heat-killed bacterial cells were used as control treatment. The data are showed as the mean  $\pm$  SD of at least three independent measurements.

This Br8-inherent enzymatic activity is responsible for releasing orthophosphates, by using G2P, which may precipitate U(VI) as uranyl phosphate minerals. It should be noted that other organic phosphate sources than G2P like sodium glycerophosphate have been demonstrated to play the same role in presence of bacterial phosphatase activity (Tu et al., 2019). The amount of the orthophosphate detected after incubation increased as the U concentration decreased (Fig. S-2). Abiotic and killed-cells controls showed very low values of released orthophosphate, a finding supported by the P-ase activity results shown above (Fig. 2).

### ***STEM-HAADF analysis***

The STEM-HAADF/EDX technique was used to determine the cellular location of U precipitated by the bacterium Br8 and to elucidate the key mechanism through which this strain copes with the radionuclide's toxicity. Micrographs of ultrathin sections of 0.1 and 1 mM U-treated-cells of *Stenotrophomonas* sp. Br8 (48 h, pH 6.3, 5 mM G2P) are presented in Fig. 3. Needle-like U precipitates were localized at the cell surface and in the

extracellular space. No intracellular U accumulation was observed, suggesting the ability of this strain to overcome U toxicity by avoiding its uptake. The precipitation of U around the cell surface is probably due to the localization of P-ase enzymes at this level and, consequently, to the potential abundance of phosphate groups (Kulkarni et al., 2016; Chandwadkar et al., 2018). Potentiometric titration of the cells of a similar strain (*S. bentonitica* BII-R7) revealed a high amount of phosphate groups at the cell surface,  $10.78 \pm 0.31 \times 10^{-4}$  mol/g higher than those of other bacterial strains (Ruiz-Fresneda, submitted to Environmental Science and Technology). In general, microbes inhabiting U contaminated environments accumulate biogenic metal minerals in the extracellular space as a defensive mechanism. A similar strategy was observed for *Stenotrophomonas* sp. U18 when incubated for 1h in a solution containing U (Islam and Sar, 2016). Intracellular U-containing accumulates have been observed in the closely-related bacterial strain *S. maltophilia* JG-2, isolated from U mining wastes (Merroun and Selenska-Pobell, 2008).

EDX spectra and elemental mapping analysis indicated that the electron-dense accumulations observed extracellularly and on the cell surface are composed mainly of U and P (Fig. 3). These observations confirm the high P-ase activity of this bacterial strain and its key role in the formation of U-phosphate minerals, which are considered to be very stable for long periods over a wide range of pH, and to not re-oxidize and re-mobilize easily as is the case for U reduction byproducts (Lloyd et al., 2002; Senko et al., 2002; Beazley et al., 2011).

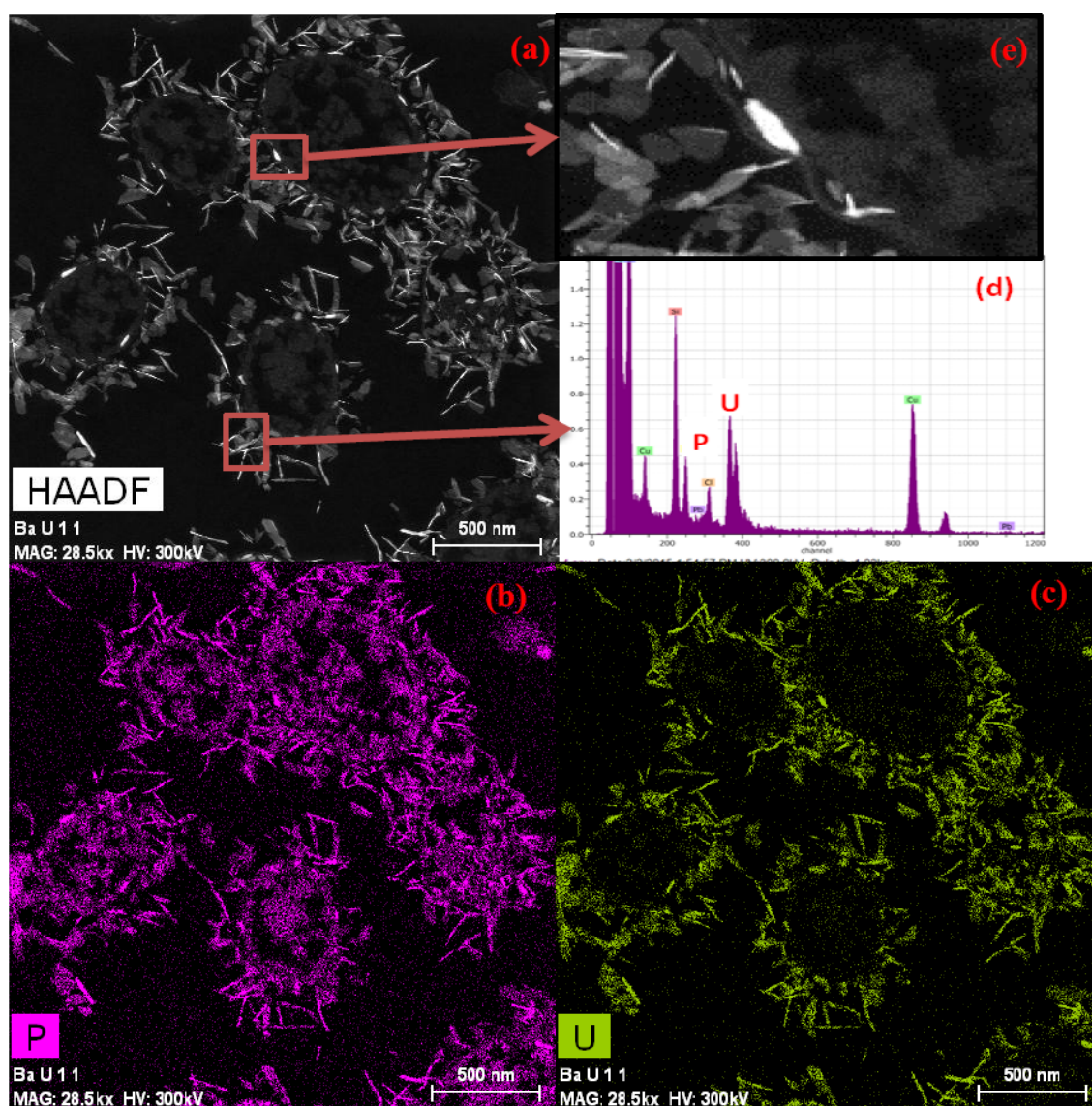


**Figure 3.** HAADF-STEM micrograph (a) of a thin section showing U precipitates around Br8 cells recovered after their incubation (48h; 28°C; 165 rpm) in MOPS-buffered (20 mM) distilled water (pH 6.3) amended with G2P (5 mM) and U (1 mM). EDX element-distribution maps for P (b) and U (c), and EDXS spectrum (d) of the point marked with a red square in (a) image, indicated that precipitates observed are mainly composed of P and U. Zoomed-in view (e) showed U precipitates located at cell surface level.

### *EXAFS analysis*

The  $L_{III}$ -edge EXAFS spectra of the U complexes formed by Br8 cells at 0.1 and 1 mM metal concentration, and that of inorganic uranyl phosphate (m-autunite) used as a standard compound for comparison, along with their Fourier Transforms (FT), are presented in Fig. 4. The EXAFS spectra of the two experimental samples highly resemble each other and the m-autunite spectrum, indicating that the local coordination of U(VI) within the two samples consists of U phosphates.

The FT of the EXAFS spectra of the two U bacterial samples show 5 significant peaks (Fig. 4). Quantitative fit results (Table 2) (distances are phase shift corrected) showed that U(VI) has two  $O_{ax}$  at a distance of 1.78 Å and 4  $O_{eq}$  at  $2.29 \pm 0.02$  Å. The second peak of the FTs ( $R+\Delta \sim 1.8$  Å) was related to the backscattering contribution of the equatorial oxygen atoms. The MS path of the axial oxygen atoms, as well as the SS and MS of the phosphate atoms, can be seen in the FTs in the region between  $R+\Delta=2.8$  and 3.4 Å, respectively. The U-O<sub>eq</sub> bond distance in the two samples is within the range of previously reported values for the oxygen atom of the phosphate bound to uranyl (Merroun et al., 2003, 2011; Nedelkova et al., 2007). The fourth FT peak, which appears at  $R+\Delta \sim 3$  Å (radial distance  $R = 3.61$  Å) is a result of back-scattering from phosphorus atoms. This distance is typical for a monodentate coordination of U(VI) by phosphate. A fifth peak at bond distance of  $5.20-5.22 \pm 0.02$  Å was fitted to a U-U. The EXAFS spectra of the U-treated bacterial cell samples at 2 U concentrations are similar to that of m-autunite with regard to the U-O<sub>eq</sub>, U-P and U-U distances, suggesting that an inorganic m-autunite-like uranyl phosphate phase was precipitated by the Br8 cells in these two samples. These results are in agreement with those obtained on the high P-ase activity of the Br8 strain, leading to the release of inorganic phosphate needed for U precipitation as U phosphate phases, with a local coordination similar to that of m-autunite.

**Table 2.** Structural parameters of the uranium complexes formed by the cells of the strain *Stenotrophomonas* sp. Br8 exposed to 1 and 0,1 mM U(VI), pH 5.5 and in presence of G2P.

Sample	Shell	N <sup>a</sup>	R(Å) <sup>b</sup>	$\sigma^2$ (Å <sup>2</sup> ) <sup>c</sup>	$\Delta E$ (eV)
Br8/G2P/1mMU	U-O <sub>ax</sub>	2 <sup>d</sup>	1.78	0.0037	0.82
	U-O <sub>eq1</sub>	$3.7 \pm 0,2$	2.29	0.0032	
	U-P	$5.5 \pm 1,7$	3.61	0.0093	
	U- O <sub>eq1</sub> -P (MS)	11,0 <sup>e</sup>	3.71	0.0093 <sup>f</sup>	
	U-U	$2.7 \pm 1.7$	5.22	0.008 <sup>d</sup>	
Br8/G2P/0.1mMU	U-O <sub>ax</sub>	2 <sup>d</sup>	1.78	0.0043	0.42
	U-O <sub>eq1</sub>	$4.1 \pm 0.3$	2.29	0.0051	
	U-P	$2.6 \pm 0.7$	3.61	0.0024	
	U- O <sub>eq1</sub> -P (MS)	5,2 <sup>e</sup>	3.71	0.0024 <sup>f</sup>	
	U-U	$2.1 \pm 0.9$	5.20	0.008 <sup>d</sup>	

<sup>a</sup> Errors in coordination numbers are  $\pm 25\%$ , and standard deviations, as estimated by EXAFSPAK, are given in parentheses.

<sup>b</sup> Errors in distance are  $\pm 0.02$  Å.

<sup>c</sup> Debye-Waller factor.

<sup>d</sup> Value fixed for calculation.

<sup>e</sup> Coordination numbers for U-P and U-O<sub>eq1</sub>-P MS were linked.

<sup>f</sup> Debye Waller factors for U-P and U-O<sub>eq1</sub>-P MS were linked.



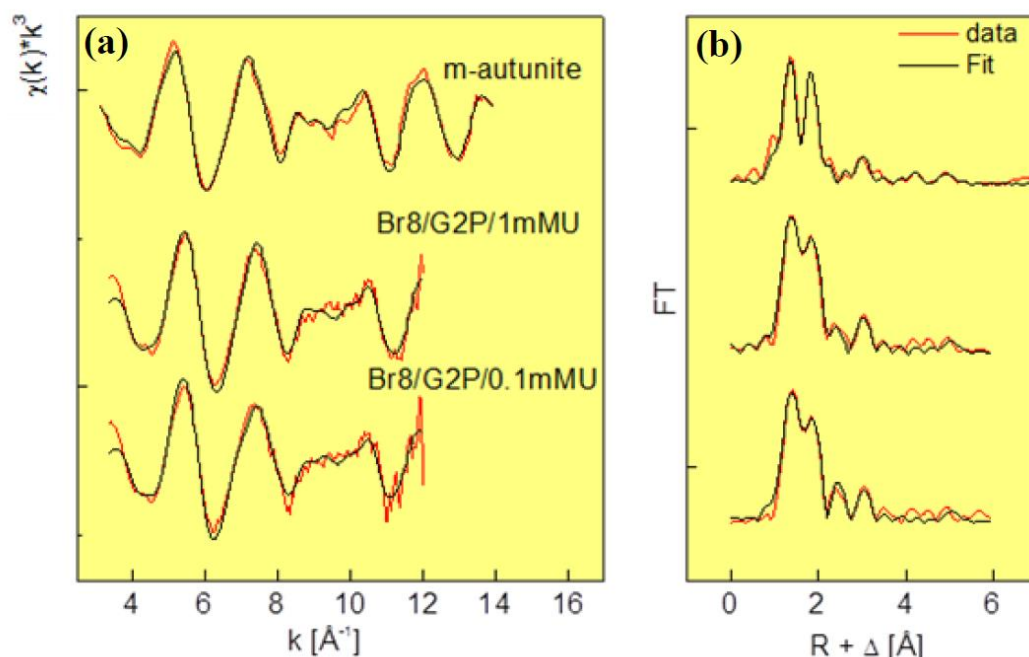


**Figure 4.** (a) Uranium  $L_{III}$ -edge  $k^3$ -weighted EXAFS spectra and (b) the corresponding Fourier Transforms (FT) of the uranium complexes formed by *Stenotrophomonas* sp. Br8 cells at U concentrations of 1 mM and 0.1 mM in MOPS-buffered (20 mM) distilled water amended with G2P (5 mM), and reference compound (m-autunite).

### *Uranium-immobilization performance by Br8-cells: influencing factors*

#### *Time: kinetics of the uranium immobilization process*

The uranium removal capacity of the strain Br8 monitored at different incubation times is presented in Fig. 5. The results indicate increased U removal rate of 16.2, 20.7 and  $\approx 50\%$  after 5, 30 and 180 min, respectively, stabilizing at  $\approx 98\%$  after 20 h. Abiotic controls showed a background U precipitation of  $\approx 3\text{-}4\%$  at 10 min, reaching values around 10%-15% after 24 h (Fig. 5). Orthophosphates in solution are first detected at a significant concentration at 24 h (Fig. S-3), once the U(VI) precipitation percentage had reached its maximum (Fig. 5).

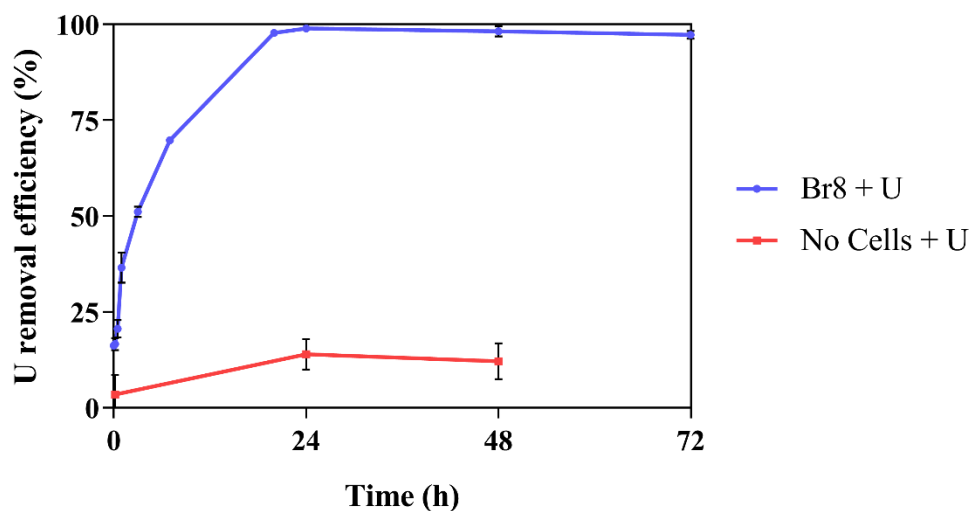


**Figure 5.** Uranium removal efficiency (%) kinetics during incubation (72 h; 28°C; 165 rpm) of MOPS-buffered (20 mM) distilled water (pH 6.3) amended with G2P (5 mM) and U (0.5 mM) in presence of *Stenotrophomonas* sp. Br8 cells (0.5 mg dry biomass per ml of medium, equivalent OD<sub>600nm</sub> ≈ 0.5). Flasks without cells were used as control treatment. The data are showed as the mean ± SD of at least three independent measurements.

As suggested above, these findings support the implication of active and passive mechanisms in aerobic U immobilization. Metabolically independent mechanisms likely based on U sorption onto the cell surface of the bacterium are first to be detected in this time-course experiment. Previous reports describe similarly fast actinides sequestration, interpreting them as passive events (Gerber et al., 2016; Shukla et al., 2017). A large number of bacterial functional groups at the cell surface (e.g. carboxyl, hydroxyl, amino and phosphoryl) are known to effectively provide binding sites for metals and other toxic elements (Fein et al., 2005; Ojeda et al., 2008; Merroun et al., 2011; Moll et al., 2014; Reitz et al., 2015). Phosphate groups have been found to be particularly abundant at the cell surface level in the Br8 closely related bacterial strain *S. bentonitica* BII-R7 in comparison to other bacteria (Ruiz-Fresneda, submitted to Environmental Science and Technology). In terms of biomineralization active mechanisms, the lack of orthophosphates in excess in the incubation medium before 24 h suggests that the process kinetics at this U concentration are governed by the rate of release of enzymatic inorganic phosphates. While soluble U(VI) is available in the system, free orthophosphates bound rapidly to it, making its detection impossible. Subsequent sampling times (48 and 72 h) show a linear increase of orthophosphates in the medium (Fig. S-3), indicating a continuous orthophosphates release

via P-ase activity. No-cell control treatments evidenced an abiotic removal process most likely produced by spontaneous chemical conversion of G2P into orthophosphates, which may interact with the solved U fraction. This background abiotic U removal (approx. 10%-15%) was repeatedly obtained in our work.

### *Biomass concentration*

The effect of biomass concentration (0.25, 0.5 and 1 mg/mL dry biomass) in the U immobilization process was investigated to determine the optimal Br8 cell concentration for removing U in solution in the presence of G2P. The uranium precipitation ability of this strain was not affected by this biological parameter. Removal rates at the studied biomass concentrations (0.25, 0.5 and 1 mg/mL dry weight) did not differ significantly (Fig. S-4a). Even at the lowest concentration (0.25 mg/mL dry weight), U removal (94.8%) remained at the same level as in previous assays (Fig. S-4a). However, the measured concentrations of orthophosphates released in the medium varied clearly depending on the biomass concentration (Fig. S-4b). These changes in the amount of inorganic phosphates released are not proportional to the biomass concentration, indicating a nonlinear relationship. Considering these results, limitation of the U biomineralization process is imposed by Br8 enzymatic activity and not by the G2P concentration, which is clearly in excess in our experiments. Since the minimum biomass concentration tested in this case (0.25 mg/mL dry weight) resulted in maximum U removal values, further optimization experiments are needed to determine the minimum biomass applicable for satisfactory U removal rates.

### *pH*

The effect of pH in the U biomineralization mediated by Br8 cells was also investigated in order to determine whether this process is suitable for bioremediation of acidic or alkaline U contaminated waters. For this purpose, slightly acidic (pH 5) and alkaline (pH 8) conditions were investigated. Similar U removal rates (93%-99%; Fig. S-5a) as those observed in previous experiments at circumneutral pH (92%-95%; Fig. 1) were obtained for acidic and alkaline pH conditions, regardless of the U concentrations assayed (0.1, 0.5 and 1 mM U) (Fig. S-5a). The chemical speciation of U in the studied systems (Table S-1) showed that at pH 5, U largely formed positively charged uranium hydroxide complexes

(e.g.  $(\text{UO}_2)_3(\text{OH})^{5+}$ ,  $\text{UO}_2^{2+}$ ,  $\text{UO}_2\text{OH}^+$ ,  $(\text{UO}_2)_2(\text{OH})_2^{2+}$ ), while at pH 8, the negatively charged uranyl hydroxide  $(\text{UO}_2)_3(\text{OH})^{7-}$  occurred also in a significant proportion (14.6-18.5%, depending on U initial concentration; Table S-1). Thus, the passive initial phase of U biosorption is expectable to be more pronounced under slightly acidic pH, where the positively charged hydroxide complexes are more represented, rather than under pH 8. Concerning active mechanisms, the release of orthophosphates by Br8 cells was higher at alkaline pH, where an excess of orthophosphates in solution was detected for all U concentrations at 48 h (Fig. S-5b). Under acidic conditions, the inorganic phosphate concentration in solution decreased significantly at all U concentrations. Yet it should be noted that even under these conditions, the cells released sufficient orthophosphates to precipitate most of the U in solution (94.6% for 1 mM initial U concentration). The measurements of P-ase activity gave values of 40  $\mu\text{mol}$  (per h and g) at both alkaline and acidic pHs for all three U concentrations tested, except in the case of pH 5 and 0.5 mM U, where this activity showed a maximum value of 60-62  $\mu\text{mol}$  (per h and g).

Since previous experiments at circumneutral pH showed higher P-ase activity (Fig. 2), in accordance with previous investigations (Macaskie et al., 1994; Kulkarni et al., 2016), we hypothesize that at these pH conditions both types of phosphatases may act with a summative effect. The unexpected high P-ase activity associated with low levels of orthophosphates released seen at pH 5 and 0.5 mM U would indicate a reduction in the efficiency of Br8 enzymatic activity. Similar contradictory results were recently reported by Chandwadkar et al (2018), who observed slower U precipitation kinetics at pH 5 but a higher P-ase activity when compared to the same test at pH 7 and 9. Several studies with enterobacteria demonstrate that a high P-ase activity is not enough to confer metal immobilization properties (Macaskie et al., 1994; Jeong and Macaskie, 1995). *Serratia* bacterial cells were found to be damaged and lysed at pH 5, allowing solved uranyl to penetrate and precipitate within the cytoplasm (Chandwadkar et al., 2018), likely affecting the sensitive P-ase activity (Macaskie et al., 2000). On the other hand, at alkaline pH (8), the presence of carbonates may hinder uranyl phosphate precipitation because of the formation of highly soluble uranyl carbonate complexes (Nilgiriwala et al., 2008; Kulkarni et al., 2016). At any rate, no intracellular U precipitates are normally found under these alkaline conditions, maintaining cell viability intact (Kulkarni et al., 2016).

Since U removal values at pH 8 resulted slightly higher than those obtained under circumneutral and acidic conditions (Figs. S-5a and 1), microscopic STEM observations

were made to investigate the interaction mechanisms involved in this case. Microscopy images (Fig. S-6) reveal the presence of flake-shaped accumulates, located extracellularly and at the cell surface level, larger than those found previously under circumneutral conditions (Fig. 3). Similarly to those analyzed before at pH 6.3, EDX spectra and elemental mapping analysis indicated that the precipitates formed are composed mainly of U and P (Fig. S-6). Through XRD analysis, structures resembling  $\text{Rb}[(\text{UO}_2)(\text{PO}_4)](\text{H}_2\text{O})_3$  and autunite  $[\text{CaU}(\text{PO}_4)_2]$  were identified in the precipitates resulting under alkaline and acidic conditions, respectively (Fig. S-7).

### *Temperature*

Regarding the temperature effect in the bio-immobilization process at 48 h, maximum removal efficiencies (>90%) were observed at 28 °C and 37 °C (Fig. S-8a). Orthophosphate concentrations measured at 48 h (Fig. S-8b) suggest higher enzymatic activity at 37 °C. At 15 °C, Br8 U precipitation ability decreased approximately 20% (Fig. S-8a).

For most mesophiles, metabolic capacity in general and P-ase enzymatic activity in particular are known to be reduced when temperature drops under 20 °-25 °C (González et al., 1994; Lee et al., 2015; Behera et al., 2017). As pointed out in the previous section, the U removal mechanism reported in this work is highly dependent upon the metabolic capacity of Br8 cells, which is clearly higher at moderate temperatures (28 °- 37°C) than at lower ones such as 15 °C.

### **Conclusions**

This study describes a highly efficient process for soluble U(VI) immobilization mediated by a bacterial strain from the genus *Stenotrophomonas* (Br8) in presence of G2P as organophosphate source at different pH values (5, 7 and 8). Although U removal from aqueous solutions mediated by certain bacterial strains in presence of an organophosphate compound has already been reported (Macaskie et al., 1992, 1994; Beazley et al., 2007 and 2009; Martinez et al., 2007; Merroun et al., 2011), the present work demonstrates the ability of the strain Br8 for tolerating and immobilizing aerobically high U concentrations in a

short period of time under changing environmental conditions. The biogenic U phosphate phases precipitated by this strain presented a local coordination similar to that of autunite groups, characterized by their high long-term stability.

In summary, these results have direct implications for understanding bacterial U tolerance mechanisms and the impact of the strain *Stenotrophomonas* sp. (Br8) on mobility and biogeochemical U cycling in nature. They also demonstrate the potential of this bacterial strain for U bioremediation as a result of a complex process combining passive and active mechanisms, including fast biosorption to the cell surfaces and a subsequent P-ase enzyme-mediated biomineralization phase (e.g. Chandwadkar et al., 2018). Moreover, since phosphatases are also activated under anaerobic conditions (Rossolini et al., 1998), the U biomineralization presented here may be an alternative to bioreduction in the presence of G2P when the presence of oxygen is limited. Despite these promising data presented, further research is needed on the performance of this process when applied to real U-polluted mining waters through column experiments for the design of appropriate application procedures.

### **Declaration of competing interest**

The authors declare that they have no known competing financial interests or personal relationships that could have appeared to influence the work reported in this paper.

### **Acknowledgements**

This work was supported by ORANO Mining (France) [collaborative research contract n° 3022 OTRI-UGR]. It results from a Joint Research Project between Orano Mining R&D Department and the Department of Microbiology of the University of Granada. We acknowledge the assistance at the STEM-HAADF and XRD measurements of Maria del Mar Abad Ortega, Concepción Hernández Castillo and José Romero Garzón (Centro de Instrumentación Científica, University of Granada, Spain). We also acknowledge SOLEIL for provision of synchrotron radiation facilities.

## References

- Acharya, C., 2015. Uranium bioremediation: approaches and challenges. In: Sukla, L.B., Pradhan, N., Panda, S., Mishra, B.K. (Eds.), *Environmental Microbial Biotechnology*, pp. 119–132. <http://www.springer.com/978-3-319-19017-4>.
- Alonso, A., Sanchez, P., Martinez, J.L., 2000. *Stenotrophomonas maltophilia* D457R contains a cluster of genes from Gram-positive bacteria involved in antibiotic and heavy metal resistance. *Antimicrob. Agents Chemother.* 44, 1778–1782.
- Ankudinov, A., Ravel, B., Rehr, J., Conradson, S., 1998. Real-space multiple-scattering calculation and interpretation of x-ray-absorption near-edge structure. *Phys. Rev. B* 58, 7565.
- Bader, M., Müller, K., Foerstendorf, H., Drobot, B., Schmidt, M., Musat, N., Swanson, J., Reed, D., Stump, T., Cherkouk, A., 2017. Multistage bioassociation of uranium onto an extremely halophilic archaeon revealed by a unique combination of spectroscopic and microscopic techniques. *J. Hazard. Mater.* 327, 225–232.
- Banerjee, M., Yesmin, L., 2002. Sulfur-oxidizing plant growth promoting rhizobacteria for enhanced canola performance. US Patent 07491535.
- Bargar, J.R., Bernier-Latmani, R., Giammar, D.E., Tebo, B.M., 2008. Biogenic uraninite nanoparticles and their importance for uranium remediation. *Elements* 4, 407–412.
- Beazley, M.J., Martinez, R.J., Sobecky, P.A., Webb, S.M., Taillefert, M., 2007. Uranium biomineralization as a result of bacterial phosphatase activity: insights from bacterial isolates from a contaminated subsurface. *Environ. Sci. Technol.* 41, 5701–5707.
- Beazley, M.J., Martinez, R.J., Sobecky, P.A., Webb, S.M., Taillefert, M., 2009. Nonreductive biomineralization of uranium(VI) phosphate via microbial phosphatase activity in anaerobic conditions. *Geomicrobiol. J.* 26, 431–441. 10.1080/01490450903060780.
- Beazley, M.J., Martinez, R.J., Webb, S.M., Sobecky, P.A., Taillefert, M., 2011. The effect of pH and natural microbial phosphatase activity on the speciation of uranium in subsurface soils. *Geochim. Cosmochim. Acta* 75, 5648–5663.
- Behera, B.C., Yadav, H., Singh, S.K., Mishra, R.R., Sethi, B.K., Dutta, S.K., Thatoi, H.N., 2017. Phosphate solubilization and acid phosphatase activity of *Serratia* sp. isolated from mangrove soil of Mahanadi river delta, Odisha, India. *J. Genet. Eng. Biotechnol.* 15, 169–178.
- Chandwadkar, P., Misra, H.S., Acharya, C., 2018. Uranium biomineralization induced by a metal tolerant *Serratia* strain under acid, alkaline and irradiated conditions. *Metallomics* 10, 1078–1088.
- Ding, L., Tan, W.-F., Xie, S.-B., Mumford, K., Lv, J.-W., Wang, H.-Q., Fang, Q., Zhang, X.-W., Wu, X.-Y., Li, M., 2018. Uranium adsorption and subsequent re-oxidation under aerobic conditions by *Leifsonia* sp. - Coated biochar as green trapping agent. *Environ. Pollut.* 242, 778–787.
- Fein, J.B., Boily, J.-F., Yee, N., Gorman-Lewis, D., Turner, B.F., 2005. Potentiometric titrations of *Bacillus subtilis* cells to low pH and a comparison of modeling approaches. *Geochim. Cosmochim. Acta* 69, 1123–1132.
- Gavrilescu, M., Pavel, L.V., Cretescu, I., 2009. Characterization and remediation of soils contaminated with uranium. *J. Hazard. Mater.* 163, 475–510.
- Gerber, U., Zirnstein, I., Krawczyk-Bärsch, E., Lünsdorf, H., Arnold, T., Merroun, M.L., 2016. Combined use of flow cytometry and microscopy to study the interactions between the gram-negative betaproteobacterium *Acidovorax facilis* and uranium (VI). *J. Hazard Mater.* 317, 127–134.
- German, D.P., Weintraub, M.N., Grandy, A.S., Lauber, C.L., Rinkes, Z.L., Allison, S.D., 2011. Optimization of hydrolytic and oxidative enzyme methods for ecosystem studies. *Soil Biol. Biochem.* 43, 1387–1397.
- González, D.F., Fárez-Vidal, M.E., Arias, J.M., Montoya, E., 1994. Partial purification and biochemical properties of acid and alkaline phosphatases from *Myxococcus coralloides*. *J. Appl. Bacteriol.* 77, 567–573.

- Hsi, C.D., Langmuir, D., 1985. Adsorption of uranyl onto ferric oxyhydroxides: application of the surface complexation site-binding model. *Geochim. Cosmochim. Acta*, 49, 1931-1941. 10.1016/0016-7037(85)90088-2.
- Hudson, E., Allen, P., Terminello, L., Denecke, M., Reich, T., 1996. Polarized x-ray-absorption spectroscopy of the uranyl ion: comparison of experiment and theory. *Phys. Rev. B* 54, 156.
- Ikemoto, S., Suzuki, K., Kaneko, T., Komagata, K., 1980. Characterization of strains of *Pseudomonas maltophilia* which do not require methionine. *Int. J. Syst. Bacteriol.* 30, 437-447.
- Islam, E., Sar, P., 2011. Culture-dependent and -independent molecular analysis of bacterial community within uranium ore. *J. Basic Microbiol.* 51, 1-13.
- Islam, E., Sar, P., 2016. Diversity, metal resistance and uranium sequestration abilities of bacteria from uranium ore deposit in deep earth stratum. *Ecotoxicol. Environ. Saf.* 127, 12-21.
- Jeong, B.C., Macaskie, L.E., 1995. PhoN-type acid phosphatases of a heavy metal-accumulating *Citrobacter* sp.: resistance to heavy metals and affinity towards phosphomonoester substrates. *FEMS Microbiol. Lett.* 130, 211-214.
- Kolhe, N., Zinjarde, S., Acharya, C., 2018. Responses exhibited by various microbial groups relevant to uranium exposure. *Biotechnol. Adv.* 36, 1828-1846.
- Kong, L., Ruan, Y., Zheng, Q., Su, M., Diao, Z., Chen, D., Hou, L.A., Chang, X., Shih, K., 2020. Uranium extraction using hydroxyapatite recovered from phosphorus containing wastewater. *J. Hazard. Mater.* 382, 120784.
- Krawczyk-Bärsch, E., Gerber, U., Müller, K., Moll, H., Rossberg, A., Steudtner, R., Merroun, M.L., 2018. Multidisciplinary characterization of U(VI) sequestration by *Acidovorax facilis* for bioremediation purposes. *J. Hazard. Mater.* 347, 233-241.
- Kulkarni, S., Ballal, A., Apte, S.K., 2013. Bioprecipitation of uranium from alkaline waste solutions using recombinant *Deinococcus radiodurans*. *J. Hazard. Mater.* 262, 853-861.
- Kulkarni, S., Misra, C.S., Gupta, A., Ballal, A., Apte, S.K., 2016. Interaction of uranium with bacterial cell surfaces: inferences from phosphatase-mediated uranium precipitation. *Appl. Environ. Microb.* 82, 4965-4974.
- Langmuir, D., 1978. Uranium solution-mineral equilibria at low temperatures with applications to sedimentary ore deposits. *Geochim. Cosmochim. Acta* 42, 547-569.
- Lee, D.-H., Choi S.-L., Rha, E., Kim, S.J., Yeom, S.-J., Moon, J.-H., Lee, S.-G., 2015. A novel psychrophilic alkaline phosphatase from the metagenome of tidal flat sediments. *BMC Biotechnol.* 15, 1.
- Li, X., Gu, A.Z., Zhang, Y., Xie, B., Li, D., Chen J., 2019. Sub-lethal concentrations of heavy metals induce antibiotic resistance via mutagenesis. *J. Hazard. Mater.* 369, 9-16.
- Lloyd, J.R., Chesnes, J., Glasauer, S., Bunker, D.J., Livens, F.R., Lovley, D.R., 2002. Reduction of actinides and fission products by Fe(III)-reducing bacteria. *Geomicrobiol. J.* 19, 103-120.
- López-Fernández, M., Fernández-Sanfrancisco, O., Moreno-García, A., Martín-Sánchez, I., Sánchez-Castro, I., Merroun, M.L., 2014. Microbial communities in bentonite formations and their interactions with uranium. *Appl. Geochem.* 49, 77-86.
- Lovley, D.R., Phillips, E.J.P., Gorby, Y.A., Landa, E.R., 1991. Microbial reduction of uranium. *Nature* 350, 413-416.
- Lovley, D.R., Phillips, E.J.P., 1992. Bioremediation of uranium contamination with enzymatic uranium reduction. *Environ. Sci. Technol.* 26, 2228-2234. <https://doi.org/10.1021/es00035a023>.
- Lovley, D.R., 2001. Bioremediation anaerobes to the rescue. *Science*, 293, 1444-1446.
- Macaskie, L.E., Empson, R.M., Cheetham, A.K., Grey, C.P., Skarnulis, A.J., 1992. Uranium bioaccumulation by a *Citrobacter* sp. as a result of enzymically mediated growth of polycrystalline  $\text{eHUO}_2\text{PO}_4$ . *Science* 257, 782-784. 10.1126/science.1496397.
- Macaskie, L.E., Bonthron, K.M., Rouch, D.M., 1994. Phosphatase-mediated heavy



- metal accumulation by a *Citrobacter* sp. and related enterobacteria. FEMS Microbiol. Lett. 121, 141-146.
- Macaskie, L.E., Bonthron, K.M., Yong, P., Goddard, D.T., 2000. Enzymically mediated bioprecipitation of uranium by a *Citrobacter* sp.: a concerted role for exocellular lipopolysaccharide and associated phosphatase in biomineral formation. Microbiology 146, 1855–1867.
- Makarov, E., Ivanov, V., 1960. The crystalline structure of  $\text{Ca}(\text{UO}_2)_2(\text{PO}_4)_2 \cdot 6\text{H}_2\text{O}$  meta-tenite  
Dokl. Akad. Nauk SSSR 132, 673-676.
- Martinez, R.J., Beazley, M.J., Taillefert, M., Arakaki, A.K., Skolnick, J., Sobecky, P.A., 2007. Aerobic uranium (VI) bioprecipitation by metal-resistant bacteria isolated from radionuclide- and metal-contaminated subsurface soils. Environ. Microbiol. 9, 3122-3133. 10.1111/j.1462-2920.2007.01422.x.
- Mehta, V.S., Maillot, F., Wang, Z., Gatalano, J.G., Giammar, D.E., 2013. Effect of co-solutes on the products and solubility of uranium(VI) precipitated with phosphate. Chem. Geol. 364, 66-75.
- Merroun, M.L., Hennig, C., Rossberg, A., Reich, T., Selenska-Pobell, S., 2003. Characterization of U (VI)-*Acidithiobacillus ferrooxidans* complexes using EXAFS, transmission electron microscopy, and energy-dispersive X-ray analysis. Radiochim. Acta 91, 583-592.
- Merroun, M.L., Raff, J., Rossberg, A., Hennig, C., Reich, T., Selenska-Pobell, S., 2005. Complexation of uranium by cells and S-layer sheets of *Bacillus sphaericus* JG-A12. Appl. Environ. Microbiol. 71, 5532-5543.
- Merroun, M.L., Selenska-Pobell, S., 2008. Bacterial interactions with uranium: An environmental perspective. J. Contam. Hydrol. 102, 285-295.
- Merroun, M.L., Nedelkova, M., Ojeda, J.J., Reitz, T., López-Fernández, M., Arias, J.M., Romero-González, M., Selenska-Pobell, S., 2011. Bio-precipitation of uranium by two bacterial isolates recovered from extreme environments as estimated by potentiometric titration, TEM and X-ray absorption spectroscopic analyses. J. Hazard. Mater. 197, 1-10.
- Moll, H., Lütke, L., Bachvarova, V., Cherkouk, A., Selenska-Pobell, S., Bernhard, G., 2014. Interactions of the Mont Terri Opalinus Clay isolate *Sporomusa* sp. MT-2.99 with curium(III) and europium(III). Geomicrobiol. J. 31, 682-696. doi:10.1080/01490451.2014.889975.
- Murphy, J., Riley, J.P., 1962. A modified single-solution method for the determination of phosphorus in natural waters. Anal. Chim. Acta 27, 31-36.
- Nazina, T.N., Lukyanova, E.A., Zakharova, E.V., Konstantinova, L.I., Kalmykov, S.N., Poltarau, A.B., Zubkova, A.A., 2010. Microorganisms in a disposal site for liquid radioactive wastes and their influence on radionuclides. Geomicrobiol. J. 27, 473-486.
- Nedelkova, M., Merroun, M.L., Rossberg, A., Hennig, C., Selenska-Pobell, S., 2007. *Microbacterium* isolates from the vicinity of a radioactive waste depository and their interactions with uranium. FEMS Microbiol. Ecol. 59, 694-705.
- Neill, T.S., Morris, K., Pearce, C.I., Sherriff, N.K., Burke, M.G., Chater, P.A., Janssen, A., Natrajan, L., Shaw, S., 2018. Stability, composition, and core-shell particle structure of uranium(IV)-silicate colloids. Environ. Sci. Technol. 52, 9118-9127.
- Newsome, L., Morris, K., Trivedi, D., Bewsher, A., Lloyd, J.R., 2015. Biostimulation by glycerol phosphate to precipitate recalcitrant uranium(IV) phosphate. Environ. Sci. Technol. 49, 11070-11078.
- Nilgiriwala, K.S., Alahari, A., Rao, A.S., Apte, S.K., 2008. Cloning and overexpression of alkaline phosphatase PhoK from *Sphingomonas* sp strain BSAR-1 for bioprecipitation of uranium from alkaline solutions. Appl. Environ. Microbiol. 74, 5516-5523.
- Ojeda, J.J., Romero-González, M.E., Bachmann, R.T., Edyvean, R.G., Banwart, S.A., 2008. Characterization of the cell surface and cell wall chemistry of drinking water bacteria by combining XPS, FTIR spectroscopy, modeling, and potentiometric titrations. Langmuir 24, 4032-4040.

- Page, D., Rose, J., Conrod, S., Cuine, S., Carrier, P., Heulin, T., Achouak, W., 2008. Heavy metal tolerance in *Stenotrophomonas maltophilia*. PLoS ONE 3, e1539.
- Pan, X., Chen, Z., Chen, F., Cheng, Y., Lin, Z., Guan, X., 2015. The mechanism of uranium transformation from U (VI) into nano-uramphite by two indigenous *Bacillus thuringiensis* strains. J. Hazard. Mater. 297, 313–319. dx.doi.org/10.1016/j.jhazmat.2015.05.019.
- Park, M., Kim, C., Yang, J., Lee, H., Shin, W., Kim, S., Sa, T., 2005. Isolation and characterization of diazotrophic growth promoting bacteria from rhizosphere of agricultural crops of Korea. Microbiol. Res. 160, 127–133.
- Ravel, B., Newville, M.A., 2005. ARTEMIS, HEPHAESTUS: data analysis for X-ray absorption spectroscopy using IFEFFIT. J. Synchrotron Radiat. 12, 537-541.
- Reitz, T., Rossberg, A., Barkleit, A., Selenska-Pobell, S., Merroun, M.L., 2014. Decrease of U (VI) immobilization capability of the facultative anaerobic strain *Paenibacillus* sp. JG-TB8 under anoxic conditions due to strongly reduced phosphatase activity. PLoS One 9 e102447.
- Reitz, T., Rossberg, A., Barkleit, A., Steudtner, R., Selenska-Pobell, S., Merroun, M.L., 2015. Spectroscopic study on uranyl carboxylate complexes formed at the surface layer of *Sulfolobus acidocaldarius*. Dalton Trans. 44, 2684-2692.
- Rossolini, G.M., Shipa, S., Riccio, M.L., Berlutti, F., Macaskie, L.E., Thaller, M.C., 1998. Bacterial non-specific acid phosphatases: physiology, evolution, and use as tools in microbial biotechnology. Cell Mol. Life Sci. 54, 833–850.
- Ruiz Fresneda, M.A., Delgado-Martín, J., Gómez-Bolívar, J., Fernández-Cantos, M.V., Bosch-Estévez, G., Martínez Moreno, M.F., Merroun, M.L., 2018. Green synthesis and biotransformation of amorphous Se nanospheres to trigonal 1D Se nanostructures: impact on Se mobility within the concept of radioactive waste disposal. Environ. Sci. Nano 5, 2103-2116. 10.1039/C8EN00221E
- Ruiz Fresneda, M.A., Gómez-Bolívar, J., Delgado-Martín, J., Abad-Ortega, M.M., Guerra-Tschuschke, I., Merroun, M.L., 2019. The bioreduction of selenite under anaerobic and alkaline conditions analogous to those expected for a deep geological repository system. Molecules 24, 3868.
- Ryan, R.P., Monchy, S., Cardinale, M., Taghavi, S., Crossman, L., Avison, M.B., Berg, G., van der Lelie, D., Dow, J.M., 2009. The versatility and adaptation of bacteria from the genus *Stenotrophomonas*. Nat. Rev. Microbiol. 7, 514-525.
- Sánchez-Castro, I., Amador-García, A., Moreno-Romero, C., López-Fernández, M., Phrommavanh, V., Nos, J., Descostes, M., Merroun, M.L., 2017a. Screening of bacterial strains isolated from uranium mill tailings porewaters for bioremediation purposes. J. Environ. Radioact. 166, 130-141.
- Sánchez-Castro, I., Ruiz-Fresneda, M.A., Bakkali, M., Kämpfer, P., Glaeser, S.P., Busse, H.J., López-Fernández, M., Martínez-Rodríguez, P., Merroun, M.L., 2017b. *Stenotrophomonas bentonitica* sp. nov., isolated from bentonite formations. Int. J. Syst. Evol. Microbiol. 67, 2779–2786. doi: 10.1099/ijsem.0.002016.
- Schindler, M., Lussier, A.J., Bellrose, J., Rouvimov, S., Burns, P.C., Kurt Kyser, T., 2017. Mobilization and agglomeration of uraninite nanoparticles: A nano-mineralogical study of samples from the Matoush Uranium ore deposit. Am. Mineral. 102, 1776-1787.
- Senko, J.M., Istok, J.D., Suflita, J.M., Krumholz, L.R., 2002. In situ evidence for uranium immobilization and remobilization. Environ. Sci. Technol. 36, 1491-1496.
- Shen, Y., Zheng, X., Wang, X., Wang, T., 2018. The biomineralization process of uranium(VI) by *Saccharomyces cerevisiae*-transformation from amorphous U(VI) to crystalline chernikovite. Appl. Microbiol. Biotechnol. 102, 4217-4229.
- Shukla, A., Parmar, P., Saraf, M., 2017. Radiation, radionuclides and bacteria: an in-perspective review. J. Environ. Radioact. 180, 27-35.
- Shukla, S.K., Hariharan, S., Rao, T.S., 2019. Uranium bioremediation by acid

- phosphatase activity of *Staphylococcus aureus* biofilms: Can a foe turn a friend? *J. Hazard. Mater.* 121316, 10.1016/j.jhazmat.2019.121316. In press
- Sitaud, B., Solari, P. L., Schlutig, S., Llorens, I., Hermange, H., 2012. Characterization of radioactive materials using the MARS beamline at the synchrotron SOLEIL. *J. Nucl. Mat.* 425, 238-243.
- Song, J., Han, B., Song, H., Yang, J., Zhang, L., Ning, P., Lin, Z., 2019. Nonreductive biomineralization of uranium by *Bacillus subtilis* ATCC-6633 under aerobic conditions. *J. Environ. Radioactiv.* 208–209, 106027.
- Sousa, T., Chung, A.P., Pereira, A., Piedade, A.P., Morais, P.V., 2013. Aerobic uranium immobilization by *Rhodanobacter* A2-61 through formation of intracellular uranium-phosphate complexes. *Metallomics* 5, 390–397. doi: 10.1039/c3mt00052d.
- Spycher, N.F., Issarangkun, M., Stewart, B.D., Sevinç Şengör, S., Belding, E., Ginn, T.R., Peyton, B.M., Sani, R.K., 2011. Biogenic uraninite precipitation and its reoxidation by iron(III) (hydr)oxides: a reaction modeling approach. *Geochim. Cosmochim. Acta*, 75, 4426-4440.
- Suzuki, Y., Banfield, J.F., 1999. Geomicrobiology of uranium. In: Burns, P.C., Finch, R. (Eds.), *Uranium: Mineralogy, Geochemistry and the Environment*. Mineralogical Society of America, Washington, DC, pp. 393-432.
- Swarup, G., Cohen, S., Garbers, D.L., 1982. Inhibition of membrane phosphotyrosyl-protein phosphatase activity by vanadate. *Biochem. Bioph. Res. Co.* 107, 1104-1109.
- Tabaldi, L., Ruppenthal, R., Cargnelutti, D., Morsch, V., Pereira, L., Schetinger, M., 2007. Effects of metal elements on acid phosphatase activity in cucumber (*Cucumis sativus* L.) seedlings. *Environ. Exp. Bot.* 59, 43-48.
- Tu, H., Guo, Y.Y., Zhao, C.S., Liu, J., Li, F.Z., Yang, J.J., Liao, J.L., Yang, Y.Y., Liu, N., 2019. U-phosphate biomineralization induced by *Bacillus* sp. dw-2 in the presence of organic acids. *Nucl. Eng. Technol.* 51, 1322–1332.
- VanEngelen, M.R., Field, E.K., Gerlach, R., Lee, B.D., Apel, W.A., Peyton, B.M., 2010.  $UO_2^{2+}$  speciation determines uranium toxicity and bioaccumulation in an environmental *Pseudomonas* sp. isolate. *Environ. Toxicol. Chem.* 29, 763–769.
- Waite, T.D., Davis, J.A., Payne, T.E., Waychunas, G.A., Xu, N., 1994. Uranium(VI) adsorption to ferrihydrite: application of a surface complexation model. *Geochim. Cosmochim. Acta* 58, 5465-5478. 10.1016/0016-7037(94)90243-7.
- Wall, J.D., Krumholz, L., 2006. Uranium reduction. *Annu. Rev. Microbiol.* 60, 149-166.
- Wan, J., Tokunaga, T.K., Brodie, E., Wang, Z., Zheng, Z., Herman, D., Hazen, T.C., Firestone, M.K., Sutton, S.R., 2005. Reoxidation of bioreduced uranium under reducing conditions. *Environ. Sci. Technol.* 39, 6162-6169.
- Wan, J., Tokunaga, T.K., Kim, Y., Brodie, E., Daly, R., Hazen, T.C., Firestone, M.K., 2008. Effects of organic carbon supply rates on uranium mobility in a previously bioreduced contaminated sediment. *Environ. Sci. Technol.* 42, 7573-7579.
- Wang, Z.M., Lee, S.-W.W., Kapoor, P., Tebo, B.M., Giammar, D.E., 2013. Uraninite oxidation and dissolution induced by manganese oxide: a redox reaction between two insoluble minerals. *Geochim. Cosmochim. Acta* 100, 24-40.
- Watson, D.B., Wu, W.M., Mehlhorn, T., Tang, G.P., Earles, J., Lowe, K., Gihring, T.M., Zhang, G.X., Phillips, J., Boyanov, M.I., Spalding, B.P., Schadt, C., Kemner, K.M., Criddle, C.S., Jardine, P.M., Brooks, S.C., 2013. In situ bioremediation of uranium with emulsified vegetable oil as the electron donor. *Environ. Sci. Technol.* 47, 6440–6448.
- Weber, M., Schünemann, W., Fuß, J., Kämpfer, P., Lipski, A., 2018. *Stenotrophomonas lactitubi* sp. nov. and *Stenotrophomonas indicatrix* sp. nov., isolated from surfaces with food contact. *Int. J. Syst. Evol. Microbiol.* 68, 1830–1838.
- Wiegand, I., Hilpert, K., Hancock, R., 2008. Agar and broth dilution methods to determine the minimal inhibitory concentration (MIC) of antimicrobial substances. *Nat. Protoc.* 3, 163–175.
- Wu, W.-M., Carley, J., Gentry, T., Ginder-Vogel, M.A., Fienen, M., Mehlhorn, T., Yan, H.,

- Carroll S., Pace, M.N., Nyman, J., Luo, J., Gentile, M.E., Fields, M.W., Hickey, R.F., Gu, B., Watson, D., Cirpka, O.A., Zhou, J., Fendorf, S., Kitanidis, P.K., Jardine, P.M., Criddle, C.S., 2006. Pilot-scale in situ bioremediation of uranium in a highly contaminated aquifer. 2. Reduction of U(VI) and geochemical control of U(VI) bioavailability. *Environ. Sci. Technol.* 40, 3986-3995.
- Wu, W.- M., Carley, J., Luo, J., Ginder-Vogel, M.A., Cardenas, E., Leigh, M.B., Hwang, C., Kelly, S.D., Ruan, C., Wu, L., Van Nostrand, J., Gentry, T., Lowe, K., Mehlhorn, T., Carroll, S., Luo, W., Fields, M.W., Gu, B., Watson, D., Kemner, K.M., Marsh, T., Tiedje, J., Zhou, J., Fendorf, S., Kitanidis, P.K., Jardine, P.M., Criddle, C.S., 2007. In situ bioreduction of uranium (VI) to submicromolar levels and reoxidation by dissolved oxygen. *Environ. Sci. Technol.* 41, 5716-5723.
- Wu, W.M., Carley, J., Green, S.J., Luo, J., Kelly, S.D., van Nostrand, J., Lowe, K., Mehlhorn, T., Carroll, S., Boonchayanant, B., Löffler, F.E., Watson, D., Kemner, K.M., Zhou, J., Kitanidis, P.K., Kostka, J.E., Jardine, P.M., Criddle, C.S., 2010. Effects of nitrate on the stability of uranium in a bioreduced region of the subsurface. *Environ. Sci. Technol.* 44, 5104-5111.
- Xie, J.C., Lin, J.F., Zhou, X.H., 2018. pH-dependent microbial reduction of uranium(VI) in carbonate-free: UV-vis, XPS, TEM, and thermodynamic studies. *Environ. Sci. Pollut. Res.* 10.1007/s11356-018-2326-2.
- Xu, A.G., Chao, L., Xiao, H.B., Sui, Y.Y., Liu, J., Xie, Q.J., Yao, S.Z., 2018. Ultrasensitive electrochemical sensing of Hg<sup>2+</sup> based on thymine-Hg<sup>2+</sup>-thymine interaction and signal amplification of alkaline phosphatase catalyzed silver deposition. *Biosens. Bioelectron.* 104, 95-101.
- Yong, P., Macaskie, L.E., 1995. Enhancement of uranium bioaccumulation by a *Citrobacter* sp. via enzymically-mediated growth of polycrystalline NH<sub>4</sub>UO<sub>2</sub>PO<sub>4</sub>. *J. Chem. Technol. Biotechnol.* 63, 101-108.
- Zhang, J., Song, H., Chen, Z., Liu, S., Wei, Y., Huang, J., Guo, C., Dang, Z., Lin, Z., 2018. Biomineralization mechanism of U(VI) induced by *Bacillus cereus* 12-2: The role of functional groups and enzymes. *Chemosphere* 206, 682-692.

## Supplementary data

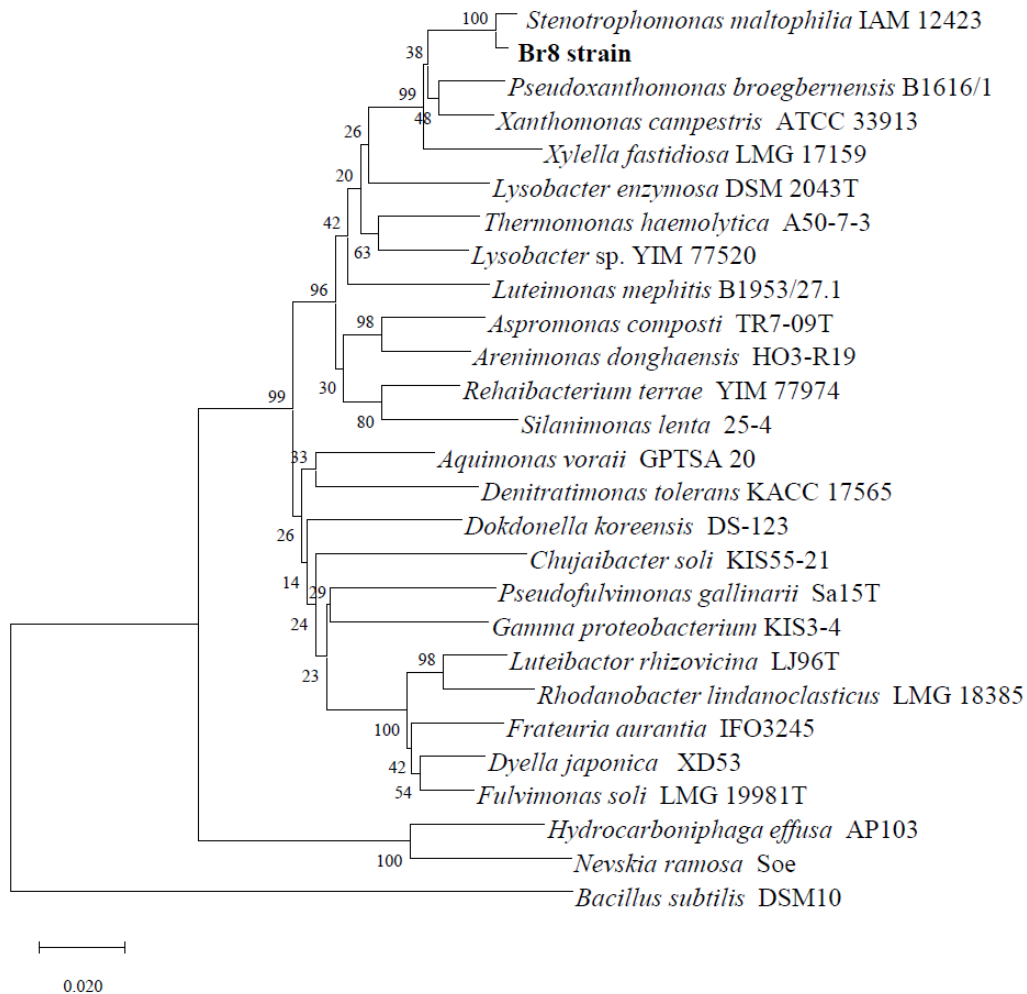


**Figure Supplementary 1.** Phylogenetic dendrogram obtained by neighbor-joining clustering of 16S rRNA gene sequences, showing the position of strain Br8 among the type strains of recognised genera within *Xanthomonadaceae* family. *Bacillus subtilis* DSM10 was used as the outgroup. Bootstrap values (expressed as percentages of 1000 replications) are shown at branch points. Bar 0.020 substitutions per nucleotide position.

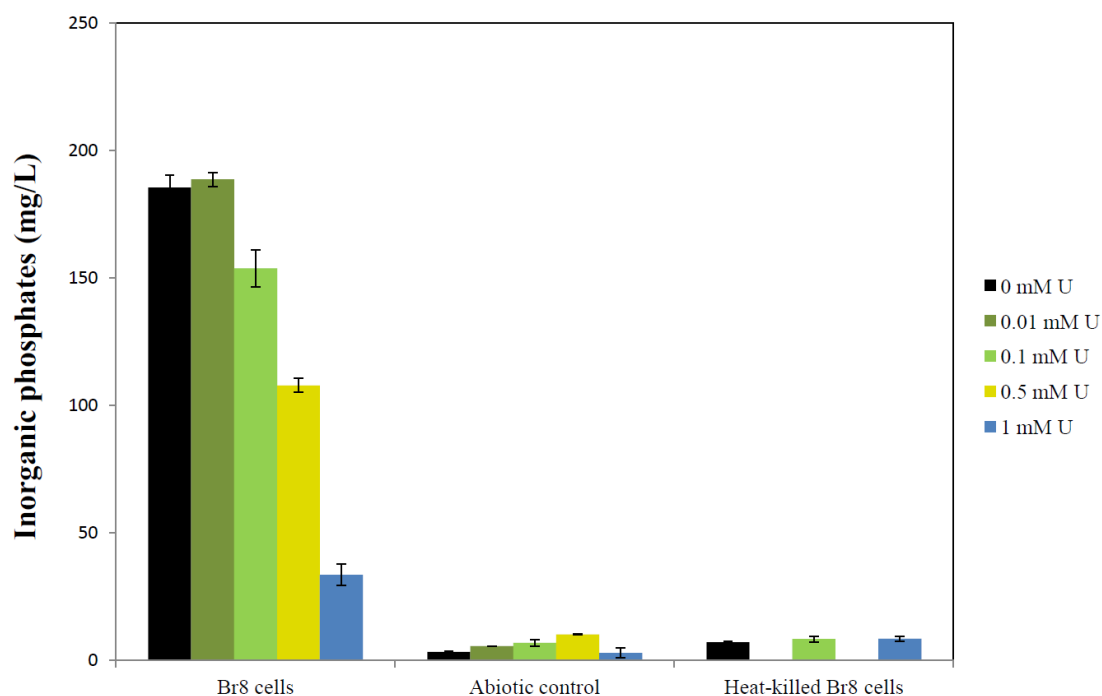


**Figure Supplementary 2.** Inorganic phosphates in solution (mg/L) detected after incubation (48h; 28°C; 165 rpm) of MOPS-buffered (20 mM) distilled water (pH 6.3) amended with G2P (5 mM) and various U concentrations (0, 0.01, 0.1, 0.5 and 1 mM) in presence of *Stenotrophomonas* sp. Br8 cells (0.5 mg dry biomass per ml of medium, equivalent OD600nm  $\approx$  0.5). Flasks without cells and including heat-killed bacterial cells were used as control treatments. The data are showed as the mean  $\pm$  SD of at least three independent measurements.

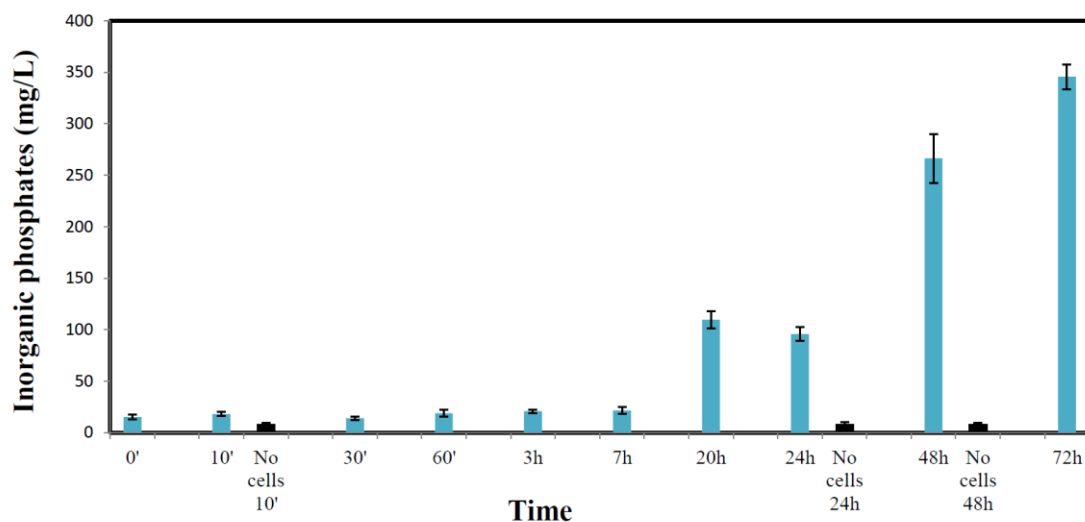


**Figure Supplementary 3.** Inorganic phosphates in solution (mg/L) kinetics detected during incubation (72 h; 28°C; 165 rpm) of MOPS-buffered (20 mM) distilled water (pH 6.3) amended with G2P (5 mM) and U (0.5 mM) in presence of *Stenotrophomonas* sp. Br8 cells (0.5 mg dry biomass per ml of medium, equivalent OD600nm  $\approx$  0.5). Flasks without cells were used as control treatment. The data are showed as the mean  $\pm$  SD of at least three independent measurements.

## CAPÍTULO IV

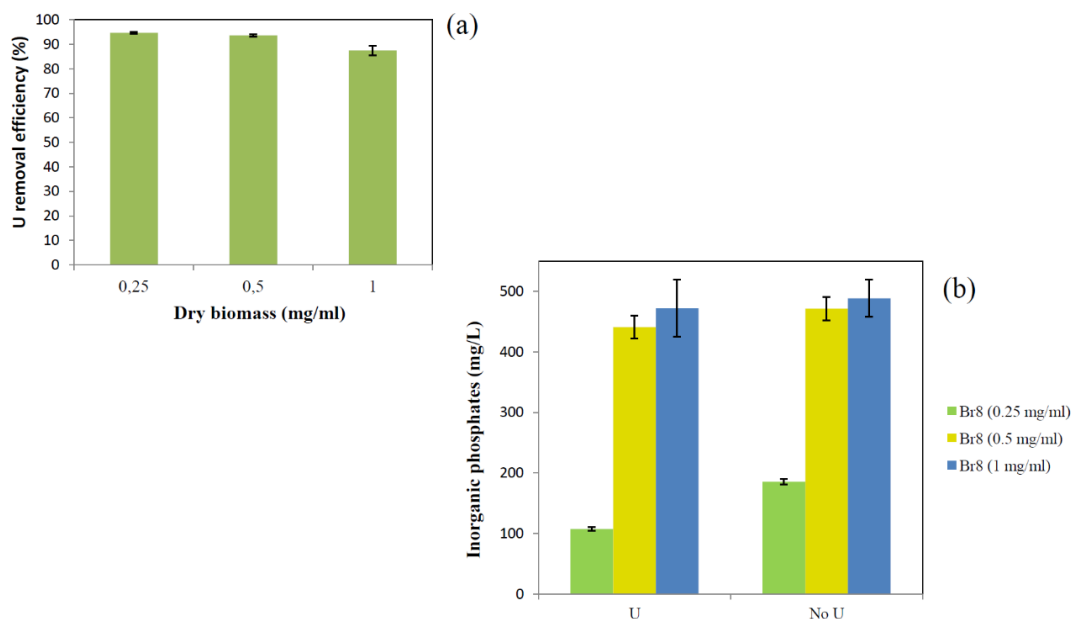


**Figure Supplementary 4.** Uranium removal efficiency (%) (a) and inorganic phosphates in solution (mg/L) (b) after incubation (48 h; 28°C; 165 rpm) of MOPS-buffered (20 mM) distilled water (pH 6.3) amended with G2P (5 mM) and U (0.5 mM) in presence of *Stenotrophomonas* sp. Br8 cells at different concentrations (0.25, 0.5 and 1 mg dry biomass per ml of medium). Flasks without U were used as control treatment for inorganic phosphates measurements. The data are showed as the mean  $\pm$  SD of at least three independent measurements.

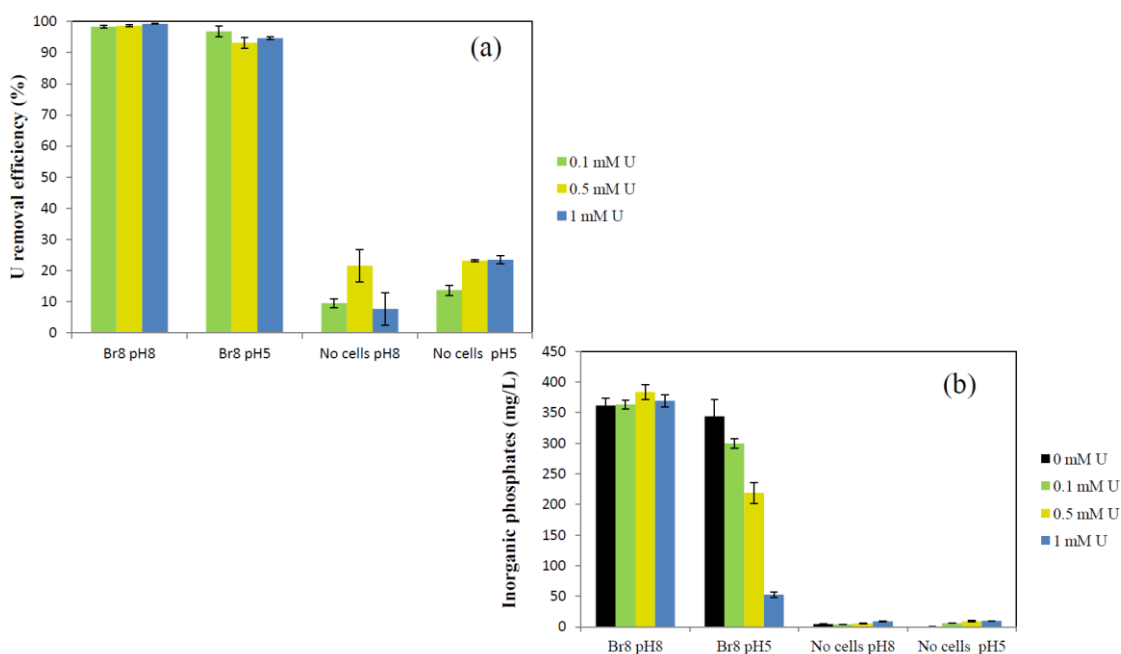


**Figure Supplementary 5.** Uranium removal efficiency (%) (a) and inorganic phosphates in solution (mg/L) (b) after incubation (48 h; 28°C; 165 rpm) of MOPS-buffered (20 mM) distilled water (pH 5 and pH 8) amended with G2P (5 mM) and various U concentrations (0, 0.1, 0.5 and 1 mM) in presence of *Stenotrophomonas* sp. Br8 cells (0.5 mg dry biomass per ml of medium, equivalent OD600nm  $\approx$ 0.5). Flasks without bacterial cells were used as control treatment. The data are showed as the mean  $\pm$  SD of at least three independent measurements.

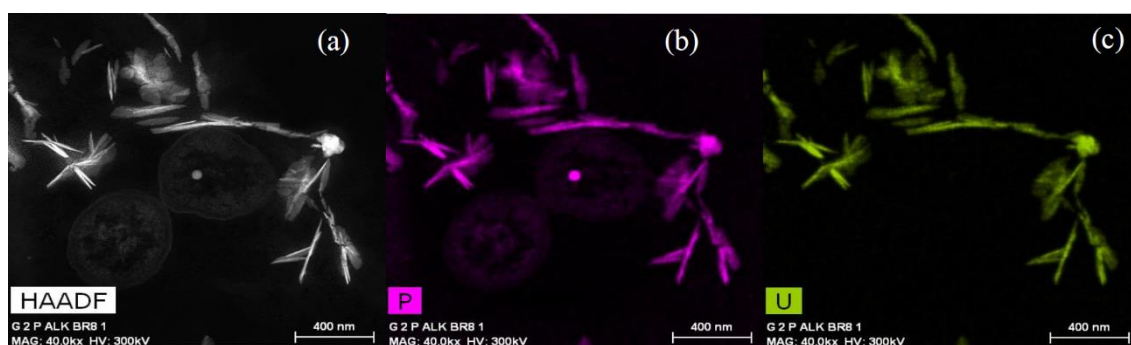


**Figure Supplementary 6.** HAADF-STEM micrograph (a) of a thin section showing U precipitates around Br8 cells recovered after their incubation (48h; 28°C; 165 rpm) in MOPS-buffered (20 mM) distilled water (pH 8) amended with G2P (5 mM) and U (1 mM). EDX element-distribution maps for P (b) and U (c) indicated that precipitates observed are mainly composed of P and U.

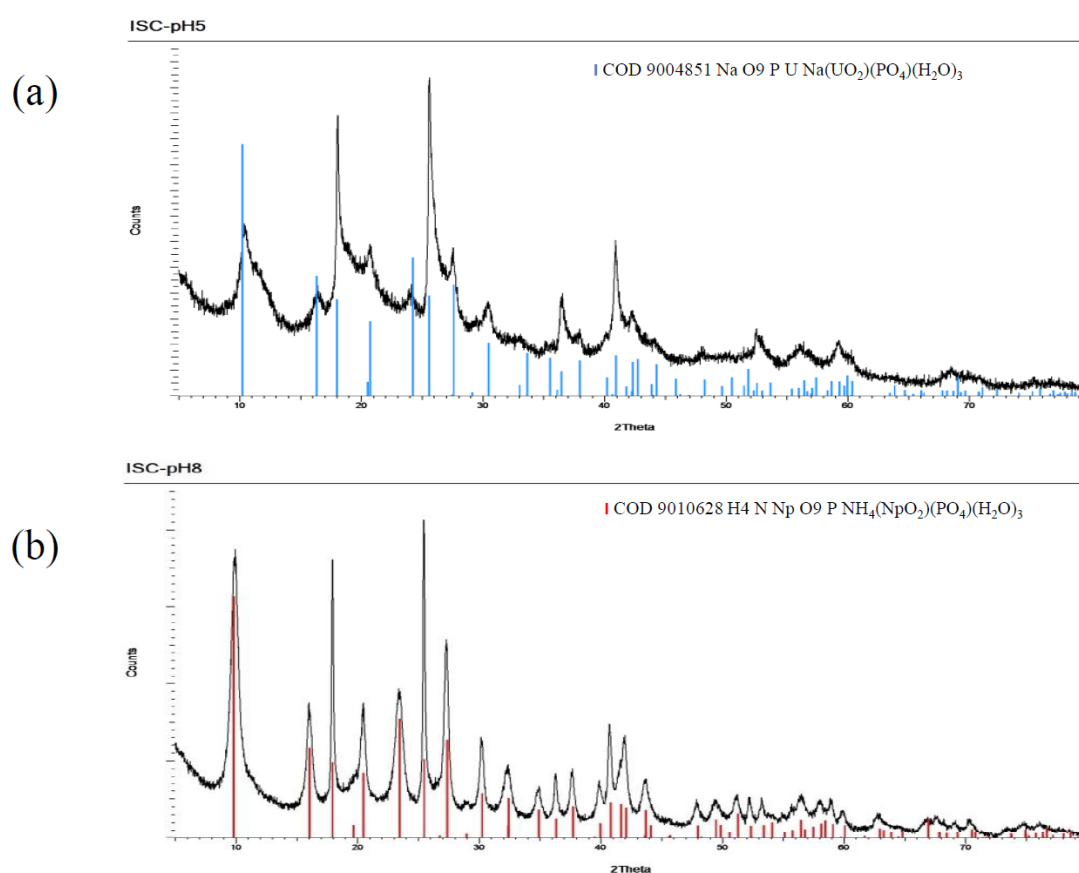


**Figure Supplementary 7.** XRD pattern of precipitates recovered after *Stenotrophomonas* sp. Br8 cells incubation (48h; 28°C; 165 rpm) in MOPS-buffered (20 mM) distilled water at pH 5 (a) and pH 8 (b) amended with G2P (5 mM) and U (1 mM).



## CAPÍTULO IV

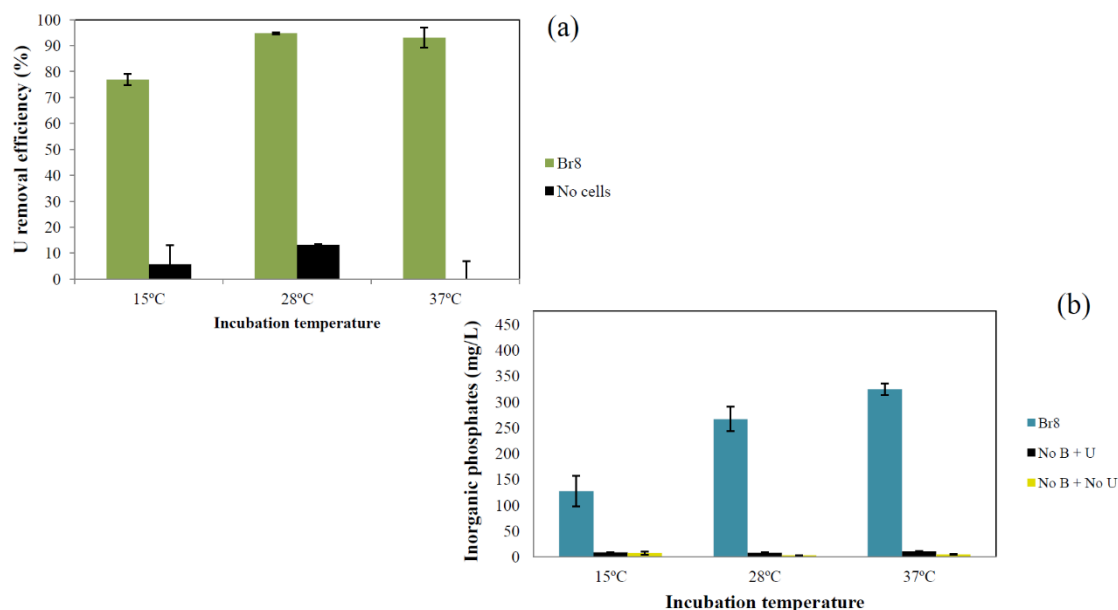


**Figure Supplementary 8.** Uranium removal efficiency (%) (a) and inorganic phosphates in solution (mg/L) (b) after incubation (48 h; 15°C, 28°C and 37°C; 165 rpm) of MOPS-buffered (20 mM) distilled water (pH 6.3) amended with G2P (5 mM) and U (0.5 mM) in presence of *Stenotrophomonas* sp. Br8 cells (0.5 mg dry biomass per ml of medium, equivalent OD600nm  $\approx$ 0.5). Flasks without bacterial cells and without U were used as control treatments. The data are showed as the mean  $\pm$  SD of at least three independent measurements.

**Table Supplementary 1.** Uranium speciation obtained under all different experimental conditions used in the present study.

Component	Species name	pH 6.3						pH 5			pH 8		
		0.01 mM	0.1 mM	0.5 mM	1 mM	0.5 mM	0.5 mM	0.1 mM	0.5 mM	1 mM	0.1 mM	0.5 mM	1 mM
		28°C						28°C			28°C		
		% of total concentration											
UO <sub>2</sub> <sup>2+</sup>	UO <sub>2</sub> <sup>2+</sup>	0.847	0.184	0.062	0.038	0.079	0.046	20.626	7.996	5.205	-	-	-
	UO <sub>2</sub> OH <sup>+</sup>	8.38	1.814	0.604	0.375	0.359	0.737	10.881	4.174	2.685	0.116	0.038	0.023
	(UO <sub>2</sub> ) <sub>2</sub> (OH) <sub>2</sub> <sup>2+</sup>	1.067	0.501	0.279	0.216	0.238	0.236	17.262	12.79	10.667	-	-	-
	(UO <sub>2</sub> ) <sub>3</sub> (OH) <sup>5+</sup>	79.668	80.79	74.317	70.497	28.675	91.084	45.646	63.948	67.542	48.579	41.813	38.421
	(UO <sub>2</sub> ) <sub>4</sub> (OH) <sup>7+</sup>	7.252	15.915	24.328	28.544	70.513	7.11	2.76	7.39	10.001	29.36	41.089	46.222
	(UO <sub>2</sub> ) <sub>3</sub> (OH) <sup>7-</sup>	0.012	0.012	0.011	0.011	-	0.064	2.459	-	-	18.525	15.945	14.65
	(UO <sub>2</sub> ) <sub>3</sub> (OH) <sub>4</sub> <sup>2+</sup>	0.229	0.232	0.215	0.206	0.103	0.229	0.195	3.482	3.721	-	-	-
	UO <sub>2</sub> (OH) <sup>3-</sup>	0.051	0.011	-	-	-	0.015	-	-	-	1.763	0.574	0.352
	UO <sub>2</sub> (OH) <sub>2</sub> (aq)	2.494	0.54	0.179	0.111	0.032	0.478	0.166	0.063	0.041	1.651	0.537	0.329
	(UO <sub>2</sub> ) <sub>2</sub> OH <sup>3+</sup>	-	-	-	-	-	-	-	0.147	0.125	-	-	-
	UO <sub>2</sub> NO <sup>3+</sup>	-	-	-	-	-	-	-	0.011	0.014	-	-	-
NO <sub>3</sub> <sup>1-</sup>	NO <sub>3</sub> <sup>1-</sup>	99.885	99.885	99.886	99.886	99.885	99.886	99.877	99.876	99.875	99.895	99.895	99.895
	NaNO <sub>3</sub> (aq)	0.115	0.115	0.114	0.114	0.115	0.114	0.12	0.119	0.118	0.105	0.105	0.105
MOPS	MOPS <sup>1-</sup>	13.594	13.6	13.628	13.661	9.737	16.779	0.766	0.769	0.772	89.196	89.209	89.225
	H <sup>+</sup> MOPS (aq)	86.406	86.4	86.372	86.339	90.263	83.221	99.234	99.231	99.228	10.804	10.791	10.775
Gly-2-phosphate	GlyPhos-2	36.998	37.034	37.19	37.379	38.247	36.556	2.692	2.72	2.752	97.101	97.112	97.124
	H-GlyPhos-	63.002	62.966	62.809	62.621	61.752	63.443	97.3	97.272	97.241	2.899	2.888	2.876
Na <sup>1+</sup>	Na <sup>1+</sup>	100	99.995	99.977	99.955	99.977	99.977	99.995	99.976	99.953	99.996	99.979	99.958
	NaNO <sub>3</sub> (aq)	-	-	0.023	0.045	0.023	0.023	-	0.024	0.047	-	0.021	0.042

aq, aqueous.

## CAPÍTULO V:

### **Uranium removal from complex mining waters by alginate beads doped with cells of *Stenotrophomonas* sp. Br8: novel perspectives for metal bioremediation**

Iván Sánchez-Castro<sup>1\*</sup>, Pablo Martínez-Rodríguez<sup>1\*</sup>, María M. Abad<sup>2</sup>, Michael Descostes<sup>3,4</sup>,  
Mohamed Larbi Merroun<sup>1</sup>

<sup>1</sup> Department of Microbiology, University of Granada, Campus Fuentenueva s/n, 18071 Granada, Spain.

<sup>2</sup> Centro de Instrumentación Científica (CIC), University of Granada, Campus Fuentenueva, Granada, Spain.

<sup>3</sup> ORANO Mining, Environmental R&D Department, 125 Avenue de Paris, 92330, Châtillon, France.

<sup>4</sup> PSL University/Mines ParisTech, Centre de Géosciences, 35 rue Saint-Honoré, 77305, Fontainebleau, France.

\*These authors contributed equally.

Este capítulo ha sido publicado en la revista Journal of Environmental Management:

Sánchez-Castro, I., Martínez-Rodríguez, P., Abad, M.M., Descostes, M., Merroun, M.L., 2021. Uranium removal from complex mining waters by alginate beads doped with cells of *Stenotrophomonas* sp. Br8: Novel perspectives for metal bioremediation. J. Environ. Manage. 296, 1–10. <https://doi.org/10.1016/j.jenvman.2021.113411>



**Abstract**

Uranium-containing effluents generated by nuclear energy industry must be efficiently remediated before release to the environment. Currently, numerous microbial-based strategies are being developed for this purpose. In particular, the bacterial strain *Stenotrophomonas* sp. Br8, isolated from U mill tailings porewaters, has been already shown to efficiently precipitate U(VI) as stable U phosphates mediated by phosphatase activity. However, the upscaling of this strategy should overcome some constraints regarding cell exposure to harsh environmental conditions. In the present study, the immobilization of Br8 biomass in an inorganic matrix was optimized to provide protection to the cells as well as to make the process more convenient for real-scale utilization. The use of biocompatible, highly porous alginate beads for Br8 cells immobilization resulted the best alternative when investigating by a multidisciplinary approach (High-Angle Annular Dark-Field Scanning Transmission Electron Microscopy (HAADF-STEM), Environmental Scanning Electron Microscopy (ESEM), Fourier Transform Infrared Spectroscopy with Attenuated Total Reflectance, etc.) several consolidated entrapment methods. This biomaterial was applied to complex real U mining porewaters (containing 47 mg/L U) in presence of an organic phosphate source (glycerol-2-phosphate) to produce reactive free orthophosphates through Br8 phosphatase activity. Uranium immobilization rates around 98% were observed after one cycle of 72 h. In terms of U removal ability as a function of biomass, Br8-doped alginate beads were determined to remove up to 1199.5 mg U/g dry biomass over two treatment cycles. Additionally, optimized conditions for storing Br8-doped beads and for a correct application were assessed. Results for U accumulation kinetics and HAADF-STEM/ESEM analyses revealed that U removal by the immobilized cells is a biphasic process combining a first passive U sorption onto bead and/or cell surfaces and a second slow active biomineralization. This work provides new practical insights into the biological and physico-chemical parameters governing a high-efficient U bioremediation process based on the phosphatase activity of immobilized bacterial cells when applied to complex mining waters under laboratory conditions.

**Keywords:** Mining waters; Bioremediation; Biomineralization; Uranium; Bacteria immobilization; Alginate beads

## Introduction

Uranium (U) mining as well as nuclear plants/reactors generate a large volume of hazardous wastewaters containing U and other heavy metals. To prevent potential contamination of nearby water bodies with highly soluble U compounds and subsequent U introduction into the trophic chain, these effluents must be efficiently treated. Conventional physicochemical-based methodologies for processing heavy metals polluted wastewaters are known to be inherently costly at economical and environmental level, as well as inefficient at low heavy metals concentrations (Birungi and Chirwa, 2015; Jaafari and Yaghmaeian, 2019). In contrast, biological technologies emerge as an attractive approach for metal remediation mainly due to its low environmental impact and high efficiency at rather low heavy metals concentration (Das and Osborne, 2018). Numerous recent studies exhibited the great prospects of applying selected microbes to decontaminate heavy metals polluted waters through different interaction mechanisms (reviewed in Soni et al., 2019). In the case of U, main processes reported to be involved in microbial-based bioremediation strategies are biosorption (Acharya et al., 2009; Akhtar et al., 2009), bioprecipitation (Martinez et al., 2007; Nedelkova et al., 2007; Choudhary and Sar, 2011; Merroun et al., 2011; Pinel et al., 2021) and enzymatic reduction (Lovley and Phillips, 1992; Williams et al., 2013). Recently, it was demonstrated the ability of the bacterial strain *Stenotrophomonas* sp. Br8 to precipitate U(VI) as long-term stable U phosphates mediated by inorganic phosphates which are generated via phosphatase enzymes under different environmental conditions relevant for U contaminated waters (pH, temperature, etc.) (Sánchez-Castro et al., 2020). This microbial-driven U immobilization procedure is considered particularly attractive (Benzerara et al., 2011) in comparison with other extensively reported biological methods like the bioreduction of U(VI) to U(IV) showing stability issues of the resulting compounds (e.g. Bargar et al., 2008).

In order to make this Br8-based U(VI) biomineralization process (Sánchez-Castro et al., 2020) applicable at field scale, several issues like cell exposure to harsh environmental conditions (Prabhakaran et al., 2016) or potential up-scaling drawbacks should be overcome. In addition, the use of cells in planktonic state may result in microbial activity reduction because of cell washout in continuously operated reactors (Baskaran and Nemati, 2006). In this sense, the immobilization of microorganisms is a procedure known to provide a series of advantages in different biotechnological applications such as bio-fuel production or wastewaters purification (Ranganathan et al., 2008; Covarrubias et al., 2012). The micro-

environments created within these immobilization matrices can improve the preservation of cell integrity under limiting conditions as well as provide specific properties to microbes (Bouabidi et al., 2019). Many other practical reasons such as easy transportation and handling, the possibility to use it repeatedly and easy separation/recuperation of cells and elements accumulated in the matrix (Dianawati et al., 2016; Shi et al., 2018) make this alternative more efficient at multiple levels (e.g. operational, economical), and thus, convenient for real-scale application.

A great variety of biomass immobilization technologies have been proposed in the last decades (Dzionek et al., 2016). Those based on the immobilization of microbial biomass in the supporting material through the use of different chemical agents are the most commonly used (Bouabidi et al., 2019). In this way, methods such as adsorption (including ionic and covalent binding to a solid support), cell cross-linking to obtain the formation of stable cellular aggregates and mainly, biomass entrapment in a polymeric matrix have been already tested with satisfactory results (Bouabidi et al., 2019). In relation to this last method, different natural (mainly isolated from algae such as agar, chitosan, carrageenan, cellulose or alginate salt) and synthetic polymers (e.g. polyacrylamide, poly(carbamoyl) sulphonate, silica, polyethylene glycol, polyurethane or polyvinyl alcohol) showing specific features are proposed depending on the nature of the biomass to be immobilized (Wang et al., 2010; Kumari et al., 2017; Kiran et al., 2018). To enhance the effectiveness of the immobilization process for a particular biotic agent, and therefore the application performance of the immobilized-biomass system, an optimization process by assessing supporting materials with different characteristics seems essential. Some desirable features to apply this type of biomaterials in water treatment are hydrophilicity, inertness towards any kind of external bioactivity, biocompatibility, resistance to biotic and abiotic harmful agents and low production costs (Brodelius and Mosbach, 1987).

The main aim of the present work is to optimize a suitable U immobilization procedure based in the use of *Stenotrophomonas* sp. Br8, a strain isolated from U-mining porewaters, which in planktonic form efficiently precipitates soluble species of U(VI) in chemically stable U-phosphate mineral phases with a structure similar to that of meta-autunite (Sánchez-Castro et al., 2020). For this purpose, several immobilization strategies were tested and final products were characterized at multiple levels (matrix physico-chemical properties, cells distribution and viability, etc.). Biomass immobilized under optimized conditions was applied to perform batch-scale experiments for U removal from mining

porewaters containing glycerol-2-phosphate (G2P; source of organic phosphates) amended to produce reactive free orthophosphates through Br8 phosphatase activity. So far, few works have demonstrated the applicability of immobilized bacteria to successfully treat real complex U-containing mining porewaters. The present study is essential to determine optimal application conditions to scale-up the proposed low-cost removal process. Moreover, this type of studies is clearly necessary as a preliminary step towards the field application of innovative technologies for heavy metals bioremediation.

## **Materials and methods**

Experimental procedures related to the study of the effect of incubation time/biomass concentration/biomaterial storage as well as microscopic analyses (HAADF-STEM/EDAX and ESEM) are provided as Supplementary Material.

### ***Bacterial strain Br8 and optimization of a biomass immobilization procedure***

The bacterial strain *Stenotrophomonas* sp. Br8 was isolated from U mill tailings porewaters in the vicinity of former mining sites in France (Sánchez-Castro et al., 2017). This strain showed great U removal potential as planktonic cells under different conditions (Sánchez-Castro et al., 2020). Cells of this bacterial isolate were employed to assess and enhance previously described biomass immobilization procedures for the decontamination of U polluted waters.

*Stenotrophomonas* sp. Br8 cells were grown in LB broth (casein peptone 10 g/L, yeast extract 5 g/L, pH 7.2; Scharlau Chemie, SA) at 28°C under shaking at 160 rpm for 24 h. Subsequently, mid-exponential growth phase cells were recovered by centrifugation (10,000 x g for 5 min at 4°C) and washed twice with 0.9% NaCl solution. Afterwards, the washed biomass was immobilized similarly as indicated in the different reference protocols considered (stated below), but using always the same biomass concentration ( $\sim 1.5 \cdot 10^7$  CFU/g biomaterial) to make comparable at biotic level all biomaterials generated. Well-established entrapment methods were used as baseline to optimize Br8 cells immobilization. Firstly, the Na-alginate entrapment technique by Smidsrod and Skjak-Braek (1990) is based on the formation of beads by dripping through a syringe a mixture of cells and an aqueous solution of Na<sup>+</sup> alginate into a solution containing Ca<sup>2+</sup> ions. The

second method used as reference produces sol–gel ceramics by gelling and drying a mixture of biomass and aqueous silica nanosols composed of tetraethyl orthosilicate (Raff et al., 2003; Soltmann et al., 2003). And finally, alternative approaches combining both methodologies stated above were also considered to develop this work (Pannier et al., 2014; Perullini et al., 2014).

Resulting Br8-doped biomaterials (biocer, beads, etc.) were investigated at multiple levels using a multidisciplinary approach combining microscopy, spectroscopy, etc. Thus, external and internal morphology and cell distribution within the matrix were characterized using environmental scanning electron microscopy (ESEM, model FEI Quanta 650 FEG, Thermofisher-FEI) analysis as described below. Presence and identification of major types of functional groups at surface level were determined by Fourier Transform Infrared Spectroscopy with Attenuated Total Reflectance (FTIR-ATR). The analyses were performed with a Jasco 6200 spectrometer, with a total of 32 scans per measure and a resolution of  $0.25\text{ cm}^{-1}$  in the mid-infrared region ( $4000\text{--}400\text{ cm}^{-1}$ ). Abiotic matrices corresponding to each method applied were prepared for comparison and for the evaluation of the effect of biomass in the immobilization support at structural level (mechanical stability, porosity, etc.).

### ***Chemical characterization and U speciation in the studied mining water***

Real U mining porewaters, under the monitoring of ORANO Mining, were used as incubation medium in all cases. Geochemical characterization and aqueous uranium speciation in this mining water, named COMI\_79, was already given in Reiller and Descostes (2020). Uranium concentration was estimated in 47.4 mg/L and U(VI) was mainly found under  $\text{Ca}_n\text{UO}_2(\text{CO}_3)_3^{4-2n}$  aqueous species. pH of the mining water was 7.75. Porewater samples received were analyzed in our laboratory and characteristics previously reported were confirmed (data not shown). This mine water was chosen as its composition is characteristic of U mining context, that is to say high U content and relatively high ionic strength.

### ***Uranium removal batch experiments***

Batch U removal experiments applying the previously optimized *Stenotrophomonas* sp. Br8-doped biomaterial were performed using 100 mL acid-washed glass Erlenmeyer flasks filled with 25 mL of non-filtered COMI\_79 mining water as incubation medium. G2P (Sigma Aldrich) was selected as phosphate source (5 mM). Flasks including: a) cell-free beads; b) cell-free G2P-containing system; or c) phosphate-free system, were assayed as controls to validate the results obtained. To distinguish between the role of the bacterial strain Br8 and that of naturally occurring microbes in the mining water used as incubation medium, 0.22  $\mu\text{m}$  filter-sterilized COMI\_79 mining water was also evaluated. Moreover, to investigate the potential reusability of the biomaterial for U removal, two 48-h-incubation cycles were assayed by using the same biomaterial but changing mining water solution between both cycles. Incubation was conducted at 28°C for 48-72 h and under continuous shaking (165 rpm) in all cases.

After incubation, 5-mL aliquots of the mining water used as incubation solution from all replicates were centrifuged at 10000 g for 10 min at 4°C, and supernatants were stored for further analysis. Recovered biomaterials were washed twice with 0.9% NaCl to remove the interfering elements of the incubating solution before analyzing. Uranium removal efficiency was evaluated by estimating the precipitation of dissolved U(VI) under defined experimental conditions. Chemical composition variations in the incubation mining water solution were determined through ICP-MS.

All treatments were conducted in triplicate and all subsequent analyses utilized all replicates data for statistical analysis.

### ***Multilevel batch experiments evaluation***

#### ***Determination of inorganic phosphates ( $P_i$ ) released***

The IP concentration in solution after the incubation period was determined by means of the “ammonium-molybdate method” (Murphy and Riley, 1962). This technique is based in the reaction of the orthophosphate ions with ammonium-molybdate in acidic solution forming phosphomolybdic acid. Upon reduction with ascorbic acid, this compound produces a blue complex whose intensity is quantified spectrophotometrically at 850 nm.



### *Quantification of uranium removal ratio*

Concentration of U(VI) in solution was determined spectrophotometrically by using the Arsenazo III method (Jauberty et al., 2013). In brief, 1 mL of a disodium salt of 2,7-bis(2-arsenophenylazo)-1,8-dihydroxynaphthalene-3,6-disulfonic acid (also called Arsenazo-III) solution was mixed with 250  $\mu$ L of supernatant and absorbance was measured at 651 nm after 30 s incubation. Reagent was prepared by dissolving 70 mg of Arsenazo-III into 1 l of 3 M HClO<sub>4</sub>. Uranium concentrations were determined by comparison with a scale of uranyl nitrate accounting for 1–15 mg/L. The percentage of U removed from solution was calculated by the difference between the initial and final U concentrations.

### *Recovered biomaterial evaluation*

Mechanical stability of the beads was assessed taking into account the morphology intactness using optical microscope and scanning transmission electron microscope (STEM) as described below. Viability of the immobilized biomass after incubations was evaluated by grinding surface-sterilized biomaterial and culturing it in LB plates for 48-72 h at 28 °C.

### *Statistical analysis*

Data in this manuscript are presented as averages and standard deviations (SD) for at least three independent replicates per experimental condition tested. Analyses of variance (ANOVA) were performed together with the post hoc Tukey's test to detect significant differences among all treatment means. Significant differences ( $p < 0.05$ ) among treatments after ANOVA and Tuckey's test ( $n = 3$ ) were represented by different letters. All statistical analyses and data visualization were done using GraphPad Prism 8.0.2 (GraphPad Software, San Diego, California USA) and R Project software (R Core Team, 2020).

## Results

### *Selection and optimization of the biomass immobilization method*

Methods based on the use of tetraethyl orthosilicate (Raff et al., 2003; Soltmann et al., 2003) and Na-alginate (Smidsrod and Skjak-Braek, 1990) as inorganic supports, as well as modified versions of other enhanced approaches (Pannier et al., 2014; Perullini et al., 2014), were implemented with Br8 cells. Multiple parameters like mechanical and chemical stability, identity of functional groups at surface level, biocompatibility, and external/internal morphology (e.g. porosity, cell distribution) were evaluated in comparison with control abiotic immobilization matrices. Taking into account these results (illustrated in Table S1 and Figs. S1-S7 of the Supporting Information (SI)), an optimized immobilization procedure, based on that described by Smidsrod and Skjak-Braek (1990) using Na-alginate as inorganic support, was developed. Modifications of the original protocol, aimed to enhance long-term stability of the biomaterial produced, which in turn would lead to decrease the economic costs of the U removal process proposed. The main modifications were related to increase the concentration of the aqueous stock solution of Na-alginate (5% instead of 2-4%) and the mixing proportion of Na-alginate solution to concentrated washed-cells solution (4:1 instead 1:1) to achieve the desired cells dosage and a final alginate concentration of 4%. In addition, concentration of CaCl<sub>2</sub>-based solidifying solution (increased from 0.02-0.1 M to 0.3 M) and incubation time in this hardening solution (2-3 h instead 5-30 min) were modified in relation to the original method (Smidsrod and Skjak-Braek, 1990) as they yielded better stability.

### *Characterization of the biomass immobilization system*

The enhanced immobilization procedure resulted in the formation of beads with a size of about 1.5-2 mm as it is shown in Fig. 1. FTIR-ATR spectroscopy results (Fig. S1) are provided as Supplementary Material.

By microscopic observation (ESEM and HAADF-STEM), the structure of the inner section of the bead was shown to contain numerous macro- and micro-pores suggesting a good ratio surface/volume and high diffusion rates (Figs. S2-S7). In addition, cells entrapped within the beads were confirmed to be abundant and homogeneously distributed (Figs. S2-S7). Although the beads demonstrated very high mechanical stability since no relevant

alterations were observed through optical microscope after 120-days incubation in saline solution under agitation, a Na-citrate solution (50mM) dissolved them after 30-60 minutes. This fact is the main weakness of alginate beads since they are widely known to be chemically unstable in the presence of calcium chelators such as phosphate, lactate or citrate (Ching et al., 2017).

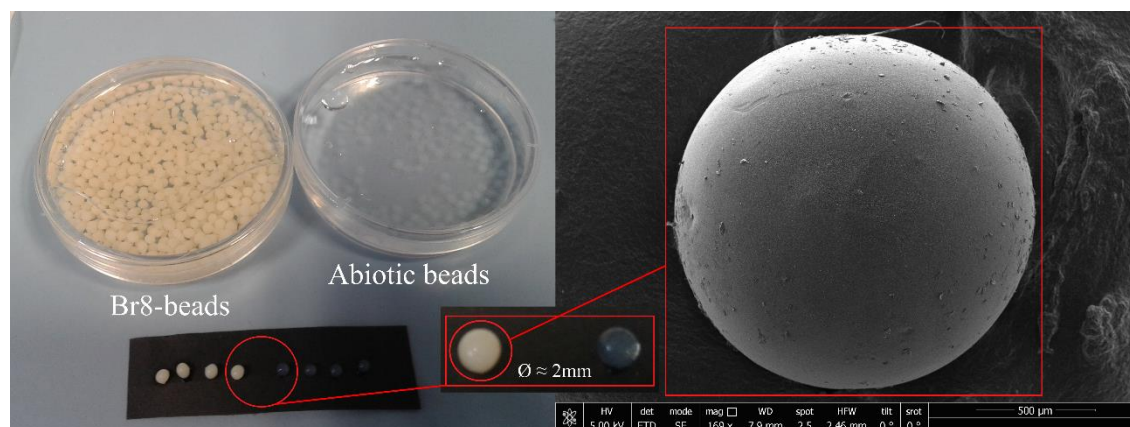


**Figure 1.** Alginate beads, with and without *Stenotrophomonas* sp. Br8 cells, generated with the enhanced method based in the protocol of Smidsrod and Skjak Braek (1990). Right micrograph was obtained with Environmental Scanning Electron Microscope FEI Quanta 400

### ***Batch studies of U removal using Br8 immobilized biomass***

The interaction mechanisms occurring when contacting Br8 immobilized cells with U-containing mining waters (COMI\_79) and optimal application conditions for U removal were investigated. A series of batch assays considering the effect of biomass-water contact time, biomass concentration and beads storage conditions were conducted. Additionally, resulting precipitates were characterized by HAADF-STEM and ESEM microscopic observations.

#### ***Contact time effect: kinetics study***

The immobilized cells obtained using the modified procedure described above were characterized for its potential in the removal of U from real mining waters. Br8-doped beads efficiency to precipitate solved U(VI) in presence of G2P increased gradually with longer contact times (from 0.08 h to 72 h), reaching a highest value of 97.8% at the end of the incubation (72 h) (Fig. 2a). Planktonic Br8 cells provoked the U immobilization in a shorter time, although the final removal rate is quite similar than that of the immobilized cells at

final incubation time (72 h; Fig. 2a). Release of inorganic phosphates resulted slower for the Br8-beads in comparison to planktonic cells (Fig. 2b). This fact is probably explained by the easier accessibility of Br8 phosphatases to the amended G2P in planktonic cells than in embedded ones.

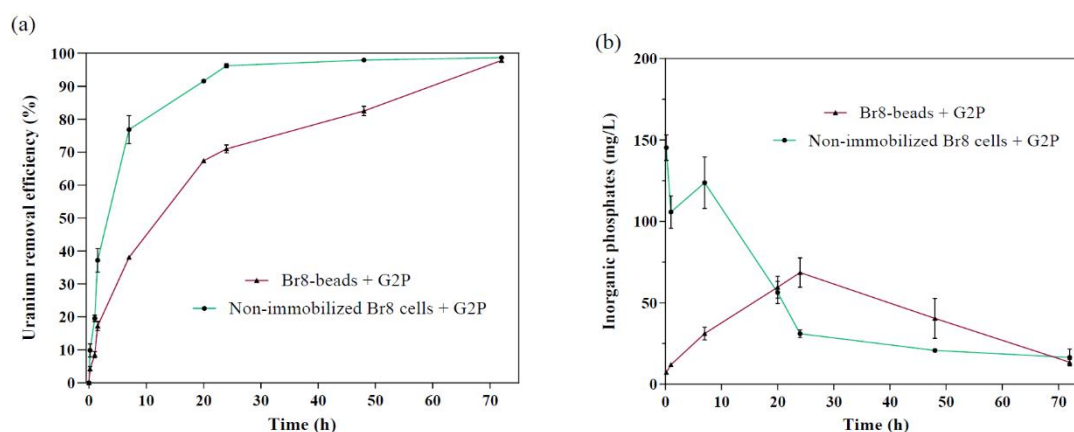


**Figure 2.** Uranium removal efficiency (%) kinetics (a) and inorganic phosphates in solution (mg/L) detected (b) during incubation (28°C; 165 rpm) of natural COMI\_79 mining water (initial U concentration 47.4 mg/L; pH 7.75; amended with 5 mM G2P) in presence of 4% Na-alginate beads doped with *Stenotrophomonas* sp. Br8 cells ( $\sim 1.5 \cdot 10^7$  CFU / g bead). Flasks with non-immobilized Br8 cells were used as control treatment. Data are showed as the mean  $\pm$ SD of at least three independent measurements. For some points, the error bars are shorter than the height of the symbol.

Control experiments confirmed the results presented above (Fig. 3). For instance, cell-free beads (abiotic control beads) in presence of G2P could remove less than 4% of the initial U concentration. Contrary to our results, some studies described a significant contribution of cell-free alginate beads in the removal of uranium from dilute aqueous solutions at different optimized conditions (Gok and Aytas, 2009; Kulkarni et al., 2013; Yu et al., 2017). In the case of exogenous phosphate-free treatments, no significant U removal was evidenced (Fig. 3). When using filter-sterilized COMI\_79 mining water no relevant changes were observed in comparison with non-filtered water, confirming that indigenous microbial populations inhabiting this mining water have no relevant role on the U removal process (Fig. 3).

The U removal ability of the immobilized Br8 cells over two treatment cycles was determined to be up to 1,199.5 mg U/g dry biomass (637.5 and 562 mgU/g dry biomass for the first and second cycle, respectively). Residual U concentration increased approximately 10% after the second treatment cycle, exhibiting a final removal rate of 87.4%. This data

clearly revealed that immobilized Br8 beads can be reused at least for two cycles achieving high U removal rates. Application of additional cycles with the same batch of beads would suppose a significant increase in the total U precipitation capacity of immobilized Br8 biomass, although our data suggested a decrease in removal efficiency after each cycle in agreement with recent surveys (e.g. Shi et al., 2018). Conversely, other studies reported no detrimental effects on heavy metals removal rates after multiple applications of the beads (Kiran et al., 2018).

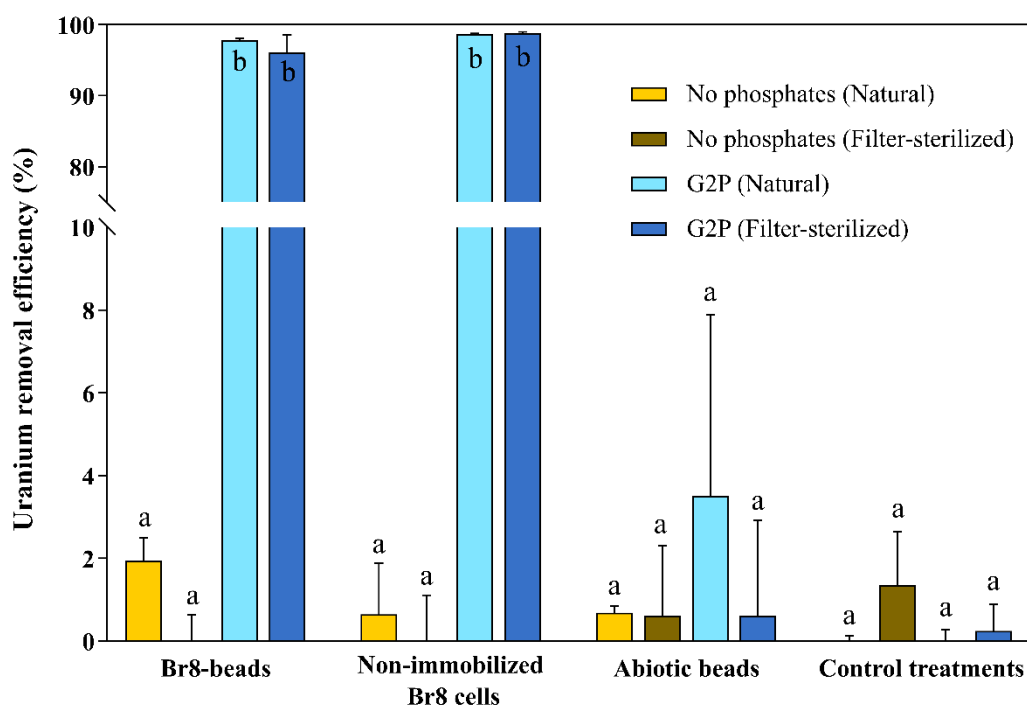


**Figure 3.** Uranium removal efficiency (%) after incubation (72 h; 28°C; 165 rpm) of natural and filter-sterilized COMI\_79 mining water (initial U concentration 47.4 mg/L; pH 7.75; amended either with 5 mM G2P or without amended phosphates) in presence of 4% Na-alginate beads doped with *Stenotrophomonas* sp. Br8 cells (~1.5·10<sup>7</sup>CFU/g bead). Flasks with non-immobilized Br8 cells, abiotic beads, and without Br8 cells were used as control treatments. Data are showed as the mean ±SD of at least three independent measurements.

#### *Microscopic characterization of U immobilization process*

HAADF-STEM and ESEM analyses showed that Br8-doped beads incubated for 72 h in G2P-amended COMI\_79 water displayed apparently intact macro-morphological properties besides complex nature of the treated water (Reiller and Descostes, 2020). STEM micrographs of thin sections of the Br8-doped beads and ESEM images revealed the presence of needle-like U precipitates distributed at surface and inner areas of the beads

(Figs. 4 and S8-S9). Uranium precipitates within the beads were mainly found around the cells, what is likely caused by the localization of phosphatases at this level (Kulkarni et al., 2016; Chandwadkar et al., 2018). No intracellular U precipitates were observed as it was also reported for U treated planktonic cells (Sánchez-Castro et al., 2020). Cell-free beads (abiotic control) showed no significant U precipitation (data not shown) confirming the key role of Br8 in the U removal process described above. Further microscopic and spectroscopic analyses revealed U and P as main elements composing resulting precipitates (Fig. 5), what suggests formation of biogenic uranium phosphates of amorphous nature as indicated by XRD analysis (Fig. S10).

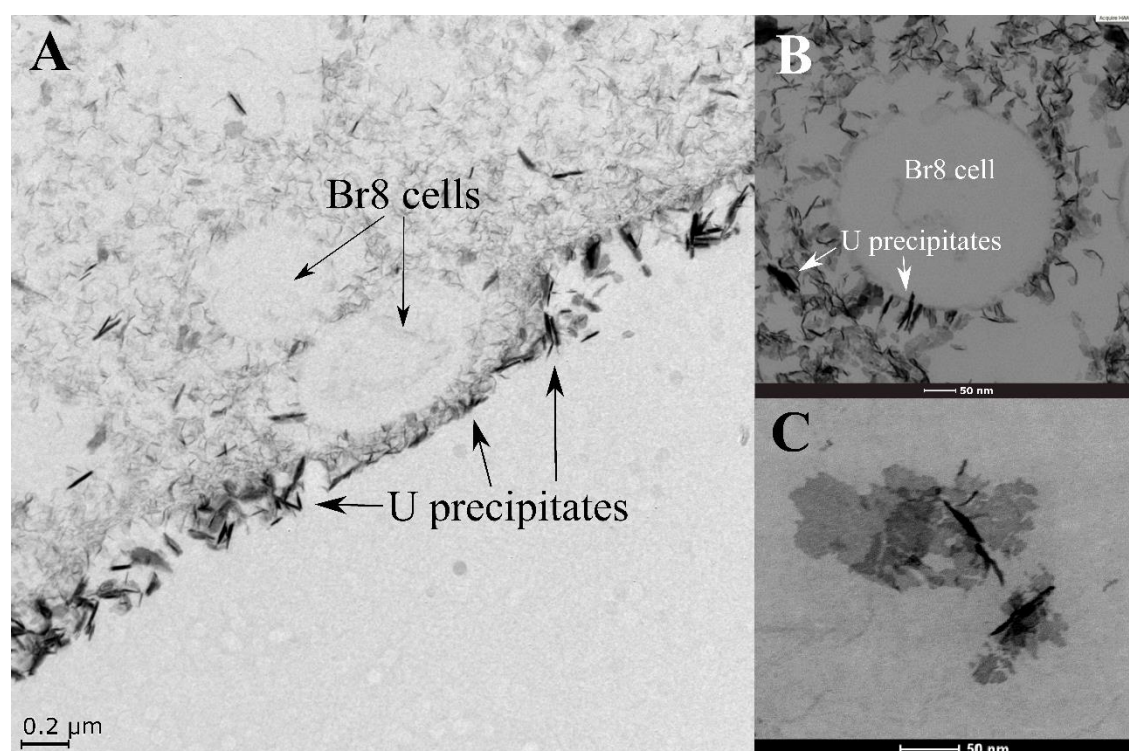


**Figure 4.** HAADF-STEM micrographs of thin sections of 4 % Na-alginate beads doped with *Stenotrophomonas* sp. Br8 cells ( $\sim 1.5 \cdot 10^7$  CFU/g bead) recovered after incubation (72 h; 28 °C; 165 rpm) in natural COMI\_79 mining water (initial U concentration 47.4 mg/L; pH 7.75; amended with 5 mM G2P). Image A shows the edge of the bead. Image B focused in a Br8 cell immobilized within the bead and image C shows a zoomed-in view of U-phosphate precipitates.

#### *Effect of the biomass concentration on U removal*

The effect of biomass dosage and number of beads used per mL of tested mining water was investigated. As stated in Materials and Methods section, simple dosage will be considered  $\sim 1.5 \cdot 10^7$  CFU/g biomaterial. Use of 1 or 2 beads per mL with simple cell dosage or 1 bead per mL with double cell dosage showed all similar U precipitation rates over 90% (Fig. 6a)



after 72 h incubation. The use of 0.5 Br8-beads per mL with simple cell dosage reduced the U removal efficiency in 15-20%, reaching a maximum value of 77%. In the same trend, the release of inorganic phosphates was similar in all cases except for treatment using 0.5 beads (simple dosage) per mL which resulted in a lower orthophosphates release (Fig. 6b).

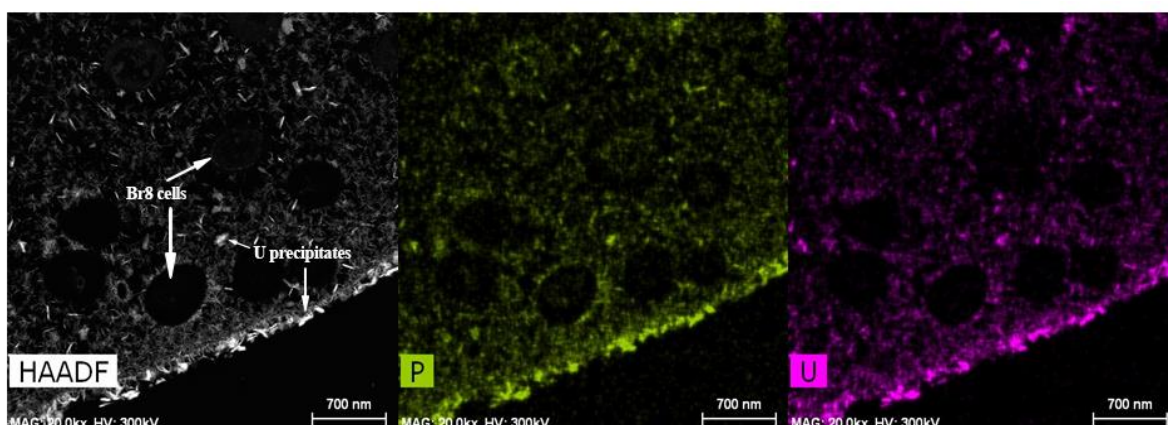


**Figure 5.** EDX element-distribution maps for P and U and HAADF-STEM micrograph of a thin section showing U-phosphate precipitates in the inner part of a 4 % Na- alginate bead doped with *Stenotrophomonas* sp. Br8 cells ( $\sim 1.5 \cdot 10^7$  CFU/g bead) recovered after incubation (72 h; 28 °C; 165 rpm) in natural COMI\_79 mining water (initial U concentration 47.4 mg/L; pH 7.75; amended with 5 mM G2P).

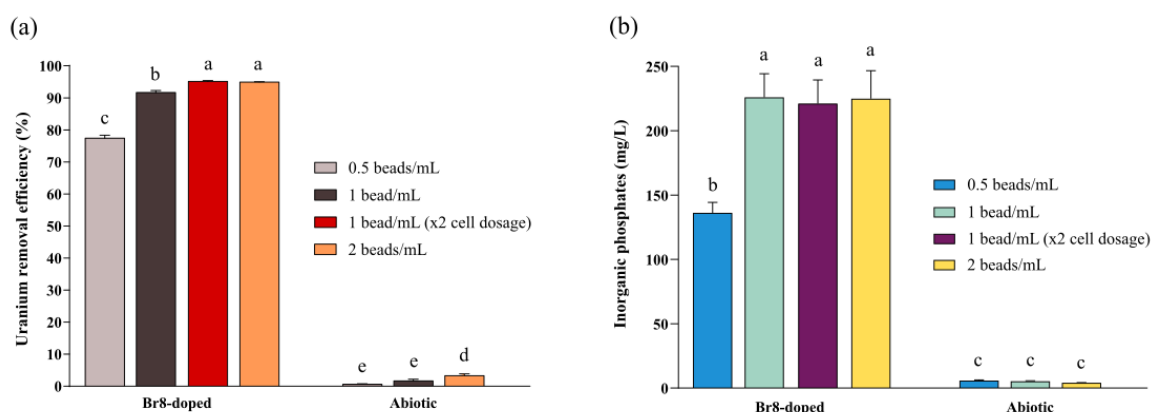


**Figure 6.** Uranium removal efficiency (%) (a) and inorganic phosphates in solution (mg/L) detected (b) after incubation (72 h; 28 °C; 165 rpm) of natural COMI\_79 mining water (initial U concentration 47.4 mg/L; pH 7.75; amended with 5 mM G2P) in presence of different number of 4 % Na-alginate beads doped with *Stenotrophomonas* sp. Br8 cells ( $\sim 1.5 \cdot 10^7$  or  $\sim 3 \cdot 10^7$  CFU/g bead). Flasks with different number of abiotic beads were used as control treatments. Data are showed as the mean  $\pm$  SD of at least three independent measurements. Different letters mean significant differences ( $p < 0.05$ ).

### *Effect of the immobilized biomass storage conditions*

To enhance the applicability of the proposed biomaterial, different storage conditions (temperature, time and physical state) were tested before using it and investigating their impact on its U removal performance. At U immobilization level, no significant differences were found after storing non-freeze-dried beads at 4°C for 7 d, 90 d and 300 d, as well as after storing freeze-dried beads at 25°C for 90 d, reaching in all cases values between 90-95% after 72 h (Fig. 7a). However, non-freeze-dried beads stored at 25°C for 90 d evidenced a dramatic decrease to removal values under 3%, what may be explained by a low cell viability which produced a poor release of inorganic phosphates (Fig. 7b). Although non-freeze-dried beads conserved for 300 d (4°C) and freeze-dried beads after rehydration showed some alterations in their external morphology, these changes seemed not to affect their performance as stated above (Fig. 7).

## **Discussion**

### *Optimization of the immobilization process of *Stenotrophomonas* sp. Br8 bacterial biomass*

*Stenotrophomonas* spp. are described for their high versatility and capacity for remediating a variety of metals like uranium (Merroun and Selenska-Pobell, 2008; Nazina et al., 2010; Islam and Sar, 2016), selenium (Ruiz-Fresneda et al., 2018, 2019 and 2020), gold (Song et al., 2008), arsenic (Bahar et al., 2012), copper (Ghosh et al., 2020; Gopi et al., 2020), chromium (Ge and Ge, 2016; Aslam et al., 2020), zinc (Ge and Ge, 2016), nickel (Aslam et al., 2020; Ghosh et al., 2020), or lead (Aslam et al., 2020) through different mechanisms (e.g. biomineralization, bioreduction, bioaccumulation). In fact, the biomass of planktonic cells of the same *Stenotrophomonas* isolate used in this case (*Stenotrophomonas* sp. Br8) was previously characterized for its high U removal capacity in U nitrates solution amended with G2P at different metal concentrations (Sánchez-Castro et al., 2020). The present work goes a step beyond by evidencing their high capacity for efficiently immobilizing U from real U mining waters. For enhancing the applicability of this remediation strategy through protecting planktonic bacterial cells from toxicity provoked by high U (and other heavy metals) concentration and improving their stability, biomass immobilization through well-established entrapment protocols was evaluated.



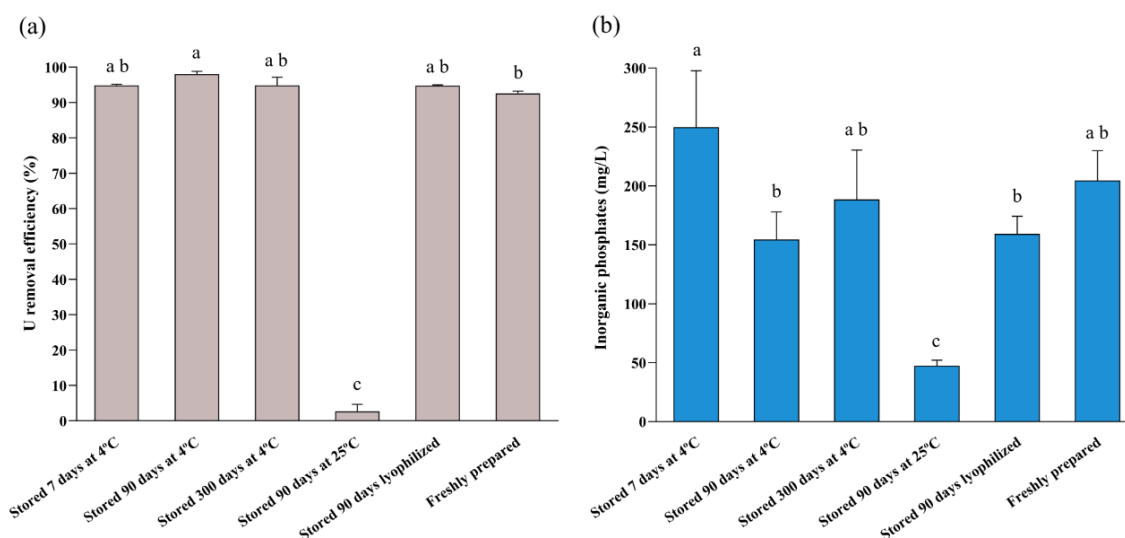


**Figure 7.** Uranium removal efficiency (%) (a) and inorganic phosphates in solution (mg/L) detected (b) after incubation (72h; 28 °C; 165 rpm) of natural COMI\_79 mining water (initial U concentration 47.4 mg/L; pH 7.75; amended with 5 mM G2P) in presence of 4 % Na-alginate beads doped with *Stenotrophomonas* sp. Br8 cells (~1.5·10<sup>7</sup> CFU/g bead) and stored under different conditions before application. Flasks with freshly prepared Br8-doped beads were used as control treatment. Data are showed as the mean ± SD of at least three independent measurements. Different letters mean significant differences (p < 0.05).

In this study, evaluation of parameters like mechanical/chemical stability, presence of certain functional groups, biocompatibility, and external/internal morphology demonstrated the high efficiency of alginate as inorganic matrix for Br8 cell immobilization. Despite its poor chemical stability in presence of Ca<sup>2+</sup> chelators, this natural polymer is preferred over other materials for active cell immobilization, mainly because of its high biocompatibility, hydrophilicity, presence of carboxylic groups (which enhance heavy metal ion adsorption; Romera et al., 2007), low economical cost, easy availability and low-biodegradability under different conditions (Lozinsky and Plieva, 1998; Wani et al., 2016). Similarly, as proposed in the present work where alginate final concentration was increased to 4% to gain stability, modifications of the original alginate beads production protocol (Smidsrod and Skjak-Braek, 1990) were repeatedly reported aiming to enhance its performance (e.g. increasing stability; Kiran et al., 2018). Furthermore, some studies demonstrated higher efficiency in bioremediation by using immobilized cells in comparison to planktonic cells likely due to immobilization matrix sorption capacity as well as better conservation in the bacterial activity (Shi et al., 2018).

Other advantages such as better storage stability and better reutilizing ability are also addressed (Dianawati et al., 2016; Shi et al., 2018). For these reasons, alginate matrices doped with bacterial cells have been repeatedly investigated in the last years as efficient bioremediation agents of metals like lead (Zhang et al., 2020), chromium (Wu et al., 2019; El-Naggar et al., 2020), cadmium (Shi et al., 2018), uranium (Kulkarni et al., 2013), or copper and zinc simultaneously (Kiran et al., 2018). Moreover, cell-free alginate matrices have been also shown to produce comparable results (Yu et al., 2017).

### ***Ability of Br8 immobilized biomass to remove U from mining water***

In the present study we demonstrated the ability of immobilized cells, belonging to a strain of the genus *Stenotrophomonas*, for U immobilization. It was already reported multiple benefits of immobilizing cells from different strains of the genus in alginate beads or inert polyurethane foam to remediate colored textile wastewaters (Galai et al., 2010; Rajendran et al., 2015, respectively) or organic pollutants (Mukherjee and Roy, 2013), as well as being applied as biocontrol agents in agriculture (Ahmad et al., 2012). Likewise, catechol dioxygenases obtained from *Stenotrophomonas maltophilia* KB2 strain were immobilized in alginate hydrogels for enhancing the bioremediation and detoxification of xenobiotic-contaminated environments (Wojcieszynska et al., 2012; Guzik et al., 2014). Regarding metals bioremediation, other microbes than *Stenotrophomonas* immobilized in alginate beads have been effectively used (Kiran et al., 2018; Leong and Chang, 2020). In particular, fungal cells (genus *Trichoderma*; Akhtar et al., 2007 and 2009; and genus *Aspergillus*; Wang et al., 2010) immobilized in alginate beads have been successfully assessed to recover uranium from aqueous solutions. However, this is the first study describing the metal phosphate biomineralization as strategy to remove U from U contaminated water.

The fact that U immobilization process by Br8-doped alginate beads showed a first rapid metal removal phase (38% in 7h) followed by a gradual slower phase where a maximum removal value (98%) was achieved at 72 h, suggests that several interaction mechanisms are co-occurring in the system. During the first hours, passive mechanisms seem to mediate the immobilization of the uranium by sorption onto bead and/or cell surfaces, as observed in other studies (Gok and Aytas, 2009; Wang et al., 2010; Yu et al., 2017; Sánchez-Castro et al., 2020). Besides bacterial functional groups known to provide binding sites for U sorption (e.g. carboxyl and phosphoryl), other reactive groups detected on beads surface

(e.g. hydroxyl and alkoxy groups) are likely participating (cell-free beads removed around 4% of the total solved U; Fig. 3) in this first metabolism-independent phase (Yu et al., 2017). In a similar way as described in Sánchez-Castro et al. (2020), the rate of release of inorganic phosphates (mediated by phosphatase enzymes; Chandwadkar et al., 2018) by Br8 is presumably controlling the process kinetics of the subsequent U immobilization phase based on phosphate biomineralization active mechanisms. Cells' immobilization technology optimized in the present work seems not to affect phosphatase enzymes activity (97.8% U removal after 72 h) although this kinetics study showed a delay in the process in comparison to planktonic Br8 cells application (Fig. 2).

As described in Sánchez-Castro et al. (2020), U precipitates within the beads were mainly localized around the cells, what is likely caused by the presence of phosphatases at this level (Kulkarni et al., 2016; Chandwadkar et al., 2018). No intracellular U precipitates were observed as it was also found for U treated planktonic cells (Sánchez-Castro et al., 2020), suggesting that cells remained viable during the U removal process. Elemental mapping (performed through STEM) and additional spectroscopic analyses indicated formation of biogenic U phosphates. These compounds which are known to be highly stable in comparison to other U precipitates showing chemical fragility such as U carbonate complexes (Duff et al., 2004), has been already reported for planktonic bacterial cells (Beazley et al., 2007 and 2009; Choudhary and Sar, 2011; Povedano-Priego et al., 2019). Specifically, planktonic cells of the strain *Stenotrophomonas* sp. Br8 were already demonstrated to precipitate U as long-term stable U phosphate mineral phases with a structure similar to that of meta-autunite (Sánchez-Castro et al., 2020). In this study, cells from the same strain formed similar stable biogenic U phosphates after being immobilized within alginate beads. So far, most previous works using alginate beads (doped with microbes or not) for U immobilization are based on sorption mechanisms (Gok and Aytas, 2009; Wang et al., 2010; Yu et al., 2017) and then resulting in unstable U precipitates.

### ***Novel uranium removal mechanism proposed and optimal application conditions to treat U mining waters***

Considering all results presented above, the proposed U removal mechanism observed consist of a multi-step process starting with a first fast sorption phase where a portion of the soluble U(VI) is bound mainly onto functional groups at the surface of the cells

embedded within the alginate beads. Concomitantly, a Br8-phosphatase-mediated release of inorganic phosphates from amended G2P occurred. Then, these orthophosphates generated associate with bio-available and soluble uranyl ions in the mining water forming stable U phosphates phases.

In addition, key biological and physicochemical parameters like biomass concentration within the beads, storage conditions of the alginate beads before using, bead/water contact time, and amendment of an external organic phosphate source were assessed to enhance the applicability of this U removal process. Thus, use of 1 bead (containing approx.  $1.8 \cdot 10^5$  CFU) per mL is estimated as the optimal amount to achieve an efficient U removal from COMI\_79 mining waters. Alternatively, the use of the same number of cells distributed in a lower number of beads would reduce substantially the economic costs inherent to the immobilization process while offering comparable U removal efficiency rates. The possibility of storing this biomaterial under certain conditions (4°C) for at least 300 days without compromising its U removal capacity, clearly enhance the relevance of the strategy proposed in this work. Previous studies reported a good conservation of viability in bacterial cells immobilized in similar inorganic matrices after 120d (Ontañón et al., 2017) and 180d (Brachkova et al., 2010; Zommere and Nikolajeva, 2017). However, to the best of our knowledge, no longer storage periods of time than 300d have been assessed before for bacterial cells immobilized in Na-alginate beads. Regarding freeze-drying process, it should be noted that it requires a sharp decrease in temperature which might have deadly effects on bacterial cells (Crittenden et al., 2006; Chavarri et al., 2010; Amine et al., 2014), mainly caused by water crystallization, protein denaturation or membranes injury (De Giulio et al., 2005). In this sense, the use of inorganic matrices for bacterial cells immobilization plays a protective role which may reduce the physiological deterioration, maintaining, at least partially, cells viability, metabolic potential and operational stability (Amine et al., 2014). Other key considerations to apply efficiently the strategy proposed is the amendment of an organic phosphates source like G2P or the incubation of the system for at least 72 h.

## **Conclusions**

Uranium, particularly at high concentrations, is known to produce serious detrimental effects on bacterial diversity and activity. By embedding bacterial cells in an alginate

matrix acting as a protective barrier, U cytotoxic effects can be reduced significantly through preventing direct contact between this hazardous agent and the cells. In this sense, it was developed an enhanced biomass immobilization method, based on previous consolidated protocols, resulting in biocompatible, highly porous Na-alginate beads. This biomaterial was thoroughly characterized and successfully applied, for one or multiple cycles, to immobilize soluble U from real mining wastewaters. Microscopic and spectroscopic characterization of the immobilized U solid phases confirmed formation of highly-stable U phosphates at bead surface level but also in their inner sections, associated to Br8 cells but never inside them. Chemical stability issues and potential Br8 cells leakage during removal process should be investigated by carrying out further studies focused on increasing the mechanical and chemical stability of the carrier material. Although U removal from non-natural U-containing solutions has received considerable attention, immobilization of U from real mining wastewaters remains relatively unexplored so far. The U precipitation as uranyl phosphate from real mining waters is of great scientific and environmental relevance but rather difficult on account of water chemical complexity. However, the process proposed in this study including an active enzymatic release of inorganic phosphates may overcome these difficulties and precipitate efficiently solved U(VI) and, likely, other heavy metals from these polluted wastewaters. In addition, key parameters like biomass dosage or biomaterial storage conditions were optimized for obtaining a cost-effective and applicable technology to remediate heavy-metals-containing water.

In conclusion, this lab-scale study revealed that U removal from complex mining waters employing alginate beads doped with cells of *Stenotrophomonas* sp. Br8 bacterial strain is a promising strategy even at high initial concentrations. Further research should focus on the scale-up of this highly efficient and low-cost process to develop eco-friendly heavy-metals-containing water treatment stations.

### **Declaration of competing interest**

The authors declare that they have no known competing financial interests or personal relationships that could have appeared to influence the work reported in this paper.

## Acknowledgements

This work was supported by ORANO Mining (France) [collaborative research contract n° 3022 OTRI-UGR]. It results from a Joint Research Project between Orano Mining R&D Department and the Department of Microbiology of the University of Granada. We acknowledge the assistance at the ESEM of Isabel Sánchez Almazo and Concepción Hernández Castillo (Centro de Instrumentación Científica, University of Granada, Spain).

## References

- Acharya, C., Joseph, D., Apte, S.K., 2009. Uranium sequestration by a marine cyanobacterium, *Synechococcus elongatus* strain BDU/75042. *Bioresour. Technol.* 100, 2176–2181. <https://doi.org/10.1016/j.biortech.2008.10.047>
- Ahmad, M., Ahmad, M.M., Hamid, R., Abdin, M.Z., Javed, S., 2012. In vitro inhibition study against *A. flavus* with *Stenotrophomonas maltophilia* immobilized in calcium alginate gel beads. *J. Pure Appl. Microbiol.* 6, 597–608.
- Akhtar, K., Waheed Akhtar, M., Khalid, A.M., 2007. Removal and recovery of uranium from aqueous solutions by *Trichoderma harzianum*. *Water Res.* 41, 1366–1378. <https://doi.org/10.1016/j.watres.2006.12.009>
- Akhtar, K., Khalid, A.M., Akhtar, M.W., Ghauri, M.A., 2009. Removal and recovery of uranium from aqueous solutions by Calcium alginate immobilized *Trichoderma harzianum*. *Bioresour. Technol.* 100, 4551–4558. <https://doi.org/10.1016/j.biortech.2009.03.073>
- Amine, K.M., Champagne, C.P., Salmieri, S., Britten, M., St-Gelais, D., Fustier, P., Lacroix, M., 2014. Effect of palmitoylated alginate microencapsulation on viability of *Bifidobacterium longum* during freeze-drying. *LWT - Food Sci. Technol.* 56, 111–117. <https://doi.org/10.1016/j.lwt.2013.11.003>
- Aslam, F., Yasmin, A., Sohail, S., 2020. Bioaccumulation of lead, chromium, and nickel by bacteria from three different genera isolated from industrial effluent. *Int. Microbiol.* 23, 253–261. <https://doi.org/10.1007/s10123-019-00098-w>
- Bahar, M.M., Megharaj, M., Naidu, R., 2012. Arsenic bioremediation potential of a new arsenite-oxidizing bacterium *Stenotrophomonas* sp. MM-7 isolated from soil. *Biodegradation* 23, 803–812. <https://doi.org/10.1007/s10532-012-9567-4>
- Bargar, J.R., Bernier-Latmani, R., Giammar, D.E., Tebo, B.M., 2008. Biogenic Uraninite Nanoparticles and Their Importance for Uranium Remediation. *Elements* 4, 407–412. <https://doi.org/10.2113/gselements.4.6.407>
- Baskaran, V., Nemati, M., 2006. Anaerobic reduction of sulfate in immobilized cell bioreactors, using a microbial culture originated from an oil reservoir. *Biochem. Eng. J.* 31, 148–159. <https://doi.org/10.1016/j.bej.2006.07.007>
- Beazley, M.J., Martinez, R.J., Sobecky, P.A., Webb, S.M., Taillefert, M., 2007. Uranium biomineralization as a result of bacterial phosphatase activity: Insights from bacterial isolates from a contaminated subsurface. *Environ. Sci. Technol.* 41, 5701–5707. <https://doi.org/10.1021/es070567g>
- Beazley, M.J., Martinez, R.J., Sobecky, P.A., Webb, S.M., Taillefert, M., 2009. Nonreductive biomineralization of uranium(VI) phosphate via microbial phosphatase activity in anaerobic conditions. *Geomicrobiol. J.* 26, 431–441. <https://doi.org/10.1080/0149045090306>

- 0780
- Benzerara, K., Miot, J., Morin, G., Ona-Nguema, G., Skouri-Panet, F., Férard, C., 2011. Importance, mécanismes et implications environnementales de la biominéralisation par les microorganismes. *Comptes Rendus - Geosci.* 343, 160–167. <https://doi.org/10.1016/j.crte.2010.09.002>
- Birungi, Z.S., Chirwa, E.M.N., 2015. The adsorption potential and recovery of thallium using green micro-algae from eutrophic water sources. *J. Hazard. Mater.* 299, 67–77. <https://doi.org/10.1016/j.jhazmat.2015.06.011>
- Bouabidi, Z.B., El-Naas, M.H., Zhang, Z., 2019. Immobilization of microbial cells for the biotreatment of wastewater: A review. *Environ. Chem. Lett.* 17, 241–257. <https://doi.org/10.1007/s10311-018-0795-7>
- Brachkova, M.I., Duarte, M.A., Pinto, J.F., 2010. Preservation of viability and antibacterial activity of *Lactobacillus* spp. in calcium alginate beads. *Eur. J. Pharm. Sci.* 41, 589–596. <https://doi.org/10.1016/j.ejps.2010.08.008>
- Brodelius, P., Mosbach, K., 1987. Immobilization techniques for cells/organelles, in: *Methods in Enzymology*. Academic Press, pp. 173–454. [https://doi.org/10.1016/0076-6879\(87\)35075-X](https://doi.org/10.1016/0076-6879(87)35075-X)
- Chandwadkar, P., Misra, H.S., Acharya, C., 2018. Uranium biomineralization induced by a metal tolerant: *Serratia* strain under acid, alkaline and irradiated conditions. *Metallomics* 10, 1078–1088. <https://doi.org/10.1039/c8mt00061a>
- Chávarri, M., Marañón, I., Ares, R., Ibáñez, F.C., Marzo, F., Villarán, M. del C., 2010. Microencapsulation of a probiotic and prebiotic in alginate-chitosan capsules improves survival in simulated gastrointestinal conditions. *Int. J. Food Microbiol.* 142, 185–189. <https://doi.org/10.1016/j.ijfoodmicro.2010.06.022>
- Ching, S.H., Bansal, N., Bhandari, B., 2017. Alginate gel particles—A review of production techniques and physical properties. *Crit. Rev. Food Sci. Nutr.* 57, 1133–1152. <https://doi.org/10.1080/10408398.2014.965773>
- Choudhary, S., Sar, P., 2011. Uranium biomineralization by a metal resistant *Pseudomonas aeruginosa* strain isolated from contaminated mine waste. *J. Hazard. Mater.* 186, 336–343. <https://doi.org/10.1016/j.jhazmat.2010.11.004>
- Covarrubias, S.A., De-Bashan, L.E., Moreno, M., Bashan, Y., 2012. Alginate beads provide a beneficial physical barrier against native microorganisms in wastewater treated with immobilized bacteria and microalgae. *Appl. Microbiol. Biotechnol.* 93, 2669–2680. <https://doi.org/10.1007/s00253-011-3585-8>
- Crittenden, R., Weerakkody, R., Sanguansri, L., Augustin, M., 2006. Synbiotic microcapsules that enhance microbial viability during nonrefrigerated storage and gastrointestinal transit. *Appl. Environ. Microbiol.* 72, 2280–2282. <https://doi.org/10.1128/AEM.72.3.2280-2282.2006>
- Das, A., Osborne, J.W., 2018. Bioremediation of Heavy Metals, in: Gothandam, K.M., Ranjan, S., Dasgupta, N., Ramalingam, C., Lichtfouse, E. (Eds.), *Nanotechnology, Food Security and Water Treatment*. Springer International Publishing, Cham, pp. 277–311. [https://doi.org/10.1007/978-3-319-70166-0\\_9](https://doi.org/10.1007/978-3-319-70166-0_9)
- De Giulio, B., Orlando, P., Barba, G., Coppola, R., De Rosa, M., Sada, A., De Prisco, P.P., Nazzaro, F., 2005. Use of alginate and cryo-protective sugars to improve the viability of lactic acid bacteria after freezing and freeze-drying. *World J. Microbiol. Biotechnol.* 21, 739–746. <https://doi.org/10.1007/s11274-004-4735-2>
- Dianawati, D., Mishra, V., Shah, N.P., 2016. Survival of Microencapsulated Probiotic Bacteria after Processing and during Storage: A Review. *Crit. Rev. Food Sci. Nutr.* 56, 1685–1716. <https://doi.org/10.1080/10408398.2013.798779>
- Duff, M.C., Hunter, D.B., Hobbs, D.T., Fink, S.D., Dai, Z., Bradley, J.P., 2004. Mechanisms of strontium and uranium

- removal from high-level radioactive waste simulant solution by the sorbent monosodium titanate. *Environ. Sci. Technol.* 38, 5201–5207. <https://doi.org/10.1021/es035415+>
- Dzionic, A., Wojcieszynska, D., Guzik, U., 2016. Natural carriers in bioremediation: A review. *Electron. J. Biotechnol.* 23, 28–36. <https://doi.org/10.1016/j.ejbt.2016.07.003>
- El-Naggar, N.E.A., El-khateeb, A.Y., Ghoniem, A.A., El-Hersh, M.S., Saber, W.E.I.A., 2020. Innovative low-cost biosorption process of Cr<sup>6+</sup> by *Pseudomonas alcaliphila* NEWG-2. *Sci. Rep.* 10, 1–18. <https://doi.org/10.1038/s41598-020-70473-5>
- Galai, S., Limam, F., Marzouki, M.N., 2010. Decolorization of an industrial effluent by free and immobilized cells of *Stenotrophomonas maltophilia* AAP56. Implementation of efficient down flow column reactor. *World J. Microbiol. Biotechnol.* 26, 1341–1347. <https://doi.org/10.1007/s11274-010-0306-x>
- Ge, S., Ge, S.C., 2016. Simultaneous Cr(VI) reduction and Zn(II) biosorption by *Stenotrophomonas* sp. and constitutive expression of related genes. *Biotechnol. Lett.* 38, 877–884. <https://doi.org/10.1007/s10529-016-2057-8>
- Ghosh, A., Ali, S., Mukherjee, S.K., Saha, S., Kaviraj, A., 2020. Bioremediation of Copper and Nickel from Freshwater Fish *Cyprinus carpio* Using Rhizoplane Bacteria Isolated from *Pistia stratiotes*. *Environ. Process.* 7, 443–461. <https://doi.org/10.1007/s40710-020-00436-5>
- Gok, C., Aytas, S., 2009. Biosorption of uranium(VI) from aqueous solution using calcium alginate beads. *J. Hazard. Mater.* 168, 369–375. <https://doi.org/10.1016/j.jhazmat.2009.02.063>
- Gopi, K., Jinal, H.N., Pritesh, P., Kartik, V.P., Amaresan, N., 2020. Effect of copper-resistant *Stenotrophomonas maltophilia* on maize (*Zea mays*) growth, physiological properties, and copper accumulation: potential for phytoremediation into biofortification. *Int. J. Phytoremediation* 22, 662–668. <https://doi.org/10.1080/15226514.2019.1707161>
- Guzik, U., Hupert-Kocurek, K., Marchlewicz, A., Wojcieszynska, D., 2014. Enhancement of biodegradation potential of catechol 1,2-dioxygenase through its immobilization in calcium alginate gel. *Electron. J. Biotechnol.* 17, 83–88. <https://doi.org/10.1016/j.ejbt.2014.02.001>
- Islam, E., Sar, P., 2016. Diversity, metal resistance and uranium sequestration abilities of bacteria from uranium ore deposit in deep earth stratum. *Ecotoxicol. Environ. Saf.* 127, 12–21. <https://doi.org/10.1016/j.ecoenv.2016.01.001>
- Jaafari, J., Yaghmaeian, K., 2019. Optimization of heavy metal biosorption onto freshwater algae (*Chlorella coloniales*) using response surface methodology (RSM). *Chemosphere* 217, 447–455. <https://doi.org/10.1016/j.chemosphere.2018.10.205>
- Jauberty, L., Drogat, N., Decossas, J.L., Delpech, V., Gloaguen, V., Sol, V., 2013. Optimization of the arsenazo-III method for the determination of uranium in water and plant samples. *Talanta* 115, 751–754. <https://doi.org/10.1016/j.talanta.2013.06.046>
- Kiran, M.G., Pakshirajan, K., Das, G., 2018. Heavy metal removal from aqueous solution using sodium alginate immobilized sulfate reducing bacteria: Mechanism and process optimization. *J. Environ. Manage.* 218, 486–496. <https://doi.org/10.1016/j.jenvman.2018.03.020>
- Kulkarni, S., Ballal, A., Apte, S.K., 2013. Bioprecipitation of uranium from alkaline waste solutions using recombinant *Deinococcus radiodurans*. *J. Hazard. Mater.* 262, 853–861. <https://doi.org/10.1016/j.jhazmat.2013.09.057>
- Kulkarni, S., Misra, C.S., Gupta, A., Ballal, A., Apte, S.K., 2016. Interaction of uranium with bacterial cell surfaces: Inferences from phosphatase-mediated uranium precipitation. *Appl. Environ. Microbiol.* 82, 4965–4974. <https://doi.org/10.1128/AEM.00728-16>



- Kumari, S., Mahapatra, S., Das, S., 2017. Calcium alginate as a support matrix for Pb(II) biosorption with immobilized biofilm associated extracellular polymeric substances of *Pseudomonas aeruginosa* N6P6. *Chem. Eng. J.* 328, 556–566. <https://doi.org/10.1016/j.cej.2017.07.102>
- Leong, Y.K., Chang, J.S., 2020. Bioremediation of heavy metals using microalgae: Recent advances and mechanisms. *Bioresour. Technol.* 303, 122886. <https://doi.org/10.1016/j.biortech.2020.122886>
- Lovley, D.R., Phillips, E.J.P., 1992. Reduction of uranium by *Desulfovibrio desulfuricans*. *Appl. Environ. Microbiol.* 58, 850–856. <https://doi.org/10.1128/aem.58.3.850-856.1992>
- Lozinsky, V.I., Plieva, F.M., 1998. Poly(vinyl alcohol) cryogels employed as matrices for cell immobilization. 3. Overview of recent research and developments. *Enzyme Microb. Technol.* 23, 227–242. [https://doi.org/10.1016/S0141-0229\(98\)00036-2](https://doi.org/10.1016/S0141-0229(98)00036-2)
- Martinez, R.J., Beazley, M.J., Taillefert, M., Arakaki, A.K., Skolnick, J., Sobecky, P.A., 2007. Aerobic uranium (VI) bioprecipitation by metal-resistant bacteria isolated from radionuclide- and metal-contaminated subsurface soils. *Environ. Microbiol.* 9, 3122–3133. <https://doi.org/10.1111/j.1462-2920.2007.01422.x>
- Merroun, M.L., Selenska-Pobell, S., 2008. Bacterial interactions with uranium: An environmental perspective. *J. Contam. Hydrol.* 102, 285–295. <https://doi.org/10.1016/j.jconhyd.2008.09.019>
- Merroun, M.L., Nedelkova, M., Ojeda, J.J., Reitz, T., Fernández, M.L., Arias, J.M., Romero-González, M., Selenska-Pobell, S., 2011. Bio-precipitation of uranium by two bacterial isolates recovered from extreme environments as estimated by potentiometric titration, TEM and X-ray absorption spectroscopic analyses. *J. Hazard. Mater.* 197, 1–10. <https://doi.org/10.1016/j.jhazmat.2011.09.049>
- Mukherjee, P., Roy, P., 2013. Persistent organic pollutants induced protein expression and immunocrossreactivity by *Stenotrophomonas maltophilia* PM102: A prospective bioremediating candidate. *Biomed Res. Int.* 2013. <https://doi.org/10.1155/2013/714232>
- Murphy, J., Riley, J.P., 1962. A modified single solution method for the determination of phosphate in natural waters. *Anal. Chim. Acta* 27, 31–36. [https://doi.org/10.1016/S0003-2670\(00\)88444-5](https://doi.org/10.1016/S0003-2670(00)88444-5)
- Nazina, T.N., Luk'yanova, E.A., Zakharova, E. V., Konstantinova, L.I., Kalmykov, S.N., Poltarau, A.B., Zubkov, A.A., 2010. Microorganisms in a Disposal Site for liquid radioactive wastes and their influence on radionuclides. *Geomicrobiol. J.* 27, 473–486. <https://doi.org/10.1080/01490451003719044>
- Nedelkova, M., Merroun, M.L., Rossberg, A., Hennig, C., Selenska-Pobell, S., 2007. Microbacterium isolates from the vicinity of a radioactive waste depository and their interactions with uranium. *FEMS Microbiol. Ecol.* 59, 694–705. <https://doi.org/10.1111/j.1574-6941.2006.00261.x>
- Ontañón, O.M., González, P.S., Barros, G.G., Agostini, E., 2017. Improvement of simultaneous Cr(VI) and phenol removal by an immobilised bacterial consortium and characterisation of biodegradation products. *N. Biotechnol.* 37, 172–179. <https://doi.org/10.1016/j.nbt.2017.02.003>
- Pannier, A., Soltmann, U., Soltmann, B., Altenburger, R., Schmitt-Jansen, M., 2014. Alginate/silica hybrid materials for immobilization of green microalgae *Chlorella vulgaris* for cell-based sensor arrays. *J. Mater. Chem. B* 2, 7896–7909. <https://doi.org/10.1039/C4TB00944D>
- Perullini, M., Orias, F., Durrieu, C., Jobbágy, M., Bilmes, S.A., 2014. Co-encapsulation of *Daphnia magna* and microalgae in silica matrices, a stepping stone toward a portable microcosm. *Biotechnol. Reports* 4, 147–150. <https://doi.org/10.1016/j.btre.2014.10.002>
- Pinel-Cabello, M., Iroundi, F., López-Fernández, M., Geffers, R., Jarek, M., Jauregui, R., Link, A., Vílchez-Vargas, R., Merroun, M.L., 2021. Multisystem combined uranium resistance mechanisms and

- bioremediation potential of *Stenotrophomonas bentonitica* BII-R7: Transcriptomics and microscopic study. *J. Hazard. Mater.* 403. <https://doi.org/10.1016/j.jhazmat.2020.123858>
- Povedano-Priego, C., Jroundi, F., Lopez-Fernandez, M., Sánchez-Castro, I., Martín-Sánchez, I., Huertas, F.J., Merroun, M.L., 2019. Shifts in bentonite bacterial community and mineralogy in response to uranium and glycerol-2-phosphate exposure. *Sci. Total Environ.* 692, 219–232. <https://doi.org/10.1016/j.scitotenv.2019.07.228>
- Prabhakaran, P., Ashraf, M.A., Aqma, W.S., 2016. Microbial stress response to heavy metals in the environment. *RSC Adv.* 6, 109862–109877. <https://doi.org/10.1039/c6ra10966g>
- R Core Team, 2020. R: A language and environment for statistical computing. R Foundation for Statistical Computing, Vienna, Austria. URL: <https://www.R-project.org/>.
- Raff, J., Soltmann, U., Matys, S., Selenska-Pobell, S., Böttcher, H., Pompe, W., 2003. Biosorption of uranium and copper by biocers. *Chem. Mater.* 15, 240–244. <https://doi.org/10.1021/cm021213l>
- Rajendran, R., Prabhavathi, P., Karthiksundaram, S., Pattabi, S., Kumar, S.D., Santhanam, P., 2015. Biodecolorization and bioremediation of denim industrial wastewater by adapted bacterial consortium immobilized on inert polyurethane foam (PUF) matrix: A first approach with biobarrier model. *Polish J. Microbiol.* 64, 329–338. <https://doi.org/10.5604/17331331.1185230>
- Ranganathan, S.V., Narasimhan, S.L., Muthukumar, K., 2008. An overview of enzymatic production of biodiesel. *Bioresour. Technol.* 99, 3975–3981. <https://doi.org/10.1016/j.biortech.2007.04.060>
- Reiller, P.E., Descostes, M., 2020. Development and application of the thermodynamic database PRODATA dedicated to the monitoring of mining activities from exploration to remediation. *Chemosphere* 251. <https://doi.org/10.1016/j.chemosphere.2020.126301>
- Romera, E., González, F., Ballester, A., Blázquez, M.L., Muñoz, J.A., 2007. Comparative study of biosorption of heavy metals using different types of algae. *Bioresour. Technol.* 98, 3344–3353. <https://doi.org/10.1016/j.biortech.2006.09.026>
- Ruiz-Fresneda, M.A., Delgado-Martín, J., Gómez-Bolívar, J., Fernández-Cantos, M. V., Bosch-Estévez, G., Martínez-Moreno, M.F., Merroun, M.L., 2018. Green synthesis and biotransformation of amorphous Se nanospheres to trigonal 1D Se nanostructures: Impact on Se mobility within the concept of radioactive waste disposal. *Environ. Sci. Nano* 5, 2103–2116. <https://doi.org/10.1039/c8en00221e>
- Ruiz-Fresneda, M.A., Gomez-Bolivar, J., Delgado-Martin, J., del Mar Abad-Ortega, M., Guerra-Tschuschke, I., Merroun, M.L., 2019. The bioreduction of selenite under anaerobic and alkaline conditions analogous to those expected for a deep geological repository system. *Molecules* 24. <https://doi.org/10.3390/molecules24213868>
- Ruiz-Fresneda, M.A., Eswayah, A.S., Romero-González, M., Gardiner, P.H.E., Solari, P.L., Merroun, M.L., 2020. Chemical and structural characterization of SeIV biotransformations by: *Stenotrophomonas bentonitica* into Se0 nanostructures and volatiles Se species. *Environ. Sci. Nano* 7, 2140–2155. <https://doi.org/10.1039/d0en00507j>
- Sánchez-Castro, I., Amador-García, A., Moreno-Romero, C., López-Fernández, M., Phrommavanh, V., Nos, J., Descostes, M., Merroun, M.L., 2017. Screening of bacterial strains isolated from uranium mill tailings porewaters for bioremediation purposes. *J. Environ. Radioact.* 166, 130–141. <https://doi.org/10.1016/j.jenvrad.2016.03.016>
- Sánchez-Castro, I., Martínez-Rodríguez, P., Jroundi, F., Lorenzo, P., Descostes, M., L. Merroun, M., 2020. High-efficient microbial immobilization of solvated U(VI) by the *Stenotrophomonas* strain Br8. *Water Res.* 183. <https://doi.org/10.1016/j.watres.2020.11>

- 6110
- Shi, X., Zhou, G., Liao, S., Shan, S., Wang, G., Guo, Z., 2018. Immobilization of cadmium by immobilized *Alishewanella* sp. WH16-1 with alginate-lotus seed pods in pot experiments of Cd-contaminated paddy soil. *J. Hazard. Mater.* 357, 431–439. <https://doi.org/10.1016/j.jhazmat.2018.06.027>
- Smidsrød, O., Skjakbraek, G., 1990. Alginate as immobilization matrix for cells. *Rev. Philos. Psychol.* 8, 71–78. [https://doi.org/10.1016/0167-7799\(90\)90139-O](https://doi.org/10.1016/0167-7799(90)90139-O)
- Soltmann, U., Raff, J., Selenska-Pobell, S., Matys, S., Pompe, W., Böttcher, H., 2003. Biosorption of heavy metals by sol-gel immobilized *Bacillus sphaericus* cells, spores and S-layers. *J. Sol-Gel Sci. Technol.* 26, 1209–1212. <https://doi.org/10.1023/A:1020768420872>
- Song, H.P., Li, X.G., Sun, J.S., Xu, S.M., Han, X., 2008. Application of a magnetotactic bacterium, *Stenotrophomonas* sp. to the removal of Au(III) from contaminated wastewater with a magnetic separator. *Chemosphere* 72, 616–621. <https://doi.org/10.1016/j.chemosphere.2008.02.064>
- Soni, R., Dash, B., Kumar, P., Mishra, U.N., Goel, R., 2019. Microbes for Bioremediation of Heavy Metals, in: Singh, D.P., Prabha, R. (Eds.), *Microbial Interventions in Agriculture and Environment: Volume 3: Soil and Crop Health Management*. Springer Singapore, Singapore, pp. 129–141. [https://doi.org/10.1007/978-981-32-9084-6\\_6](https://doi.org/10.1007/978-981-32-9084-6_6)
- Wang, J., Hu, X., Liu, Y., Xie, S., Bao, Z., 2010. Biosorption of uranium (VI) by immobilized *Aspergillus fumigatus* beads. *J. Environ. Radioact.* 101, 504–508. <https://doi.org/10.1016/j.jenvrad.2010.03.002>
- Wani, P., Olamide, A., Rafi, N., Wahid, S., Wasiu, I., Sunday, O., 2016. Sodium Alginate/Polyvinyl Alcohol Immobilization of *Brevibacillus brevis* OZF6 Isolated from Waste Water and Its Role in the Removal of Toxic Chromate. *Br. Biotechnol. J.* 15, 1–10. <https://doi.org/10.9734/bbj/2016/27341>
- Williams, K.H., Bargar, J.R., Lloyd, J.R., Lovley, D.R., 2013. Bioremediation of uranium-contaminated groundwater: A systems approach to subsurface biogeochemistry. *Curr. Opin. Biotechnol.* 24, 489–497. <https://doi.org/10.1016/j.copbio.2012.10.008>
- Wojcieszynska, D., Hupert-Kocurek, K., Jankowska, A., Guzik, U., 2012. Properties of catechol 2,3-dioxygenase from crude extract of *Stenotrophomonas maltophilia* strain KB2 immobilized in calcium alginate hydrogels. *Biochem. Eng. J.* 66, 1–7. <https://doi.org/10.1016/j.bej.2012.04.008>
- Wu, M., Li, Y., Li, J., Wang, Y., Xu, H., Zhao, Y., 2019. Bioreduction of hexavalent chromium using a novel strain CRB-7 immobilized on multiple materials. *J. Hazard. Mater.* 368, 412–420. <https://doi.org/10.1016/j.jhazmat.2019.01.059>
- Yu, J., Wang, J., Jiang, Y., 2017. Removal of Uranium from Aqueous Solution by Alginate Beads. *Nucl. Eng. Technol.* 49, 534–540. <https://doi.org/10.1016/j.net.2016.09.004>
- Zhang, K., Teng, Z., Shao, W., Wang, Y., Li, M., Lam, S.S., 2020. Effective passivation of lead by phosphate solubilizing bacteria capsules containing tricalcium phosphate. *J. Hazard. Mater.* 397, 122754. <https://doi.org/10.1016/j.jhazmat.2020.122754>
- Zommere, Ž., Nikolajeva, V., 2017. Immobilization of bacterial association in alginate beads for bioremediation of oil-contaminated lands. *Environ. Exp. Biol.* <https://doi.org/10.22364/eeb.15.09>

## Supplementary data

### *Supplementary materials and methods*

#### *Effect of incubation time, biomass concentration and biomaterial storage conditions in U removal*

A time-dependent study (0.08 h, 0.16 h, 1 h, 1.5 h, 7 h, 20 h, 24 h, 48 h and 72 h) was performed to investigate the kinetics of the U removal process mediated by immobilized Br8 strain cells. Effect of biomass dosage was also evaluated by testing different amounts of biomaterial (0.5, 1 and 2 beads per mL of mining water), and different biomass concentration used to prepare the beads ( $\sim 1.5 \cdot 10^7$  and  $\sim 3 \cdot 10^7$  CFU per g of biomaterial, corresponding to simple dosage and double dosage respectively). In addition, the effect on U removal performance of determined biomaterial storage conditions (at 4°C, non-freeze-dried, for 7 d, 90 d and 300d; and at 25°C, freeze-dried and non-freeze-dried, for 90 d) was also investigated. Incubations were conducted in the presence of 5 mM G2P under conditions indicated above (28°C; 72 h; and 165 rpm). Resulting treated water solution and biomaterial were subjected to analyses for determining the efficiency of the process under assayed conditions.

#### *Morphological characterization of biomaterials and localization of uranium precipitates through microscopic analyses: HAADF-STEM/EDAX and ESEM*

For high-angle annular dark field scanning transmission electron microscope (HAADF-STEM) and ESEM analyses, biomaterials newly produced and those already used in batch experiments were surface-washed twice with 0.9% NaCl and Na-cacodylate buffer (0.1 M, pH 7.4). Then, the samples were fixed with 2.5% glutaraldehyde in Na-cacodylate buffer. Later on, they were rinsed three times in the same buffer, stained with osmium tetroxide (1%, 1 h), and rinsed again three times with deionized water. Finally, the samples were progressively dehydrated: first, at increasing ethanol concentrations (50%, 70%, 80%, 90%, 95%, 100%); and then at critical point with CO<sub>2</sub> (Anderson, 1951) in a Leica EM CPD300 equipment.

For HAADF-STEM observation, samples were embedded in epoxy resin. Ultrathin sections (0.1  $\mu\text{m}$ ) of the samples, obtained using an ultra-microtome, were loaded in carbon coated copper grid and analysed by FEI TITAN G2 80-300 equipment. The TEM

specimen's holders were clean by plasma prior to STEM analysis to minimize contamination. The high-resolution STEM is equipped with HAADF detector and EDAX energy dispersive X-ray, which provides elemental information via the analysis of X-ray emissions caused by a high-energy electron beam.

To analyze the samples by ESEM equipment (Quanta 650 FEG, Thermofisher-FEI), they were placed in aluminum stubs with double carbon tape and carbon coating (EMITECH K975X) and imaged with an ETD secondary electron detector operated at 5 kV. For recognition of the uranium phosphates, BSE high resolution images (backscatter images) were collected using a circular backscatter (CBS) detector and a beam deceleration at a landing energy of 5 kV.

### *Supplementary results*

#### *FTIR-ATR spectroscopy analysis*

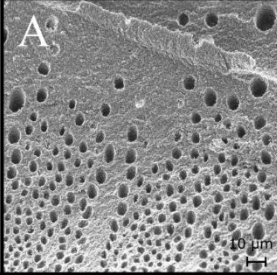
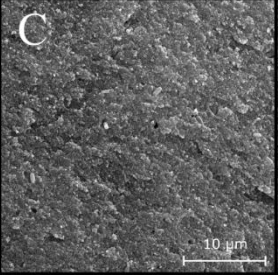
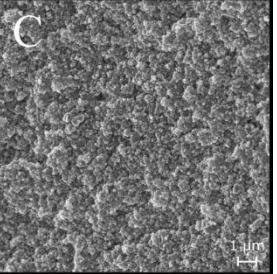
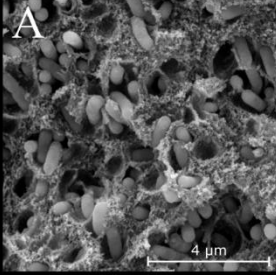
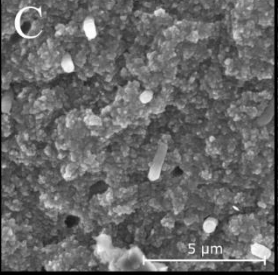
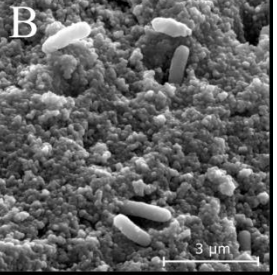
FTIR-ATR spectroscopy measurements performed to characterize the chemical properties of the beads at surface level evidenced presence of a variety of functional groups in beads with and without cells (Fig. S1). When analyzing the alginate sample, the high frequency region between 3500-3000  $\text{cm}^{-1}$  exhibited stretching vibrations of -O-H bonds of alginate (Manuja et al., 2014). The region around 1598  $\text{cm}^{-1}$  was likely assigned to the vibration of adsorbed water on the beads (Yu et al., 2017). Additionally, two characteristic bands at 1418  $\text{cm}^{-1}$  and 1305  $\text{cm}^{-1}$  were also attributed to hydroxyl groups (Yu et al., 2017) and that one at 938  $\text{cm}^{-1}$  to the C-O stretching vibration of ring and the C-O stretching with contributions from C-C-H and C-O-H deformation (Larosa et al., 2018). An ether group (-O-C-O-) was identified at 1079  $\text{cm}^{-1}$  and a carbonyl group (C=O) at 1022  $\text{cm}^{-1}$ , although some authors attribute some peaks in this area to alkoxy groups (Yu et al., 2017). Other minor peaks observed at 887  $\text{cm}^{-1}$  and 815  $\text{cm}^{-1}$  probably represented functional groups associated to residues of uronic or mannuronic acids present in the alginate structure (Cardenas-Jiron et al., 2011). In the case of Br8 cells sample (Fig. S1), the region between 3000 and 2800  $\text{cm}^{-1}$  presented the typical C-H stretching vibrations (VC-H) corresponding to the CH<sub>3</sub> and >CH<sub>2</sub> functional groups of macromolecules like lipids, and the O-H stretching band (VO-H) corresponding to hydroxyl groups of bacterial cells (Ruiz-Fresneda et al., 2020). In particular, the peak at 2917  $\text{cm}^{-1}$  corresponded to stretching vibrations of -C-H- aliphatic groups (Larosa et al.,

2018). The region between 1800 and 750  $\text{cm}^{-1}$ , exhibited vibrations of C–H,  $>\text{CH}_2$ , and  $\text{CH}_3$  groups, amides, carbonyl groups, and polysaccharides. For instance, 1639 and 1535  $\text{cm}^{-1}$  were attributed to proteins containing amide I (stretching  $\text{C}=\text{O}$  ( $\nu_{\text{C}=\text{O}}$ )) and amide II (combination of bending N–H ( $\delta_{\text{N-H}}$ ) and contributions from stretching C–N ( $\nu_{\text{C-N}}$ ) groups) bands, respectively (Ojeda et al., 2008). The peak around 1404  $\text{cm}^{-1}$  is due to the symmetric stretching C–O of carboxylate groups ( $\nu_{\text{sym COO}^-}$ ). Bands related to phosphate containing macromolecules included 1237  $\text{cm}^{-1}$  peak (double bond stretching of  $>\text{P}=\text{O}$  of general phosphoryl groups and phosphodiester of nucleic acids), 1070  $\text{cm}^{-1}$  peak (stretching of  $\text{P}=\text{O}$  groups from polyphosphates, nucleic acids phosphodiesters and phosphorylated proteins), and 933  $\text{cm}^{-1}$  peak (asymmetric O–P–O stretching modes) (Jiang et al., 2004; Yee et al., 2004; Dittrich and Sibling, 2005). However, for the third sample, that of alginate with Br8 biomass (Fig. S1), it should be noted that only two bands corresponding to 1237  $\text{cm}^{-1}$  (related to phosphate containing macromolecules, able to complex metals (Merroun et al., 2003)) and 1539  $\text{cm}^{-1}$  (NH bending of the secondary amide group CONH (amide II band; Merroun et al., 2003)) were associated to Br8 cells since all other peaks corresponded to abiotic alginate sample, as showed above. The position of some of the peaks present in Br8-doped beads resulted to be shifted in comparison with those obtained when analyzing abiotic beads (Fig. S1), suggesting their potential role in the interaction process between cells and the alginate bead (Vodnar et al., 2010; Vaziri et al., 2018). Some of the groups detected in these samples (alkynyl, hydroxyl, and alkoxy) have been already detected in the surface of Ca-alginate beads and proposed to be involved in the U(VI) adsorption process by providing unshared pair electrons (Yu et al., 2017).

*Supplementary figures/tables*

**Table Supplementary 1.** Multiparameter evaluation of the different biomass immobilization systems selected in this study: Na-alginate beads, tetraethyl orthosilicate (TEOS)-based system, and a hybrid approach.

A – High, B – Medium, C – Low.

	<b>Alginate beads</b>	<b>TEOS</b> (Tetraethyl orthosilicate)	<b>Hybrid approach</b>
<i>Mechanical stability</i> * <sup>1</sup>	High	Low	Low
<i>Chemical stability</i> * <sup>2</sup>	Medium	High	Medium
<i>Matrix porosity</i>			
<i>Cell distribution</i>			

\*<sup>1</sup>Mechanical stability was assessed taking into account the morphology intactness using optical microscope and scanning transmission electron microscope after continuous shaking (165 rpm) for 24h.

\*<sup>2</sup>Chemical stability was assessed taking into account the morphology intactness using optical microscope and scanning transmission electron microscope after exposing to different chemical agents for 1h, 5h and 24h.

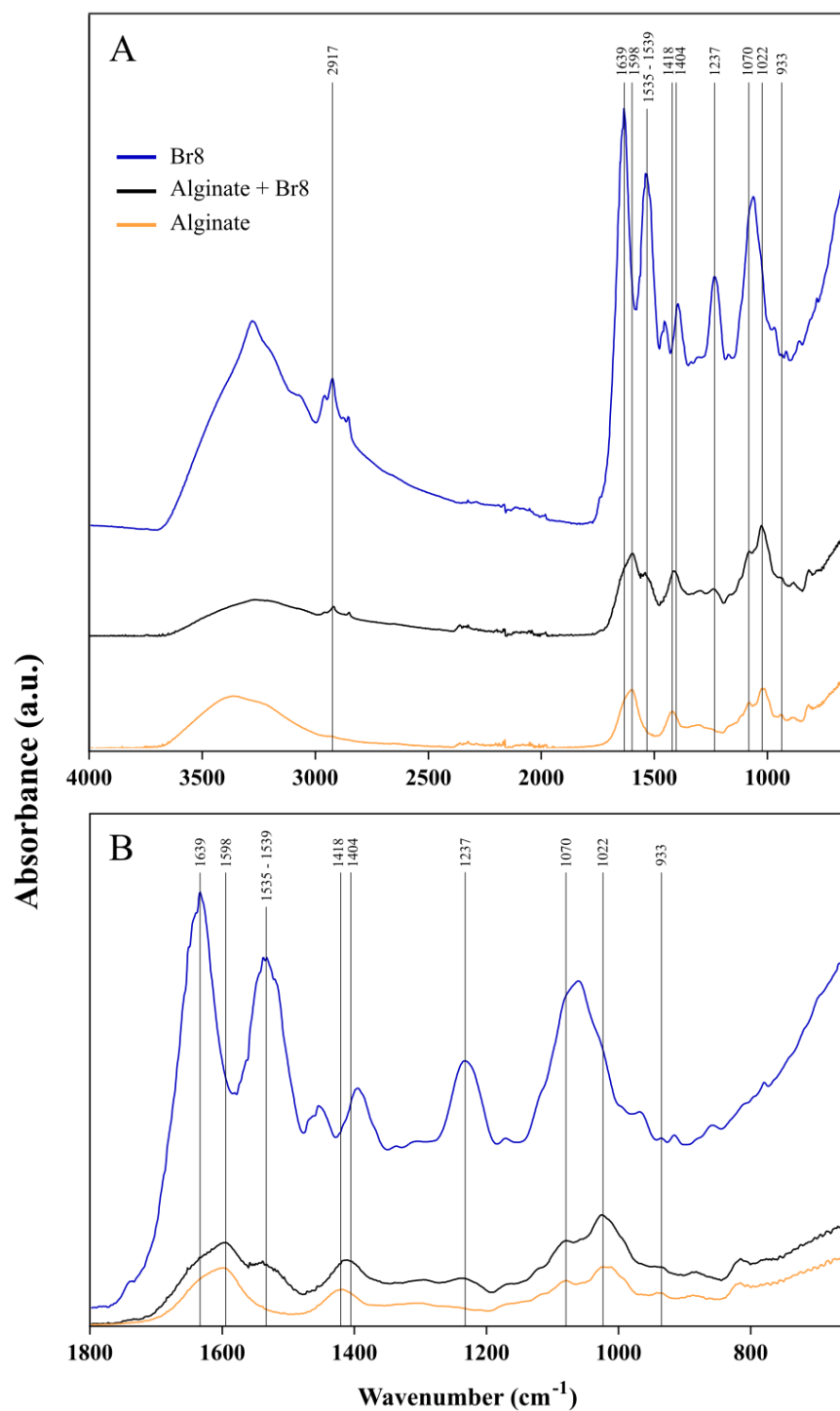


**Fig. Supplementary 1.** Fourier Transform Infrared spectra obtained from samples of Br8-cells, Br8-cells embedded in Na-alginate matrix and abiotic Na-alginate matrix (A). Region between 1800 and 600 cm<sup>-1</sup> was amplified for detailed analysis (B).



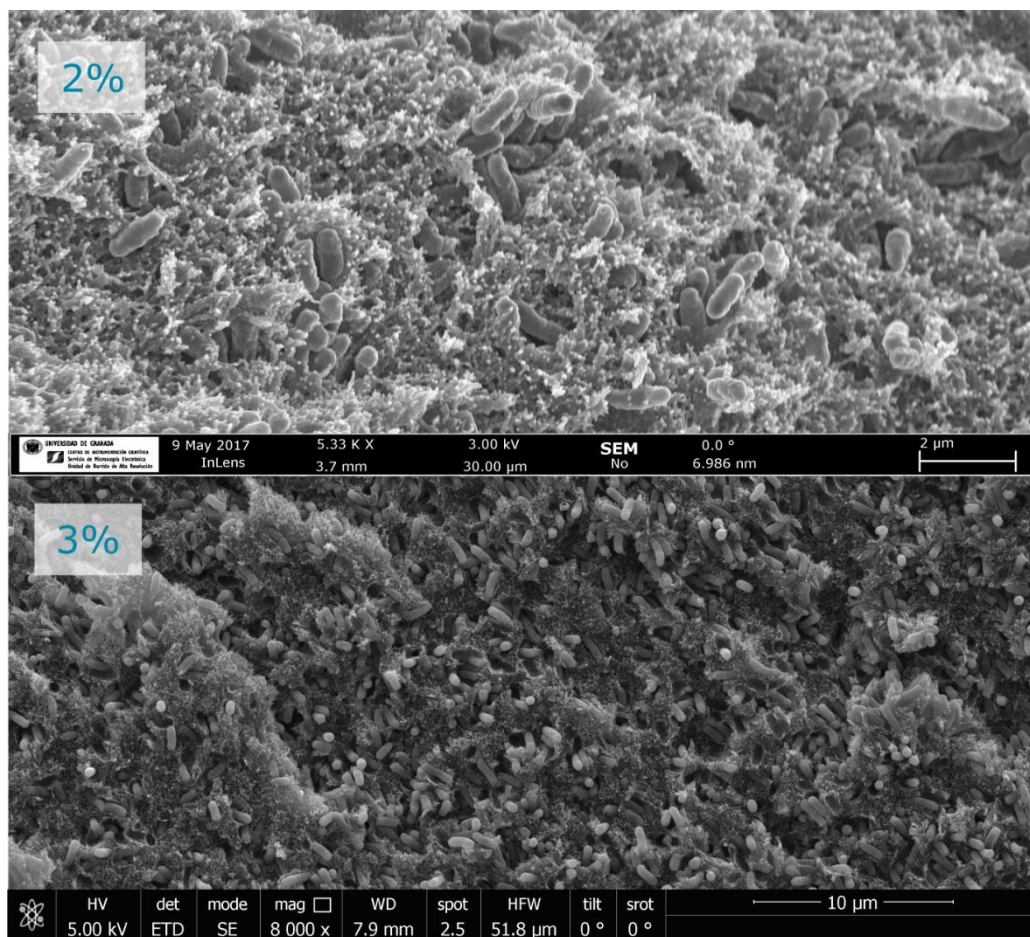


**Fig. Supplementary 2.** ESEM micrographs of the inner part of 2% and 3% Na-alginate beads doped with *Stenotrophomonas* sp. Br8 cells showing homogeneous distribution of cells.

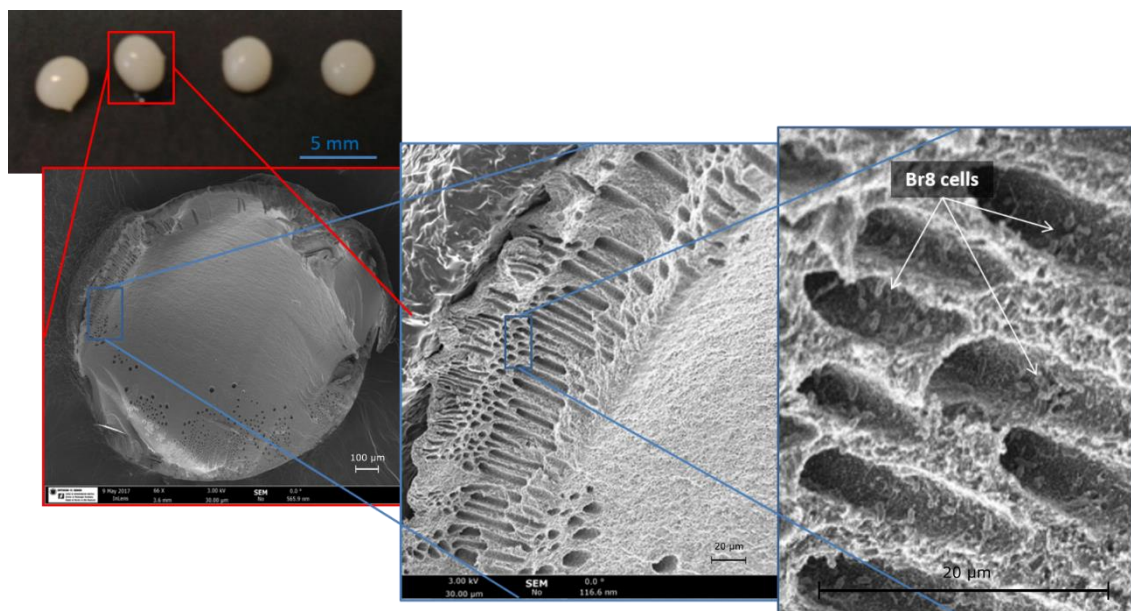


**Fig. Supplementary 3.** ESEM micrographs of the inner part of 4% Na-alginate beads doped with *Stenotrophomonas* sp. Br8 cells ( $\sim 1.5 \cdot 10^7$  CFU / g bead). Upper left image shows a bead seen without microscope. The other 3 images show the view of the same bead under different SEM microscopy magnifications.

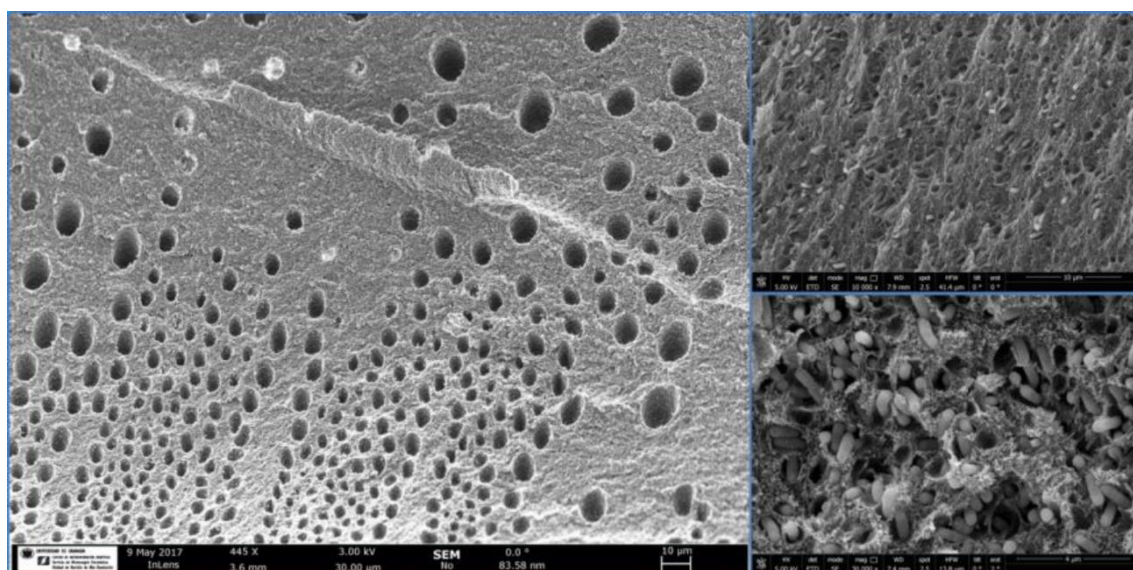


**Fig. Supplementary 4.** ESEM micrographs of the inner part of 4% Na-alginate beads doped with *Stenotrophomonas* sp. Br8 cells ( $\sim 1.5 \cdot 10^7$  CFU / g bead). Macro-pores are present at surface level in different areas of the bead surface (left). Numerous micro-pores were also observed inside (right).

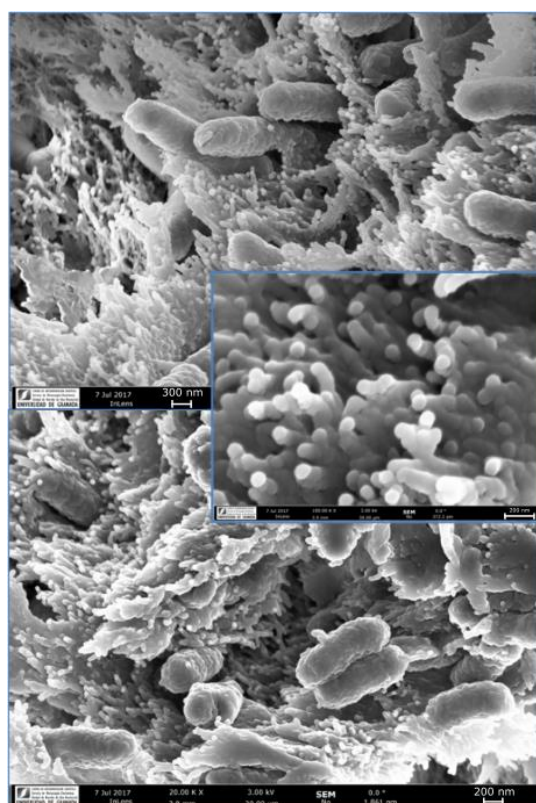


**Fig. Supplementary 5.** ESEM micrographs of the inner part of 4% Na-alginate beads doped with *Stenotrophomonas* sp. Br8 cells ( $\sim 1.5 \cdot 10^7$  CFU / g bead) showing matrix structure in detail.



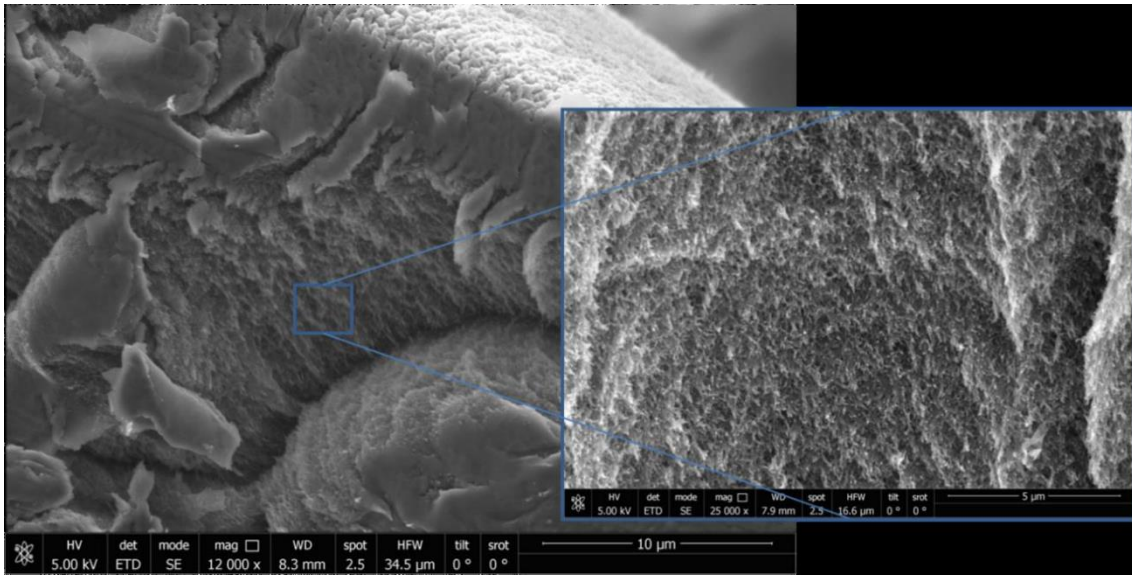


**Fig. Supplementary 6.** ESEM micrographs of the inner part of 4% abiotic Na-alginate beads showing matrix structure.

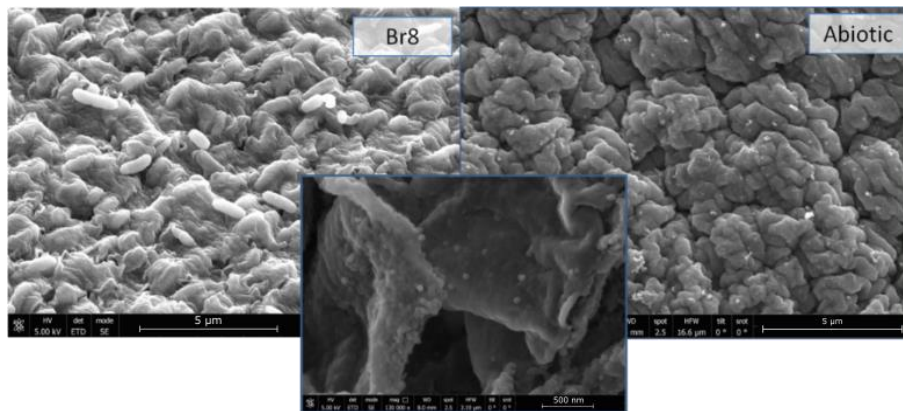


**Fig. Supplementary 7.** ESEM micrographs of the surface of 4% Na-alginate beads doped and no-doped with *Stenotrophomonas* sp. Br8 cells. The image below is a detail of the surface where the round-shaped particles observed previously seem to be also forming this surface layer.

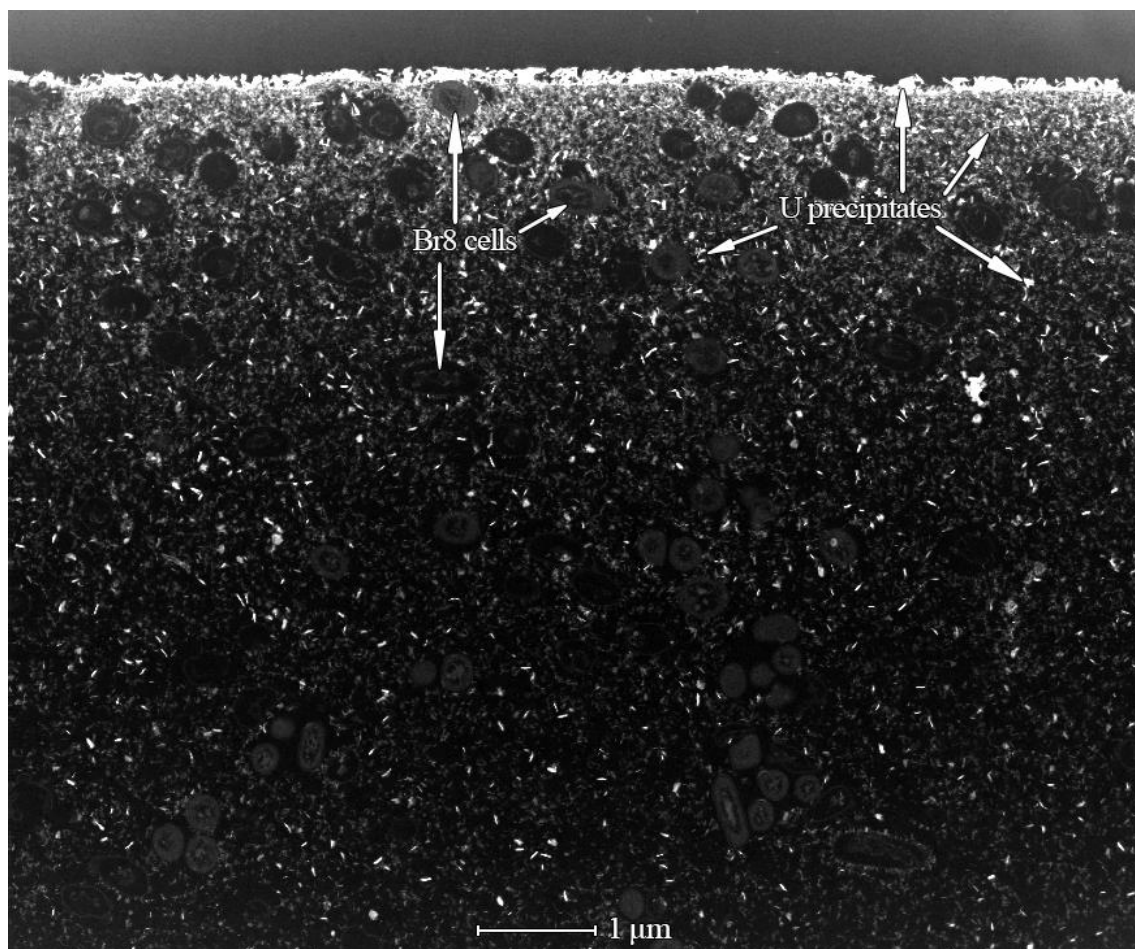


**Fig. Supplementary 8.** HAADF-STEM micrograph of a thin section of a 4% Na-alginate bead doped with *Stenotrophomonas* sp. Br8 cells ( $\sim 1.5 \cdot 10^7$  CFU / g bead) recovered after incubation (72 h; 28°C; 165 rpm) in natural COMI\_79 mining water (initial U concentration 47.4 mg/L; pH 7.75; amended with 5 mM G2P).

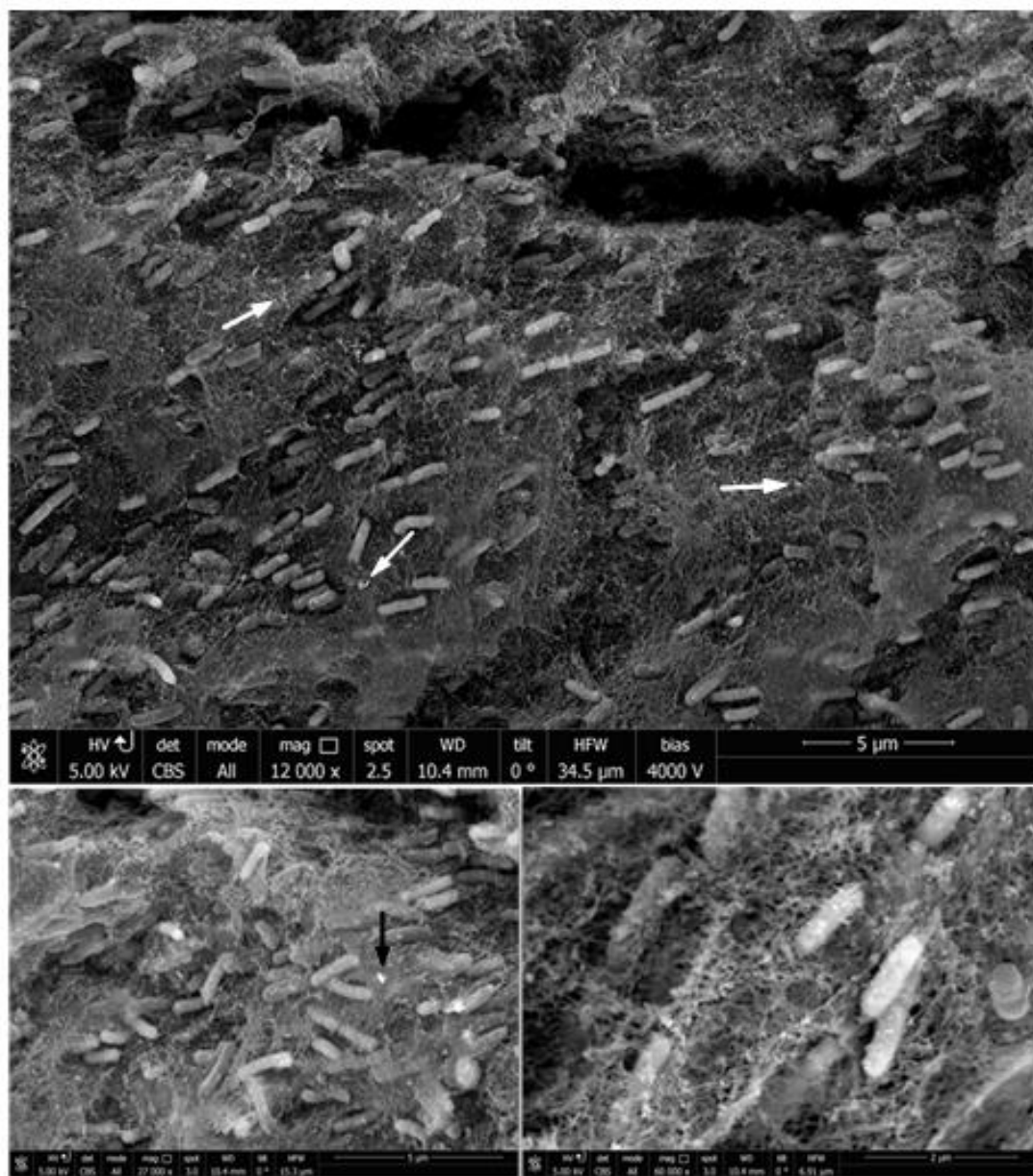


**Fig. Supplementary 9.** ESEM micrographs of the inner part of 4% Na-alginate beads doped with *Stenotrophomonas* sp. Br8 cells ( $\sim 1.5 \cdot 10^7$  CFU / g bead) recovered after incubation (72 h; 28°C; 165 rpm) in natural COMI\_79 mining water (initial U concentration 47.4 mg/L; pH 7.75; amended with 5 mM G2P). U precipitates are indicated with arrows.

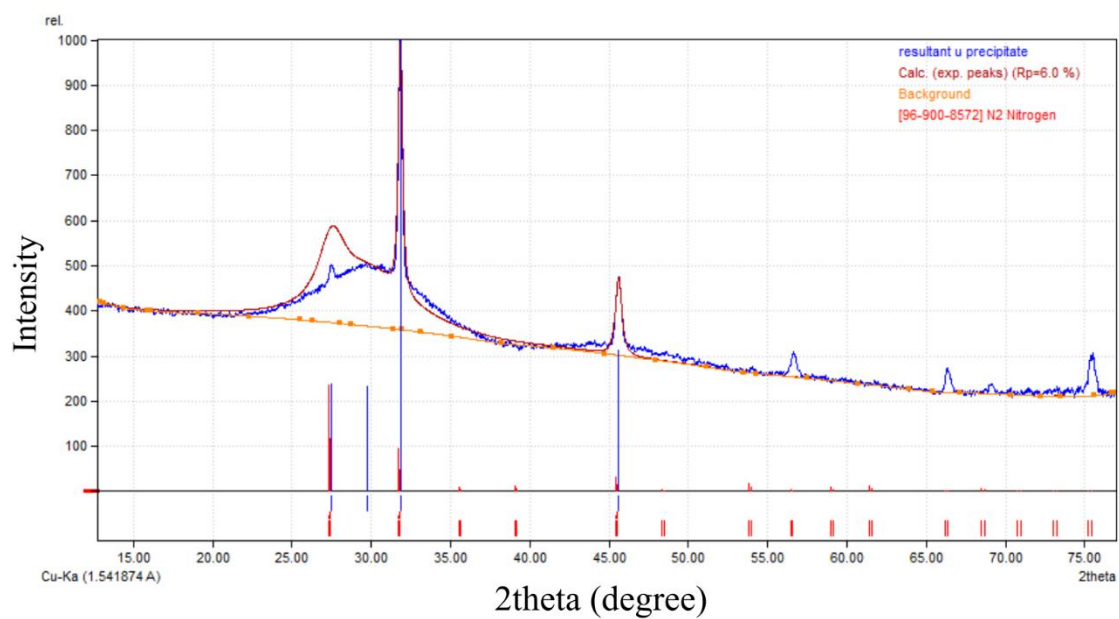


**Fig. Supplementary 10.** XRD analysis of precipitate generated during uranium biomineralization process.



# **DISCUSIÓN GENERAL**





Los microorganismos son los únicos seres vivos que han sido capaces de colonizar todos los nichos ecológicos conocidos (Baquero et al., 2021), siendo esenciales para el adecuado funcionamiento de los diferentes ecosistemas. Esta ubicuidad es debida a su alta versatilidad metabólica que les permite tomar parte de un gran número de reacciones (Knoll et al., 2012), entre ellas, frente a metales pesados. Estas interacciones entre microorganismos y metales pesados pueden ser aprovechadas para reducir la concentración de dichos elementos bajo determinadas condiciones. En los últimos años, el uso de microorganismos para la eliminación de metales pesados presentes en aguas contaminadas ha sido ampliamente estudiado con el objetivo de desarrollar tecnologías de biorremediación a gran escala aplicables en el medio ambiente (Areco et al., 2018; George et al., 2016; Miao et al., 2020; Nanda et al., 2019; Saunders et al., 2018; Sharma et al., 2021; Varjani and Upasani, 2021). Entre estos metales pesados contaminantes, el U es uno de los principales debido a su alta toxicidad (Gao et al., 2019). Su uso y manipulación en diferentes campos puede provocar la acumulación de altas concentraciones de este radionucleido que deben ser gestionadas adecuadamente para evitar graves efectos adversos. En esta tesis doctoral se estudió el uso de cepas bacterianas para su aplicación en biorremediación de U y se desarrolló una posible estrategia mediante la inmovilización de células en diferentes materiales inertes. Con el fin de seleccionar las cepas bacterianas más prometedoras se diseñó un proceso de evaluación de las propiedades más relevantes en biorremediación. En trabajos previos, llevados a cabo en el Grupo BIO103, se realizó el aislamiento de cepas microbianas presentes en aguas subterráneas de relaves cercanas a una antigua mina de U, caracterizando el potencial enzimático, uso de sustratos y su alta tolerancia a diferentes metales pesados (Sánchez-Castro et al., 2017). Tras este proceso de aislamiento y selección, las cepas *Stenotrophomonas* sp. Br8 y *Microbacterium* sp. Be9 fueron las más prometedoras para el desarrollo de este trabajo, principalmente debido a su tolerancia al U y capacidad de biomineralización de fosfatos de este radionucleido.

En primer lugar, **la caracterización a nivel molecular, fisiológico y bioquímico** de ambas cepas proporcionó información tanto de su identificación taxonómica como de sus capacidades de interacción con radionucleidos, en concreto con U. La anotación de sus genomas permitió obtener información sobre las secuencias codificantes de proteínas involucradas con la tolerancia al U y poder dilucidar los mecanismos activos/pasivos responsables en la bioabsorción y/o biomineralización de este metal pesado. La cepa Be9 fue clasificada en el género *Microbacterium*, el cual se distribuye ampliamente en diversos

## DISCUSIÓN GENERAL

ambientes naturales, como suelos, aguas, productos lácteos u otros organismos vivos (Kook et al., 2014; Lee et al., 2006; Yan et al., 2017). Esta cepa bacteriana mostró previamente tolerancia a diferentes metales como U, Pb, Zn o Se (Sánchez-Castro et al., 2017). Mediante la anotación de su genoma se predijeron secuencias codificantes de proteínas, destacando aquellas que correspondían a proteínas relacionadas con la resistencia a antibióticos y compuestos tóxicos, a transportadores de membrana y a respuestas frente al estrés. En su secuencia se identificaron la presencia de diversos genes o regiones codificantes para proteínas (p. ej. *amt*, *CzcD*, sideróforos ABC-type Fe<sup>3+</sup>, *CopC*, *DedA*, *ArsR*) vinculadas con una expresión regulada en presencia de metales y/o U (Fierros-Romer et al., 2016; Gallois et al., 2018; Mouser et al., 2009). También se predijeron secuencias codificantes para proteínas relacionadas con la solubilización de fosfatos, como *PstA*, *PstB* y *PstC*, las cuales se expresan ante situaciones limitantes de P (Brito et al., 2020; N'Guessan et al., 2010), o secuencias de glucosa deshidrogenasas, principales responsables de la solubilización de P inorgánicos (Liang et al., 2020). Por otro lado, la cepa Br8 fue identificada como *Stenotrophomonas lactitubi* mediante un análisis ANI (*Average Nucleotide Identity*) con todos los genomas de las especies tipo del género, al superar el umbral establecido para nuevas especies (95-96%) (Richter and Rosselló-Móra, 2009). Esta cepa mostró alta tolerancia a diferentes metales como U, Cd, Se, Eu o Zn, además de una alta actividad enzimática de la fosfatasa alcalina y ácida, confirmando su potencial en la biomineralización de metales pesados. La anotación de su genoma predijo secuencias codificantes de proteínas, pertenecientes a transporte de membrana, resistencia de antibióticos y compuestos tóxicos, y respuestas de estrés metabólico. En concreto, destacó la presencia de regiones codificantes para transportadores tipo-ABC glicerol-3-fosfato y glicerol-3-fosfato aciltransferasas, los cuales han mostrado una expresión alta ante la presencia de U (Gallois et al., 2018). Además, los genes *phoU*, *phoB* y *phoR* están presentes en el genoma de Br8, cuya función en la captación de P en condiciones limitantes (Hirota et al., 2010) podría estar involucrada con su actividad de biomineralización. Regiones codificantes de la superóxido dismutasa, la glutatión sintetasa y glutaredoxinas, las cuales tienen un papel defensivo contra el estrés oxidativo provocado en ocasiones por concentraciones altas de U (Dekker et al., 2016; Orellana et al., 2014), se encontraron en el genoma de Br8, al igual que regiones relacionadas con la homeostasis de Fe, asociadas a genes expresados en microorganismos en presencia de U (Khare et al., 2020) y Cr (Gao et al., 2020). Recientemente, se ha demostrado que la cepa BII-R7, perteneciente al género *Stenotrophomonas*, aumenta la expresión de genes implicados en la síntesis de la pared

celular (CreD y OmpA), el transporte de compuestos tóxicos, y de fosfatasa ácidas/alcalinas ante la exposición de U (Pinel-Cabello et al., 2021).

Gracias a toda la información obtenida, ambas cepas fueron seleccionadas y ensayadas en presencia de U para el desarrollo de posibles estrategias de biorremediación.

En primer lugar, se investigó el proceso de eliminación de U en soluciones acuosas mediante la cepa *Microbacterium* sp. **Be9**. Tras varios ensayos, se comprobó que la presencia de fosfatos afectaba a la capacidad de precipitación del metal, de modo que se investigó el efecto de la ausencia y presencia de fosfatos orgánicos e inorgánicos en la biomineralización de U. En estudios previos, se han investigado multitud de factores ambientales que pueden afectar a la biomineralización de U, como el pH (Beazley et al., 2007; Chandwadkar et al., 2018; Zhang et al., 2018), temperatura (Li et al., 2013), presencia de carbonatos (Wei et al., 2019), adición de  $\text{NH}_4^+$  (Yong and Macaskie, 1995) o la presencia de materia orgánica (Boiteau et al., 2018; Medina et al., 2017). En los ensayos realizados en el marco de esta tesis doctoral, se demostró que, en presencia tanto de fosfatos orgánicos como inorgánicos, la capacidad de eliminación de U por la cepa Be9 se reduce drásticamente, sin embargo, en un sistema libre de fosfatos eliminó hasta el 88% a través de biomineralización intracelular de U. Posteriormente, se confirmó que en presencia de fosfatos de U previamente precipitados, la cepa Be9 es capaz de solubilizar el metal a través de un proceso metabólicamente activo.

En el modelo propuesto en este capítulo, la primera etapa del proceso de biomineralización sería una bioadsorción superficial en la membrana de las células de Be9. Las superficies bacterianas actúan como sitios de unión donde se forman compuestos de U, para posteriormente, combinar un proceso de sorción hacia el interior de la célula, con otro de biomineralización de fosfatos de U mediante enzimas fosfatasa (Pan et al., 2015; Theodorakopoulos et al., 2015). Las membranas desempeñan un papel importante en la adsorción de metales debido a la contribución de interacciones electrostáticas entre las especies metálicas con carga positiva y grupos funcionales de carga negativa (p. ej. los grupos fosfato o carboxilato). Las bacterias Gram positivas (como la cepa Be9) exhiben una mayor capacidad de bioadsorción que las Gram negativas debido a los componentes de su envoltura celular (Hufton et al., 2021). En Liu et al., (2015) demostraron el papel de los grupos funcionales carboxilo, fosforilo y amino de la cepa *Synechococcus* sp. PCC 7002 como ligandos a nivel de superficie para elementos metálicos mediante estudios

## DISCUSIÓN GENERAL

potenciométricos. De forma similar, se caracterizaron las propiedades químicas de la superficie celular de la cepa Be9 mediante titulación potenciométrica y análisis por la técnica XPS. La carga de cero protones de pH ( $\text{pH}_{\text{zpc}}$ ) detectada fue alrededor de  $6.61 \pm 0.07$ , lo que indicó que las células Be9 desarrollan una carga neta negativa bajo el valor de pH estudiado en este trabajo (pH 7). Estos datos mostraron que la atracción electrostática es favorable entre grupos ionizantes negativamente (p. ej. grupos carboxilo, fosforilo e hidroxilo) con especies U cargadas positivamente (p. ej.  $(\text{UO}_2)_3(\text{OH})_5^+$  o  $(\text{UO}_2)_4(\text{OH})_7^+$ ), siendo estas dos últimas especies las más presentes en la solución estudiada (78% y 20%, respectivamente). En el caso del sistema libre de fosfatos, los grupos ionizantes negativos de la pared celular podrían adsorber el 70% de los compuestos de U cargados positivamente en los primeros 10 minutos, como se detectó en los estudios de cinética de eliminación de U. Por otro lado, el análisis por XPS mostró una alta proporción de polisacáridos en la superficie celular de la cepa Be9, los cuales han sido descritos como responsables de un papel importante en la mejora de la tolerancia de los microorganismos bajo estrés por metales (Sun et al., 2020). Previamente, en superficies celulares de *Pseudomonas putida* se obtuvieron porcentajes de péptidos similares a los de Be9, estando involucrados en la interacción con partículas nZVI/Pd (Lv et al., 2017).

Tras el mecanismo de adsorción en superficie, la segunda etapa sería una precipitación metabólicamente activa de fosfatos de U tanto intracelular como extracelularmente. La mayor capacidad de eliminación de U en el sistema libre de fosfatos se alcanzó a las 24 h, demostrando que, tras la primera etapa rápida mediada por un proceso pasivo, esta segunda etapa es más lenta, inducida por procesos metabólicos, como la acumulación intracelular y/o la biomineralización. Este mecanismo de eliminación de U bifásico también ha sido descrito en otros trabajos con diferentes cepas bacterianas como *Acidovorax facilis* (Gerber et al., 2016), *Stenotrophomonas bentonitica* BII-R7 (Pinel-Cabello et al., 2021) o *Microbacterium* sp. A9 (Theodorakopoulos et al., 2015). La alta capacidad de eliminación de U de esta cepa de *Microbacterium* es comparable a la de otras cepas del mismo género. Por ejemplo, *Microbacterium* sp. Ni1, *Microbacterium* sp. Ni7, *Microbacterium* sp. Ni17 y *Microbacterium* sp. CrF acumularon entre un 52 – 90% a las 12 h y un 38 – 60% del U presente a las 48 h (Islam and Sar, 2016). Además, alrededor de 77 mg de U se lograron eliminar mediante la cepa *Microbacterium oxydans* S15-M2 (Nedelkova et al., 2007), y entre un 86 – 94 % de eliminación de U fue detectada por *Microbacterium* sp. A9 tras 24 h a diferentes concentraciones (Theodorakopoulos et al., 2015). Las micrografías obtenidas

por STEM (*Scanning transmission electron microscopy*) mostraron precipitados en forma de *agujas* en el espacio intracelular, los cuales estaban formados por U y P. Esta morfología de los fosfatos de U en forma de *agujas* fue observada previamente en otros trabajos (Lopez-Fernandez et al., 2018), y también en el género *Microbacterium* (Theodorakopoulos et al., 2015). En este trabajo, aunque la actividad fosfatasa detectada en la cepa Be9 era débil, se evidenció la presencia de biominerales identificados como fosfatos de U, lo cual puede indicar que la biomineralización no esté asociada a dicha actividad fosfatasa. La presencia de estas estructuras en forma de *aguja* podría surgir de la interacción del U con los ortofosfatos ya existentes en el interior celular, como gránulos de polifosfatos (poli-Ps), ya que no se agregó ninguna fuente exógena en este caso. Trabajos previos han descrito algunas cepas bacterianas capaces de precipitar U sin fuentes adicionales de fósforo (Pan et al., 2015; Zhang et al., 2018). Estos gránulos de polifosfatos son polímeros ubicuos que se encuentran en muchos microorganismos (Seufferheld et al., 2008), los cuales contienen grandes cantidades de ortofosfatos unidos mediante enlaces fosfoanhídrido formando polímeros lineales (Mandala et al., 2020). Los poli-Ps poseen varias funciones biológicas incluida la eliminación de fosfato, la quelación de metales, respuesta al estrés (Achbergerová and Nahálka, 2011), o acumulación de metales pesados y radionúclidos (Acharya and Apte, 2013; Brim et al., 2000; Villagrasa et al., 2020).

En el caso concreto del U, numerosos estudios han mostrado la inmovilización de este metal mediante polifosfatos intracelulares a través de diferentes análisis como TEM (*Transmission electron microscopy*) y EDX (*Energy-dispersive X-ray spectroscopy*) (Li et al., 2016; Merroun et al., 2006, 2003; Suzuki and Banfield, 2004). En el presente trabajo se deduce que la presencia de U en el interior de las células Be9 induce la actividad de enzimas como la exopolifosfatasa para degradar polifosfatos ya presentes, liberando así ortofosfatos que provocan la biomineralización de U. En Theodorakopoulos et al., (2015) se propone una inducción de vías enzimáticas en una cepa de *Microbacterium* que causa la ruptura de los gránulos de poli-Ps presentes en el citoplasma para la posterior biomineralización intracelular de U. No obstante, para producir esta inmovilización intracelularmente, es necesaria una absorción del U al interior, para lo cual se ha descrito un mecanismo principal compuesto de dos etapas: en primer lugar, un proceso activo mediante transportadores de metales para elementos esenciales y tras esto, un proceso pasivo provocado por el aumento de la permeabilidad de la membrana celular ante el daño provocado por metales tóxicos (Suzuki and Banfield, 1999). En el caso del género

## DISCUSIÓN GENERAL

*Microbacterium*, se ha demostrado que las proteínas transportadoras de Fe están involucradas en la acumulación intracelular de U por parte de *Microbacterium oleivorans* A9 (Gallois et al., 2018). Recientemente, ha sido descrita una proteína transmembrana presente en diferentes cepas de *Microbacterium* tolerantes a U, con afinidad específica de unión por los iones  $\text{UO}_2^{2+}$  y  $\text{Fe}^{3+}$  (Gallois et al., 2022). En el caso de la cepa Be9 se identificaron numerosas secuencias codificadoras de proteínas en su genoma, entre ellas, proteínas transportadoras de sideróforos  $\text{Fe}^{3+}$  tipo ABC (Martínez-Rodríguez et al., 2020), las cuales podrían estar implicadas en la captación de U.

En presencia de G2P como fuente de fosfatos orgánicos, las células de Be9 mostraron una baja capacidad de eliminación de U (10%) en comparación con el tratamiento libre de fosfatos. A pesar de que no se detectó actividad fosfatasa, la cual sería responsable de catalizar la hidrólisis del G2P en glicerol y ortofosfatos (Beazley et al., 2011; Liang et al., 2016; Merroun et al., 2011), se detectó una cierta concentración de ortofosfatos libres en solución. Por tanto, dado que el G2P añadido no es degradado extracelularmente, es probable que sea transportado intracelularmente para ser utilizado como fuente de carbono orgánico durante el metabolismo de carbohidratos y lípidos. Esta hipótesis está respaldada por el hecho de que en la secuencia del genoma de Be9 se identificaron genes que codifican proteínas para la captación y utilización de G3P y glicerol (p. ej. transportadores ABC de glicerol-3-fosfato, proteína de unión a ATP UgpC, glicerol-3-fosfato deshidrogenasa o glicerofosforil diéster fosfodiesterasa). Gallois et al., (2018) revelaron una regulación positiva de proteínas que implican el transporte de glicerol-3-fosfato en las células de *Microbacterium oleivorans* A9 tratadas con U. En contraste con las condiciones anteriores (sistema libre de fosfato), la viabilidad celular bajo la presencia de U y G2P aumentó de 24 a 48 h de incubación, lo que apoya la suposición de que las células Be9 utilizan G2P como fuente de carbono o fósforo.

En el caso de los ensayos abióticos en presencia de una fuente de fosfatos inorgánicos, se observó que prácticamente la totalidad del U era precipitada (92 – 99%) en forma de fosfatos y carbonatos de U. Sin embargo, en presencia de actividad bacteriana se redujo su eliminación notablemente (13 – 23%), señalando que su metabolismo afecta a la precipitación previamente mostrada. Esto se demostró en ensayos posteriores, donde la presencia de las células de Be9 provocó la re-solubilización de los fosfatos de U añadidos (94,5%). Los microorganismos conocidos como PSB (*Phosphate solubilizing bacteria*), entre los que se encuentran algunas especies del género *Microbacterium*, son capaces de

solubilizar compuestos insolubles de fósforo orgánico e inorgánico (Ahemad, 2015). Se conoce que los mecanismos de solubilización de fosfato por parte de cepas PSB involucran a grupos hidroxilo y carboxilo presentes en las células o en los ácidos orgánicos liberados (Chen et al., 2006). Además, han sido descritos una serie de genes que codifican enzimas responsables de la solubilización de P (p. ej. *gcd* que codifica la quinoproteína glucosa deshidrogenasa, la subunidad de liasa *phnP* C-P (PhnP), la fosfatasa alcalina *phoA* (PhoA), la fosfatasa alcalina *phoD* (PhoD) y la fosfatasa ácida *phoN* (clase A)) (Rawat et al., 2021). En el presente trabajo, se detectó la actividad movilizadora de U por parte de *Microbacterium* Be9 al reaccionar con fosfatos inorgánicos, confirmando su comportamiento como cepa perteneciente al grupo de PSB. Este hecho indicó que el mecanismo que lleva a cabo dicha cepa bacteriana puede implicar la solubilización de fosfatos previamente precipitados y, en consecuencia, la liberación del metal pesado asociado, volviendo a un estado soluble, y, por tanto, más tóxico. Estos resultados proporcionan nuevos conocimientos sobre el impacto de las bacterias en el ciclo biogeoquímico del U en presencia de diferentes formas de fosfatos, lo que permite comprender las condiciones relacionadas con las fases minerales biogénicas de fosfato de U y las estrategias de biomineralización limitantes en condiciones oxidantes. Por lo tanto, la importancia de conocer la diversidad microbiana y su papel en este tipo de procesos es crucial para lograr la correcta aplicación de la tecnología de biorremediación seleccionada.

En el capítulo 4, se investigó la capacidad de eliminación de U soluble por parte de la cepa bacteriana *Stenotrophomonas* sp. **Br8** en presencia de G2P. Se estudiaron diferentes factores que influyen en este proceso, como el tiempo de incubación, la concentración de biomasa, el pH y la temperatura. Aunque ya se han documentado ciertos trabajos sobre la eliminación de U en soluciones acuosas mediante cepas bacterianas en presencia de una fuente de fosfatos orgánicos (Beazley et al., 2009; Nie et al., 2022; Povedano-Priego et al., 2019), en esta sección de la tesis doctoral se ensayó el potencial de esta cepa, previamente aislada en nuestro grupo de investigación, para tolerar e inmovilizar altas concentraciones de U de forma eficiente bajo diferentes condiciones. Los ensayos en presencia de la cepa Br8 mostraron altos valores de precipitación de U en soluciones acuosas tanto a tiempos finales (aprox. 90% en 48 h), como en tiempos más tempranos (aprox. 50% en 3 h). Estos resultados sugirieron que la interacción entre el U y las células de Br8 podría ocurrir en dos etapas: a través de mecanismos mediados por procesos pasivos (p. ej. biosorción) y activos (p. ej. biomineralización). Los mecanismos metabólicamente independientes basados en la



## DISCUSIÓN GENERAL

captación del U en la superficie celular son los primeros que parecen detectarse en estos ensayos, coincidiendo con otros trabajos que han descrito la captación pasiva de radionucleidos de forma muy similar e igualmente rápida (Gerber et al., 2016; Huang et al., 2017; Manobala et al., 2019; Nie et al., 2022). Es conocido que diferentes grupos funcionales presentes en las membranas celulares (carboxilos, fosforilos o hidroxilo entre otros) proporcionan sitios de unión para metales u otros elementos tóxicos (Merroun et al., 2011; Moll et al., 2014; Ojeda et al., 2008; Reitz et al., 2015). Con respecto a los mecanismos activos de precipitación de U soluble mostrados por la cepa Br8, se confirmó que la actividad fosfatasa era la responsable de la eliminación del metal en esta etapa. La baja cantidad de fosfatos inorgánicos detectada en el medio durante las primeras 24 h sugieren que la cinética de este proceso está dirigida por la velocidad de liberación de dichos ortofosfatos, de modo que, mientras el U es soluble, los ortofosfatos libres se unen rápidamente a él, haciendo imposible su detección.

Los estudios llevados a cabo sobre el efecto de diferentes concentraciones de biomasa en el proceso de eliminación de U descrito, concluyeron que dicha capacidad no se vio afectada significativamente por este parámetro biológico, pero, sin embargo, la cantidad de ortofosfatos liberados variaron de forma no lineal dependiendo de la concentración de biomasa empleada. Por otro lado, el efecto del pH no resultó tampoco significativo en cuanto a las tasas de eliminación de U observadas, aunque la especiación del metal si presentó variaciones al variar el valor de pH, siendo la fase de biosorción pasiva más pronunciada a pH ligeramente ácido. Esto se debería a la presencia de complejos de hidroxilo cargados positivamente frente a complejos hidroxilo cargados negativamente a pH más alcalino. Se plantea la hipótesis de que, en esas condiciones de pH, ambos tipos de fosfatasas (alcalinas y ácidas) pudieran actuar con un efecto acumulativo, dado a que tanto en ensayos previos propios, como en trabajos de otros autores (Ambreen et al., 2020; Kulkarni et al., 2016), mostraron una mayor actividad enzimática. Sin embargo, la alta actividad fosfatasa asociada con niveles bajos de ortofosfatos liberados en condiciones de pH 5 y 0.5 mM U indicaron una reducción de la eficiencia enzimática, lo que coincide con lo descrito en otros trabajos (Chandwadkar et al., 2018). En cuanto al efecto de la temperatura, se observaron las máximas eficiencias de eliminación a 28 y 37 °C, mientras que la mayor concentración de fosfatos inorgánicos libres se detectó a 37 °C. Para la mayor parte de organismos mesófilos es bien conocido que la capacidad metabólica y enzimática (en particular la de la fosfatasa) se reduce cuando la temperatura es menor de 20°C (Behera et al., 2017;

González et al., 1994; Lee et al., 2015), lo cual se vio reflejado en la cepa Br8. Pocos estudios han logrado anteriormente tasas de eliminación similares en presencia de concentraciones de U y G2P como las presentadas aquí. En otros trabajos, únicamente al ensayar concentraciones de U más bajas con diferentes cepas bacterianas aisladas de ambientes con altos niveles de U, como *Rahnella* sp. Y9602, *Leifsonia* sp. J5 o *Serratia* sp. OT-II-7, se observaron tasas de inmovilización del metal superiores a 90% (Chandwadkar et al., 2018; Ding et al., 2018; Zeng et al., 2022). En Nazina et al., (2010), se lograron tasas de eliminación de U mucho más bajas mediante dos cepas del género *Stenotrophomonas* aisladas de vertederos de minería.

Tras la caracterización molecular realizada en este trabajo y en otros estudios previos, se confirma que las especies del género *Stenotrophomonas* pueden expresar una actividad fosfatasa alta. Por tanto, se evaluó el papel de esta enzima, presente en la cepa Br8, en la eliminación de U en forma de fosfatos. Los resultados señalaron que la actividad enzimática de Br8 depende de la concentración de U usada, siendo mayor en las concentraciones intermedias (0,1 y 0,5 mM) que en las altas (1 mM). Esto se puede deber a que, aunque la presencia de U potencia la actividad fosfatasa como protección a la toxicidad del metal, altas concentraciones de U y otros metales podrían disminuir la eficiencia de este mecanismo (Macaskie et al., 2000; Tabaldi et al., 2007; Vanadate et al., 1982; Xu et al., 2018). Esta actividad fosfatasa detectada en Br8 es la responsable de liberar fosfatos inorgánicos a partir del G2P añadido, los cuales pueden asociarse con el U soluble formando fosfatos de U(VI).

La técnica de microscopía STEM-HAADF/EDX fue utilizada para determinar la localización celular de los precipitados de U y dilucidar el mecanismo a través del cual la cepa Br8 inmoviliza el metal. En las micrografías obtenidas se localizaron precipitados de U en forma de “agujas” tanto en la superficie celular como en el espacio extracelular, mientras que intracelularmente no se observaron. Gracias a los datos obtenidos en los análisis de mapeo elemental y EDX, se confirmó que estas acumulaciones estaban compuestas principalmente por U y P. Los precipitados de U a nivel de la membrana celular probablemente se deban a la localización de las enzimas fosfatasa en dicha capa y, en consecuencia, a la potencial abundancia de grupos fosfato (Chandwadkar et al., 2018; Kulkarni et al., 2016). Esto sugirió que la cepa Br8 se protege de la toxicidad del U evitando su absorción y precipitándolo en el exterior. En general, los microorganismos que habitan en ambientes contaminados con metales pesados los acumulan en forma de minerales en el

espacio extracelular como mecanismo de defensa. En la cepa *Stenotrophomonas* sp. U18 se observó una estrategia similar cuando es incubada durante 1 h en una solución con una concentración de U de 160 mg/L (Islam and Sar, 2016). También se han observado precipitados intracelulares que contienen U en la cepa bacteriana *Stenotrophomonas maltophilia* JG-2, la cual fue aislada de desechos mineros de U (Merroun and Selenska-Pobell, 2008). Estos precipitados de U formados son muy estables durante largos periodos de tiempo en un amplio rango de pH, y su solubilidad no se ve alterada fácilmente, al contrario que los subproductos de la reducción del U (Beazley et al., 2011; Lloyd and Macaskie, 2002; Senko et al., 2002). Por otro lado, mediante la técnica EXAFS se obtuvieron datos estructurales sobre los minerales formados, los cuales mostraron una gran semejanza tanto entre sí como con el espectro control de minerales de fosfatos de U del grupo de meta-autunita ( $\text{Ca}(\text{UO}_2)_2(\text{PO}_4)_2 \cdot 10\text{-}12\text{H}_2\text{O}$ ). Esto indicó que la coordinación local de U(VI) dentro de las dos muestras consistía en fosfatos de U. Las transformadas de Fourier de los espectros mostraron 5 picos principales (U-O<sub>ax</sub>, U-O<sub>eq1</sub>, U-P, U-O<sub>eq1</sub>-P(MS) y U-U), dentro de los cuales la distancia del enlace U-O<sub>eq</sub> en ambas muestras coincide con los valores encontrados previamente entre el átomo de oxígeno presente en el enlace entre fosfato y uranilo (Merroun et al., 2011, 2003; Nedelkova et al., 2007). Los espectros EXAFS de las muestras bióticas tratadas con ambas concentraciones de U son similares a los de la m-autunita con respecto a las distancias de los enlaces U-O<sub>eq</sub>, U-P y U-U, lo que sugiere que este fosfato de uranio precipitado por las células Br8 es similar a la m-autunita.

En definitiva, todos estos resultados obtenidos mediante un amplio espectro de técnicas, ayudan a comprender los mecanismos de tolerancia bacteriana al U y el impacto de la cepa *Stenotrophomonas* sp. Br8 en la movilidad y el ciclo biogeoquímico de dicho metal. Al contrario que la cepa Be9, ésta presenta un comportamiento estable frente al U bajo condiciones diversas. También queda demostrado el potencial de esta cepa para la biorremediación de U mediante la combinación de procesos pasivos y activos, como son la biosorción y la posterior biomineralización de fosfatos de U(VI) (Chandwadkar et al., 2018). Además, dado que las enzimas fosfatasa también se activan en condiciones anaeróbicas (Rossolini et al., 1998), la biomineralización de la cepa Br8 puede ser una alternativa a la bio-reducción en presencia de G2P cuando la presencia de oxígeno es limitada. Por tanto, estos prometedores resultados fueron la base de los siguientes estudios en los que se usaron aguas mineras reales contaminadas con U y células de la cepa *Stenotrophomonas* sp. Br8 inmovilizadas en una matriz.

Para mejorar la aplicabilidad de esta prometedora tecnología, se evaluó la posibilidad de inmovilizar la biomasa de la cepa bacteriana objeto de estudio en una matriz inorgánica. Las estrategias de biorremediación mediante el uso de células inmovilizadas han mostrado una mayor eficiencia en comparación con estrategias basadas en el uso de células planctónicas, debido a la propia capacidad de sorción de la matriz usada, así como por una mejor conservación de la viabilidad y actividad bacteriana (Shi et al., 2018). Estas estrategias también suponen una serie de ventajas como una mayor estabilidad de almacenamiento y una mejor capacidad de reutilización (Dianawati et al., 2016; Shi et al., 2018). Con la finalidad de evaluar las diferentes estrategias para inmovilizar células de la cepa Br8, en el capítulo 5 se muestran resultados del estudio de diversos parámetros como la estabilidad mecánica/química, la presencia de grupos funcionales, la biocompatibilidad con la cepa Br8 y la morfología interna/externa. En el caso de las matrices de alginato, a pesar de que su estabilidad química es débil frente a quelantes de  $\text{Ca}^{2+}$ , este polímero es preferible a otros materiales principalmente debido a su alta biocompatibilidad, hidrofilia, presencia de grupos carboxilo (los cuales mejoran la adsorción de iones de metales pesados; Romera et al., 2007), su bajo coste económico, fácil adquisición y su baja biodegradabilidad ante diferentes condiciones (Lozinsky and Plieva, 1998; Wani et al., 2016).

El uso de matrices de alginato inoculadas con cepas bacterianas ha sido estudiado en repetidas ocasiones a lo largo de los últimos años como estrategia de biorremediación frente a metales como el plomo (Zhang et al., 2020), el cromo (El-Naggar et al., 2020; Wu et al., 2019), cadmio (Shi et al., 2018), uranio (Kulkarni et al., 2013) o cobre y zinc simultáneamente (Gopi Kiran et al., 2018). Además, su espectro de aplicación es muy amplio pues se han usado para remediar aguas residuales procedentes de industrias textiles (Galai et al., 2010; Rajendran et al., 2015) o contaminantes orgánicos (Mukherjee and Roy, 2013), así como agentes de control en agricultura (Ahmad et al., 2012). Dentro del propio género *Stenotrophomonas* también existen estudios centrados en la inmovilización de biocomponentes. Catecol dioxigenasas obtenidas de la cepa *S. maltophilia* KB2 fueron inmovilizadas en hidrogeles de alginato para biorremediar y desintoxicar ambientes contaminados con xenobióticos (Wojcieszynska et al., 2012). En cuanto a la eliminación de metales, otras cepas bacterianas han sido eficazmente inmovilizadas en microesferas de alginato (Gopi Kiran et al., 2018; Leong and Chang, 2020). En concreto, células del género *Trichoderma* (Akhtar et al., 2009, 2007) o del género *Aspergillus* (Wang et al., 2010) fueron inmovilizadas en microesferas de alginato exitosamente para recuperar el U procedente de

## DISCUSIÓN GENERAL

soluciones acuosas. Sin embargo, el capítulo 5 de esta tesis doctoral muestra resultados novedosos en la descripción y desarrollo de la biomineralización de fosfatos metálicos como estrategia de biorremediación. A pesar de que la inmovilización en esferas en alginato ha sido estudiada ampliamente, este trabajo profundiza y optimiza la precipitación de U presente en aguas reales contaminadas mediante células inmovilizadas de la cepa *Stenotrophomonas* sp. Br8 en microesferas de alginato.

Los ensayos cinéticos del proceso de inmovilización de U mediante el uso de la cepa Br8 inmovilizada en microesferas de alginato, mostraron una primera etapa de eliminación rápida del metal (un 38% en 7 h) seguida de una segunda etapa gradual más lenta donde se alcanzó el valor máximo (98% a las 72 h). Estos resultados sugieren que existen varios tipos de interacción durante el proceso, ya que en las primeras horas parece tener lugar un mecanismo pasivo de bioadsorción del U en la superficie de las células y/o en la propia matriz de las microesferas, como se ha observado en otros estudios (Gok and Aytas, 2009; Sánchez-Castro et al., 2020; Wang et al., 2010; Yu et al., 2017). Además de los grupos funcionales presentes en las membranas bacterianas responsables de la unión del U (como se describe anteriormente en los mecanismos de las cepas Be9 y Br8), es probable que participen grupos detectados en la superficie de las microesferas (como grupos hidroxilo y alcoxi) (Yu et al., 2017) debido a que las microesferas abióticas lograron eliminar un 4% del U presente en la primera etapa pasiva. De forma similar a como se observó en los ensayos de eliminación de U con células libres de Br8 (capítulo 4), la tasa de liberación de fosfatos inorgánicos a través de enzimas fosfatasa controla la cinética de la inmovilización del U. El proceso de inmovilización de las células Br8 parece no afectar a la actividad fosfatasa de éstas, aunque en estos ensayos se demostró un retardo en la liberación en comparación con las células planctónicas.

De forma similar a lo observado en los ensayos de células planctónicas de Br8, los precipitados de U detectados por microscopía electrónica se localizaron principalmente alrededor de las células, probablemente debido a la mayor abundancia de fosfatasas en este nivel (Chandwadkar et al., 2018; Kulkarni et al., 2016). Del mismo modo que en los ensayos previos, no se observaron precipitados intracelulares, sugiriendo que las células permanecieron viables durante todo el proceso. Mediante mapeos elementales realizados por STEM y análisis espectroscópicos adicionales se observó que los precipitados formados eran fosfatos de U. Dichos compuestos ya han sido demostrados ser formados por diferentes cepas bacterianas (Beazley et al., 2009, 2007; Choudhary and Sar, 2011;

Povedano-Priego et al., 2019) y ser altamente estables en comparación con otros precipitados de U, como los complejos de carbonatos de U (Duff et al., 2004). Hasta ahora, la mayoría de trabajos que han utilizado la inmovilización de biomasa en microesferas de alginato para la eliminación de U se basan principalmente en mecanismos de sorción (Chen et al., 2020; Kolhe et al., 2020; Wang et al., 2010; Yu et al., 2017), que acaban generando precipitados de U de baja estabilidad.

Además, tras la evaluación de parámetros biológicos y fisicoquímicos determinantes en la eficiencia del proceso, se concluyó que el uso de un mismo número de células en un menor número de microesferas reduciría de forma significativa el coste económico del proceso de inmovilización, al mismo tiempo que ofrece unas tasas de eficiencia de eliminación de U prácticamente iguales. La posibilidad de almacenar este biomaterial en condiciones de bajas temperaturas (4°C) durante al menos 300 días sin comprometer su capacidad de biorremediación refuerza la relevancia de la estrategia planteada aquí. En trabajos previos lograron una buena conservación de la viabilidad de las células inmovilizadas en matrices inorgánicas similares tras 120 días (Ontañón et al., 2017) y 180 días (Brachkova et al., 2010; Zommere and Nikolajeva, 2017). En cuanto al proceso de liofilización aplicado y su alta efectividad en este trabajo, queda claro que la matriz de alginato juega un papel protector que puede reducir el deterioro fisiológico, manteniendo la viabilidad celular, el potencial metabólico y la estabilidad operativa (Amine et al., 2014).

En conclusión, este estudio determinó que la eliminación de U presente en aguas mineras reales mediante la inmovilización de la cepa *Stenotrophomonas* sp. Br8 en microesferas de alginato es una estrategia muy prometedora. Aunque la eliminación de U en soluciones acuosas es un tema que ha recibido una atención considerable en los últimos años, el tratamiento de aguas mineras reales permanece relativamente inexplorado. La precipitación de fosfatos de U en aguas mineras reales tiene una gran relevancia científica y ambiental, pero es un mecanismo difícil debido a la complejidad química del agua. Sin embargo, el proceso propuesto en este trabajo que incluye una liberación enzimática de fosfatos inorgánicos puede superar estas dificultades y precipitar eficientemente el U disuelto y, probablemente, otros metales pesados presentes en las aguas contaminadas.

## Bibliografía

- Acharya, C., Apte, S.K., 2013. Novel surface associated polyphosphate bodies sequester uranium in the filamentous, marine cyanobacterium, *Anabaena torulosa*. *Metallomics* 5, 1595–1598. <https://doi.org/10.1039/c3mt00139c>
- Achbergerová, L., Nahálka, J., 2011. Polyphosphate - an ancient energy source and active metabolic regulator. *Microb. Cell Fact.* 10, 1–14. <https://doi.org/10.1186/1475-2859-10-63>
- Ahemad, M., 2015. Phosphate-solubilizing bacteria-assisted phytoremediation of metalliferous soils: a review. *3 Biotech* 5, 111–121. <https://doi.org/10.1007/s13205-014-0206-0>
- Ahmad, M., Ahmad, M.M., Hamid, R., Abdin, M.Z., Javed, S., 2012. In vitro inhibition study against *A. flavus* with *Stenotrophomonas maltophilia* immobilized in calcium alginate gel beads. *J. Pure Appl. Microbiol.* 6, 597–608.
- Akhtar, K., Khalid, A.M., Akhtar, M.W., Ghauri, M.A., 2009. Removal and recovery of uranium from aqueous solutions by Calcium alginate immobilized *Trichoderma harzianum*. *Bioresour. Technol.* 100, 4551–4558. <https://doi.org/10.1016/j.biortech.2009.03.073>
- Akhtar, K., Waheed Akhtar, M., Khalid, A.M., 2007. Removal and recovery of uranium from aqueous solutions by *Trichoderma harzianum*. *Water Res.* 41, 1366–1378. <https://doi.org/10.1016/j.watres.2006.12.009>
- Ambreen, S., Yasmin, A., Aziz, S., 2020. Isolation and characterization of organophosphorus phosphatases from *Bacillus thuringiensis* MB497 capable of degrading Chlorpyrifos, Triazophos and Dimethoate. *Heliyon* 6, e04221. <https://doi.org/10.1016/j.heliyon.2020.e04221>
- Amine, K.M., Champagne, C.P., Salmieri, S., Britten, M., St-Gelais, D., Fustier, P., Lacroix, M., 2014. Effect of palmitoylated alginate microencapsulation on viability of *Bifidobacterium longum* during freeze-drying. *LWT - Food Sci. Technol.* 56, 111–117. <https://doi.org/10.1016/j.lwt.2013.11.003>
- Areco, M.M., Haug, E., Curutchet, G., 2018. Studies on bioremediation of Zn and acid waters using *Botryococcus braunii*. *J. Environ. Chem. Eng.* 6, 3849–3859. <https://doi.org/10.1016/j.jece.2018.05.041>
- Baquero, F., Coque, T.M., Galán, J.C., Martínez, J.L., 2021. The Origin of Niches and Species in the Bacterial World. *Front. Microbiol.* 12, 1–13. <https://doi.org/10.3389/fmicb.2021.657986>
- Beazley, M.J., Martínez, R.J., Sobecky, P.A., Webb, S.M., Taillefert, M., 2009. Nonreductive biomineralization of uranium(VI) phosphate via microbial phosphatase activity in anaerobic conditions. *Geomicrobiol. J.* 26, 431–441. <https://doi.org/10.1080/01490450903060780>
- Beazley, M.J., Martínez, R.J., Sobecky, P.A., Webb, S.M., Taillefert, M., 2007. Uranium biomineralization as a result of bacterial phosphatase activity: Insights from bacterial isolates from a contaminated subsurface. *Environ. Sci. Technol.* 41, 5701–5707. <https://doi.org/10.1021/es070567g>
- Beazley, M.J., Martínez, R.J., Webb, S.M., Sobecky, P.A., Taillefert, M., 2011. The effect of pH and natural microbial phosphatase activity on the speciation of uranium in subsurface soils. *Geochim. Cosmochim. Acta* 75, 5648–5663. <https://doi.org/10.1016/j.gca.2011.07.006>
- Behera, B.C., Yadav, H., Singh, S.K., Mishra, R.R., Sethi, B.K., Dutta, S.K., Thatoi, H.N., 2017. Phosphate solubilization and acid phosphatase activity of *Serratia* sp. isolated from mangrove soil of Mahanadi river delta, Odisha, India. *J. Genet. Eng. Biotechnol.* 15, 169–178. <https://doi.org/10.1016/j.jgeb.2017.01.003>
- Boiteau, R.M., Shaw, J.B., Pasa-Tolic, L., Koppelaar, D.W., Jansson, J.K., 2018. Micronutrient metal speciation is

- controlled by competitive organic chelation in grassland soils. *Soil Biol. Biochem.* 120, 283–291. <https://doi.org/10.1016/j.soilbio.2018.02.018>
- Brachkova, M.I., Duarte, M.A., Pinto, J.F., 2010. Preservation of viability and antibacterial activity of *Lactobacillus* spp. in calcium alginate beads. *Eur. J. Pharm. Sci.* 41, 589–596. <https://doi.org/10.1016/j.ejps.2010.08.008>
- Brim, H., McFarlan, S.C., Fredrickson, J.K., Minton, K.W., Zhai, M., Wackett, L.P., Daly, M.J., 2000. Engineering *Deinococcus radiodurans* for metal remediation in radioactive mixed waste environments. *Nat. Biotechnol.* 18, 85–90. <https://doi.org/10.1038/71986>
- Brito, L.F., López, M.G., Straube, L., Passaglia, L.M.P., Wendisch, V.F., 2020. Inorganic Phosphate Solubilization by Rhizosphere Bacterium *Paenibacillus sonchi*: Gene Expression and Physiological Functions. *Front. Microbiol.* 11, 1–21. <https://doi.org/10.3389/fmicb.2020.588605>
- Chandwadkar, P., Misra, H.S., Acharya, C., 2018. Uranium biomineralization induced by a metal tolerant: *Serratia* strain under acid, alkaline and irradiated conditions. *Metallomics* 10, 1078–1088. <https://doi.org/10.1039/c8mt00061a>
- Chen, C., Hu, J., Wang, J., 2020. Uranium biosorption by immobilized active yeast cells entrapped in calcium-alginate-PVA-GO-crosslinked gel beads. *Radiochim. Acta* 108, 273–286. <https://doi.org/10.1515/ract-2019-3150>
- Chen, Y.P., Rekha, P.D., Arun, A.B., Shen, F.T., Lai, W., Young, C.C., 2006. Phosphate solubilizing bacteria from subtropical soil and their tricalcium phosphate solubilizing abilities 34, 33–41. <https://doi.org/10.1016/j.apsoil.2005.12.002>
- Choudhary, S., Sar, P., 2011. Uranium biomineralization by a metal resistant *Pseudomonas aeruginosa* strain isolated from contaminated mine waste. *J. Hazard. Mater.* 186, 336–343. <https://doi.org/10.1016/j.jhazmat.2010.11.004>
- Dekker, L., Arsène-Ploetze, F., Santini, J.M., 2016. Comparative proteomics of *Acidithiobacillus ferrooxidans* grown in the presence and absence of uranium. *Res. Microbiol.* 167, 234–239. <https://doi.org/10.1016/j.resmic.2016.01.007>
- Dianawati, D., Mishra, V., Shah, N.P., 2016. Survival of Microencapsulated Probiotic Bacteria after Processing and during Storage: A Review. *Crit. Rev. Food Sci. Nutr.* 56, 1685–1716. <https://doi.org/10.1080/10408398.2013.798779>
- Ding, L., Tan, W. fa, Xie, S. bo, Mumford, K., Lv, J. wen, Wang, H. qiang, Fang, Q., Zhang, X. wen, Wu, X. yan, Li, M., 2018. Uranium adsorption and subsequent re-oxidation under aerobic conditions by *Leifsonia* sp. - Coated biochar as green trapping agent. *Environ. Pollut.* 242, 778–787. <https://doi.org/10.1016/j.envpol.2018.07.050>
- Duff, M.C., Hunter, D.B., Hobbs, D.T., Fink, S.D., Dai, Z., Bradley, J.P., 2004. Mechanisms of strontium and uranium removal from high-level radioactive waste simulant solution by the sorbent monosodium titanate. *Environ. Sci. Technol.* 38, 5201–5207. <https://doi.org/10.1021/es035415+>
- El-Naggar, N.E.A., El-khateeb, A.Y., Ghoniem, A.A., El-Hersh, M.S., Saber, W.E.I.A., 2020. Innovative low-cost biosorption process of Cr<sup>6+</sup> by *Pseudomonas alcaliphila* NEWG-2. *Sci. Rep.* 10, 1–18. <https://doi.org/10.1038/s41598-020-70473-5>
- Fierros-Romer, G., Gómez-Ramírez, M., Arenas-Isaac, G.E., Pless, R.C., Rojas-Avelizapa, N.G., 2016. Identification of *Bacillus megaterium* and *Microbacterium liquefaciens* genes involved in metal resistance and metal removal. *Can. J. Microbiol.* 62, 505–513. <https://doi.org/10.1139/cjm-2015-0507>
- Galai, S., Limam, F., Marzouki, M.N., 2010. Decolorization of an industrial effluent by free and immobilized cells of *Stenotrophomonas maltophilia* AAP56. Implementation of efficient down flow column reactor. *World J. Microbiol. Biotechnol.* 26, 1341–1347. <https://doi.org/10.1007/s11274-010-0306-x>



## DISCUSIÓN GENERAL

- Gallois, N., Alpha-Bazin, B., Bremond, N., Ortet, P., Barakat, M., Piette, L., Mohamad Ali, A., Lemaire, D., Legrand, P., Theodorakopoulos, N., Floriani, M., Février, L., Den Auwer, C., Arnoux, P., Berthomieu, C., Armengaud, J., Chapon, V., 2022. Discovery and characterization of UipA, a uranium- and iron-binding PepSY protein involved in uranium tolerance by soil bacteria. *ISME J.* 16, 705–716. <https://doi.org/10.1038/s41396-021-01113-7>
- Gallois, N., Alpha-Bazin, B., Ortet, P., Barakat, M., Piette, L., Long, J., Berthomieu, C., Armengaud, J., Chapon, V., 2018. Proteogenomic insights into uranium tolerance of a Chernobyl's Microbacterium bacterial isolate. *J. Proteomics* 177, 148–157. <https://doi.org/10.1016/j.jprot.2017.11.021>
- Gao, J., Wu, Shimin, Liu, Y., Wu, Shanghua, Jiang, C., Li, X., Wang, R., Bai, Z., Zhuang, G., Zhuang, X., 2020. Characterization and transcriptomic analysis of a highly Cr(VI)-resistant and -reductive plant-growth-promoting rhizobacterium *Stenotrophomonas rhizophila* DSM14405T. *Environ. Pollut.* 263, 114622. <https://doi.org/10.1016/j.envpol.2020.114622>
- Gao, N., Huang, Z., Liu, H., Hou, J., Liu, X., 2019. Advances on the toxicity of uranium to different organisms. *Chemosphere* 237, 124548. <https://doi.org/10.1016/j.chemosphere.2019.124548>
- George, K.S., Revathi, K.B., Deepa, N., Sheregar, C.P., Ashwini, T.S., Das, S., 2016. A Study on the Potential of Moringa Leaf and Bark Extract in Bioremediation of Heavy Metals from Water Collected from Various Lakes in Bangalore. *Procedia Environ. Sci.* 35, 869–880. <https://doi.org/10.1016/j.proenv.2016.07.104>
- Gerber, U., Zirnstein, I., Krawczyk-bärsch, E., Lünsdorf, H., Arnold, T., Merroun, M.L., 2016. Combined use of flow cytometry and microscopy to study the interactions between the gram-negative betaproteobacterium *Acidovorax facilis* and uranium(VI). *J. Hazard. Mater.* 317, 127–134. <https://doi.org/10.1016/j.jhazmat.2016.05.062>
- Gok, C., Aytas, S., 2009. Biosorption of uranium(VI) from aqueous solution using calcium alginate beads. *J. Hazard. Mater.* 168, 369–375. <https://doi.org/10.1016/j.jhazmat.2009.02.063>
- González, F., Martínez-Cañamero, M.M., Fárez-Vidal, M.E., Arias, J.M., 1994. Localization of acid and alkaline phosphatases in *Myxococcus coralloides* D. *Lett. Appl. Microbiol.* 18, 264–267. <https://doi.org/10.1111/j.1472-765X.1994.tb00865.x>
- Gopi Kiran, M., Pakshirajan, K., Das, G., 2018. Heavy metal removal from aqueous solution using sodium alginate immobilized sulfate reducing bacteria: Mechanism and process optimization. *J. Environ. Manage.* 218, 486–496. <https://doi.org/10.1016/j.jenvman.2018.03.020>
- Hirota, R., Kuroda, A., Kato, J., Ohtake, H., 2010. Bacterial phosphate metabolism and its application to phosphorus recovery and industrial bioprocesses. *J. Biosci. Bioeng.* 109, 423–432. <https://doi.org/10.1016/j.jbiosc.2009.10.018>
- Huang, W., Cheng, W., Nie, X., Dong, F., Ding, C., Liu, M., Li, Z., Hayat, T., Alharbi, N.S., 2017. Microscopic and Spectroscopic Insights into Uranium Phosphate Mineral Precipitated by *Bacillus Mucilaginosus*. *ACS Earth Sp. Chem.* 1, 483–492. <https://doi.org/10.1021/acsearthspacechem.7b00060>
- Hufton, J., Harding, J., Smith, T., Romero-González, M.E., 2021. The importance of the bacterial cell wall in uranium(vi) biosorption. *Phys. Chem. Chem. Phys.* 23, 1566–1576. <https://doi.org/10.1039/d0cp04067c>
- Islam, E., Sar, P., 2016. Diversity, metal resistance and uranium sequestration abilities of bacteria from uranium ore deposit in deep earth stratum. *Ecotoxicol. Environ. Saf.* 127, 12–21. <https://doi.org/10.1016/j.ecoenv.2016.01.001>
- Khare, D., Kumar, R., Acharya, C., 2020. Genomic and functional insights into the adaptation and survival of

- Chryseobacterium sp. strain PMSZPI in uranium enriched environment. *Ecotoxicol. Environ. Saf.* 191, 110217. <https://doi.org/10.1016/j.ecoenv.2020.110217>
- Knoll, A.H., Canfield, D.E., Konhauser, K., 2012. *Fundamentals of geobiology*. Wiley Online Library.
- Kolhe, N., Zinjarde, S., Acharya, C., 2020. Removal of uranium by immobilized biomass of a tropical marine yeast *Yarrowia lipolytica*. *J. Environ. Radioact.* 223–224. <https://doi.org/10.1016/j.jenvrad.2020.106419>
- Kook, M.C., Son, H.M., Yi, T.H., 2014. *Microbacterium kyunghense* sp. nov. and *Microbacterium jejuense* sp. nov., isolated from salty soil. *Int. J. Syst. Evol. Microbiol.* 64, 2267–2273. <https://doi.org/10.1099/ijs.0.054973-0>
- Kulkarni, S., Ballal, A., Apte, S.K., 2013. Bioprecipitation of uranium from alkaline waste solutions using recombinant *Deinococcus radiodurans*. *J. Hazard. Mater.* 262, 853–861. <https://doi.org/10.1016/j.jhazmat.2013.09.057>
- Kulkarni, S., Misra, C.S., Gupta, A., Ballal, A., Apte, S.K., 2016. Interaction of uranium with bacterial cell surfaces: Inferences from phosphatase-mediated uranium precipitation. *Appl. Environ. Microbiol.* 82, 4965–4974. <https://doi.org/10.1128/AEM.00728-16>
- Lee, D.H., Choi, S.L., Rha, E., Kim, S.J., Yeom, S.J., Moon, J.H., Lee, S.G., 2015. A novel psychrophilic alkaline phosphatase from the metagenome of tidal flat sediments. *BMC Biotechnol.* 15, 1–13. <https://doi.org/10.1186/s12896-015-0115-2>
- Lee, J.S., Lee, K.C., Park, Y.H., 2006. *Microbacterium koreense* sp. nov., from sea water in the South Sea of Korea. *Int. J. Syst. Evol. Microbiol.* 56, 423–427. <https://doi.org/10.1099/ijs.0.63854-0>
- Leong, Y.K., Chang, J.S., 2020. Bioremediation of heavy metals using microalgae: Recent advances and mechanisms. *Bioresour. Technol.* 303, 122886. <https://doi.org/10.1016/j.biortech.2020.122886>
- Li, P., Liu, W., Gao, K., 2013. Effects of temperature, pH, and UV radiation on alkaline phosphatase activity in the terrestrial cyanobacterium *Nostoc flagelliforme*. *J. Appl. Phycol.* 25, 1031–1038. <https://doi.org/10.1007/s10811-012-9936-8>
- Li, X., Ding, C., Liao, J., Du, L., Sun, Q., Yang, J., Yang, Y., Zhang, D., Tang, J., Liu, N., 2016. Bioaccumulation characterization of uranium by a novel *Streptomyces sporoverrucosus* dwc-3. *J. Environ. Sci. (China)* 41, 162–171. <https://doi.org/10.1016/j.jes.2015.06.007>
- Liang, J.L., Liu, J., Jia, P., Yang, T. tao, Zeng, Q. wei, Zhang, S. chang, Liao, B., Shu, W. sheng, Li, J. tian, 2020. Novel phosphate-solubilizing bacteria enhance soil phosphorus cycling following ecological restoration of land degraded by mining. *ISME J.* 14, 1600–1613. <https://doi.org/10.1038/s41396-020-0632-4>
- Liang, X., Csetenyi, L., Gadd, G.M., 2016. Uranium bioprecipitation mediated by yeasts utilizing organic phosphorus substrates. *Appl. Microbiol. Biotechnol.* 100, 5141–5151. <https://doi.org/10.1007/s00253-016-7327-9>
- Liu, Y., Alessi, D.S., Owtrim, G.W., Petrash, D.A., Mloszewska, A.M., Lalonde, S. V., Martinez, R.E., Zhou, Q., Konhauser, K.O., 2015. Cell surface reactivity of *Synechococcus* sp. PCC 7002: Implications for metal sorption from seawater. *Geochim. Cosmochim. Acta* 169, 30–44. <https://doi.org/10.1016/j.gca.2015.07.033>
- Lloyd, J.R., Macaskie, L.E., 2002. Biochemical basis of of microbe-radionuclide interactions. *Interact. Microorg. with radionuclides* 313–342.
- Lopez-Fernandez, M., Romero-González, M., Günther, A., Solari, P.L., Merroun, M.L., 2018. Effect of U(VI) aqueous speciation on the binding of uranium by the cell surface of *Rhodotorula mucilaginosa*, a natural yeast isolate from bentonites. *Chemosphere* 199, 351–360. <https://doi.org/10.1016/j.chemosphere.2018.02.055>

## DISCUSIÓN GENERAL

- Lozinsky, V.I., Plieva, F.M., 1998. Poly(vinyl alcohol) cryogels employed as matrices for cell immobilization. 3. Overview of recent research and developments. *Enzyme Microb. Technol.* 23, 227–242. [https://doi.org/10.1016/S0141-0229\(98\)00036-2](https://doi.org/10.1016/S0141-0229(98)00036-2)
- Lv, Y., Niu, Z., Chen, Y., Hu, Y., 2017. Bacterial effects and interfacial inactivation mechanism of nZVI/Pd on *Pseudomonas putida* strain. *Water Res.* 115, 297–308. <https://doi.org/10.1016/j.watres.2017.03.012>
- Macaskie, L.E., Bonthron, K.M., Yong, P., Goddard, D.T., 2000. Enzymically mediated bioprecipitation of uranium by a *Citrobacter* sp.: A concerted role for exocellular lipopolysaccharide and associated phosphatase in biomineral formation. *Microbiology* 146, 1855–1867. <https://doi.org/10.1099/00221287-146-8-1855>
- Mandala, V.S., Loh, D.M., Shepard, S.M., Geeson, M.B., Sergeev, I. V., Nocera, D.G., Cummins, C.C., Hong, M., 2020. Bacterial phosphate granules contain cyclic polyphosphates: Evidence from <sup>31</sup>P solid-state NMR. *J. Am. Chem. Soc.* 142, 18407–18421. <https://doi.org/10.1021/jacs.0c06335>
- Manobala, T., Shukla, S.K., Rao, T.S., Kumar, M.D., 2019. Uranium sequestration by biofilm-forming bacteria isolated from marine sediment collected from Southern coastal region of India. *Int. Biodeterior. Biodegrad.* 145, 104809. <https://doi.org/10.1016/j.ibiod.2019.104809>
- Martínez-Rodríguez, P., Sánchez-Castro, I., Descostes, M., Merroun, M.L., 2020. Draft genome sequence data of *Microbacterium* sp. strain Be9 isolated from uranium-mill tailings porewaters. *Data Br.* 31, 10–14. <https://doi.org/10.1016/j.dib.2020.105732>
- Medina, J., Monreal, C., Chabot, D., Meier, S., González, M.E., Morales, E., Parillo, R., Borie, F., Cornejo, P., 2017. Microscopic and spectroscopic characterization of humic substances from a compost amended copper contaminated soil: main features and their potential effects on Cu immobilization. *Environ. Sci. Pollut. Res.* 24, 14104–14116. <https://doi.org/10.1007/s11356-017-8981-x>
- Merroun, M., Nedelkova, M., Rossberg, A., Hennig, C., Selenska-Pobell, S., 2006. Interaction mechanisms of bacterial strains isolated from extreme habitats with uranium. *Radiochim. Acta* 94, 723–729. <https://doi.org/10.1524/ract.2006.94.9-11.723>
- Merroun, M.L., Geipel, G., Nicolai, R., Heise, K.H., Selenska-Pobell, S., 2003. Complexation of uranium (VI) by three eco-types of *Acidithiobacillus* ferrooxidans studied using time-resolved laser-induced fluorescence spectroscopy and infrared spectroscopy. *BioMetals* 16, 331–339. <https://doi.org/10.1023/A:1020612600726>
- Merroun, M.L., Nedelkova, M., Ojeda, J.J., Reitz, T., Fernández, M.L., Arias, J.M., Romero-González, M., Selenska-Pobell, S., 2011. Bio-precipitation of uranium by two bacterial isolates recovered from extreme environments as estimated by potentiometric titration, TEM and X-ray absorption spectroscopic analyses. *J. Hazard. Mater.* 197, 1–10. <https://doi.org/10.1016/j.jhazmat.2011.09.049>
- Merroun, M.L., Selenska-Pobell, S., 2008. Bacterial interactions with uranium: An environmental perspective. *J. Contam. Hydrol.* 102, 285–295. <https://doi.org/10.1016/j.jconhyd.2008.09.019>
- Miao, Y., Johnson, N.W., Phan, T., Heck, K., Gedalanga, P.B., Zheng, X., Adamson, D., Newell, C., Wong, M.S., Mahendra, S., 2020. Monitoring, assessment, and prediction of microbial shifts in coupled catalysis and biodegradation of 1,4-dioxane and co-contaminants. *Water Res.* 173, 115540. <https://doi.org/10.1016/j.watres.2020.115540>
- Moll, H., Lütke, L., Bachvarova, V., Cherkouk, A., Selenska-Pobell, S., Bernhard, G., 2014. Interactions of the Mont Terri Opalinus Clay Isolate *Sporomusa* sp. MT-2.99 with Curium(III) and Europium(III). *Geomicrobiol. J.* 31, 682–696. <https://doi.org/10.1080/01490451.2014.>

889975

- Mouser, P.J., N'Guessan, A.L., Elifantz, H., Holmes, D.E., Williams, K.H., Wilkins, M.J., Long, P.E., Lovley, D.R., 2009. Influence of heterogeneous ammonium availability on bacterial community structure and the expression of nitrogen fixation and ammonium transporter genes during *in situ* bioremediation of uranium-contaminated groundwater. *Environ. Sci. Technol.* 43, 4386–4392. <https://doi.org/10.1021/es8031055>
- Mukherjee, P., Roy, P., 2013. Persistent organic pollutants induced protein expression and immunocrossreactivity by *Stenotrophomonas maltophilia* PM102: A prospective bioremediating candidate. *Biomed Res. Int.* 2013. <https://doi.org/10.1155/2013/714232>
- N'Guessan, A.L., Elifantz, H., Nevin, K.P., Mouser, P.J., Methé, B., Woodard, T.L., Manley, K., Williams, K.H., Wilkins, M.J., Larsen, J.T., Long, P.E., Lovley, D.R., 2010. Molecular analysis of phosphate limitation in *Geobacteraceae* during the bioremediation of a uranium-contaminated aquifer. *ISME J.* 4, 253–266. <https://doi.org/10.1038/ismej.2009.115>
- Nanda, M., Kumar, V., Sharma, D.K., 2019. Multimetal tolerance mechanisms in bacteria: The resistance strategies acquired by bacteria that can be exploited to 'clean-up' heavy metal contaminants from water. *Aquat. Toxicol.* 212, 1–10. <https://doi.org/10.1016/j.aquatox.2019.04.011>
- Nazina, T.N., Luk'yanova, E.A., Zakharova, E. V., Konstantinova, L.I., Kalmykov, S.N., Poltarau, A.B., Zubkov, A.A., 2010. Microorganisms in a Disposal Site for Liquid Radioactive Wastes and Their Influence on Radionuclides. *Geomicrobiol. J.* 27, 473–486. <https://doi.org/10.1080/01490451003719044>
- Nedelkova, M., Merroun, M.L., Rossberg, A., Hennig, C., Selenska-Pobell, S., 2007. Microbacterium isolates from the vicinity of a radioactive waste depository and their interactions with uranium. *FEMS Microbiol. Ecol.* 59, 694–705. <https://doi.org/10.1111/j.1574-6941.2006.00261.x>
- Nie, X., Wang, Y., Dong, F., Cheng, W., Lu, X., Ding, C., Lin, Q., Liu, M., Wang, J., Zhuan, H., Chen, G., Zhou, Y., Li, X., 2022. Surface interaction and biomineralization of uranium induced by the living and dead bacterial ghosts of *Kocuria* sp. *J. Environ. Chem. Eng.* 10, 107295. <https://doi.org/10.1016/j.jece.2022.107295>
- Ojeda, J.J., Romero-González, M.E., Bachmann, R.T., Edyvean, R.G.J., Banwart, S.A., 2008. Characterization of the cell surface and cell wall chemistry of drinking water bacteria by combining XPS, FTIR spectroscopy, modeling, and potentiometric titrations. *Langmuir* 24, 4032–4040. <https://doi.org/10.1021/la702284b>
- Ontañón, O.M., González, P.S., Barros, G.G., Agostini, E., 2017. Improvement of simultaneous Cr(VI) and phenol removal by an immobilised bacterial consortium and characterisation of biodegradation products. *N. Biotechnol.* 37, 172–179. <https://doi.org/10.1016/j.nbt.2017.02.003>
- Orellana, R., Hixson, K.K., Murphy, S., Mester, T., Sharma, M.L., Lipton, M.S., Lovley, D.R., 2014. Proteome of *Geobacter sulfurreducens* in the presence of U(VI). *Microbiol. (United Kingdom)* 160, 2607–2617. <https://doi.org/10.1099/mic.0.081398-0>
- Pan, X., Chen, Z., Chen, F., Cheng, Y., Lin, Z., Guan, X., 2015. The mechanism of uranium transformation from U(VI) into nano-uramphite by two indigenous *Bacillus thuringiensis* strains. *J. Hazard. Mater.* 297, 313–319. <https://doi.org/10.1016/j.jhazmat.2015.05.019>
- Pinel-Cabello, M., Jroundi, F., López-Fernández, M., Geffers, R., Jarek, M., Jauregui, R., Link, A., Vílchez-Vargas, R., Merroun, M.L., 2021. Multisystem combined uranium resistance mechanisms and bioremediation potential of *Stenotrophomonas bentonitica* BII-R7: Transcriptomics and microscopic study. *J. Hazard. Mater.* 403. <https://doi.org/10.1016/j.jhazmat.2020.123858>
- Povedano-Priego, C., Jroundi, F., Lopez-Fernandez, M., Sánchez-Castro, I.,

## DISCUSIÓN GENERAL

- Martin-Sánchez, I., Huertas, F.J., Merroun, M.L., 2019. Shifts in bentonite bacterial community and mineralogy in response to uranium and glycerol-2-phosphate exposure. *Sci. Total Environ.* 692, 219–232.  
<https://doi.org/10.1016/j.scitotenv.2019.07.228>
- Rajendran, R., Prabhavathi, P., Karthiksundaram, S., Pattabi, S., Kumar, S.D., Santhanam, P., 2015. Biodecolorization and bioremediation of denim industrial wastewater by adapted bacterial consortium immobilized on inert polyurethane foam (PUF) matrix: A first approach with biobarrier model. *Polish J. Microbiol.* 64, 329–338.  
<https://doi.org/10.5604/17331331.1185230>
- Rawat, P., Das, S., Shankhdhar, D., Shankhdhar, S.C., 2021. Phosphate-Solubilizing Microorganisms: Mechanism and Their Role in Phosphate Solubilization and Uptake. *J. Soil Sci. Plant Nutr.* 21, 49–68. <https://doi.org/10.1007/s42729-020-00342-7>
- Reitz, T., Rossberg, A., Barkleit, A., Steudtner, R., Selenska-Pobell, S., Merroun, M.L., 2015. Spectroscopic study on uranyl carboxylate complexes formed at the surface layer of *Sulfolobus acidocaldarius*. *Dalt. Trans.* 44, 2684–2692.  
<https://doi.org/10.1039/c4dt02555e>
- Richter, M., Rosselló-Móra, R., 2009. Shifting the genomic gold standard for the prokaryotic species definition. *Proc. Natl. Acad. Sci. U. S. A.* 106, 19126–19131.  
<https://doi.org/10.1073/pnas.0906412106>
- Romera, E., González, F., Ballester, A., Blázquez, M.L., Muñoz, J.A., 2007. Comparative study of biosorption of heavy metals using different types of algae. *Bioresour. Technol.* 98, 3344–3353.  
<https://doi.org/10.1016/j.biortech.2006.09.026>
- Rossolini, G.M., Schippa, S., Riccio, M.L., Berlutti, F., Macaskie, L.E., Thaller, M.C., 1998. Bacterial nonspecific acid phosphohydrolases: Physiology, evolution and use as tools in microbial biotechnology. *Cell. Mol. Life Sci.* 54, 833–850.  
<https://doi.org/10.1007/s000180050212>
- Sánchez-Castro, I., Amador-García, A., Moreno-Romero, C., López-Fernández, M., Phommavanh, V., Nos, J., Descostes, M., Merroun, M.L., 2017. Screening of bacterial strains isolated from uranium mill tailings porewaters for bioremediation purposes. *J. Environ. Radioact.* 166, 130–141.  
<https://doi.org/10.1016/j.jenvrad.2016.03.016>
- Sánchez-Castro, I., Martínez-Rodríguez, P., Jroundi, F., Lorenzo, P., Descostes, M., L. Merroun, M., 2020. High-efficient microbial immobilization of solvated U(VI) by the *Stenotrophomonas* strain Br8. *Water Res.* 183.  
<https://doi.org/10.1016/j.watres.2020.116110>
- Saunders, J.A., Lee, M.K., Dhakal, P., Ghandehari, S.S., Wilson, T., Billor, M.Z., Uddin, A., 2018. Bioremediation of arsenic-contaminated groundwater by sequestration of arsenic in biogenic pyrite. *Appl. Geochemistry* 96, 233–243.  
<https://doi.org/10.1016/j.apgeochem.2018.07.007>
- Senko, J.M., Istok, J.D., Suflita, J.M., Krumholz, L.R., 2002. In-situ evidence for uranium immobilization and remobilization. *Environ. Sci. Technol.* 36, 1491–1496.  
<https://doi.org/10.1021/es011240x>
- Seufferheld, M.J., Alvarez, H.M., Farias, M.E., 2008. Role of polyphosphates in microbial adaptation to extreme environments. *Appl. Environ. Microbiol.* 74, 5867–5874.  
<https://doi.org/10.1128/AEM.00501-08>
- Sharma, P., Tripathi, S., Chaturvedi, P., Chaurasia, D., Chandra, R., 2021. Newly isolated *Bacillus* sp. PS-6 assisted phytoremediation of heavy metals using *Phragmites communis*: Potential application in wastewater treatment. *Bioresour. Technol.* 320, 124353.  
<https://doi.org/10.1016/j.biortech.2020.124353>
- Shi, X., Zhou, G., Liao, S., Shan, S., Wang, G., Guo, Z., 2018. Immobilization of cadmium by immobilized *Alishewanella* sp. WH16-1 with alginate-lotus seed pods in pot experiments of Cd-contaminated paddy soil. *J. Hazard.*

- Mater. 357, 431–439.  
<https://doi.org/10.1016/j.jhazmat.2018.06.027>
- Sun, H., Meng, M., Wu, L., Zheng, X., Zhu, Z., Dai, S., 2020. Function and mechanism of polysaccharide on enhancing tolerance of *Trichoderma asperellum* under Pb<sup>2+</sup> stress. *Int. J. Biol. Macromol.* 151, 509–518.  
<https://doi.org/10.1016/j.ijbiomac.2020.02.207>
- Suzuki, Y., Banfield, J.F., 2004. Resistance to, and accumulation of, uranium by bacteria from a uranium-contaminated site. *Geomicrobiol. J.* 21, 113–121.  
<https://doi.org/10.1080/01490450490266361>
- Suzuki, Y., Banfield, J.F., 1999. 8. *Geomicrobiology of Uranium*. De Gruyter, Berlin, Boston, pp. 393–432.  
<https://doi.org/https://doi.org/10.1515/9781501509193-013>
- Tabaldi, L.A., Ruppenthal, R., Cargnelutti, D., Morsch, V.M., Pereira, L.B., Schetinger, M.R.C., 2007. Effects of metal elements on acid phosphatase activity in cucumber (*Cucumis sativus* L.) seedlings. *Environ. Exp. Bot.* 59, 43–48.  
<https://doi.org/10.1016/j.envexpbot.2005.10.009>
- Theodorakopoulos, N., Chapon, V., Coppin, F., Floriani, M., Vercouter, T., Sergeant, C., Camilleri, V., Berthomieu, C., Février, L., 2015. Use of combined microscopic and spectroscopic techniques to reveal interactions between uranium and *Microbacterium* sp. A9, a strain isolated from the Chernobyl exclusion zone. *J. Hazard. Mater.* 285, 285–293.  
<https://doi.org/10.1016/j.jhazmat.2014.12.018>
- Vanadate, B., Swarupl, G., Cohen, S., Garbers, D.L., 1982. INHIBITION OF MEMBRANE PHOSPHOTYROSYL-PROTEIN PHOSPHATASE ACTIVITY.
- Varjani, S., Upasani, V.N., 2021. Bioaugmentation of *Pseudomonas aeruginosa* NCIM 5514 – A novel oily waste degrader for treatment of petroleum hydrocarbons. *Bioresour. Technol.* 319, 124240.  
<https://doi.org/10.1016/j.biortech.2020.124240>
- Villagrasa, E., Egea, R., Ferrer-Miralles, N., Solé, A., 2020. Genomic and biotechnological insights on stress-linked polyphosphate production induced by chromium(III) in *Ochrobactrum anthropi* DE2010. *World J. Microbiol. Biotechnol.* 36, 1–10.  
<https://doi.org/10.1007/s11274-020-02875-6>
- Wang, J. song, Hu, X. jiang, Liu, Y. guo, Xie, S. bo, Bao, Z. lei, 2010. Biosorption of uranium (VI) by immobilized *Aspergillus fumigatus* beads. *J. Environ. Radioact.* 101, 504–508.  
<https://doi.org/10.1016/j.jenvrad.2010.03.002>
- Wani, P., Olamide, A., Rafi, N., Wahid, S., Wasii, I., Sunday, O., 2016. Sodium Alginate/Polyvinyl Alcohol Immobilization of *Brevibacillus brevis* OZF6 Isolated from Waste Water and Its Role in the Removal of Toxic Chromate. *Br. Biotechnol. J.* 15, 1–10.  
<https://doi.org/10.9734/bbj/2016/27341>
- Wei, Y., Chen, Z., Song, H., Zhang, J., Lin, Z., Dang, Z., Deng, H., 2019. The immobilization mechanism of U(VI) induced by *Bacillus thuringiensis* 016 and the effects of coexisting ions. *Biochem. Eng. J.* 144, 57–63.  
<https://doi.org/10.1016/j.bej.2019.01.013>
- Wojcieszynska, D., Hupert-Kocurek, K., Jankowska, A., Guzik, U., 2012. Properties of catechol 2,3-dioxygenase from crude extract of *Stenotrophomonas maltophilia* strain KB2 immobilized in calcium alginate hydrogels. *Biochem. Eng. J.* 66, 1–7.  
<https://doi.org/10.1016/j.bej.2012.04.008>
- Wu, M., Li, Y., Li, J., Wang, Y., Xu, H., Zhao, Y., 2019. Bioreduction of hexavalent chromium using a novel strain CRB-7 immobilized on multiple materials. *J. Hazard. Mater.* 368, 412–420.  
<https://doi.org/10.1016/j.jhazmat.2019.01.059>
- Xu, A., Chao, L., Xiao, H., Sui, Y., Liu, J., Xie, Q., Yao, S., 2018. Ultrasensitive electrochemical sensing of Hg<sup>2+</sup> based on thymine-Hg<sup>2+</sup>-thymine interaction and signal amplification of alkaline phosphatase catalyzed silver deposition. *Biosens. Bioelectron.* 104, 95–101.  
<https://doi.org/10.1016/j.bios.2018.01.005>

## DISCUSIÓN GENERAL

- Yan, Z.F., Lin, P., Won, K.H., Yang, J.E., Li, C.T., Kook, M.C., Wang, Q.J., Yi, T.H., 2017. *Microbacterium hibisci* sp. Nov., isolated from rhizosphere of mugunghwa (*hibiscus syriacus* L.). *Int. J. Syst. Evol. Microbiol.* 67, 3564–3569. <https://doi.org/10.1099/ijsem.0.002167>
- Yong, P., Macaskie, L.E., 1995. Enhancement of uranium bioaccumulation by a *Citrobacter* sp. via enzymically-mediated growth of polycrystalline  $\text{NH}_4\text{UO}_2\text{PO}_4$ . *J. Chem. Technol. Biotechnol.* 63, 101–108. <https://doi.org/10.1002/jctb.280630202>
- Yu, J., Wang, J., Jiang, Y., 2017. Removal of Uranium from Aqueous Solution by Alginate Beads. *Nucl. Eng. Technol.* 49, 534–540. <https://doi.org/10.1016/j.net.2016.09.004>
- Zeng, Q., Zhu, T., Wen, Y., Li, F., Cheng, Y., Chen, S., Lan, T., Yang, Y., Liao, J., Sun, Q., Liu, N., 2022. The dynamic behavior and mechanism of uranium (VI) biomineralization in *Enterobacter* sp. X57. *Chemosphere* 298. <https://doi.org/10.1016/j.chemosphere.2022.134196>
- Zhang, J., Song, H., Chen, Z., Liu, S., Wei, Y., Huang, J., Guo, C., Dang, Z., Lin, Z., 2018. Biomineralization mechanism of U(VI) induced by *Bacillus cereus* 12-2: The role of functional groups and enzymes. *Chemosphere* 206, 682–692. <https://doi.org/10.1016/j.chemosphere.2018.04.181>
- Zhang, K., Teng, Z., Shao, W., Wang, Y., Li, M., Lam, S.S., 2020. Effective passivation of lead by phosphate solubilizing bacteria capsules containing tricalcium phosphate. *J. Hazard. Mater.* 397, 122754. <https://doi.org/10.1016/j.jhazmat.2020.122754>
- Zommere, Ž., Nikolajeva, V., 2017. Immobilization of bacterial association in alginate beads for bioremediation of oil-contaminated lands. *Environ. Exp. Biol.* <https://doi.org/10.22364/eeb.15.09>

# CONCLUSIONES



## CONCLUSIONES

Tras los resultados obtenidos en esta Tesis Doctoral se proponen las siguientes conclusiones:

1. La caracterización fisiológica, bioquímica y genómica de las cepas bacterianas *Microbacterium* sp. Be9 y *Stenotrophomonas* sp. Br8 confirmó la capacidad de ambas de tolerar el U(VI) gracias a su actividad enzimática. Además, se detectaron, en ambas cepas, secuencias codificantes de proteínas que podrían estar involucradas en este proceso de interacción con U.
2. La cepa *Microbacterium* sp. Be9 mostró un comportamiento variable frente al U(VI) en función de la fuente de fosfatos presente. En ausencia de fosfatos, la cepa Be9 es capaz de precipitar intracelularmente el U soluble en forma de fosfatos de U(VI), mientras que en presencia de éstos no se detecta dicho proceso de biomineralización.
3. En presencia de fosfatos inorgánicos de U, previamente precipitados de forma abiótica, la cepa Be9 presenta la capacidad de solubilizar el metal, retornándolo a un estado móvil y disponible. Esta habilidad confirmó que la cepa Be9 pertenece al grupo de las bacterias solubilizadoras de fosfatos (*Phosphate Solubilizing Bacteria*, PSB).
4. La cepa *Stenotrophomonas* sp. Br8 mostró una alta capacidad de precipitar el U(VI) soluble como fosfatos de U(VI) en presencia de una fuente de fosfatos orgánicos (G2P) y en un amplio rango de condiciones fisicoquímicas gracias a su actividad fosfatasa.
5. Los fosfatos de U formados presentaron una coordinación estructural muy similar a la del grupo de m-autunita ( $\text{Ca}(\text{UO}_2)_2(\text{PO}_4)_2 \cdot 6\text{H}_2\text{O}$ ), sugiriendo la formación de fases minerales altamente estables. Las conclusiones detalladas en los puntos 4 y 5 llevaron a la selección de la cepa *Stenotrophomonas* sp. Br8 para posteriores ensayos de inmovilización de U en muestras de aguas mineras contaminadas.
6. Tras la caracterización de varios materiales para llevar a cabo la inmovilización de células bacterianas, se determinó que las microesferas de alginato eran las más adecuadas para la cepa *Stenotrophomonas* sp. Br8, debido a su alta biocompatibilidad, porosidad, gran estabilidad física y permeabilidad.
7. La evaluación de diferentes parámetros biológicos y fisicoquímicos, demostró que el uso de una microesfera del biomaterial por mL de agua a tratar es la cantidad óptima para lograr una eliminación de U eficiente, y que es posible almacenar las microesferas a 4°C durante, al menos, 300 días e incluso liofilizarlas sin comprometer su capacidad de bioprecipitación. Las microesferas de alginato cargadas con biomasa de Br8 demostraron ser altamente eficientes precipitando, en forma de fosfatos de U(VI), el 97,8% del U(VI) presente en aguas mineras contaminadas. Esto evidenció el gran potencial de esta estrategia para la biorremediación de aguas que presentan altas concentraciones de U así como una composición química compleja.

## CONCLUSIONES

# CONCLUSIONS

## CONCLUSIONES

After the results obtained in the present Doctoral Thesis, the following conclusions are established:

1. The physiological, biochemical and genomic characterization of *Microbacterium* sp. Be9 and *Stenotrophomonas* sp. Br8 strains confirmed their high U(VI) tolerance mediated by its specific enzymatic activity. Moreover, the presence in both strains of protein coding sequences, which could be responsible for the U-bacteria interaction, was detected.
2. *Microbacterium* sp. Be9 strain displayed a variable behavior towards U(VI) depending on the amended phosphate substrate. In absence of phosphates, Be9 strain is capable of precipitating U intracellularly as U(VI) phosphates, but in presence of phosphates, the U biomineralization process does not occur.
3. In presence of abiotically-generated U inorganic phosphates, Be9 strain showed the ability to solubilize the metal into a mobile form. This ability supported the classification of Be9 strain to the PSB group (*Phosphate Solubilizing Bacteria*).
4. *Stenotrophomonas* sp. Br8 strain showed a high capacity to precipitate soluble U(VI) into U(VI) phosphates in presence of G2P (as organic phosphates source) in a wide range of physicochemical conditions due to its phosphatase activity.
5. Generated uranium phosphates showed a similar structural coordination to that of m-autunite group ( $\text{Ca}(\text{UO}_2)_2(\text{PO}_4)_2 \cdot 6\text{H}_2\text{O}$ ), suggesting the formation of highly stable mineral phases. Conclusions number 4 and 5 entailed the selection of *Stenotrophomonas* sp. Br8 for further U immobilization assays for the bioremediation of real U mining water samples.
6. The characterization of various matrices showed that alginate beads are the most suitable immobilization system for *Stenotrophomonas* sp. Br8 strain, due to its high biocompatibility, porosity, permeability and physical stability.
7. The evaluation of different biological and physicochemical parameters showed that the optimal conditions for the U biomineralization process consisted in the use of 1 microsphere per mL of contaminated water. The lyophilization and storage of alginate beads at 4°C for, at least, 300 days did not reduce the high biomineralization potential of this biomaterial.
8. Br8 doped alginate beads demonstrated to be highly efficient precipitating up to 97.8% of the U(VI) contained in contaminated mining waters into U(VI) phosphates. This result suggests the high potential of this bioremediation strategy in waters with high U concentration and complex chemical composition.

## CONCLUSIONES



# UNIVERSIDAD DE GRANADA